SONIC INVESTIGATION OF MASONRY STRUCTURES

BY

FARHAD KOMEYLI-BIRJANDI B.Eng.

THESIS SUBMITTED TO THE UNIVERSITY OF EDINBURGH

FOR THE DEGREE OF DOCTOR OF PHILOSOPHY

DECEMBER 1986

UNIVERSITY OF EDINBURGH

DEPARTMENT OF CIVIL ENGINEERING AND BUILDING SCIENCE

1986

DECLARATION

I HEREBY DECLARE THAT THIS THESIS WAS COMPOSED BY MYSELF, AND THE ORIGINAL WORKS AND RESULTS REPORTED WERE OBTAINED SOLELY BY MYSELF, UNLESS OTHERWISE STATED.

EDINBURGH, DECEMBER 1986

F. KOMEYLI-BIRJANDI

TO MY PARENTS

ACKNOWLEDGEMENTS

The author wishes to thank Professor A.W. Hendry, head of the Department of Civil Engineering and Building Science for placing the facilities of this Department at his disposal.

The author is particularly grateful to Dr. M.C. Forde for his supervision. His suggestions, criticisms and constructive comments have been invaluable in the preparation of this thesis.

The author wishes to thank Mr. A.J. Batchelor, Civil Tech. NDT Ltd for allowing the use of the facilities of this firm in carrying out the full scale tests reported in this work.

The author is also grateful to fellow student J.D. Hill for undertaking some of the experimental work and fellow postgraduate students for their understanding and general assistance during the course of this work.

The author wishes to express his special thanks to his parents and his wife for their help, patience and encouragement at all times, which made this work possible.

The author also gratefully acknowledges the work of Mrs. J.R. Fish for typing the thesis.

NOTATIONS

$A(f)$	Fourier transform of function $a(t)$
$a(t)$	a time domain function
$a(t + \tau)$	time delayed replica of $a(t)$
$B(f)$	Fourier transform of function $b(t)$
C_{AB}	Cepstrum corresponding to length AB
$(C_{AB})_n$	Cepstrum corresponding to length AB with nth resonant frequency
C_c	complex cepstrum
$C_p(\tau)$	power cepstrum function
d	thickness of a layer
DFT	Discrete Fourier Transform
E'	apparent stiffness
f	frequency
$F(f)$	frequency function
FFT	Fast Fourier Transform
$F(k)$	frequency discrete function
F_m	maximum force
$f(n)$	time domain discrete function
FT	Fourier Transform
$f(t)$	time domain function
$F_x(f)$	frequency function in complex cepstrum
$f_x(t)$	time domain function in complex cepstrum
$F_{xx}(f)$	frequency function in power cepstrum
$H(f)$	frequency domain function
Hn-m	point on wall with vertical coordinate n and horizontal coordinate m
$h(t)$	inverse Fourier transform of $H(f)$
I	intensity of wave

I_o	initial wave intensity
I_i	intensity of incident wave
I_r	intensity of reflected wave
I_t	intensity of transmitted wave
K	a constant
ℓ,L	length of medium along which wave is propagated or reflected
R_{aa}	total power in a signal b(t)
$R_{aa}(\tau)$	auto correlation function
R_{ab}	total power in a function b(t)
$R_{ab}(\tau)$	cross correlation function
r	distance from source of energy
S	area at right angle to the direction of wave
T	period = 1/f
t,t'	transmission or reflection delay time
v	pulse, transmission or propagation velocity
v_L	longitudinal wave velocity
v_m,V_m	maximum propagation velocity
V_m/F_m	mechanical admittance
v_s	surface wave velocity
v_t	transverse wave velocity
W	rate of flow of energy
Y	Young's modulus
α_r	reflection coefficient of waves through a layer
α_t	transmission coefficient of waves through a layer
γ	coefficient of absorption
Δt	time interval
ΔV	difference in transmission velocity

λ	wavelength
λ'	bulk modulus of elasticity
μ	shear modulus of elasticity
ρ	density of medium
ρ_{aa}	auto correlation coefficient function
$\rho_{aa}(\tau)$	normalised auto correlation function
ρ_{ab}	cross correlation coefficient function
$\rho_{ab}(\tau)$	normalised cross correlation
ρv	characteristic impedance, a measure of elasticity of medium
σ	Poisson's ratio
τ	delay time between a time signal and its displaced replica

LIST OF TABLES

LIST OF PLATES

LIST OF FIGURES

LIST OF CONTENTS

The text is divided into chapters and sections. Sections are numbered decimally within each chapter. The numbers given to Figures indicate to which chapter or appendix they belong, but are not related to the section numbers.

ABSTRACT

The aim of this work was to investigate the use of sonic non-destructive testing techniques for masonry structures. Sonic techniques were used to measure the transmission velocity in masonry as an indication of quality and strength, to detect large voids or cracks and to measure the thickness of masonry.

First a review of testing techniques used for Civil Engineering materials was discussed. Then a study of masonry components, namely mortar and stone blocks, was undertaken. The results were used as a basis for testing masonry as composite.

Three shear failed reinforced brick masonry walls and several stone masonry piers were tested with the conventional time delayed methods. The purpose of these tests was to investigate the presence of cracks and also to obtain transmission velocities as an indication of quality of the material. Sonic surveys on four masonry bridges were then undertaken to study the application of the developed method to full scale structures. Both time domain and frequency domain techniques were used at this stage using digital and highly sophisticated FFT dual channel analysers and equipment.

The results were generally reliable and it can be said that from an early stage of visual inspection and transmission velocity measurement of the time domain signals, a higher degree of resolution was achieved.

CHAPTER ONE

INTRODUCTION

INTRODUCTION

Masonry structures are amongst the oldest ones which still remain standing. Their construction goes back to days before the Egyptians built the pyramids, to long before the construction of fortified castles by the Normans and to before the Great Wall of China. The chief advantages of masonry construction were durability, stability and appearance. In fact there were no other materials available to man to meet these objectives.

Today, due to the advent of alternative cheaper materials and construction methods, masonry construction is less in favour. However, quite a significant proportion of the total number of all structures in service are masonry ones. Many of them such as some Victorian arch bridges are over a century old. Their functions are now far in excess of those for which they were designed. For example, many masonry bridges are carrying loads far in excess of the designed ones. Therefore there is a widespread demand for assessment of the quality and fault detection in such structures.

Quality assessment testing of these structures and also methods of detecting faults in them are usually restricted by the fact that the appearance of many of these structures must be untouched and they are protected by law. Tests such as collapse load method, which are difficult for most structures and could cause failure, are therefore out of the question in such circumstances. Other methods like core sampling have limitations. Core sampling is not only expensive to carry out but also can damage and scar the structure. Hence other methods of testing which overcome these restrictions and meet the purposes of the test must be considered.

The type of tests usually favoured in these cases are non-destructive, where the quality assessment and fault detection are carried out without damaging the structure. Some of the non-destructive testing methods commonly used in the Civil Engineering industry include sonic/ultrasonic, acoustic emission and resistivity testing. These tests are cheap, quick and are good for

comparative and uniformity assessments. Tests such as sonic/ultrasonic methods can also give an indication of the strength of the material. However, for a more precise strength assessment other methods which cause as little damage as possible must be used.

In such cases these methods of testing plus the non-destructive test can result in thorough and reliable assessment of quality and strength of the material and the structure. Here the conventional methods of testing, for example core samples, are usually used for calibration of non-destructive methods such as sonic tests. The choice of testing methods depend upon factors such as damage to the structure, cost, speed and reliability of the results.

The non-destructive sonic method is the main technique studied in this work. It is noted that a vast amount of research has been carried out in the field of ultrasonics, which has resulted in the use of ultrasonic methods in measurement and fault detection in homogeneous materials such as metals. Its application to Civil Engineering materials has been confined to relatively homogeneous ones such as concrete on a small scale. Ultrasonic non-destructive testing techniques are not, however, appropriate to the testing of structures such as masonry ones. The very high frequency nature of these techniques results in detection of minor variations rather than the major ones. Also, because of the high rate of attenuation they are inappropriate for long path length. Therefore, a similar technique, sonic non-destructive testing method has been developed to overcome the problems of attenuation and sensitivity to minor variations.

Sonic techniques employ frequencies less than 25 kHz as opposed to ultrasonic frequencies of higher than 25 kHz. The work carried out in this thesis attempts to study the practical implications of this property and its possible application to such composite materials as masonry. It deals firstly with two main individual components of a masonry structure, that is the mortar and masonry stone or brick. The purpose of first studying the two main components of masonry is to find and develop a basis for analysing the quality of an entire structure.

In brief, this work basically investigates the viability of using sonics in the quality assessment of masonry structures and its use in fault detection and thickness measurements.

CHAPTER TWO

EXISTING METHODS OF TESTING

2.1 INTRODUCTION

There are several methods of testing Civil Engineering structures which are commonly used in practice today. They vary from a simple visual inspection to destructive loading to collapse of the structure. Although all these methods come under two major methods of destructive and non-destructive testing, there are other methods which are considered by some as different techniques of testing. These include chemical, visual inspection and semi-destructive methods of testing. Each has its own advantages and disadvantages and their functions and results are different. Chemical tests, for example, are mainly used for property determination of the materials and the destructive tests for structural behaviour and overall strength.

Non-destructive methods which include a wide variety of testing techniques from sonic testing to neutron radiography are mostly used for integrity and relative strength assessment of structures. The sonic testing method, particularly for testing masonry structures, is at an early stage of development. There is therefore a wide area of research and development yet to be covered. However, with increasing development in this field, it is being increasingly used as an alternative method to the more expensive and time consuming ones such as coring.

In this chapter a review of the existing methods commonly used in Civil Engineering practice of testing materials and structures, notably concrete and masonry, is briefly described. It will be noted that the area of testing techniques for concrete is much wider than that for masonry. Thus most of the techniques described in the chapter deal with testing concrete.

The testing techniques are usually classified into three main groups. They are destructive, partially destructive and non-destructive testing techniques. The destructive or non-destructive nature of the test is based on the degree of the damage done to the member or the structure under test. In the following the main commonly used tests for each group are briefly described.

2.2 "DESTRUCTIVE" TESTS

2.2.1 Load Testing

Load testing replaces in situ testing techniques when the latter are not adequate for determining the strength of a structure. A core taken from a bridge is in no way adequate for determining the load-deflection characteristics of the structure since a serious defect may not have been detected. In most of these cases, the main aim of the work is the proof of overall structural adequacy (1,2).

There are two types of load testing employed in Civil Engineering, selection of which depends on circumstances:

(a) in situ load testing (3,1).

(b) tests on a component of the structure removed for typically a destructive test. The results are used for the calibration and the overall strength determination of the structure (3).

2.2.1.1. The testing procedure (4)

When the proof of structural adequacy or establishing behaviour of a structure is required, load testing is performed. In the case of a complex structure the members for testing must be identified and attention to the supporting members of the structure, be paid.

Scaffolding is needed for this test and it must be provided to support the load from the likely collapse of the member or the structure. Therefore the support of the scaffolding must be made safe from collapse. Sometimes it is necessary to load a larger part of the structure to ensure that the critical members carry the required load. It is usually essential to monitor the deflection of the member, and the adjacent ones as well, to ensure that the applied load can be increased accordingly and cases of danger detected.

The test loads must always be added and removed incrementally. B.S. CP110 - 1972, has the necessary recommendations for the loads used for:

(a) deflection and cracking.

(b) ultimate strength.

There are several load application techniques, the use of which

depend on the practicalities of the situation. Water, bricks, sand bags, steel weights and hydraulic jacks are amongst the most common forms of load application methods. The first four forms are usually for uniform load applications, whereas hydraulic jacks are for point load applications. Test load for bridges for example, when a uniform load distribution is required, can be provided by distribution of loaded trucks or wagons of known weights. It is also important to provide safety measures for the personnel working in the test, during the load application and removal.

The measurement techniques are usually related to the determination of cracks or crack width and also to the load deflection characteristics of the structure.

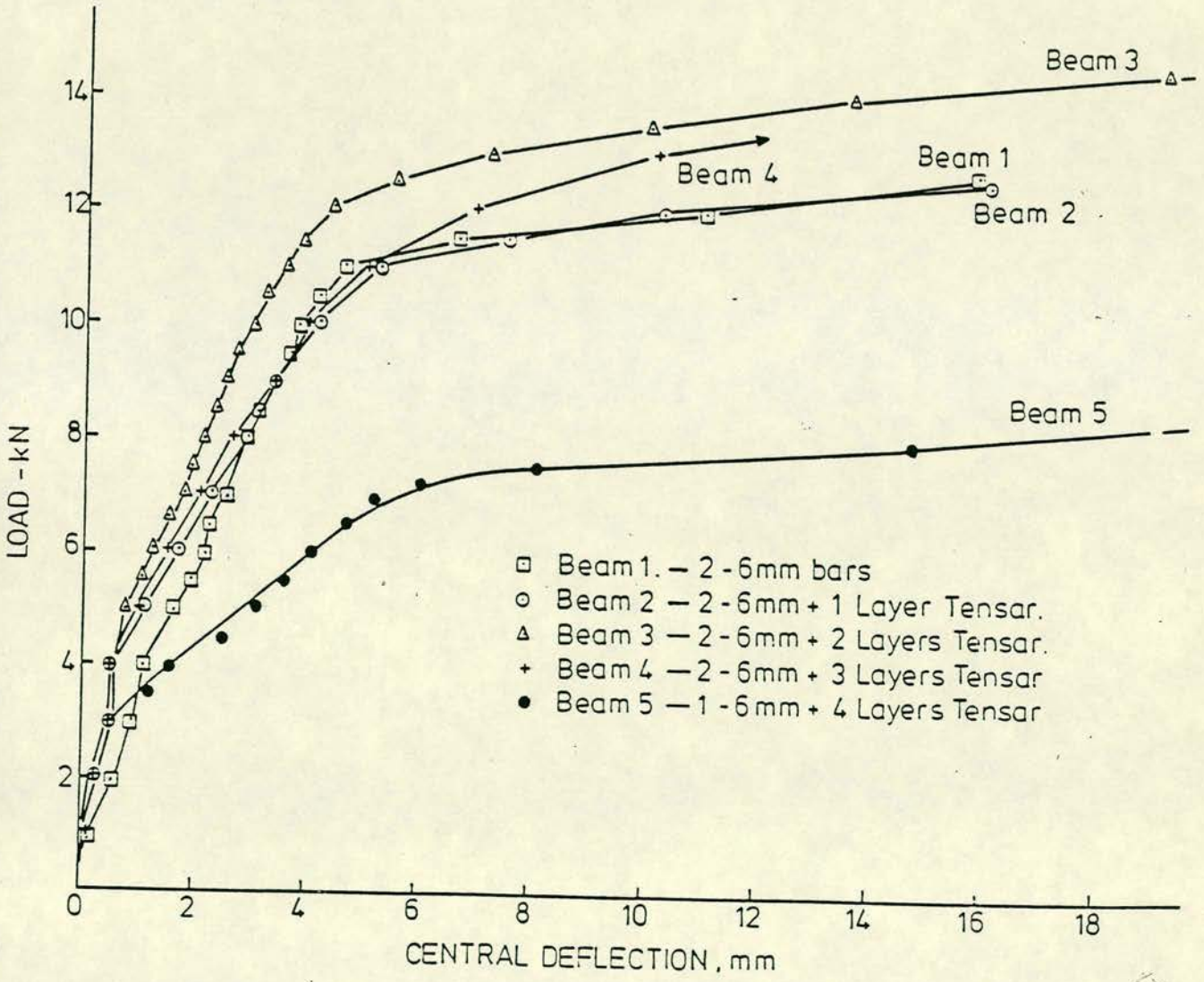

Fig. 2.1 Structural behaviour of five concrete beams under load (based on ref. 5)

For basic in situ load-deflection measurement, dial gauges are used, and for crack width measurement, optical or field surveying equipment is used. The load-deflection characteristics of the structure are of vital importance and they are mainly used for determining structural adequacy. Fig. 1, above, shows the structural behaviour of five concrete beams under load. Each beam has a different reinforcement layout as indicated. These beams were constructed to study the use of polymer grid reinforcement for corrosion control and concrete repair.

2.2.1.2 Limitations and applications

The high cost of load testing and the inconveniences it causes are serious disadvantages of load testing. Due to these two disadvantages, the time consuming nature of the test, and other restrictive practicalities, it is usually confined to one or two members of the structure being tested.

Some of the main applications of this method are:

(a) proof of the structural performance.
(b) proof of reliability of a non-standard design method.
(c) proof of performance after some structural modification and change of occupancy.
(d) proof of the structural performance of old and sub-standard structures.
(e) quantification of the deterioration of the structure due to material deterioration or physical damage.

2.2.2 Prism Testing

Prism testing is one of the very few masonry testing techniques. After load testing it is the commonest one used in practice to determine the overall strength of the structure. For example, where load testing is not practical, an alternative method is to cut out a prism of masonry from the structure under test (6).

2.2.2.1 Basic description

Masonry prisms are small specimens used for predicting the full scale properties of masonry such as compressive and shear strength. The results are also used for obtaining design compressive strengths (7).

Prisms range from two block high, stack-bonded specimens to small walls used for research purposes. Their behaviour usually reflects the characteristics of the masonry to be used in a building (8,9).

2.2.2.2 Procedure

The procedure involves capping the prism with a capping material at the top and bottom. The capping material may be gypsum plaster, mortar, fireboard, plywood, etc (9). The load is then applied in small increments depending on the size, slenderness and other factors. A number of tests must be carried out - usually a minimum of five tests when a good estimate of variation is known beforehand. A minimum of ten tests for mean strength determination is recommended (10,11).

It must be noted that the results obtained from prism tests are only estimates of the full scale test. Fig. 2.2 shows a typical prism test result for evaluating the shear strength of lintels and its comparison with full scale and derived results.

2.2.2.3 Factors influencing prism strength

As mentioned above, prism behaviour must be a reflection of the masonry, in order that a good estimate of the masonry strength can be predicted. There are a number of factors influencing the strength of the prism. Some of these factors are as follows (11):

(a) prism dimension: which in turn may depend on units, mortar, capping, method of handling and so on.

(b) number of courses, where mortar joint effects must be taken into account.

(c) height, where prism strength usually becomes constant for heights greater than 3 to 5 times the thickness.

(d) bond patterns normally do not have much effect except a few exceptions.

(e) other factors include thickness of the prism, capping method, workmanship, curing conditions, testage and load rate.

2.2.2.4 Limitations and applications

There are a number of limitations with this method of testing.

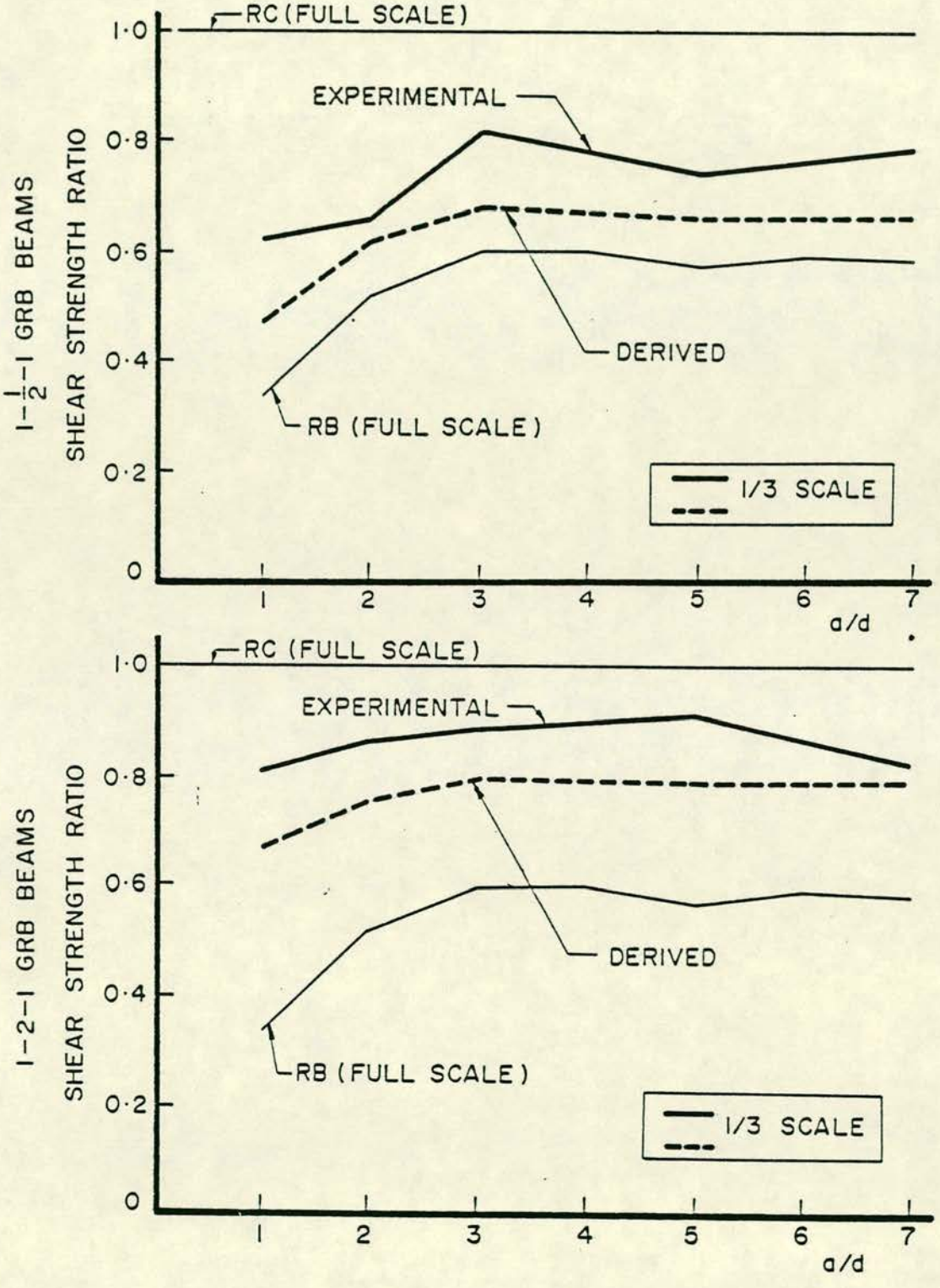

Fig. 2.2 Typical prism test results for evaluating the shear strength of lintels (based on ref. 8)

They include the effects of the factors mentioned above and the final results. The final results are not always identical to full scale ones and a correlation and correction factor must be taken into account. The major advantage of this test is that it is relatively fast and inexpensive compared to full scale tests. It is an established method of testing and the results are considered reliable. It can be done in a controlled environment, i.e. in the laboratory, so that some undesirable factors not interested in, such as moisture content, can be controlled.

The major application of this test is to predict the strength of masonry (8,9 and 13). It is also used to study the effects of the factors such as slenderness, joint reinforcements on the strength of masonry (14,15 and 16).

2.3 PARTIALLY DESTRUCTIVE TESTS

2.3.1 Core Testing Method

One of the well established methods of testing concrete and masonry is the examination of cores cut from the member under investigation. The core can be used to study the compressive strength, physical properties and tensile strength of the member. The cores can also be used for chemical testing and analysis of the materials used in the structure. The standard recommended procedure of testing and interpretation of the results are detailed in B.S. 1881 pt. 4 (17).

2.3.1.1 Procedure

First the location of the core must be identified with regard for the likely strength distribution within the member. This is important since it may result in a much wider destruction of the member. The core must also be a true representation of the material used in the structure. The length of the core taken must be as short as possible to avoid damage, high cost, variation of the material along the length and so on (18).

The core is then cut by a rotary cutting tool with diamond bits. The drilling equipment must be firmly supported on the member to prevent relative movement which may disturb or break the core. Care should be taken to ensure a uniform pressure. The performance of the test by a skilful operator is also important. The cores must then be labelled, and it is recommended that the core be immediately tested since it may require further coring with different lengths, diameters, etc. A visual inspection of the core for material type, size and characteristics must then be done. The core should be trimmed and capped to provide parallel surfaces normal to the axis of the core.

2.3.1.2 Factors influencing the core compressive strength (18)

The following factors influence the compressive strength of the core:

(i) material characteristics which include:

(a) moisture condition

(b) voids

(c) curing conditions)
(d) mix type) for concrete or mortar
(e) water/cement ratio)

(ii) testing variables such as:
(a) length/diameter ratio
(b) diameter of the core
(c) direction of drilling
(d) method of capping
(e) reinforcements

2.3.1.3 Limitations and applications

The main limitation of coring is the high cost. Inconvenience and damage caused also limit the extent of coring. The results are not very representative of the whole concrete for example used in the member. The size of the core may pose a practical problem.

Cores not only can be used for physical property determination of the material, but are the simplest method of obtaining a sample of the in situ material for different purposes. Visual inspection of the interior of the material may be very valuable for compaction and void detection. They may also be used for location and size detection of the reinforcements in the concrete.

It should be noted that cores are not always obtainable from masonry due to wash out of the mortar (especially lime mortar) by the flushing medium - which usually is water.

2.3.2 Pull Out Test

The basic principle of this test is to pull a bolt, cast in situ or inserted, from a concrete member. The force needed to do so is a measure of the compressive strength of the concrete (19). The major advantage of inserted pull out test to the cast in situ method is that it does not require preplanning. The inserted bolt pull out method, also known as drilled hole method, offers a greater flexibility and is more appropriate for field work.

The chief application of this test and other similar tests,

such as pull off and Windsor probe, is to assess the quality of concrete in a structure. The need for quality assessment of concrete arises when the strength of the structure, after a fire or due to deterioration of the concrete or perhaps due to doubts about the validity of cube results, needs re-evaluating (20). This is mainly a concrete strength assessment technique. This test cannot be used for determining the strength of masonry, due to the composite nature of the masonry. The results obtained from masonry may be an indication of the strength of the mortar and not the masonry itself.

2.3.2.1 Direct pull out method

This method of pull out test falls under the cast in situ ones. It requires a threaded insert which had already, prior to construction, been placed in the concrete. A bolt is then screwed into the insert and is pulled out by a hydraulic jack resting on a circular reaction ring. The test results in "pulling-out" a cone of concrete with the bolt from the point of testing. The force required to pull the bolt and the cone of concrete out is a measure of the compressive strength of the concrete. This compressive strength is expressed as a "pull out" strength which is based on the ratio of pull out force to the failed surface area.

2.3.2.2 BRE internal fracture test

The BRE internal fracture test was first developed at the British Research Establishment for testing high alumina cement concrete. The test, which is a type of pull out test, involves drilling a 6 mm diameter hole and then placing a wedge anchor inside it. By tightening a knot against an 80 mm diameter reaction frame and using a torque meter, the wedge anchor is then pulled out. The failure zone is a conical shape as in the case of the direct pull out test. The maximum torque on the knot gives an indication of the compressive strength of the concrete. The BRE recommends that the coefficient of variation of four internal fracture tests must not exceed 16% and has recommendations for loading technique (21,22).

2.3.2.3 Alternative methods

One of the alternative pull out test methods is the Lok-test.

This test was first developed in Denmark and it is one of the "cast in" methods. The principle difference with cast in situ direct pull out test is the shape of the insert and the loading technique (19). The test is preplanned by placing an anchor plate inside the concrete during the construction. The anchor plate is attached to a circular sleeve and at the time of testing, this sleeve is replaced by a rod which is then anchored against the concrete (23). The force required to pull the anchor plate and a cone of concrete is again a measure of the compressive strength of the concrete.

The other alternative method to the Lok-test is the Capo test. Capo or cut and pull out test is similar to Lok-test but does not require preplanning (23). The basic principle involves fixing an expanding ring into an underreamed groove and pulling the ring and a cone of concrete, at that point, out. These tests also are not suitable for masonry due to composite nature of masonry.

2.3.2.4 Advantages and limitations

The major disadvantage of this test is that it is confined to surface zones. Provided that the member under test is not thin and slender, the test gives a good indication of the compressive strength of the concrete in the surface zone and the near vicinity. There are a number of factors which influence the variability of test results. These factors include the localised nature of the test, the characteristics of the concrete surface, the imprecise load transfer mechanism and the variation in the depth of embedment of the bolt, and also the characteristics of the hole (24). Figs. 2.3 and 2.4 show the variation of test results for two different types of cement and comparison of test results carried out by different investigators.

Fig. 2.5 also shows the variation between concrete strength and torque in BRE test.

The major advantage with this test is that it is fast and relatively inexpensive. The results are immediately known and the damage is confined to surface area.

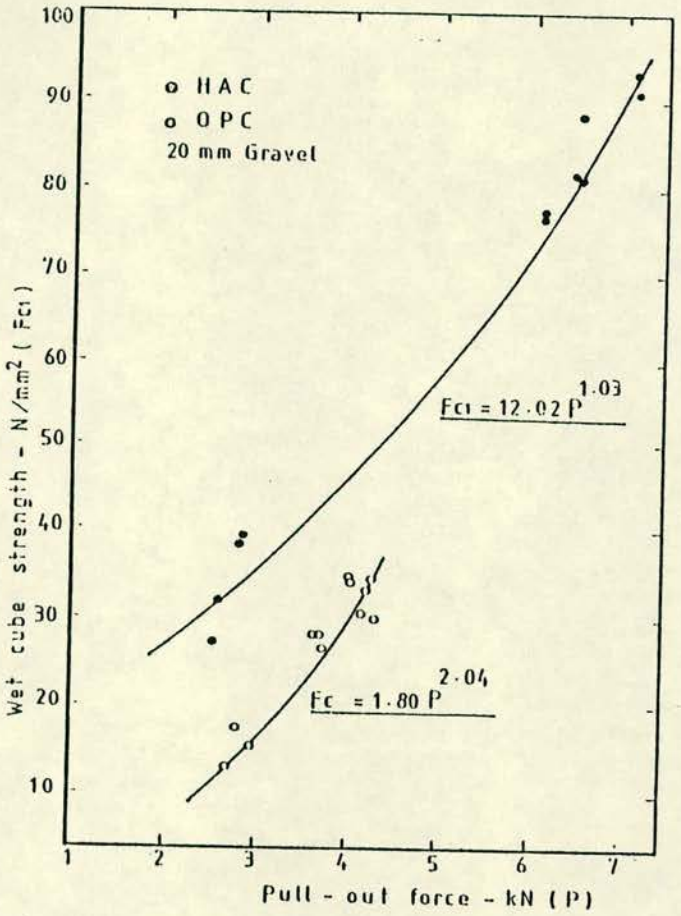

Figure 2.3 Pull-out force - wet cube strength relation (based on ref. 24)

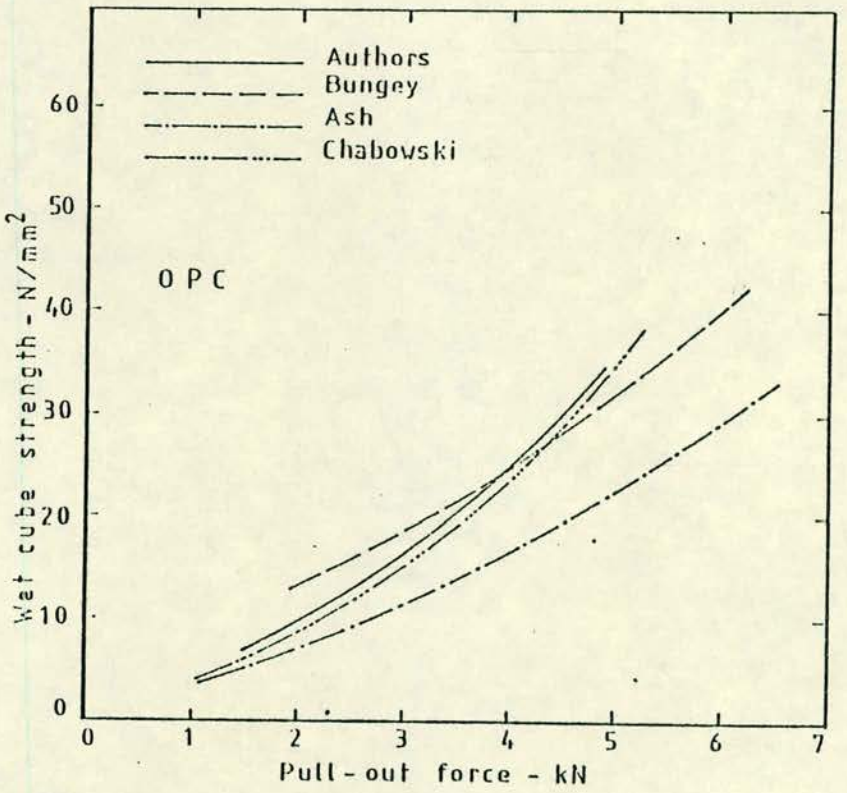

Fig. 2.4 Comparison of pull-out force and wet cube strength relation obtained by various investigations (based on ref. 24)

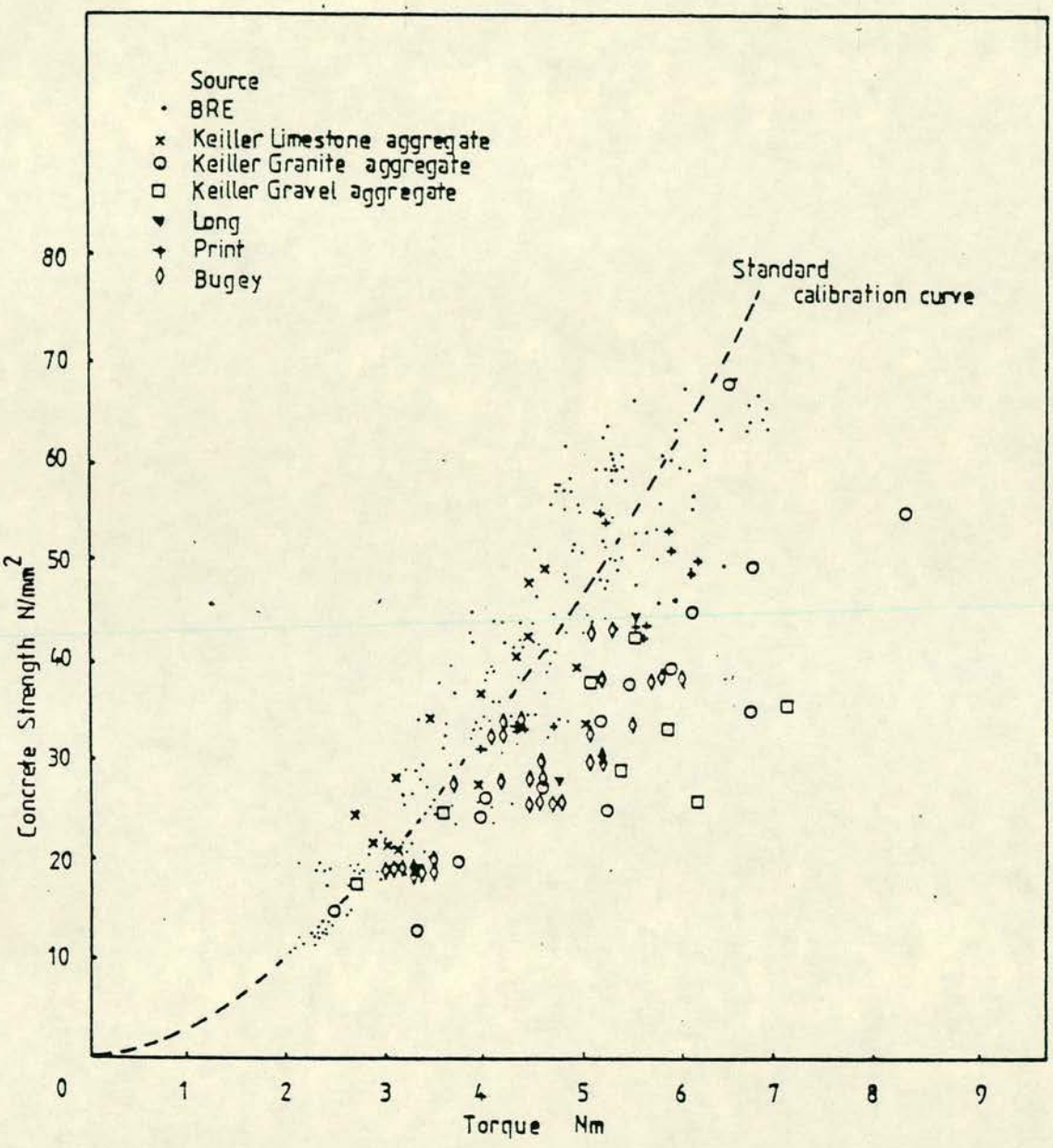

Fig. 2.5 Relationship between concrete strength and torque in BRE test (based on ref. 20)

2.3.3 Pull-Off Test

The pull off method of testing is another partially destructive testing technique used to evaluate the strength of such materials as concrete. This is one of the easiest partially destructive methods to use. The test can be performed almost anywhere without needing any preplanning. The results are a measure of the tensile strength of the material under test. As in the case of pull out tests, this test is not applicable to masonry. It may in some cases be used for determining the bond strength between brick/stone block and mortar.

Using a calibration graph, the results can be used to determine the compressive strength of the material being tested. The testing procedure described briefly below, illustrates the need for such calibration graph.

2.3.3.1 Testing procedure

This test has been developed by Long (23) at Queen's University, Belfast. The procedure basically involves bonding a circular metal probe to the surface of the concrete under investigation. The bonding can be by means of a high strength adhesive such as epoxy resin. A tensile force is then applied to the probe and is increased gradually. When the applied tensile force exceeds that of concrete at that point, the concrete fails. The area of the failure is similar to that of the probe, therefore the tensile strength of the concrete, at that point, can be calculated. Using a calibration graph, the equivalent cube compressive of the concrete can be estimated (25). Fig. 2.6 illustrates the procedure.

2.3.3.2 Factors influencing the pull off test

The success of the pull off test is said to depend on the reliability of the relationship between tensile and compressional strength of concrete. A summary of the factors affecting this relationship is as follows (26):

(i) Age of concrete - generally the tensile/compressive strength ratio decreases with increasing age of concrete.

(ii) Aggregate type and size - an allowance must be made in the calibration graph depending on the type of rock used as coarse aggregate.

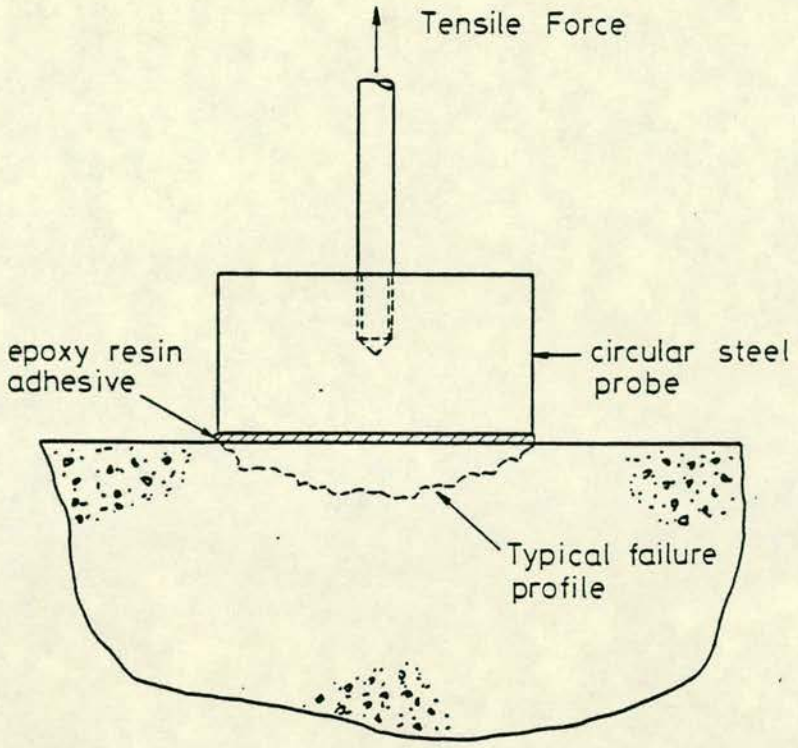

(a) Arrangement for testing uncored specimens

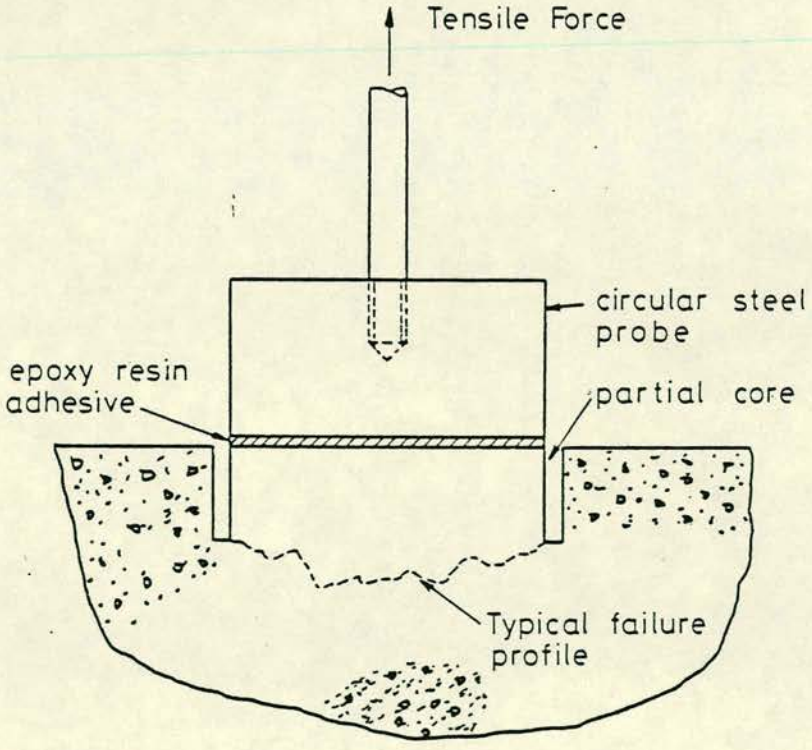

(b) Arrangement for testing partially cored specimens.

Fig. 2.6 Principle of the pull-off test (based on ref. 26)

(iii) Air entrainment: this factor clearly reduces the tensile/compressive ratio value.

(iv) Compressive stress: a concrete under compressive stress usually has a lower tensile strength. However, it is noted that because in situ concrete is not under high stress, this factor is not very influencial.

(v) Curing conditions: air cured concretes, such as in situ concrete, have lower tensile strength. The water cured ones have higher tensile strength.

Fig. 2.7 shows a typical relationship between pull-off tensile and compressional strength of concrete.

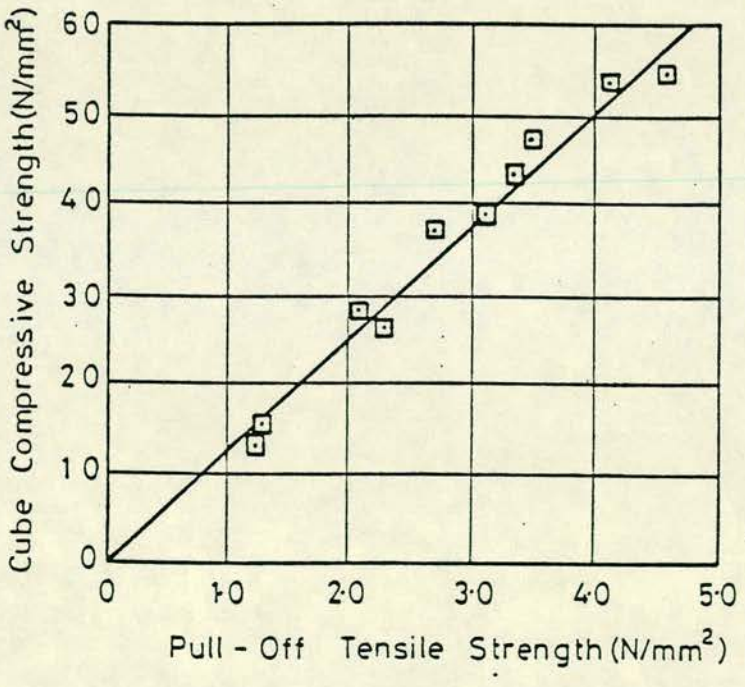

Fig. 2.7 A typical relationship between pull-off tensile strength and cube compressive strength of concrete (based on ref. 25)

2.3.3.3 Advantages and limitations

The pull off test procedure is simple and easy to perform. Unlike some other partially destructive tests such as Lok-test, it does not need preplanning. A visual inspection of the area of the failure can show whether the failure has been in the concrete or not. A surface shell failure is not a representation of concrete tensile strength. The stress at failure is a direct measure of the tensile strength of concrete. Long (23) notes that the test has been found to give reliable and consistent results. He also concludes that the pull off test is particularly suitable for HAC concrete, since the effects of hard shell can be overcome.

The main limitation of this test, as in the case of other mentioned partially destructive tests, is that it is confined to surface zones. The results obtained are not a very true indication of the strength of a thick and large concrete member in a structure. The verticality of the direction of the tensile force to the concrete surface limits the accuracy of the work. This is besides other factors, such as air entrainment, concrete age, etc, mentioned above.

2.3.4 Penetration Resistance Test

A system of penetration resistance test, also known as Windsor probe test (27) has been developed in the USA. The test measures the resistance of concrete or the material under test to penetration by a steel probe. It is a suitable and fast method of testing concrete or similar materials. It is not considered suitable for masonry, as it will only result in stone, brick or mortar resistance measurement.

2.3.4.1 Basic procedure and principle

The Windsor probe test procedure involves firing a blunt conical end bolt or probe into the surface of the concrete under test. The probe length not embedded in concrete and exposed is then measured. This length can be correlated with the compressive strength of the concrete. The results obtained are influenced by the aggregate type. The aggregate hardness affects the probe penetration and therefore must be taken into account. Several tests

must be carried out and then averaged to reduce marked effects of strong aggregates near the surface (28). The readings of the test must not vary much. As the aggregate hardness is a major factor in penetration resistance measurement, it is sometimes necessary to measure its hardness. The aggregate hardness or resistance to abrasion is measured relative to a standard scale of ten minerals, known as Moh's Scale of Hardness (MSH). The softest is chalk with MSH of 1 and the hardest is diamond with a MSH of 10 (29).

2.3.4.2 Strength and Windsor probe penetration

As discussed in the above section, the depth of penetration by the probe into the concrete depends upon the strength of the concrete. The stronger the concrete the less depth of penetration for a given power of firing the probe. Fig. 2.8 shows the variation of probe exposed length with cube strength for two given power levels. Fig. 2.9 shows the same relationship for an OPC.

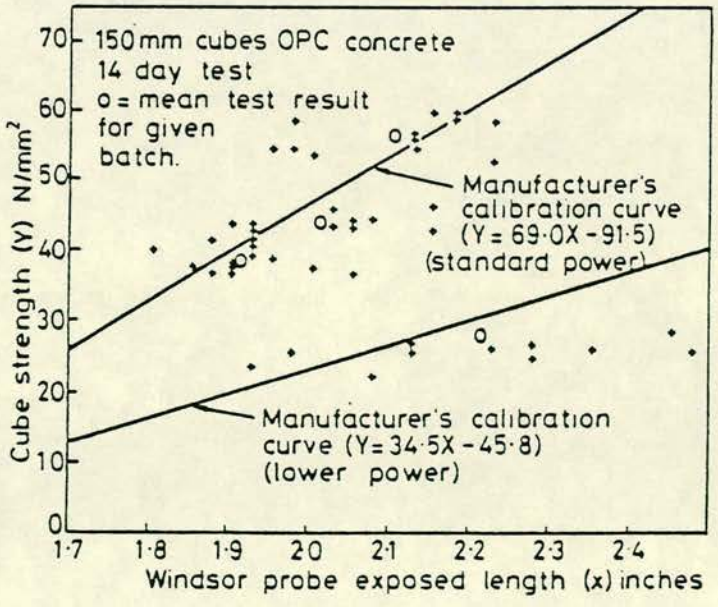

Fig. 2.8 Windsor probe test results (based on ref. 23)

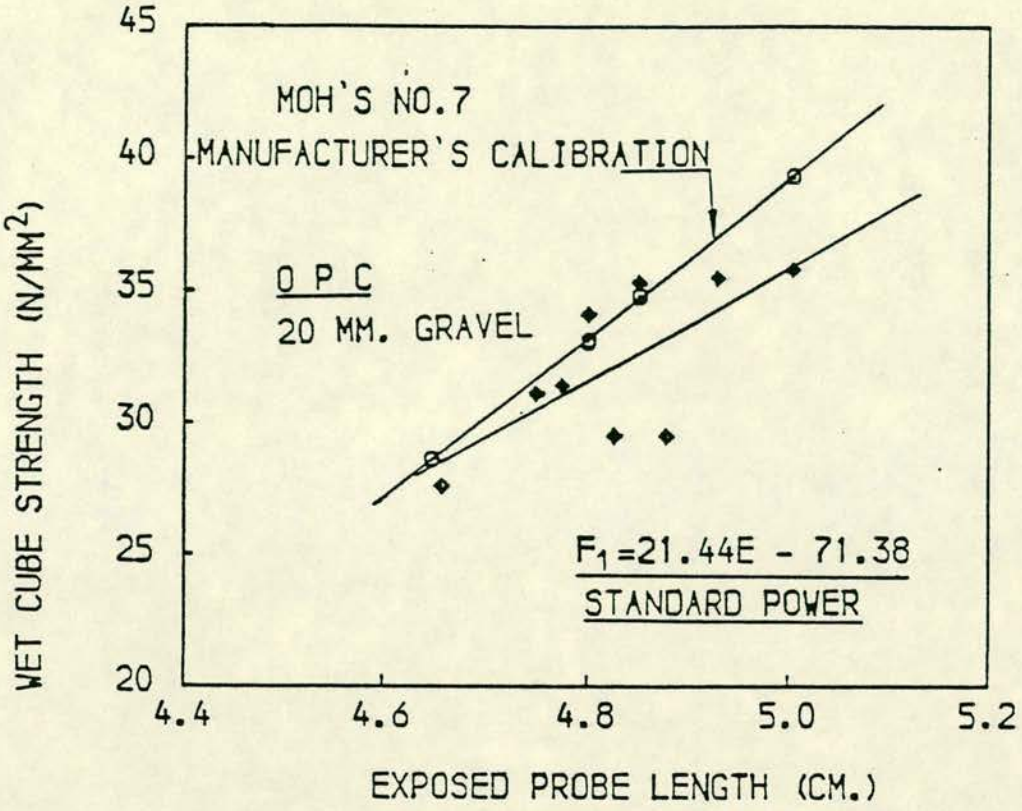

Fig. 2.9 Estimated strength from Windsor probes in relation to wet cube strength (based on ref. 24)

It was also mentioned earlier that the hardness of aggregate has a marked effect on the relationship between the exposed probe length and the strength of concrete. Fig. 2.10 illustrates this relationship for different types of aggregates. It is seen that for a given compressive strength of concrete, the stronger the aggregate, the less the depth of penetration is; basalt and granite being the hardest aggregates and limestone the weakest one.

2.3.4.3 Advantages and limitations

The main limitation of this test is that it cannot be used for thin members of a concrete structure, since there is a risk of splitting the member. Probe spacing also limits the extent of the test since too close probe spacing can cause the collapse of the member. The affected concrete areas will influence the next reading if the test is performed too close to the previous point. The verticality of the probe bolt has some effect on the strength

estimation. The presence of steel reinforcement near the point of testing is also a clear limitation.

This technique is a very quick and speedy concrete compressive strength evaluation method. The technique is not clearly applicable to masonry due to very short penetration length of the probe. The result is a better estimation of concrete strength than that of some other methods such as surface hardness method. The reason is that the probe penetrates the concrete and the result does not represent the surface strength. The results of this test are usually comparable with those of coring (30).

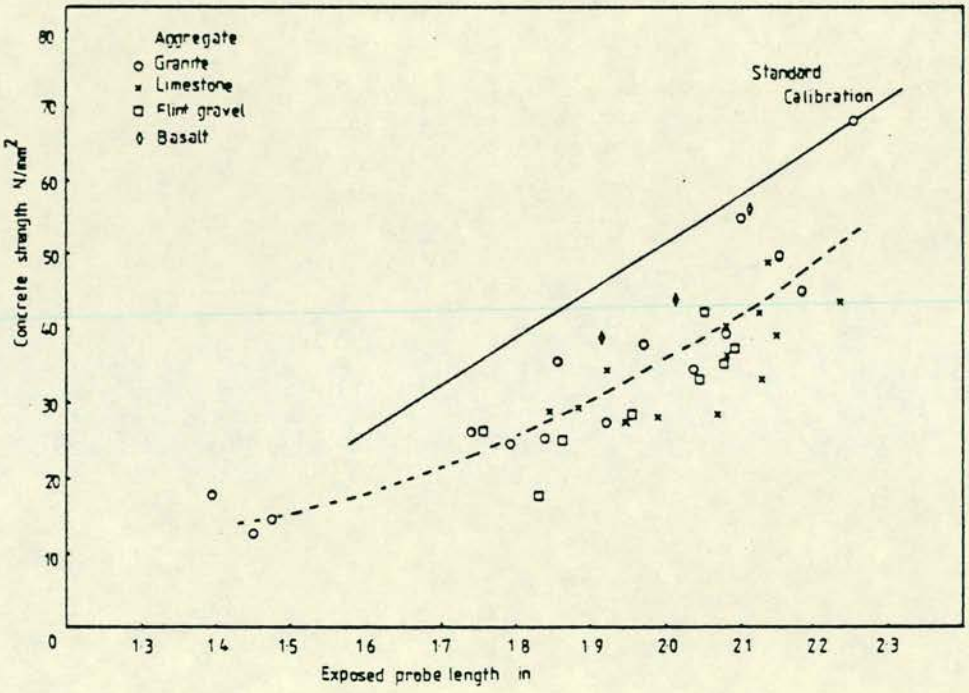

Fig. 2.10 Relationship between concrete strength and exposed probe in length in Windsor probe test (based on ref. 20)

2.3.5 Break-Off Method

This method was first developed in Norway and it was used for assessing the strength of concrete (31). The test is not suitable for masonry strength evaluation due to short length of the core and the presence of brick/stone block and mortar joints.

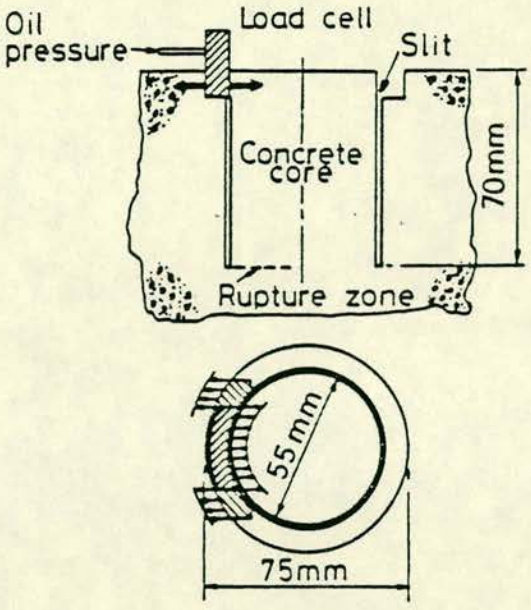

Fig. 2.11 Break-off test (based on ref. 23)

The procedures involves cutting a circular hole into the concrete. The core obtained in this way is broken by a transverse force which is applied at the top of the core. The results are a measure of flexural strength of the concrete (see Fig. 2.11).

This method of testing is quick and uncomplicated. It leaves a considerable size damage zone in the concrete.

2.3.6 Probe Hole Method

This method, which again falls under the partially destructive testing methods, is a quick and unsophisticated method of testing. The procedure consists of penetrating the areas of investigation with a small masonry bit and probing the hole with a stiff wire (32). It can be used to determine the thickness of masonry units and study the uniformity of the inner cell grout. The main disadvantage is that it is only useful for surface zones and a complete depth study is not possible. It also damages the surface of masonry which may require repair. The advantages of this method are speed, simplicity and inexpensive equipment.

2.3.7 A Brief Comparison of Partially Destructive Tests

It was seen in the previous sections that tests like the Lok-test are only suitable for preplanned investigations. This is a serious limitation on the part of these tests. The BRE internal fracture test and the Windsor probe overcome this problem. These two methods of testing plus the pull off test are the main partially destructive test methods. The table below shows that the pull off test usually attains a higher accuracy and consistency:

	Pull-Off Test	Internal Fracture Test	Windsor Probe
Range of predicted strengths as fraction of actual strength	0.85 to 1.25	0.65 to 2.77	0.75 to 1.44
Coefficient of variation	7.9%	30.4%	12.0%

Table 2.1 Comparison of test results by three methods shown (based on ref. 26)

It is also noted that coring technique can be used to study the interior such as aggregate and cement constituents of concrete. Whilst coring, pull off, pull out and Windsor probe are used for compressive strength determination, the break off method is used for flexural strength evaluation. Coring can be used for testing composite materials whereas the latter three are suitable only for concrete. The probe hole method can only be used for studying the interior of concrete or masonry. It is not a sophisticated method as break off or BRE internal fracture test which are used to obtain more detailed information about the strength of the structure. It is a simple integrity testing method.

Therefore in brief, coring, pull out, pull off and Windsor probe tests are used for compressive strength determination of concrete. Coring is also suitable for compressive strength determination of concrete and internal observation of concrete and

masonry. Depending upon the circumstances and test requirements one of these partially destructive tests can be carried out. It must be noted that these tests, except coring, mainly result in compressive strength prediction of concrete surface zones. They are not suitable for evaluating a thick and large concrete member.

2.4 NON-DESTRUCTIVE TESTS

There are many non-destructive testing methods which are applicable to a very diverse field of professions. The following testing methods are some main known NDT systems applied in the Civil Engineering industry. Each test has its own limitations and applications and depending on the testing conditions and the purpose of the test a NDT method is utilised.

2.4.1 Ultrasonics

2.4.1.1 Basic principle and procedure

Ultrasonic testing methods are used in several ways for several purposes. The major use of this is for thickness and transmission velocity measurements. The test basically consists of generating a compressional wave with a very high oscillating frequency into the material under test. The frequency range is 20 kHz and above which is inaudible. The measurement of travel time of the wave is used to calculate the transmission velocity of the medium under test or its thickness.

There are several methods of ultrasonic testing. One method is to measure directly the distance of a straight line between two points opposite each other. Another way is to calculate the transmission velocity or thickness of the medium from the reflection or refraction of the transmitted wave (33).

There are a number of commercially produced instruments. The most popular of these in Britain is "Portable Ultrasonic Non-Destructive Digital Indicating Tester" or PUNDIT (34).

It must be noted that the strength and other properties of the member under test are determined by the quality of the component materials. In the case of concrete, for example, these properties are determined by the quality of the cement used. The concrete paste usually makes up to 20% to 30% of the total path length. However, it is the aggregate type of arrangement which has the main effect and infuence upon the pulse velocity measurement (35).

Although the ultrasonic testing method is a very reliable and quick method of quality assessment, it cannot be used for big lengths of concrete or masonry. The reason is that the multiple reflections from mortar joints and low energy input will result in high attenuation and will not then be picked up by the receiver.

2.4.1.2 Factors influencing pulse velocity reading

There are quite a number of factors which influence the ultrasonic pulse velocity reading. To give an indication of the extent of the variation of such factors, some of them are listed below for concrete. B.S. 4408 lists these factors which affect the relationship between pulse velocity and strength. The factors include (36):

(a) concrete type
(b) cement content
(c) mix type
(d) aggregate type and size
(e) curing conditions
(f) age of concrete
(g) moisture conditions

The presence of reinforcement in the concrete under test also affects the ultrasonic pulse velocity reading. This is particularly significant if the reinforcement runs parallel or along the direction of the wave. B.S. 4408 includes charts for reinforcement correction factors.

2.4.1.3 Methods of measurement

There are three types of reading the transmission time value of the concrete or material under test. The first type is the direct method shown in Fig. 2.12 (a) and is most reliable for transmission time measurement. The second type is the semi-direct method. In this case if the path length or the angle between transducers are too large, there will be no signal or very low signal will exist. In this situation the sensitivity and hence the reliability will be reduced. The third type is the indirect method, shown in Fig. 2.12 (c).

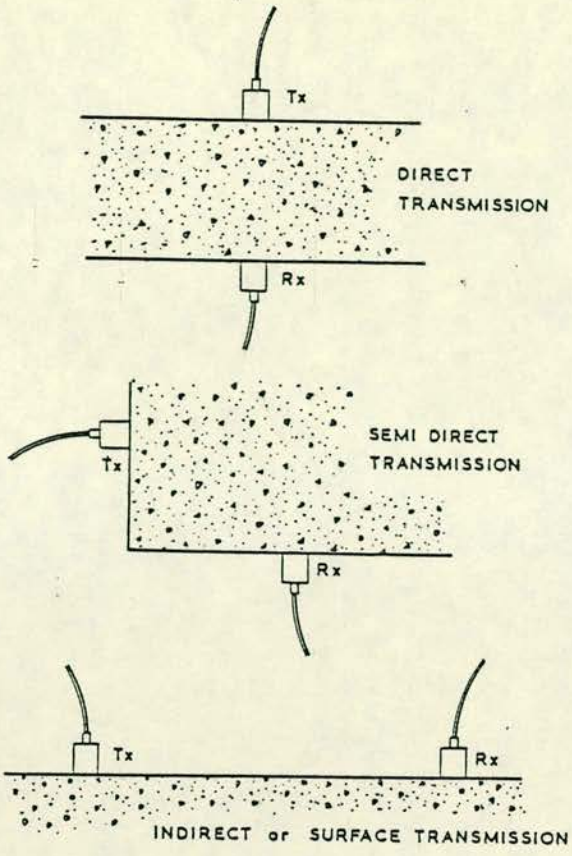

Fig. 2.12 Types of reading (based on ref. 34)

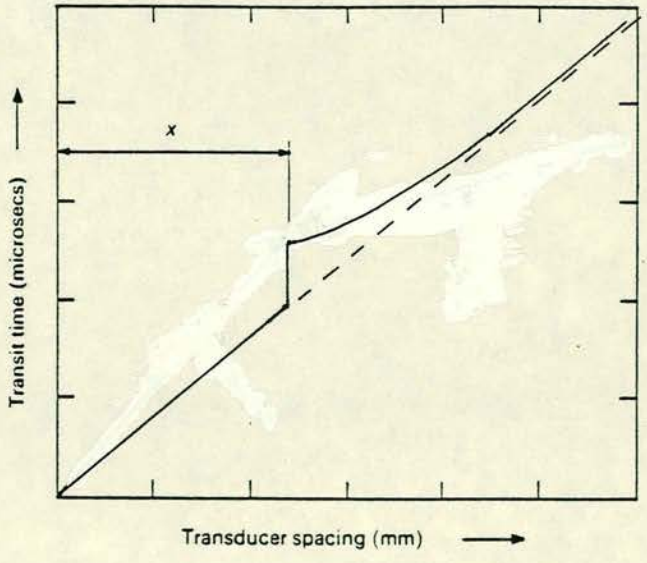

2.13 Fault detection by indirect method

The indirect method can be used for fault detection. By keeping one transducer constant and moving the other one successively, a number of readings can be taken. A graph of transmission time against transducer spacing will be a straight line. If a crack or void along the path of the transducer exists, there will be a kick in the line at that point (see Fig. 2.13).

2.4.1.4 Applications and limitations

The ultrasonic method is mainly used for pulse velocity measurement. This velocity can be used to establish: a number of applications. They include (38):

(i) investigating concrete uniformity
(ii) void or crack detection
(iii) concrete quality check
(iv) elastic modulus determination

The major limitation of the work is that it cannot be used for heterogenous and composite materials such as masonry. The high frequency nature of the pulse oscillation results in quick and fast dissipation of the energy input. It is also not suitable for large size concrete velocity measurement due to low energy input.

The main advantages are clearly speed and simplicity of reading and evaluation of the results.

2.4.2 Acoustic Emission

Acoustic emission monitoring is the detection, processing and analysis of the low level ultrasonic signals generated by materials deformation or damage. It is used for materials studies and structural inspection.

The basic principles behind acoustic emission is the rapid release of energy stored within the specimen. Some of this energy is converted into elastic waves and propagates through the structure under monitoring (39). The source of emission can be crack propagation or corrosion (40). Other sources of emission which cause the generation of elastic waves are vibration of built in structures, movement of loose parts and leakage (41).

Fig. 2.14 shows a typical acoustic emission pattern of a damaged heat exchanger. The time increase of the acoustic emission energy and the burst signals point to the vibration in the system. The jump in the energy release and the large burst signals are due to knocking noise of heat exchanges.

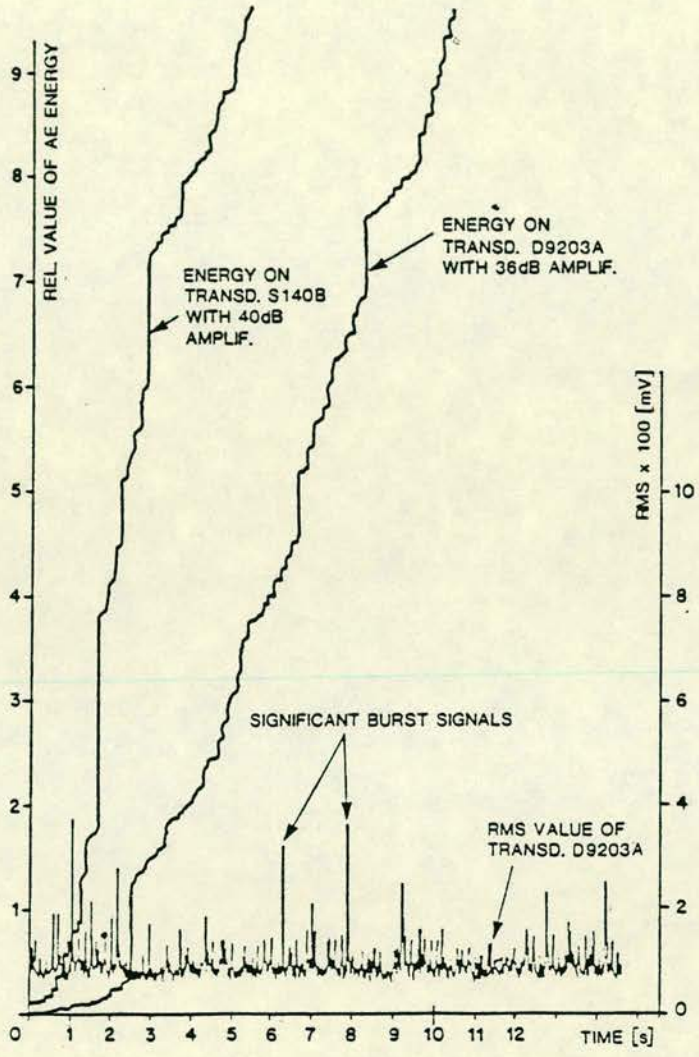

Fig. 2.14 Large time increase of the A.E. energy with burst signals of the damaged heat exchanger (based on ref. 41)

2.4.2.1 Applications and limitations

Acoustic emission technique can be used for collecting information on crack developing and monitoring the integrity status of pressure vessels. Other applications include (41,42):

(i) determination and detection of the onset of cracking in the structure under stress.

(ii) investigation of fracture mechanisms and material behaviour.

(iii) continuous surveillance of nuclear reactors for detection and location of cracks.

The main limitation of this technique is the lack of high degree resolution for integrity surveillance. Hence it is somewhat difficult to determine the severity of a crack developed in the structure.

2.4.3 Ultrasonic Spectroscopy

The basic principle of this method of testing structures is the analysis of frequency components of ultrasonic signals (43). This technique, which can be used in sonic testing as well, is associated with ultrasonic or sonic testing methods, the latter being the purpose of this thesis. Ultrasonic and sonic spectroscopy deals only with frequency analysis of the technique. Its main functions and applications are discussed in detail in this thesis. The chief application of this technique of testing in non-destructive methods is thickness measurement and the main disadvantage is the bulk and cost of the equipment. The application, however, has been confined to the inspection of metal components and welds.

2.4.4 Radioactive Methods

There are several radioactive methods. The more common techniques used in Civil Engineering, especially for testing concrete structures, are x-ray radiography and Gamma radiography (44,45,46). The x-ray radiography is mainly used for study of concrete internal composition such as aggregate spacing and arrangements. It is mainly a laboratory testing technique.

Gamma radiography is also used to produce an image of the inside of a concrete member. Its main application is reinforcement and void detection (47). This technique plus the x-ray one, due to their penetrating nature, are also sometimes called penetration radiation. The basic principle of these techniques is that the radiation gets modified by passing through the material and by defects in it.

2.4.5. Nuclear Methods

The most common technique is called neutron activation analysis. By bombarding the concrete surface with neutron, the elements composing the concrete become radioactive. The radiation from the concrete is then compared with a standard specimen. The result is mainly used for cement content determination.

The main limitation of this work is that it is expensive and requires sophisticated equipment.

2.4.6 Electrical Methods

Here again there exist several electrical methods employed in Civil Engineering work and they are mainly confined to material such as concrete and mortar. Their main applications are moisture and cement content determination and reinforcement corrosion. The reinforcement electric potential measurements are used to obtain an indication of the reinforcement corrosion. Thickness measurements can also be assessed by utilising the resistivity difference between two adjacent layers. The main methods are:

(a) Electrical resistivity technique: this method can be used to determine thickness and quality of concrete. It can also be used to determine the properties of the concrete such as moisture content, strength and so on (48). The principle of the test is based on the electrical resistivity of the material. The presence of a different material adjacent to the material under test produces a potential difference between the two materials (44). The change in the slope of the graph of resistivity versus depth gives an indication of the thickness of the material under test. Changing material properties changes its resistivity and by standardising the resistivity of the material, the change can be detected.

(b) Eddy current technique: this method uses the electric conductivity of the material to determine its physical properties. Other applications of this method of testing are detection of defects, irregularities in the structure of the member under test, cracks or void (44,49). The principle of operation is based upon the fact that when a coil carrying an alternating current is brought near to a conducting material,

eddy currents are induced in the material. The magnitude of the induced eddy current depends on the magnitude and frequency of the alternating current, electrical conductivity, magnetic permeability and shape of specimen. This magnitude of the induced eddy current can be used to determine the mentioned applications (44). This method is mainly confined to homogeneous materials and is not of direct application for many Civil Engineering situations.

2.4.7 Infra-red Thermography Method

The use of this technique is based upon taking infra-red photographs during the cooling of a heated structure. It is a useful method of detecting delamination of bridge decks. When the heated structure is being cooled, there is a difference of temperature between the surface of the structure and the surface of the hidden laminated concrete. The surface temperatures are then compared by infra-red measurements. For further details and theory see (50).

2.4.8 Photo-elastic Method

The photo-elastic method involves bonding photo-elastic coatings to the surface of the structure which will develop the same strains as the structure when subjected to loading. It is related to load testing and monitoring. Its main use is to determine patterns of behaviour at stress concentrations or the areas under an increasing load (51). There are sheets of 1 to 3 mm thickness commercially available for flat surfaces, and contoured sheets can also be produced for curved surfaces. A polariscope can be used to monitor the strain patterns. The disadvantage of this method is that it is more of a laboratory method of testing rather than a field one. It can, however, be used in field tests, but its use will be limited.

2.4.9 Hammer Test Method

The hammer test is one of the easiest and quickest of non-destructive testing methods. The procedure is used to investigate the integrity of the individual masonry units and the bond between the mortar and the masonry units (32).

The procedure involves tapping lightly the masonry unit with a hammer and listening to the resultant sound. The solid and well bonded masonry construction will have a dull thud. An unbonded and hollow masonry sounds hollow.

The limitation of this test arises from its simplicity and unsophisticated procedure, which discourages engineers to take it seriously. The other main disadvantage of this method is that it is confined to the surface zone of the masonry. It also requires an experienced operator with a good sense of hearing. The advantages of it are clearly its simplicity, speed and low cost.

2.4.10 Pachometer Test Method

The pachometer test is based on the presence of steel which will cause variation in the magnetic field of the pachometer. The pachometer itself is a magnetic detector. The variation can be correlated to the depth or the size of the reinforcement. The procedure is simple. It involves scanning the surface of the masonry with the probe. The maximum reading indicates the presence of the reinforcement under the probe. The dial reading is then used to estimate the size or the depth of the reinforcement (32).

The main limitation of this method of testing is that, when there is a heavy concentration of reinforcements, it is difficult to determine the size and depth of the reinforcement. However, it is a low cost and quick method of locating and determining the size and depth of the reinforcement.

2.4.11 Impact Method

This is a method which has been successfully used in rock mechanics to study compressive and flexural strength of rocks (52). Its use is based upon the principle that masonry is a composite structure made of bricks/stones and mortar. The properties of masonry are therefore dependent on the properties of the individual components and the quality of the bond between them.

The test procedure consists of dropping a steel weight through a cylinder from a certain height onto the brick or stone samples.

Comparing the impact response and effects of the drop, i.e. the "impact strength index" with a standard chart will result in estimating the strength and chipping properties of the masonry unit. A further detailed analysis is given in (52). It concludes that strength and durability properties of bricks (and stone units) can be inferred from the results of this test. The main advantages of the test are speed, low cost, ease and freedom in choosing the original size distribution of specimens. However, it is thought that it does not give an in-depth strength of the masonry and therefore is confined to surface area zones.

2.5 SUMMARY OF TESTING METHODS

2.5.1 Concrete

Method of testing	Advantages; Limitations, Applications
1. Surface hardness	Fast, cheap; confined to surfaces; hardness and uniformity check, also gives an indication of strength
2. Penetration resistance) 3. Pull out) 4. Pull off) 5. Break off)	Fast, inexpensive; confined to surfaces; gives an indication of strength
6. Coring	Reliable results; high cost; determination of physical properties and strength
7. Load testing	A very good proof of structural performance; expensive and time consuming
8. Acoustic emission) 9. Ultrasonic spectroscopy) 10. Radioactive methods) 11. Nuclear methods) 12. Electrical methods) 13. Infra-red thermography) 14. Photo-elastic)	Non-destructive, fast; needs sophisticated equipment and skilled operator; used for integrity testing, property determination and in some cases fault and lamination detection

Table 2.2 Summary of methods of testing concrete structures

2.5.2 Masonry

Method of testing	Advantages; Limitations; Applications
1. Coring	As above
2. Load testing	As above
3. Prism test	Good indication of strength; marked effects due to increasing courses; workmanship, capping, etc; strength determination
4. Hammer test) 5. Impact test)	Fast, cheap; surfaces only; integrity testing and indication of strength
6. Probe hole	Fast, inexpensive; surface zones only, depth determination
7. Pachometer	Fast, inexpensive; used only for light concentration of reinforcements; detecting reinforcements

Table 2.3 Summary of methods of testing masonry structures

2.6 A BRIEF REVIEW OF THE TESTING METHODS

In the previous sections a brief outline of some of the known and commonly used testing techniques was made. It was noted that the application of the methods reviewed varied from one test to another. For example, while load testing is used for measuring load bearing capacity of a structure, acoustic emission is mainly used for crack onset detection. Also the extent of the application of each test may differ from another one. To illustrate this, consider ultrasonic and sonic testing methods. Ultrasonic method employs a very high frequency oscillation and therefore the depth of penetration is limited. The energy input in this test is also very small and this adds to length limitation. At the same time sonic testing method does not have the high frequency and low energy input problems. Therefore a larger scale structure can be tested.

The cost, speed and operator's skill for running a test are other major factors infuencing the choice of the testing method.

Opting for a low cost and speedy testing technique can lead to unreliable and misleading results. Also the results of a very high cost and time consuming testing technique can be equally useless. The choice of the testing method therefore depends not only on the reliability of the results but also on the requirements of the test.

The damage to the structure done by the performance of the test is of major importance. For example, the results obtained from coring of a thin and slender column in a building may not be of any use because of the collapse of the structure! A partial, though not fatal, damage to a structure may not also prove acceptable.

The sonic non-destructive testing technique, which is the subject of the investigation in this thesis tries to overcome the above limitations. Some testing techniques are only suitable for one type of material. For example, pull out or pull off tests are only applicable to concrete and similar structures. Whereas sonic NDT can not only be applied to concrete structures but can also be used for masonry structures.

Although the test is at an early stage of development, it can be used for compressive strength determination and fault detection. Although the compressive strength results of a sonic NDT method are not directly comparable with those of prism or load testing methods, they compare favourably with those of pull out, pull off or coring techniques.

The speed with which the test is carried out is a major advantage. The comparatively low cost of performing the test is another chief advantage of sonic NDT method. The cost and speed of some conventional methods of testing such as coring or prism test methods do not compare favourably with sonic NDT cost and speed. Exactly for this reason the test can cover a much wider area than other methods. For example, coring a structure for fault detection will be confined to only a few points. On the other hand, sonic NDT method can cover a much wider area.

It is also important to note that sonic NDT tests the whole structure between two points. Other methods such as Windsor probe or pull off methods test only one point of a structure. Other techniques such as ultrasonic methods test a small proportion or a small part of a structure.

There is no damage to the structure when using sonic NDT technique, compared to the same type of results obtained from some other methods. This is an attractive advantage of sonic NDT method compared to other destructive or partially destructive techniques.

In brief, it can be said that each method of testing has its own advantages and limitations. The cost, speed, operator's skill, reliability of the results and the damage done to the structure, all play an important part. The sonic NDT method tries to overcome these limitations. Although the test does not yet compare directly with load or prism test methods, it can easily become a major rival to other methods. It has very attractive advantages which are being explored and investigated for testing masonry in this thesis.

CHAPTER THREE

OBJECTIVES OF NON-DESTRUCTIVE TESTING

OBJECTIVES OF NON-DESTRUCTIVE TESTING

Non-destructive testing methods have the advantage of being able to be used for in situ testing. For this reason a great deal of time, effort and expense can be wasted on in situ testing unless the aims of the investigation and the test are clearly established at the outset. The main objectives of non-destructive testing employed in Civil Engineering are:

(a) Transmission integrity as an indication of strength and quality of the material or the structure.

(b) Fault detection such as locating voids, cracks and cavities in a structure which may undermine the strength and performance of the structure.

(c) Thickness measurement where, for example, use of other methods are not feasible or practical. The basic principles of this test are similar to fault detection ones.

The transmission integrity as an indication of the strength of the material can be used to examine the strength of a full scale structure. It is widely used for control and compliance testing in concrete technology and practice. The most common method of non-destructive testing which meets the main aims outlind above, is sonic testing. In this method a study of the propagated wave in the material is undertaken.

In the case of transmission integrity the propagated compression wave through the material is being studied. Whereas in the case of fault detection and thickness measurement, the reflected wave is usually studied. The principle of the test is similar to earthquake seismology or seismic prospecting methods. The difference is that the state-of-the-art in seismic prospecting is very advanced, whereas it is difficult to examine shallow depths. Hence its use in Civil Engineering has been limited and it is at an early stage of development.

It must also be noted that the chief advantages of non-destructive testing in meeting the above objectives are speed and cost. Other methods such as load testing or core sampling can

prove expensive, time consuming and limited to testing of only a few members.

In the following chapters a full study of viability of sonic non-destructive testing for transmission integrity assessment, fault detection and thickness measurement in masonry, is made.

CHAPTER FOUR

CHARACTERISTICS OF MORTAR AND STONE COMPONENTS OF MASONRY

4.1 INTRODUCTION

A good quality masonry normally consists of good bricks or stone blocks and also a mortar that suits well both bricklaying and the load carrying capacity of the masonry. Different types of masonry require different materials, from low strength mortar and stone blocks in stone masonry walls to high strength brick and mortar in structural load bearing brickwork. Although the strength of masonry is affected by factors such as workmanship, mortar age, height of blocks and so on (53), it is still the stone block or brick, and to a lesser degree the mortar strength, that determines the overall strength of the masonry (see Fig. 4.1).

To investigate the quality of masonry, tests must be carried out not only on the masonry as a whole, but also on its individual components. Tests on such two components, mortar and stone, is the aim of this work. Cubes of different types of stone used in masonry construction and also cubes of varying mixes and constituents of mortar were tested ultrasonically. The results obtained were used to determine a relationship between pulse velocity and the strength of the materials tested. It was then established that the higher the pulse velocity, the higher the cube strength is.

4.2 EQUIPMENT

The testing equipment consisted of:

(a) Portable Ultrasonic Non-Destructive Digital Indicating Tester, PUNDIT, which has a frequency of 50 kHz (34).

(b) Two 54 kHz, 50 mm diameter flat surface piezoelectric transducers.

(c) 75 ohm screened coaxial cables.

(d) Two water curing tanks, the temperatures of which were monitored daily.

(e) 5 to 100 degree Celcius range thermometer.

4.3 SPECIFICATIONS

4.3.1 Mortar

The sands used in the mortar cube construction were all found to have gradings lying within the grading limits specified in B.S. 1200 (55). These sands were of three types: the coarsest having a

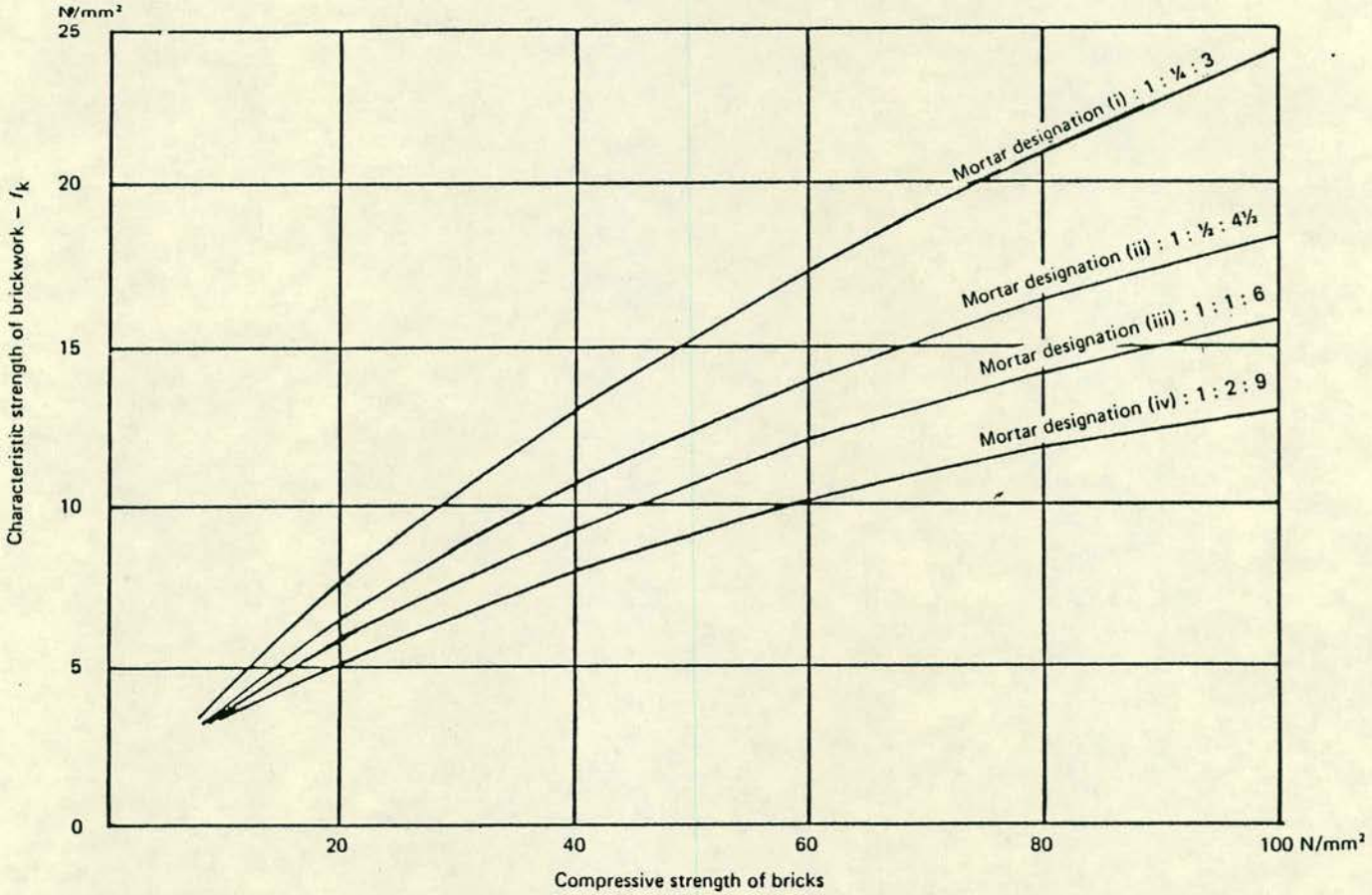

Fig. 4.1 Characteristic strength of brickwork (based on ref. 54)

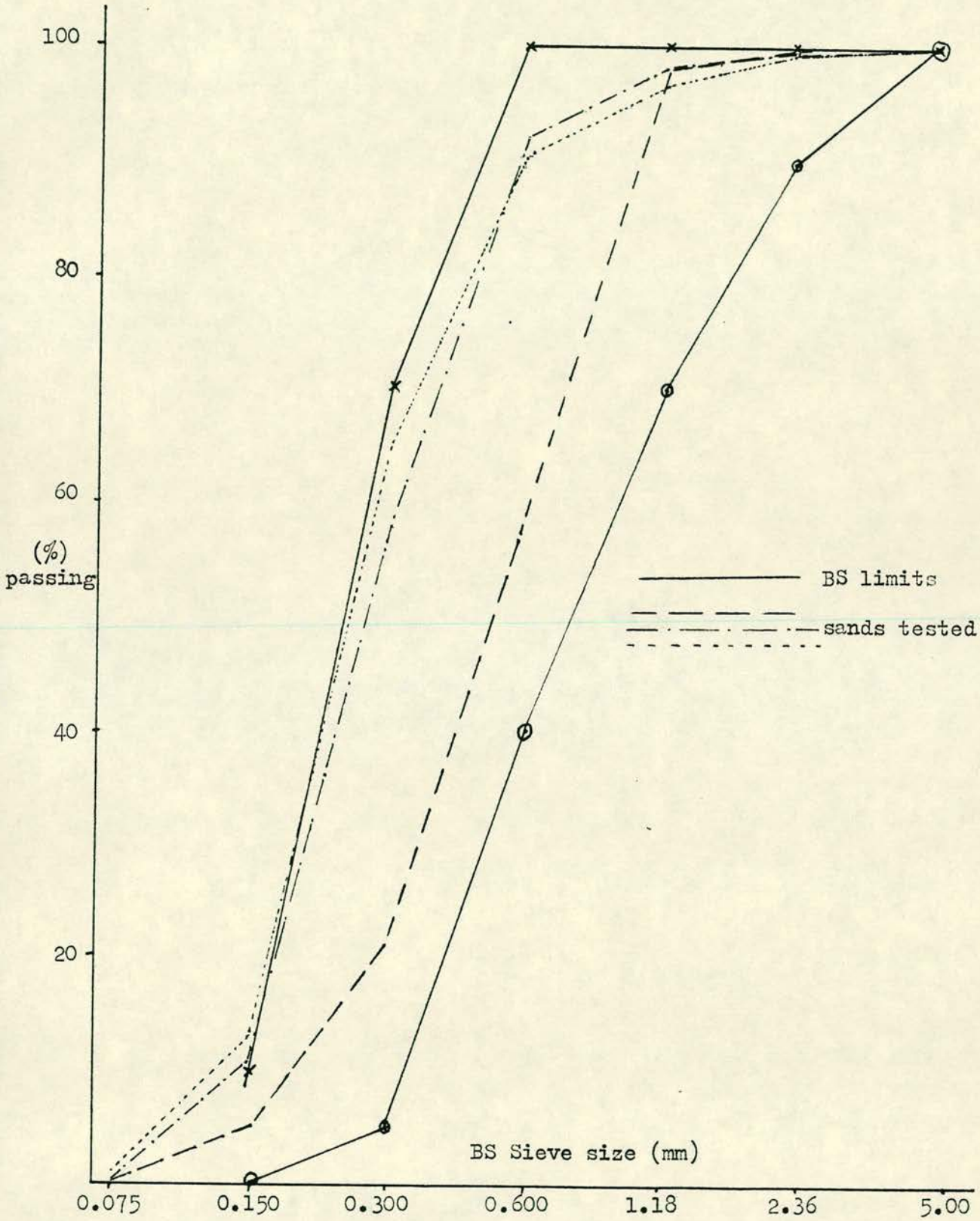

Fig. 4.2 Proposed grading limits for mortar sand and the gradings for the sands tested (based on ref. 55)

grading similar to that of Table 2 in B.S. 1200. The finest one was found to have a grading lying very close to the lower limit of the grading curve, while the third sand, which was a 1:1 mixture of the other two, had a grading somewhere between them (Fig. 4.2).

Each of these sands were used in at least four batches, each having a different mix proportion (57). The mix proportions were 1:1/4:3, 1:½:4½, 1:1:6 and 1:2:9, given by volume of cement:lime:sand. The cement used was an ordinary Portland cement and the sand was oven dried. The mixing of mortar was in accordance with the recommendations given in C.P. 121, Part 1 (58) and B.S. 5390 (59).

In addition to cubes above, two beams of dimensions 101 mm x 101 mm x 508 mm were made with the coarse sand, using a mix proportion of 1:1/4:4. The beams were used to examine the effects of path length and temperature on pulse velocity in mortar. Also one of the beams was cured in a water bath of lower temperature.

The cubes obtained were also placed in a curing tank, the temperature of which was monitored daily to ensure constant temperature. The cubes and the beams were then tested each day of their curing period using the PUNDIT.

4.3.2 Stone

The cubes tested were of various sandstones of different compressive strengths. They were cut as close as possible into 100 mm cubes with a diamond saw. It was noted that perfect cubes could not be obtained with the available cutting equipment. This would have influenced the results, especially those of the crushing compressive strength. However, it was considered that this experimental error was not large since the cubes were not significantly out of shape. The inspection of the cubes showed that they were ±2 mm out of the desired shape on each side.

4.4 EXPERIMENTAL PROCEDURE

The test procedure involved the two piezoelectric transducers being connected to the PUNDIT and to each side of the cubes; one

transducer being used as transmitter of the ultrasonic pulse and the other as a receiver. The direct transit time between the two transducers, through the cube, was displayed on the four digit crystal display screen of the PUNDIT. A very thin layer of a water pump grease was used to give a good acoustic coupling between the transducers and the cube. After applying the grease, the transducers were pressed against the cubes in opposite directions and moved several times in clockwise and anticlockwise semi-circle directions to get as thin a grease layer as possible. The two reasons for this procedure were to obtain a high resolution signal on PUNDIT and to reduce the error due to length. After each test the PUNDIT was calibrated using the Reference bar to check the instrument zero (Plate 4.1 - (cube testing)).

Noting the transmission time obtained, the cube was then placed in the cube crushing machine and the cube compressive strength was found. It was ensured that the cubes were tested in the same direction as the pulse velocity test was carried out. A relationship between the cube compressive strength and pulse velocity was then obtained.

The mortar cubes were tested during their curing period of 28 days to obtain a relationship between age and pulse velocity of mortar. The mortar beams were also tested during this curing period to observe the effect of temperature difference. One of the beams was cured in a curing tank at a temperature of 15° ±2° Celcius and the other at a temperature of 26° ±2° Celcius.

At the end of the 28 day period the beam cured at 26° C temperature was cut into different lengths from 132 mm down to 23 mm in order to monitor the effect of length on transmission or pulse velocity. The ultrasonic testing of the beams was exactly the same as the testing for the cubes.

4.5 RESULTS AND ANALYSIS

4.5.1 Mortar

The pulse velocity v (km/s) through the mortar was found using the following equation:

Plate 4.1 Mortar cube testing, pulse velocity measurement

$$v = l/t \qquad (4.1)$$

where l = the distance between the transducers or the specimen length in kilometers and

t = the time taken by the pulse to travel that distance, in seconds

Using this expression a relationship between pulse velocity of mortar and age was established (Appendix 2). Generally it was found that in the first few days as the mortar hardened, the pulse velocity increased rapidly. However, during the subsequent ageing, the rate of increase of pulse velocity decreased and the curves flattened out (Fig. 4.3).

Using pulse velocity measured just prior to crushing and the measured compressive strength, another relationship was obtained. The relationship between cube compressive strength and pulse velocity is given in Fig. 4.4 This indicates an increase in pulse velocity with an increase in compressive strength for a particular mix (Table 4.1).

Sample No	Mix Proportion	Sand Grading	Water Content (cm^3)	Compressive Strength (mN/m^2)	Pulse Velocity (Km/s)	Density (Kg/m^3)
1	1:1/4:3	Coarse	1184	17.581	3.599	2159
2	"	Medium	1330	17.451	3.451	2245
3	"	Fine	1250	17.370	3.423	2150
4	1:½:4.5	Coarse	1120	9.048	3.293	2156
5	"	Coarse	1306	6.594	3.135	2132
6	"	Medium	1410	6.844	2.962	2187
7	"	Fine	1420	7.331	2.965	2149
8	1:1:6	Coarse	1120	4.084	2.875	2117
9	"	Coarse	1330	3.722	2.720	2137
10	"	Medium	1390	3.670	2.711	2171
11	"	Fine	1420	3.514	2.633	2136
12	1:2:9	Coarse	1119	1.902	2.280	2131
13	"	Coarse	1166	1.563	2.255	2139
14	"	Medium	1420	1.555	2.264	2108
15	"	Fine	1299	1.462	2.193	2118

Table 4.1 Pulse velocity and cube compressive strength

N.B. The values obtained for each sample are the averages obtained from three mortar cubes.

Compressive strength was found by dividing the failure load by the normal cross-sectional area of the cube which was 10^4 mm^2.

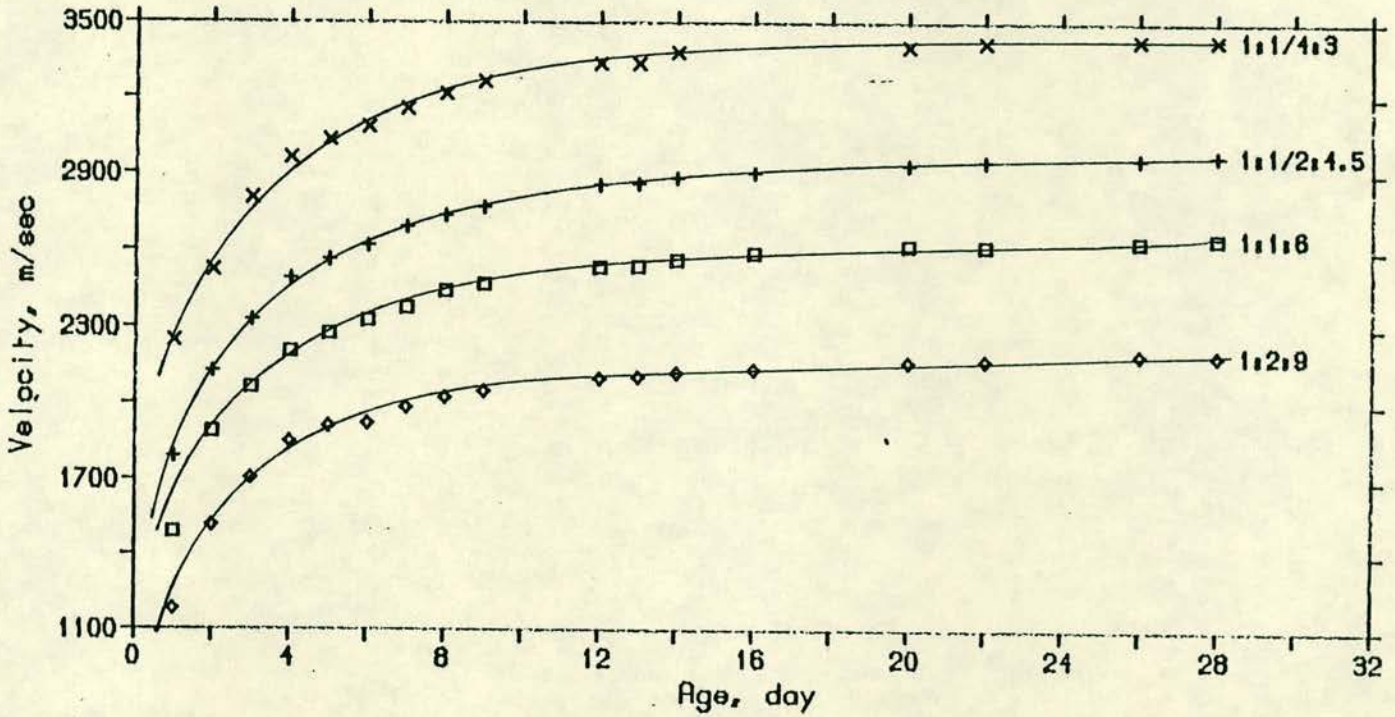

Fig. 4.3(a) Graph of mortar pulse velocity against age for FINE grade sand

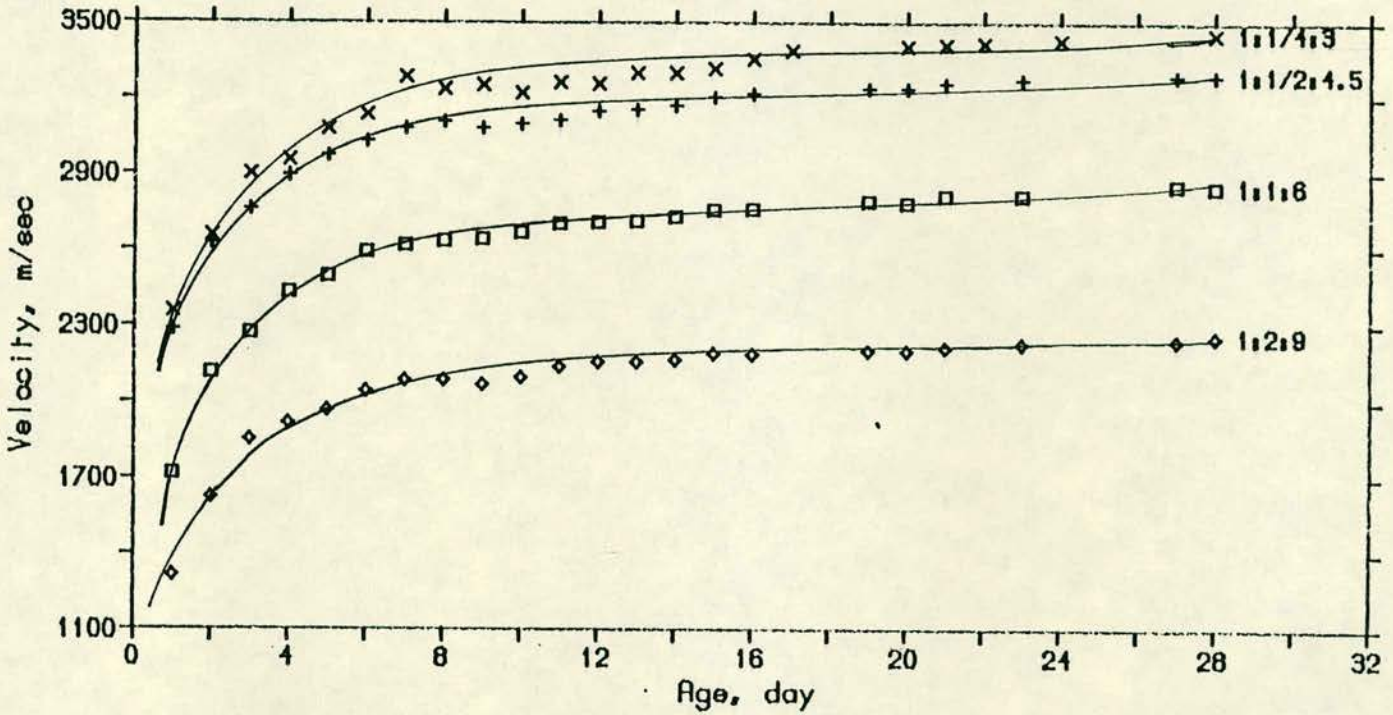

Fig. 4.3(b) Graph of mortar pulse velocity against age for MEDIUM grade sand

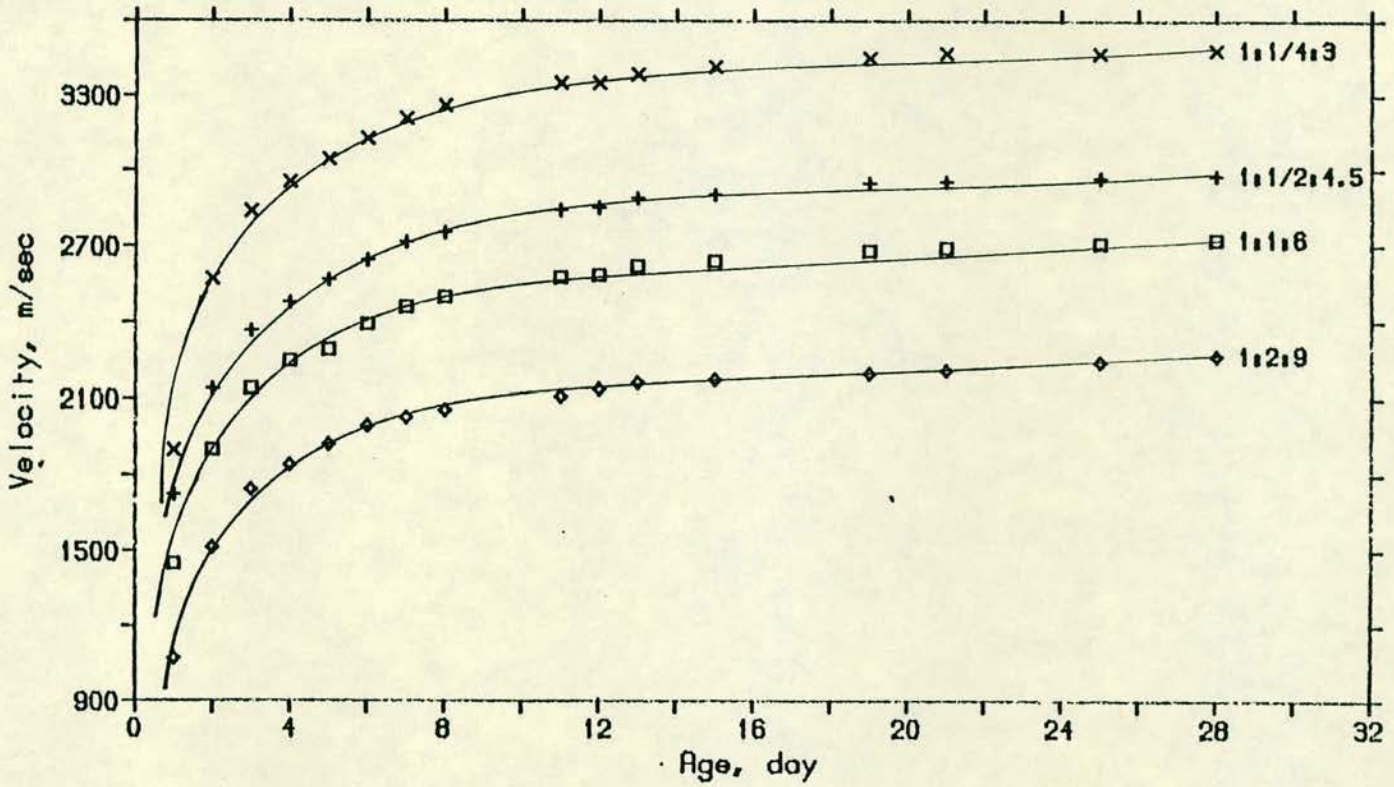

Fig. 4.3(C) Graph of mortar pulse velocity against age for COARSE grade sand

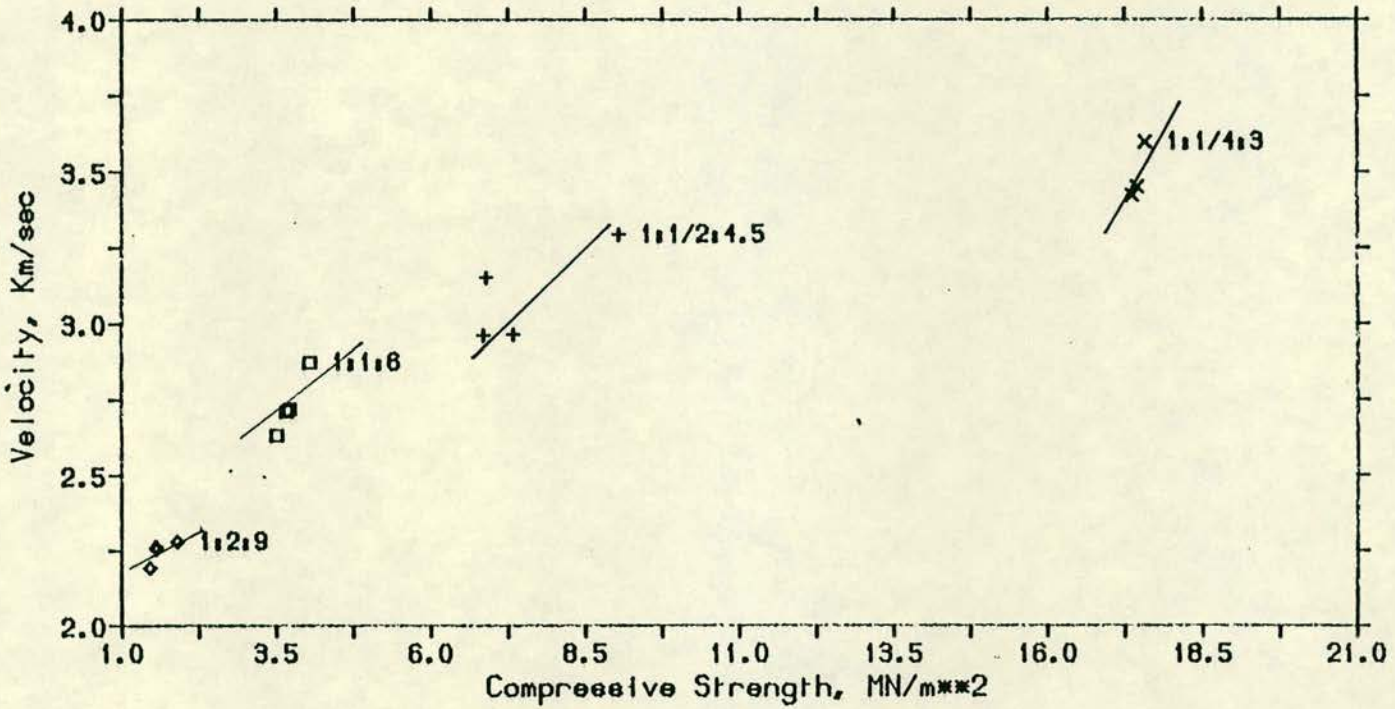

Fig. 4.4 Graph of mortar pulse velocity against cube compressive strength

Generally it was found that those cubes made with the coarse sand were the strongest in compression, followed by those with the medium sand grading. The weakest were those of the finest sand grading (Table 4.1). It was also found that by increasing the water content of a mix the strength and hence the pulse velocity were reduced. The reason is that the strength of mortar varies inversely with the water/cement ratio for each mortar grade and sand sample. Sands with a high specific surface would produce a higher water/cement ratio for a given consistence and therefore a lower strength. On the other hand, sands of a lower specific surface, i.e. the coarser grade sands, produce a lower water/cement ratio and hence a higher strength (60).

Wave velocity is known to depend on the elastic properties and mass of the medium, and hence if the mass and velocity of wave propagation are known, it is possible to assess the elastic properties. The compression velocity v, for an infinite, homogeneous, isotropic elastic medium is:

$$v = \left(\frac{(1 - \sigma)}{(1 + \sigma)(1 - 2\sigma)} \times \frac{Y}{\rho} \right)^{\frac{1}{2}} \qquad (4.2)$$

where Y is the Young's modulus of elasticity (KN/mm^2) and

σ is the Poisson's ratio (see also expression 5.11)

The modulus of elasticity Y is a measure of the stiffness of a ductile material (where stiffness is the mechanical property that defines the resistance of a material to deformation in the elastic range). The Poisson's ratio is another mechanical constant related to stiffness and is the ratio of lateral strain to axial strain in simple tension.

In the above equation, provided a reasonable estimate of σ and density ρ can be made, it is possible to calculate the elastic modulus Y, using a measured value of pulse velocity. It must, however, be noted that the above equation refers to an "ideal" material of which mortar is not necessarily one and masonry is certainly not. The complexity of the inter relationship of the constituents mean that experimental calibration of elastic modulus is normally necessary.

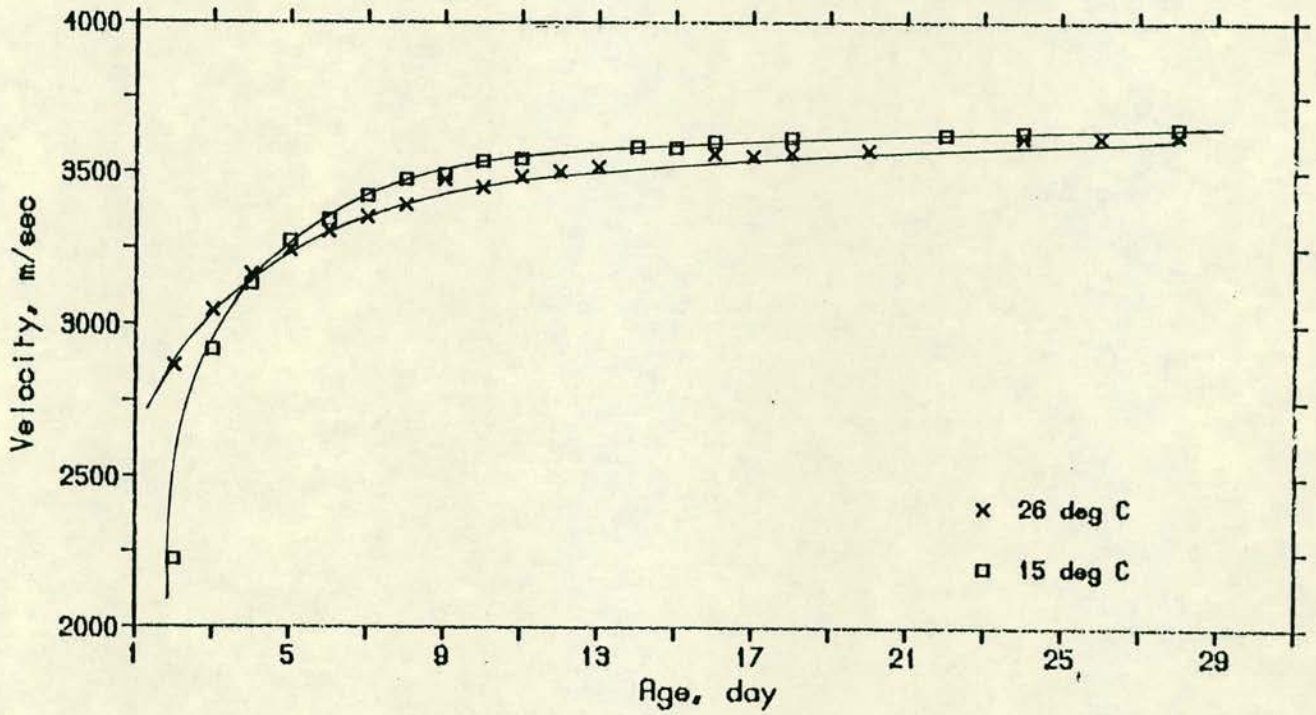

Fig. 4.5 Effect of curing temperature on mortar strength

The results for the beams constructed show that the beam cured in 26° C water produced higher pulse velocity readings in the first few days. The pulse velocity values then decreased and after several days became lower than the values obtained for the other beam cured in 15° C water (see Appendix 2 and Fig. 4.5).

It is usually thought that a higher curing temperature produces a higher strength mortar or concrete and hence a higher pulse velocity. This was true during the first few days of the experiment. However, it is suggested that a higher temperature during placing and setting, although it increases the early strength, may adversely affect the strength from about 7 days onwards (61). Figs. 4.6 and 4.7 illustrate this in more detail.

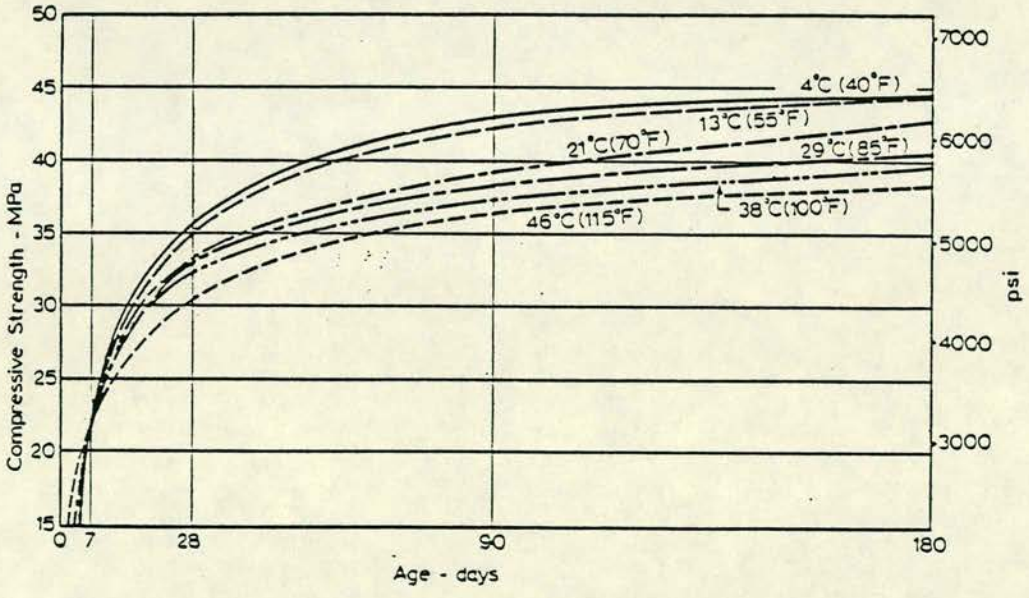

Fig. 4.6 Effect of temperature during the first two hours after casting on the development of strength - all specimens sealed and after the age of 2 hours cured at 21° C (based on ref. 61)

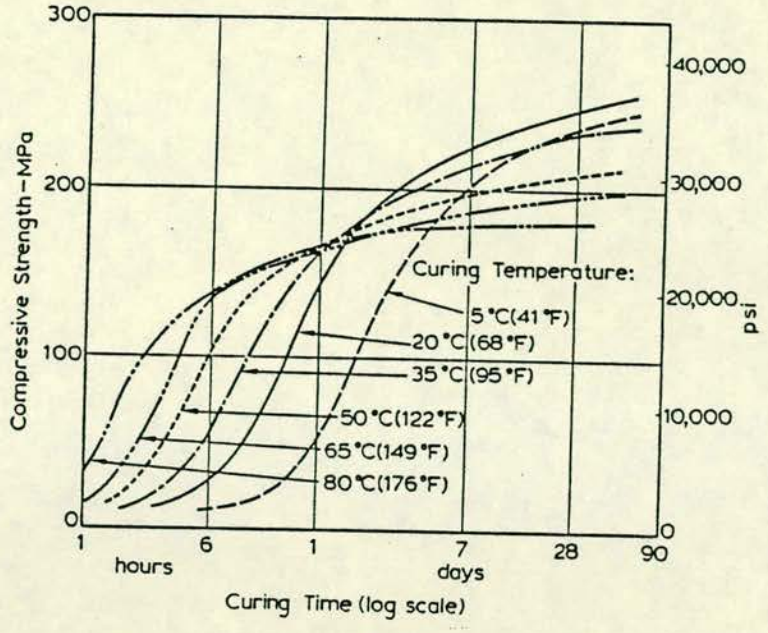

Fig. 4.7 Effect of curing temperature on compressive strength of neat cement paste compacts (based on ref. 61)

At the end of the curing period, one of the beams was cut into sections of different lengths. A relationship between path length and pulse velocity was then obtained (Table 4.2 and Fig. 4.8).

Length (mm)	Transmission time (sec x 10^{-6})	Transmission velocity (Km/sec)
23.5	8.6	2.73
29.0	10.2	2.84
40.0	13.2	3.03
49.5	16.2	3.06
60.0	19.4	3.09
71.0	22.9	3.10
80.0	25.8	3.10
132.5	42.6	3.11

Table 4.2 Path length against pulse velocity

From the graph of Fig. 4.8 it is seen that pulse velocity is relatively constant for different path lengths except when the path length is less than 60 mm. It was noted that the wave length, λ, is given by:

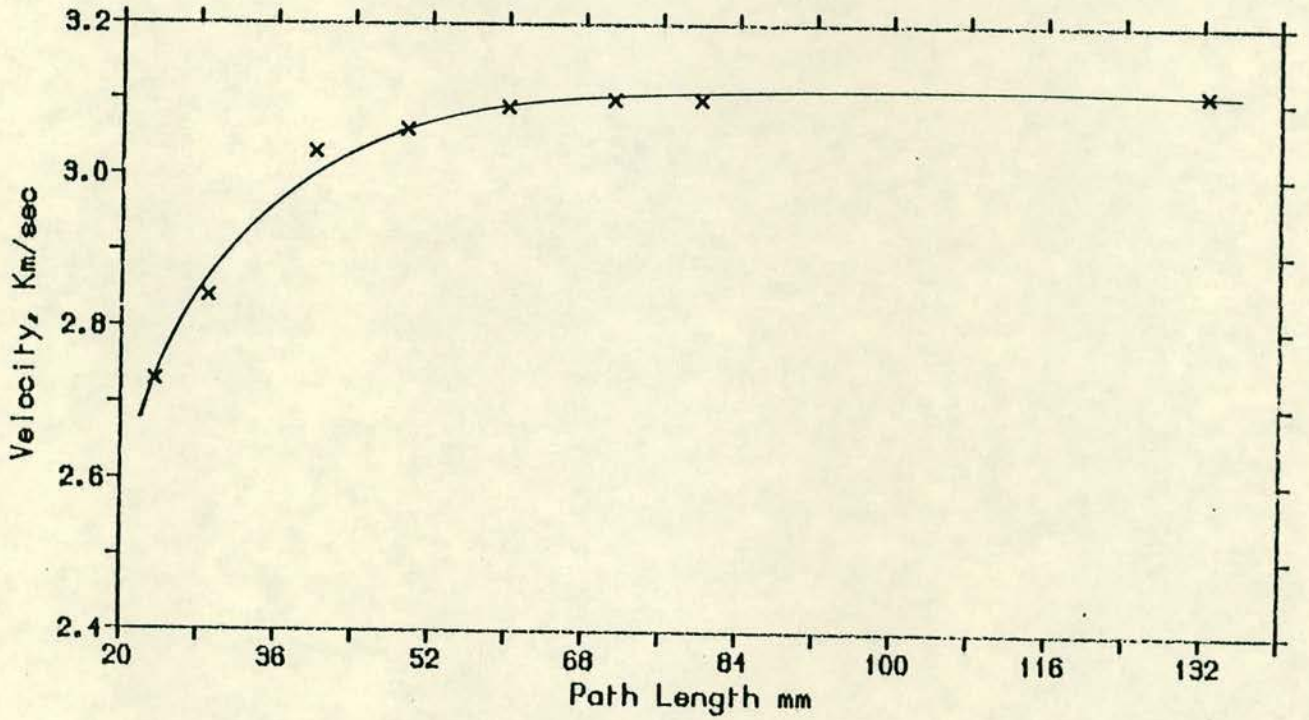

Fig. 4.8 Graph of mortar path length against pulse velocity

$$\lambda = \frac{\text{pulse velocity}}{\text{frequency (of input signal)}} \qquad (4.3)$$

$$= \frac{3.100 \text{ (Km/sec)}}{54 \text{ (kHz)}}$$

= 57.6 ≅ 60 mm for the above test.

In other words, pulse velocity is almost constant for the path lengths higher than the wave length.

4.5.2 Stone

The pulse velocity v (Km/sec) through the stone cubes was found using equation (4.1). From these values and the cubes compressive strength, a relationship between stone cube compressive strength and pulse velocity was established (Table 4.3 and Fig. 4.9).

Stone Type		Path Length (mm)	Transmission Time (μsec)	Pulse Velocity (Km/sec)	Cube Comp. Strength (mN/m²)
Yellow Sandstone	1	102.0	36.7	2.779	58.174
	2	103.0	38.9	2.648	56.910
	3	100.0	39.2	2.331	54.357
	4	103.0	35.3	2.901	51.874
	5	100.5	49.6	2.026	41.413
White Sandstone	1	102.0	41.4	2.464	25.138
	2	101.3	61.2	1.655	24.362
	3	102.0	72.3	1.410	23.986
	4	100.5	84.4	1.191	23.260
Red Sandstone	1	99.0	49.2	2.012	31.663
	2	100.0	54.2	1.835	19.784
Limestone	1	101.0	50.7	1.992	20.000
Granite*	1	140.0	27.2	5.147	known to be in range 91.2 - 145.9

Table 4.3 Stone block pulse velocity against compressive strength

* Not a cube

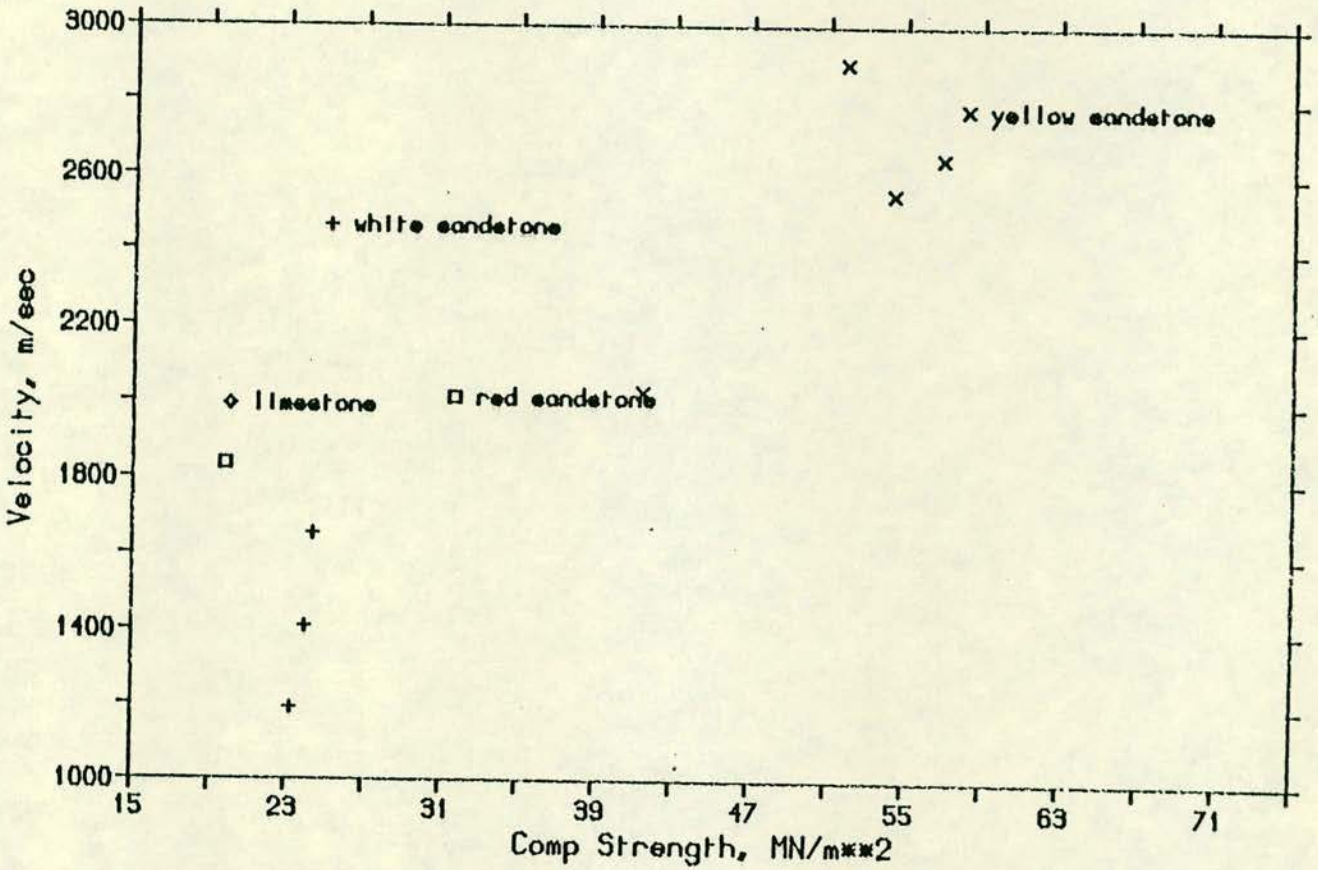

Fig. 4.9 Graph of stone cube compressive strength against pulse velocity

4.6 DISCUSSION

4.6.1 Pulse Velocity and Cube Strength

From the experimental work carried out, it is clear that the mix proportions, sand type, water/cement ratio, and maturity are all important factors which influence mortar properties and hence its strength. It was seen that the higher the mortar strength, the higher pulse velocity was, i.e. pulse velocity increased with an increase in the strength of mortar.

It was found that the coarser grained cubes of mortar had higher pulse velocity and strength than the finer grained ones. One explanation is that the mechanical interlocking of the coarse aggregate contributes to the strength of concrete in compression that is why the compressive strength of concrete is higher than that of mortar (62). The wave path in this case compared to the case of finer grained sand is more through the aggregate particles than the cement paste. The aggregate particles have clearly a very high compressive strength.

The cubes made of the weaker mixes of 1:1:6 and 1:2:9 were heavily honeycombed and produced lower compressive strength and pulse velocity. This was clearly due to the presence of air voids in the honeycombed cubes. It is evident that air voids reduce the strength of concrete. Pulse velocity has a very low value in the air and hence ultrasonic compression waves tend to pass through the mortar rather than through the air. The presence of air voids in the cubes obviously reduces the speed and produces a lower pulse velocity. This is also clear from the fact that by increasing the water/cement ratio, the strength of concrete or mortar reduces. An increase in water/cement ratio results in formation of more water and later on air voids in the mortar (or concrete). The more air voids present in the mortar, as said above, the lower the strength and pulse velocity are.

4.6.2 Pulse Velocity and Path Length

An important factor which must be taken into account when testing masonry is the strength of the mortar in the masonry. The strength of mortar in the masonry can be significantly higher than

the expected value anticipated from the mix type and the water/cement ratio. This is due to suction of water from the fresh mortar, during construction, by the dry brick or stone block. This suction results in a lower water/cement ratio. However, this "error" can be neglected as this increase in strength is largely compensated for by the decrease due to "length factor". In Fig. 4.8, section 4.5.1, it was seen that pulse velocity of mortar decreased with a decrease in length below 60 mm. The mortar joint width in masonry is usually only a few cm in length and hence it has a lower pulse velocity value than the one obtained from cube testing. Therefore when testing mortar in a masonry structure, ultrasonically, the increase in mortar strength due to suction of water may be neglected. The decrease in pulse velocity reading due to very short length of mortar compensates for that increase.

The decrease in pulse velocity measurement is attributed to physical limitations of testing equipment (63). For example in Fig. 4.8, it is seen that pulse velocity decreased with lengths below one wavelength which is nearly 60 mm. It is recommended (63) that this will always occur unless a least lateral dimension is satisfied. In this example the least lateral dimension, for the above equipment is equal to wavelength. And wavelength is the ratio of pulse velocity to input frequency.

4.6.3 Pulse Velocity and Age

From Fig. 4.3, it is seen that pulse velocity initially increases with time. The increase in pulse velocity, after construction of mortar, is very rapid for the first few days and then tends to become constant after a few weeks. In the majority of cases, after 28 days a constant pulse velocity corresponding to a constant compressive cube strength, is assumed (64). However, it is assumed that mortar and concrete strengths increase beyond these time, though only very slightly. C.P. 110, 1972, recommends that concrete after 12 months has a compressive strength 1.24 times larger than its strength at the age of one month.

It must be noted that the rate of increase of mortar strength, or concrete strength with age depends upon curing conditions. The

experimental results of beams cured in two different temperatures showed that the rate of increase for the two beams were different. The beam cured at 26° C had initially a higher rate of pulse velocity increase with time than the beam cured at 15° C. The increase in pulse velocity of the beam cured at 26° C, after a few days became lower than that of the beam cured at 15° C.

Therefore when estimating the strength of mortar, especially when it is very young, the curing conditions must be taken into account. Very cold or very hot curing environments have different effects on strength of concrete or mortar at the early stages of construction (see Figs. 4.5, 4.6 and 4.7, age against curing time).

In addition it is expected that moisture conditions also affect the mortar pulse velocity. The tests carried out on concrete have shown that wet specimens produce higher pulse velocity than the dry specimens (63), see Fig. 4.10 below.

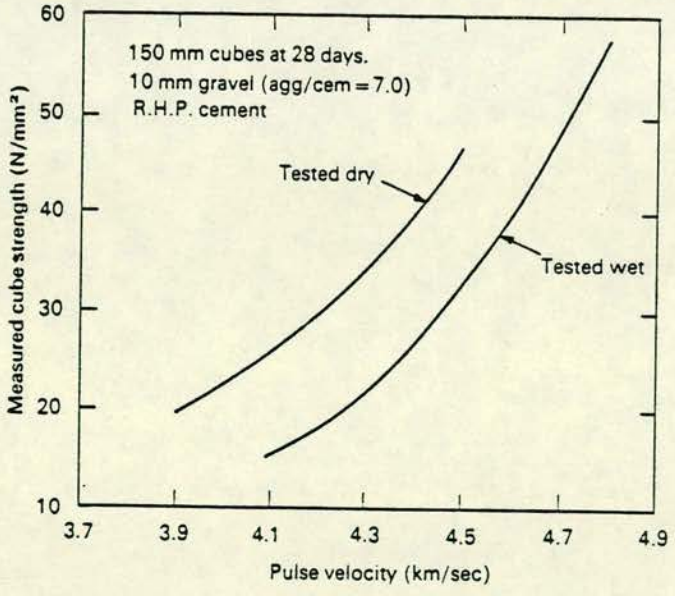

Fig. 4.10 Effect of moisture conditions on pulse velocity reading (based on ref. 63)

4.7 CONCLUSIONS

In this work, relationships between pulse velocity and age, pulse velocity and path length for mortar were found. A relationship between pulse velocity and strength for mortar and stone cubes was also established. It was found that:

(i) The stronger the mix, in a mortar, the higher the pulse velocity. This confirms that pulse velocity is dependent on the elastic properties and mass of the medium.

(ii) Pulse velocity also increases with an increase in the strength of stone block cubes.

(iii) Measured pulse velocity in mortar decreases with a decrease in path length shorter than the wavelength of the pulse. It is anticipated that this is true also for stone blocks.

(iv) This reduction in pulse velocity may be neglected when assessing the masonry strength. The higher strength of mortar caused by suction of water from fresh mortar in masonry, largely compensates for that reduction.

(v) Yellow sandstone is usually stronger than white sandstone. The coarser and better cemented granite is much stronger than sandstone, limestone and many other stone blocks used in masonry construction.

(vi) Mortar strength increases rapidly during the first few days of its construction and then the rate of increase reduces so that, as in situ case of concrete, it reaches a near constant strength at 28 days. This conclusion is dependent upon cure environment.

(vii) Pulse velocity test on mortar and stone blocks/bricks can be used to get an indication of the quality and strength of masonry.

CHAPTER FIVE

MASONRY AS COMPOSITE

5.1 INTRODUCTION

In the past few decades, there has been ongoing research into the ultrasonic testing of materials and its application in industry. The emphasis, however, has been on testing of homogeneous materials, for example metals, at high frequency (>50 kHz). Work on Civil Engineering materials has been largely confined to concrete and steel using high frequency ultrasonic devices, for example PUNDIT (34). Research into the non-destructive investigation of composite systems has been confined to concrete piles in soil where the concrete member has been the subject of integrity testing (65).

The work reported in this thesis represents the initial stages of an attempt to develop a technique for the inspection and diagnosis of composite materials, for example brick and stone masonry. Low frequency, 1 to 2 kHz, sonic investigation methods have been developed to locate cracks in, and to establish transmission velocities through shear failed brick masonry walls and stone masonry piers.

5.2 THEORY OF SONICS

The term sonics is used to describe mechanical waves propagated in materials at frequencies lower than 20 000 Hz. Characteristics of these waves are related to the mechanical properties, for example the elastic properties and the homogeneity of the structure of the medium through which they pass (66). In order to investigate this relationship a study of the waves and the time taken for the waves to travel through the material, must be made. In this section the basic concepts used in sonic testing are briefly discussed. It must be noted that the basic theory of sonics is identical to ultrasonics and the more detailed definitions and theory are given in references.

5.2.1 Wave Motion

When a sonic wave in the form of a compressional wave is generated through a medium, the particles of that medium are set into vibrations at a certain frequency. When a particle of this medium, due to the external force associated with the wave, is set into motion, the motion is resisted by the elastic forces of the

medium. Therefore, the particle comes to rest after a finite displacement. The particle then, because of its inertia, continues to move through its equilibrium position with a certain velocity and comes to rest again after being displaced in the other direction, i.e. when its kinetic energy is converted into elastic energy (potential energy). Therefore the vibrations of the medium depend on its inertia and its elasticity. Part of the energy of the vibrating particle is transmitted to neighbouring particles which, in turn, vibrate and transmit energy to their neighbouring particles. Because each particle starts its motion slightly later than the one before, the vibrational motion travels with a finite velocity v known as wave velocity. The phenomenon is defined as wave motion (66).

5.2.2 Wavelength and Frequency

Consider the wave propagation and motion in Fig. 5.1.

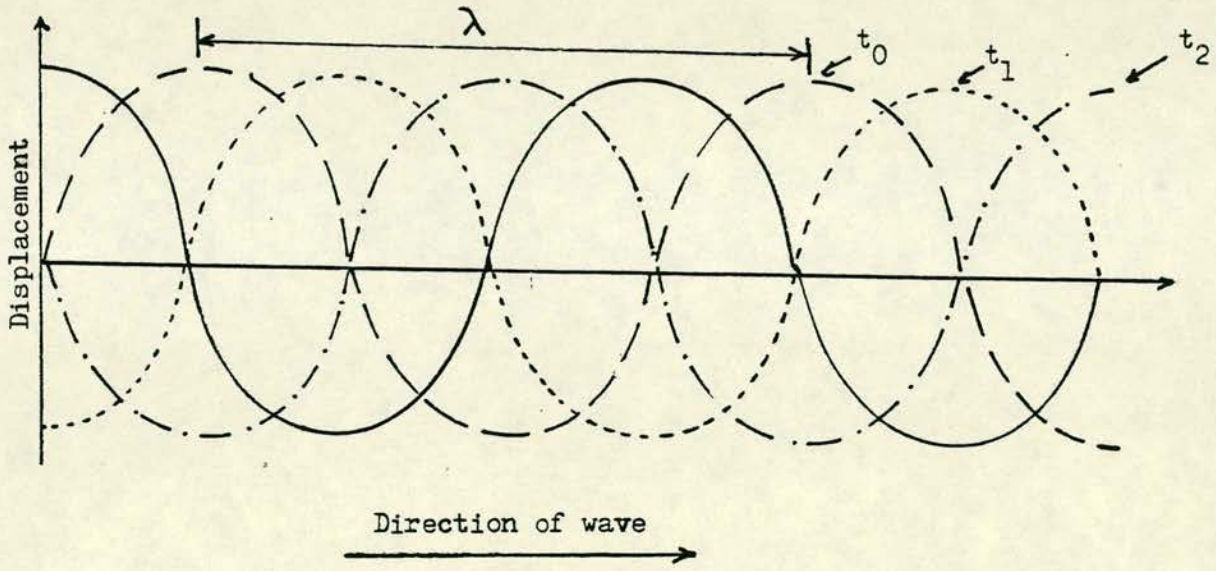

Fig. 5.1 Wave propagation along x-axis

The wavelength λ is given by the distance between two crests or troughs, the wave amplitude is the maximum or minimum value of the displacement measured from the position of equilibrium. The time taken for the wave to complete one vibration is called the time period, T, and the frequency, or cycle per second corresponding to one oscillation per second is given by:

$$f = \frac{1}{T} \qquad (5.1)$$

and the unit used is Hz.

The wave velocity v thus can be expressed by:

$$v = \frac{\lambda}{T} \qquad (5.2)$$

or $$v = \lambda f \qquad (5.3)$$

5.2.3 Reflection of Sonic Waves

When a sonic wave is generated in a semi-infinite medium and is incident normally to a boundary in the medium in contact with another semi-infinite medium some of the wave energy is reflected back and the rest is propagated or transmitted in the other medium (see Fig. 5.2).

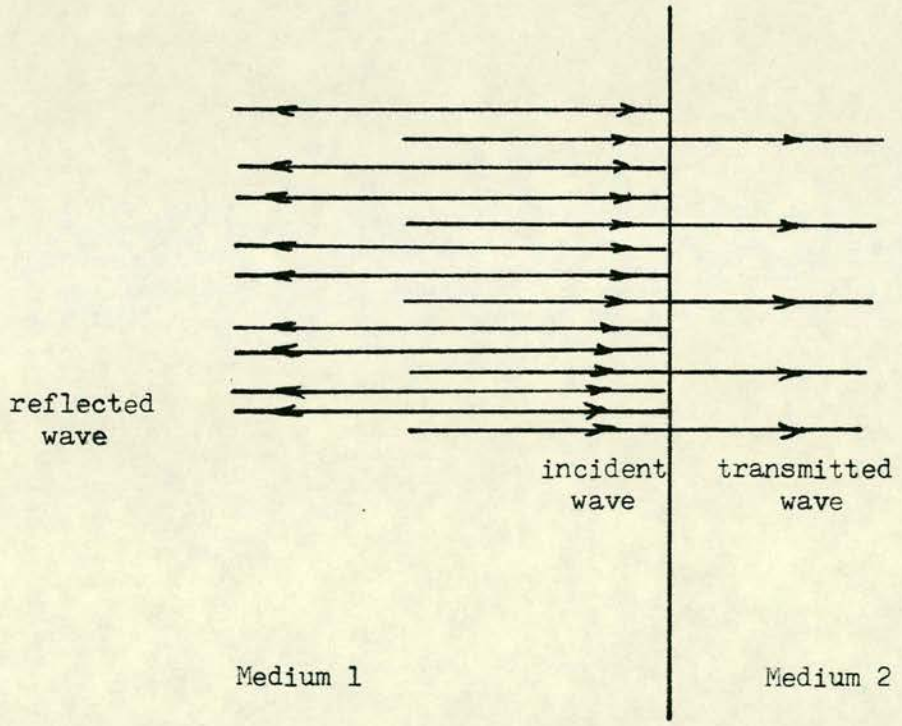

Fig. 5.2 Reflection and transmission at a boundary between two mediums

For a plane wave at normal incident between two media the transmitted coefficient α_t and reflection coefficient α_r, are given by:

$$\alpha_t = \frac{I_t}{I_i} = \frac{4\rho_1 v_2 \rho_2 v_2}{(\rho_1 v_1 + \rho_2 v_2)^2} \qquad (5.4)$$

and $$\alpha_r = \frac{I_r}{I_i} = \left(\frac{\rho_2 v_2 - \rho_1 v_1}{\rho_2 v_1 + \rho_1 v_1}\right)^2 \qquad (5.5)$$

where $$I = \frac{W}{S} \qquad (5.6)$$

I = intensity of the wave

W = rate of flow of energy

S = area at right angles to the direction of wave

I_i = intensity of incident wave

I_r = intensity of reflected wave

I_t = intensity of transmitted wave

ρ = density of the medium

v = velocity of the wave propagation in that medium

ρv = is also called characteristic impedance

Table 5.1 gives some examples of reflection of longitudinal waves incident normally to the boundary between two media:

Medium	$\rho v \times 10^{-5}$ Kg cm^{-2} sec^{-1}	Steel	Glass	Water	Air
Steel	4.6	0	31	88	100
Glass	1.8	31	0	65	100
Water	0.14	88	65	0	100
Air	0.000041	100	100	100	0

Table 5.1 Reflection coefficient (in percentage) of normally incident longitudinal wave between two different media (66)

5.2.4 Transmission of Sonic Waves through Layers

The expressions (5.4) and (5.5) are based on the assumption that the two media in contact with each other are semi-infinite. However, when the thickness of a layer is finite, or in practical terms is less than the length of the wave train propagating through it, the reflection and transmitted coefficients are given by:

$$\alpha_r = \frac{(r^2 - 1)^2}{4r^2 \cot^2 \frac{2\pi d}{\lambda} + (r^2 + 1)^2} \qquad (5.7)$$

and

$$\alpha_t = \frac{4r^2}{4r^2 \cos^2 \frac{2\pi d}{\lambda} + (r^2 + 1)^2 \sin^2 \frac{2\pi d}{\lambda}} \qquad (5.8)$$

where d = thickness of the layer

and r = distance from the source of energy where I decreases with increasing r

It should be noted that in the above case, where a layered media exists, interference occurs which violently affects the various amplitudes involved. The magnitude and direction of the interference effects depend on the phase angles. The effects are largest when (68):

(1) Attenuation losses are low.

(2) Layer thicknesses approach a few wavelengths or less.

(3) Surfaces are mismatched to give poor coupling.

(4) Provision is made for adjusting the frequency of the transmitted wave.

5.2.5 Absorption of Sonic Waves

When the medium through which the sonic wave is propagated is not perfectly elastic, i.e. change of elastic energy into kinetic energy and vice versa takes place with some losses, the intensity I can be expressed as a function of the distance ℓ in the form of

$$I = I_o e^{-\gamma \ell} \qquad (5.9)$$

where I_o = initial intensity for a distance of $\ell = o$

and γ = coefficient of absorption

Also:

$$(\rho v) = (\rho v)_o e^{-\frac{1}{2}\gamma \ell} \qquad (5.10)$$

where (ρv) is a measure of the elasticity of the medium.

5.2.6 Types of Waves

Two main kinds of waves encountered in sonic testings are longitudinal and surface waves. For longitudinal waves, the particles of the medium vibrate in the direction of propagation. This type of wave can be propagated in all types of media.

Surface wave occurs when the solid medium has a free surface. In this case the particles of the medium execute vibrations both along and perpendicular to the direction of the waves.

Another type of wave involved in sonics is the transverse wave. In this case the particles of the medium vibrate in a direction at right angles to that of propagation. Waves of this type can only be propagated in solids where shear elasticity exists.

The longitudinal wave velocity v_l, transverse velocity v_t and surface wave v_s are given by

$$v_l = \left(\frac{Y(1 - \sigma)}{\rho(1 + \sigma)(1 - 2\sigma)} \right)^{\frac{1}{2}} = \left(\frac{\lambda + \frac{3}{4}\mu}{\rho} \right)^{\frac{1}{2}} \qquad (5.11)$$

$$v_t = \left(\frac{Y}{2\rho(1 + \sigma)} \right)^{\frac{1}{2}} = \left(\frac{\mu}{\rho} \right)^{\frac{1}{2}} \qquad (5.12)$$

$$v_s = \frac{0.87 + 1.12\sigma}{1 + \sigma} \times \left(\frac{Y}{2\rho(1 + \sigma)} \right)^{\frac{1}{2}} \cong 0.9\, v_t \qquad (5.13)$$

where Y = Young's modulus of elasticity (KN/mm^2)

σ = Poisson's Ratio

λ = bulk modulus (KN/mm^2)

μ = shear modulus of elasticity (KN/mm^2)

ρ = density (Kg/m^3)

5.3 TESTING OF MASONRY

A sonic investigation of three shear failed reinforced brick masonry walls and several stone masonry piers was carried out. The objectives were to identify the position of shear cracks in the walls and to obtain an estimate of transmission velocity through cracked and uncracked brickwork, a reinforced collar joint filled with mortar and stone masonry. The sonic velocities obtained gave an indication of the relative strengths of the different materials.

5.3.1 Equipment

The testing equipment consisted of:

(1) A two channel transient recorder and flat bed plotter.
(2) 75 ohm screened coaxial cables.
(3) Two 54 kHz, 50 mm diameter piezoelectric transducers.
(4) An ordinary hammer covered with several layers of paper.
(5) Water pump grease to give good acoustic coupling.
(6) A Telequipment storage oscilloscope.
(7) PUNDIT for measuring transmission velocity through very short lengths of material.

5.3.2 Experimental Procedure

5.3.2.1 Masonry walls tested

Three shear failed reinforced brick masonry walls B2, C1 and C2 were tested (69). Each wall was of stretcher bond construction with steel embedded in the collar joint and 240 mm thick. The leaves were constructed from 102 mm wide pressed bricks and reinforcing steel was embedded in the collar joint which was 36 mm wide. Thirty-six courses of brickwork to a height of 2.7 m were capped with a 236 mm deep concrete beam. The wall base was a 300 mm deep reinforced concrete beam. Wall B2 was of 2.5 m nominal length and walls C1 and C2 of 3.5 m nominal length.

The vertical reinforcement used in each wall consisted of two 16 mm diameter bars at each end and 12 mm diameter bars uniformly distributed along the centre line of the wall. Six 8 mm diameter bars were also used horizontally and additional short starter bars, suitably anchored in the concrete base, were incorporated along the base.

Table 5.2 gives details of the dimensions and reinforcement for each wall.

Wall Designation	Wall Length (mm)	Vertical Reinforcement in Central Portion No of 12 mm dia bars	Percentage* %
B2	2465	26	0.63
C1	3483	7	0.19
C2	3483	18	0.34

All walls:	Brickwork height	2.7 m
	Total wall height	3.24 m
	Thickness	240 mm
	Horizontal reinforcement	Six 8 mm diameter bars
	Vertical reinforcement	at each end

* Percentage of reinforcement is calculated on gross cross-sectional area of the wall.

Table 5.2 Wall and Reinforcement Details (69)

The basic principle of the experimental technique entailed the propagation of a compression wave along the length of the wall, using a conventional hammer covered with several layers of soft paper, to avoid damaging the brick surface. Two piezoelectric transducers were attached to the two opposite ends of the wall, using water pump grease as an acoustic coupling medium. They were placed opposite each other at the same height above the base of the wall, 5 to 7 courses of brickwork below the concrete cap. They were connected to a two channel transient recorder and flat-bed recorder by screened cables. One transducer (A) was connected to channel (A) of the flat-bed recorder, and the other transducer (B) to the other channel (B) (Fig. 5.3). Transducer (A) triggered first.

The time scale and sensitivity of the transient recorder were adjusted such that a relatively light hammer blow, very close to

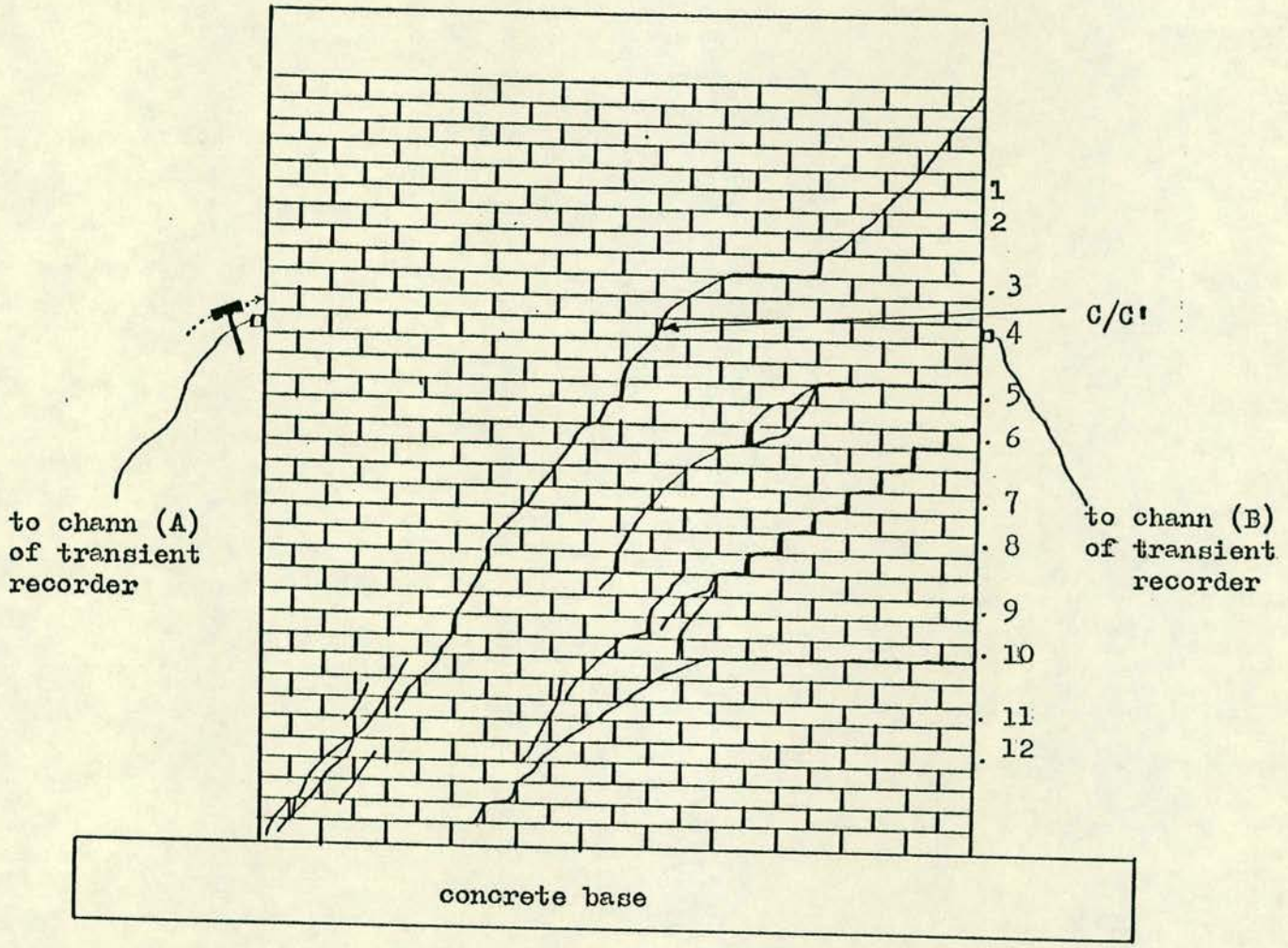

Fig. 5.3 Wall B2 - Observed crack pattern

transducer (A) would generate a compression wave which would travel along the length of the wall. A suitable recording was then obtained on the transient recorder for display on the plotter.

This procedure was repeated, moving the transducers downwards every two or three courses of brickwork. Additionally, several points on the reinforced collar joint were chosen for testing. The procedure was repeated on the concrete beams at the base of the walls.

The above technique was used on a 1.55 m uncracked length of similar brickwork in order to obtain an estimate of transmission velocity through uncracked brickwork.

The locations of the main diagonal crack and other severe visible cracks were measured with a steel tape, relative to the ends of the walls.

In setting up the transient recorder and flat-bed plotter, a suitable time scale, for accurate interpretation of results, had to be found. This was achieved by carrying out some preliminary trials to obtain sharp and well defined signals.

5.3.2.2 Stone masonry piers tested

The principle of the experimental technique for testing the piers was similar to that of masonry walls. The difference was that a storage oscilloscope was used instead of the transient recorder. This set of equipment had the advantage of a faster experimental time. The transient recorder and flat bed plotter's signal output was much larger than that of the oscilloscope, and hence it was easier to interpret. However, in masonry piers testing the early parts of the signals, for measuring the transmission velocities, were needed. Therefore the use of the oscilloscope was adequate and the results obtained were sufficiently accurate.

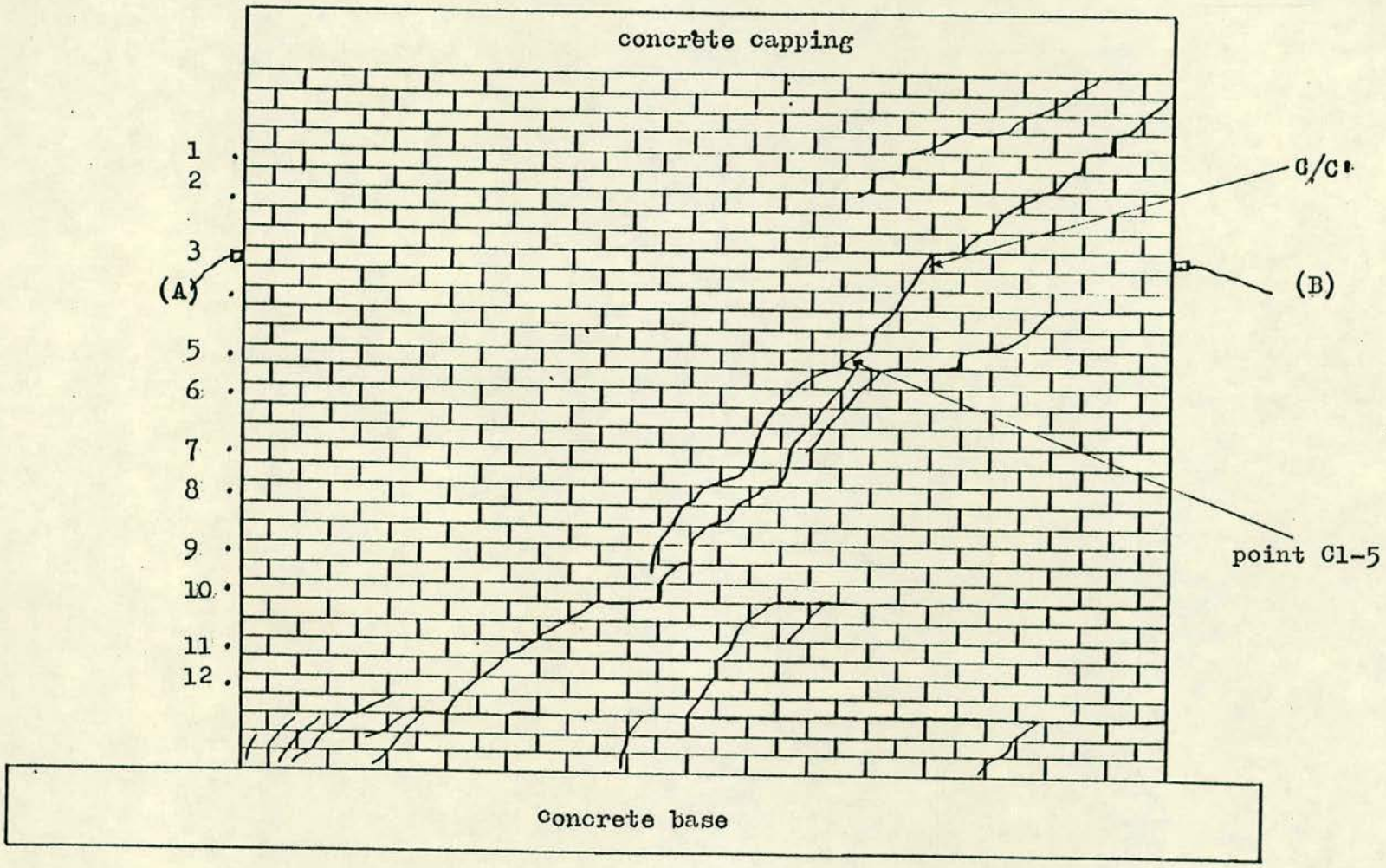

Fig. 5.4 Wall C1 - Observed cracks

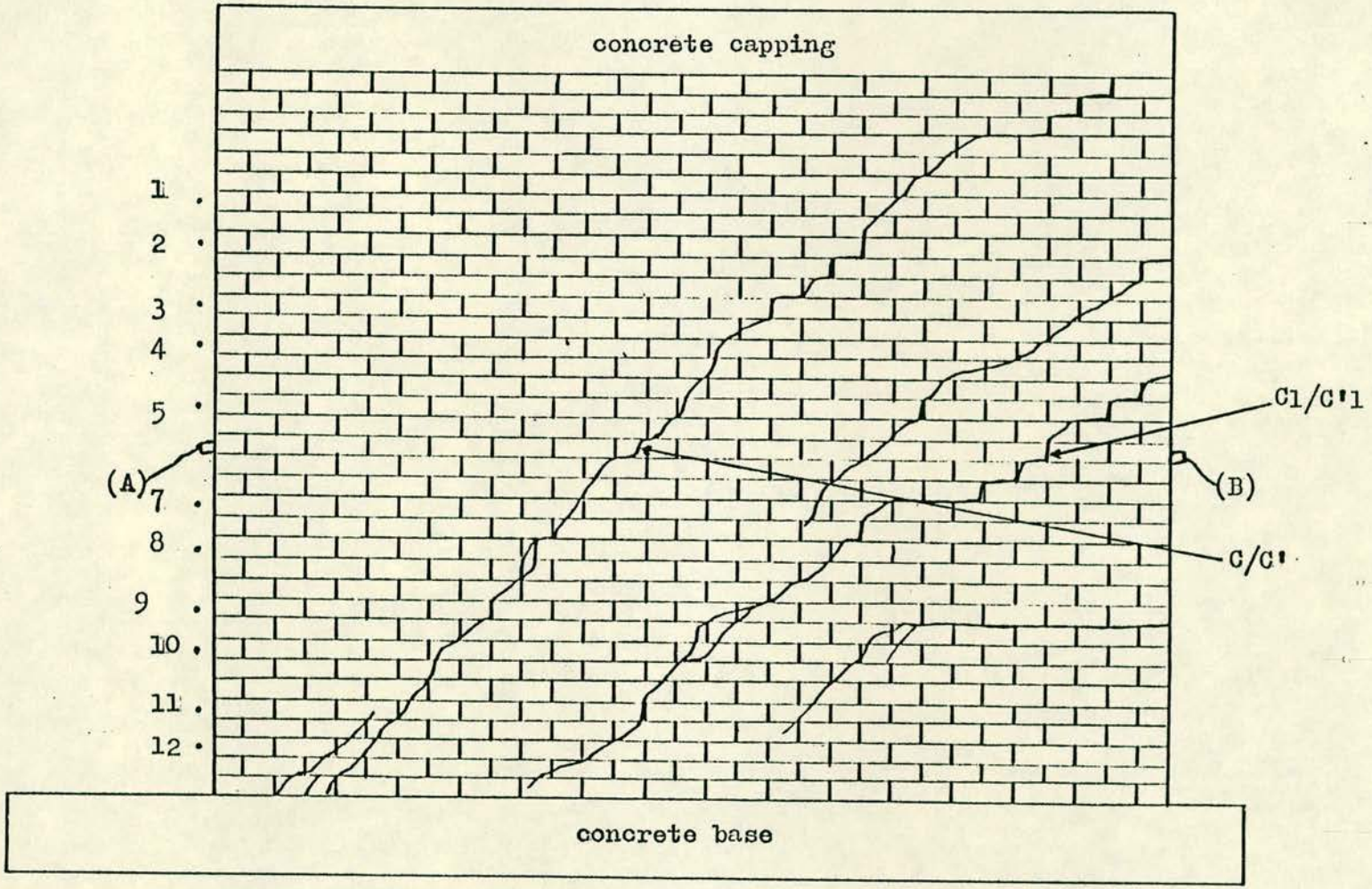

Fig. 5.5 Wall C2 - Observed cracks

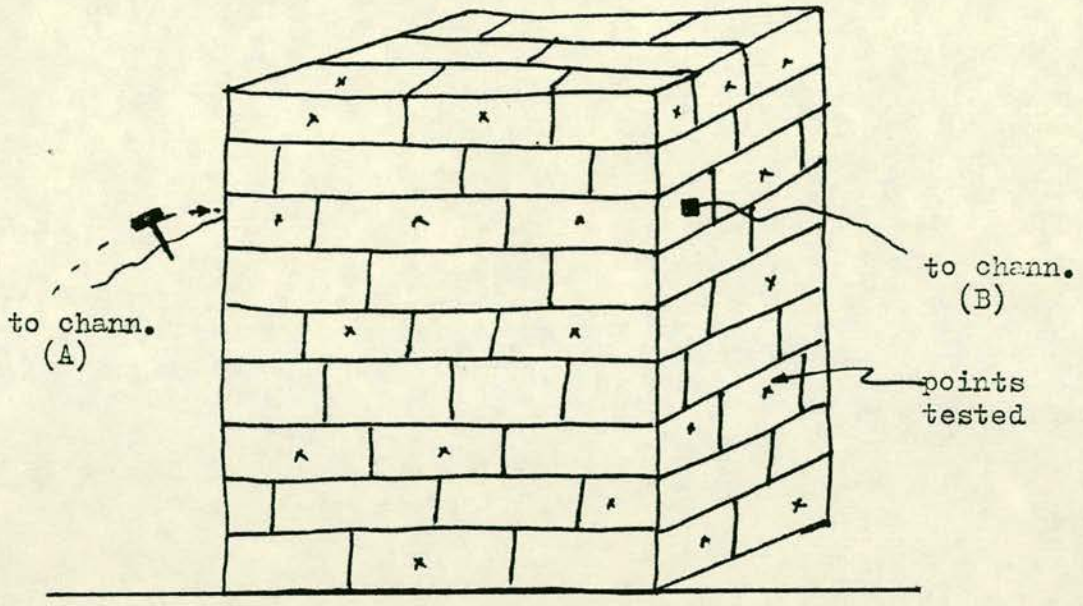

Fig. 5.6 – Masonry Pier

The masonry piers consisted of two granite, one whinstone and three various sandstone piers. Each pier had dimensions in the range 450 x 750 x 900 mm. For each pier the transmission velocity was measured at several points, on different faces. The average value was taken as the transmission or sonic velocity of the masonry.

5.4 RESULTS AND ANALYSIS

5.4.1 Interpretation of Results

Under idealised conditions, when a compression wave propagates through the masonry, it will have a shape similar to Fig. 5.7(a) which can be derived by Fourier's analysis.

This type of signal, with an exponential rise and decay, is common in ultrasonic testing (70). Indeed all the traces obtained do have this exponential rise and decay in common.

However, masonry is a heterogeneous material and additionally the walls tested were cracked. Therefore the traces obtained were

more complicated than the idealised case. The complication arises from interference of reflected waves from brick-mortar joints, any crack or discontinuity and the surface waves generated at the transducer. This is illustrated diagramatically in Fig. 5.7.

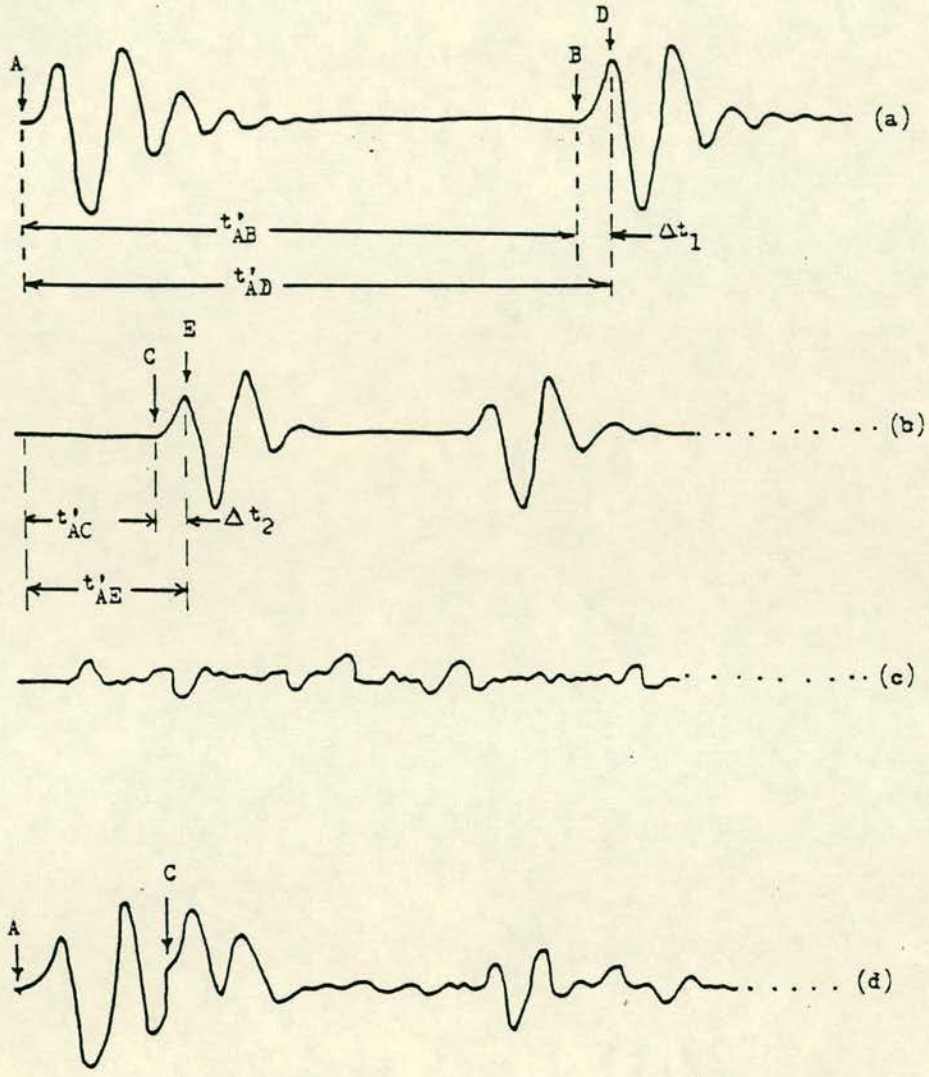

Fig. 5.7 Waveforms for cracked brickwork
(a) Transmitted signal, (b) reflected signal from a crack face, (c) reflected signal from brick-mortar joints, (d) resultant signal, i.e. the trace obtained

The relative proportion of the initial signal transmitted againt proportion reflected from a discontinuity, is dependent upon the magnitude, shape and orientation of the discontinuity. For example, a vertically continuous void results in no transmission to the end of the wall, as the characteristic impedance of air is much

higher than that of masonry and hence almost total reflection occurs (66).

As shown in Fig. 5.7, t'_{AC} and t'_{AB} correspond to delay times required by the transmitted compression wave to reach the reflectors, a crack and the end B of the wall respectively. The peak of the reflected wave from the end B of the wall occurs after a time interval of t'_{AD} and that of the reflected wave from the crack after t'_{AE}, where it can be seen from Fig. 5.4:

$$t'_{AD} = t'_{AB} + \Delta t_1$$

$$t'_{AE} = t'_{AC} + \Delta t_2$$

Δt_1 and Δt_2 are determined by the shape of the transmitted compression wave and the response of the transducer (71).

Also by using two transducers (Fig. 5.3), placed opposite each other, at the same level at the two ends of the wall, the time of arrival of a sonic pulse at each transducer could be identified and the transmission velocity measured.

Referring to Fig. 5.8, when a point close to transducer A, was excited by a hammer blow a longitudinal compression wave travelled along the length AB. This triggered first transducer A and after a time interval t_{AB} transducer B. The distance between the two triggering points A and B, on the chart, corresponded to t_{AB} i.e. the time taken for the compression wave to travel from A to B. Therefore transmission velocity V_{AB}, along the length AB was given by:

$$V_{AB} = \ell_{AB}/t_{AB}$$

where ℓ_{AB} = length of the wall between transducers A and B.

5.4.2 Sonic Assessment of Walls

In order to identify the effect of a crack or a major discontinuity along the length of the wall on the recorded trace,

the following procedure was carried out:

(1) $(V_{AB})_{uncracked}$, which had already been measured on a similar uncracked brickwork section was noted.

(2) $(V_{AB})_{cracked}$ was calculated by knowing length ℓ_{AB} and measuring t_{AB} on the trace. The distance between the start of graph A and the start of graph B, on the trace, corresponded to t_{AB}.

(3) The start of the first major distortion on the trace was marked on graph A as C. By assuming a suitable velocity V_{AC} such that $(V_{AB})_{cracked} < V_{AC} < (V_{AB})_{uncracked}$, and measuring t_{AC} on the trace, the length of the crack from face A, ℓ_{AC} was calculated.

(4) Similarly, the corresponding distortion on graph B was located and marked as C'. This helped in cross checking the existence of the discontinuity at C/C', Fig. 5.3.

It was found that most of the significant distortions in the traces obtained corresponded to a reflection from a crack face or from the opposite face of the wall. However, on several occasions, the discontinuities indicated by the sonic technique in this way were not visible on the walls, and the author suggests that these corresponded to hidden discontinuities - for example, a major void gap or an internal crack.

5.4.3 Illustrative Example

To illustrate this procedure take the example of Fig. 5.8, which corresponds to point 3 on wall C1, as a typical example:

(1) $(V_{AB})_{uncracked} = 3100$ m/s

(2) From the trace: $t_{AB} = 1.368$ ms

length of the wall C1: $\ell_{AB} = 3.50$ m

Therefore $(V_{AB})_{cracked} = \frac{3.5 \times 10^3}{1.368} \quad 2600$ m/s

(3) Point C1 on graph A of Fig. 5.8 indicates the start of a reflecting wave as there is a sudden increase in the amplitude of the graph starting at C1. It is assumed that this is the first major discontinuity on graph A of the trace, as there is no other major distortion on the graph before C1. Hence a maximum velocity of 3100 m/s is used to calculate ℓ_{AC1}.

i.e. $V_{AC1} = 3100$ m/s

From the graph: $t_{AC1} = 0.737$ ms

Therefore $\ell_{AC1} \cdot t_{AC1} = 2.28$ m which corresponds to point C1-5 (Table 5.3 and Fig. 5.4).

Note that t_{AC} = (the time taken for the transmitted signal to travel from A to C) = $\frac{1}{2}t'_{AC}$ (Fig. 5.3).

The next major distortion on graph A, starts at C2. Measuring the distance ℓ_{AC2} in the manner described above gives: $\ell_{AC} = 2.60$ m which corresponds to the diagonal crack observed at 2.58 m from A.

The trace distortions immediately following C2, on graph A, are ignored as they are very close to the end B. Interpretation of these distortions is very complicated as they may be due to interference of multiple reflections from brick-mortar joints with each other and with the reflections from C1 and C2. An attempt to interpret these complex composite signals, can lead to the apparent detection of non-existent discontinuities, unless there is a large distortion corresponding to a significant discontinuity.

The existence of C1 and C2 must be checked on graph B of the trace, to ensure that these are not due to the sum of minor reflections from brick-mortar joints. Indeed a major distortion does exist at C'2 (corresponding to C2) on graph B of the trace in Fig. 5.8. Using the method described above yields $\ell_{BC'2} = 1.0$ m.

The start of the next major distortion on graph B of Fig. 5.8 is considered to be at C'1, therefore the presence of a discontinuity at C'1 (corresponding to C1) is certain. Referring to Table 5.3 and Fig. 5.4, there is no observable discontinuity at C1. Therefore the trace distortion at C1 is considered to indicate a hidden discontinuity, for example an internal crack, at a distance 2.30 m from face A of the wall C1.

The trace distortion at C2 and C'2 corresponds to the diagonal crack observed at 2.6 m from face A.

Figs. 5.9 and 5.10 corresponding to C2-6 and B2-11 respective and the results in Tables 5.3 to 5.6 were interpreted in the same manner as described above.

5.5 DISCUSSION OF RESULTS

In general, when interpreting the results, it was found that when there was a discontinuity very close to face A (and hence when the reflecting signal fell within the first two or three peaks of graph A of a trace) it was difficult to distinguish it on graph A alone. To a lesser extent this was also true when interpreting the results from graph B alone, (when the reflecting signal fell within the first two peaks). Using two transducers in the manner described above helped to overcome this by permitting cross-checking of the presence of a discontinuity on two graphs A and B of a trace. Several of the measured distances of cracks, from face A in these tests, were first calculated from graph B and then marked on graph A.

In general, graph A for all the traces proved more difficult to interpret, compared to graph B. This was considered to be due to surface wave effects at A.

In Tables 5.3, 5.4 and 5.5, there were apparent discontinuities which were not observed on the walls. These were calculated from graph distortion and were considered to be hidden cracks or large void gaps in brick mortar joints.

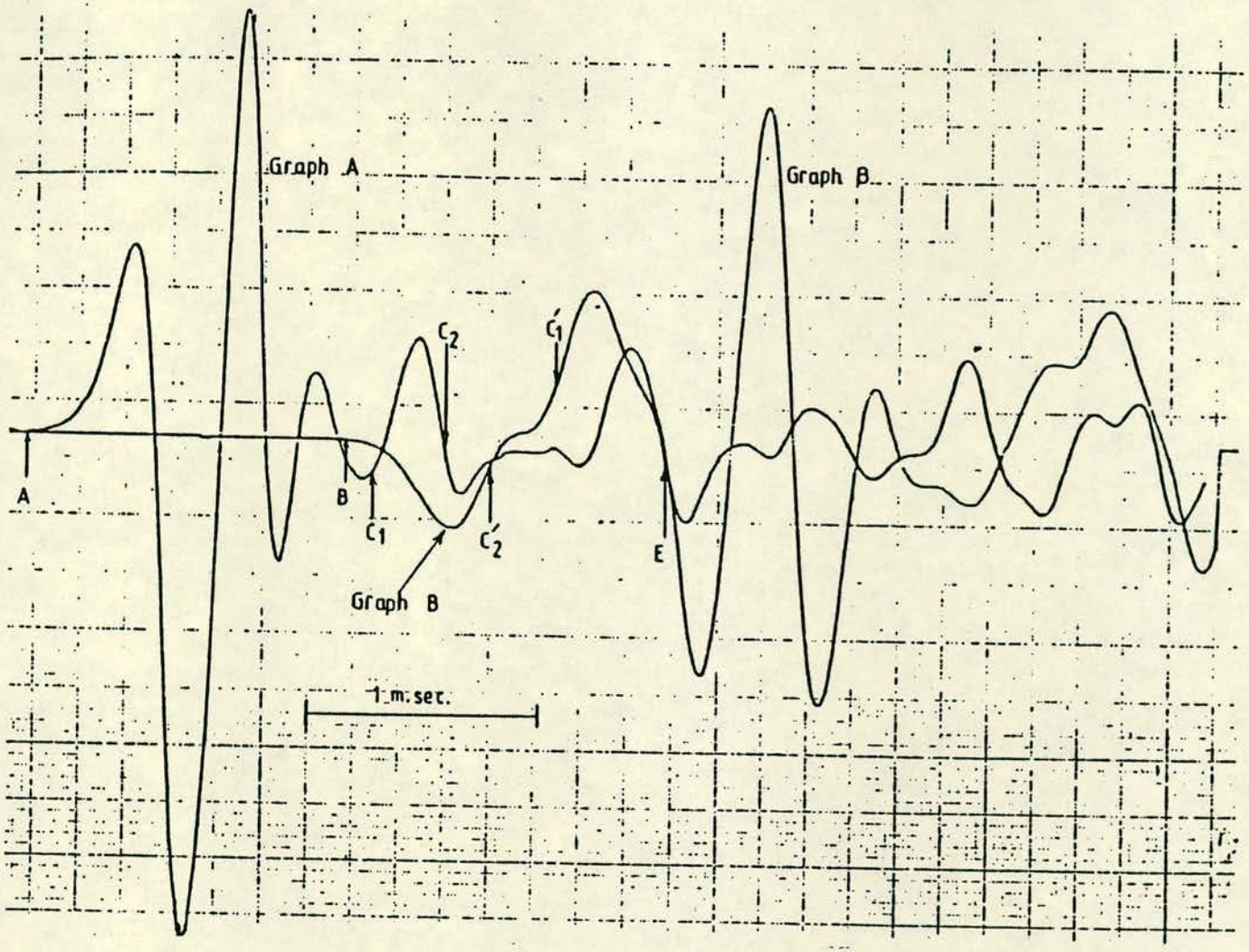

Fig. 5.8 Point C1-3

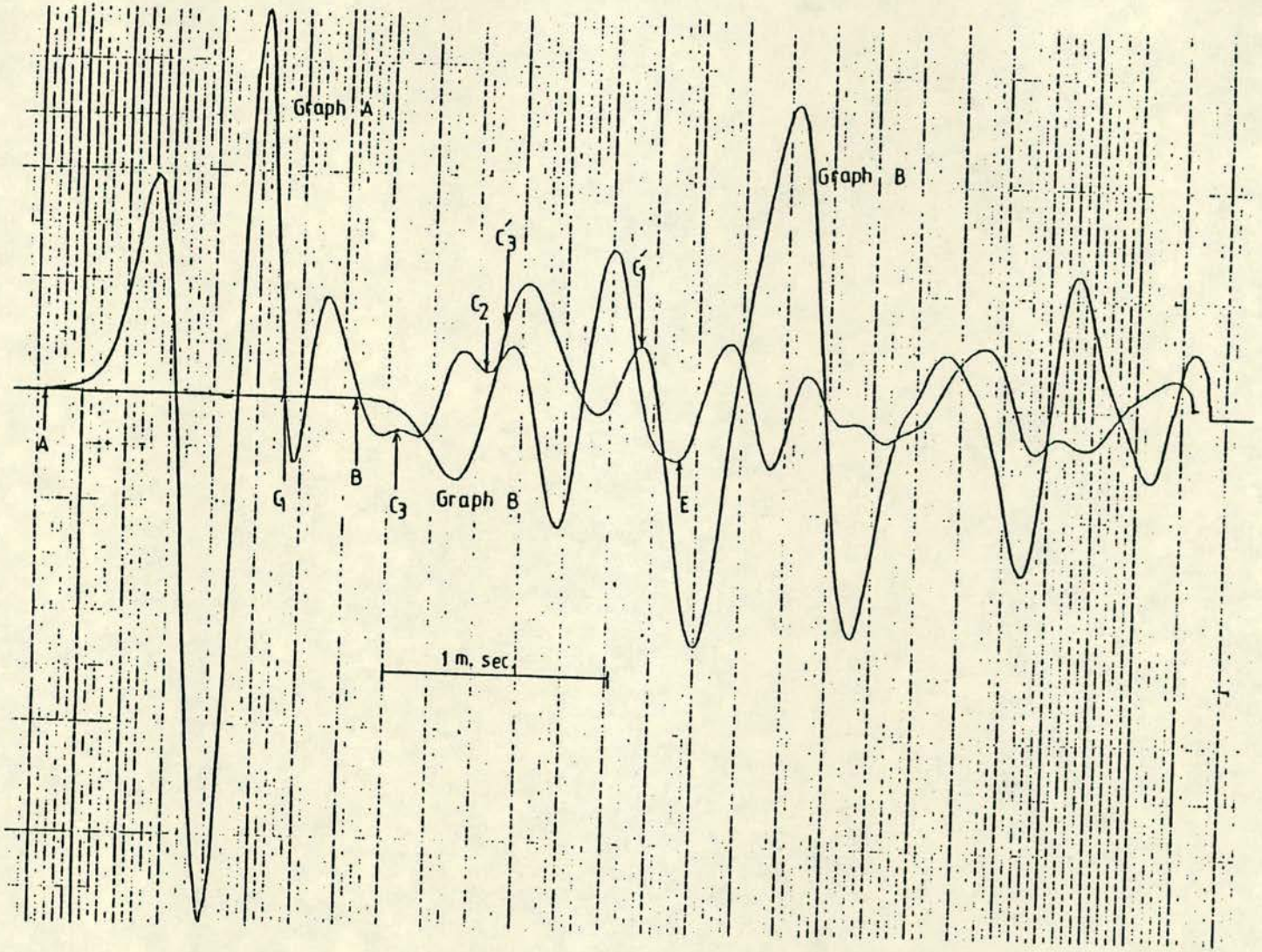

Fig. 5.9 Point C2-6

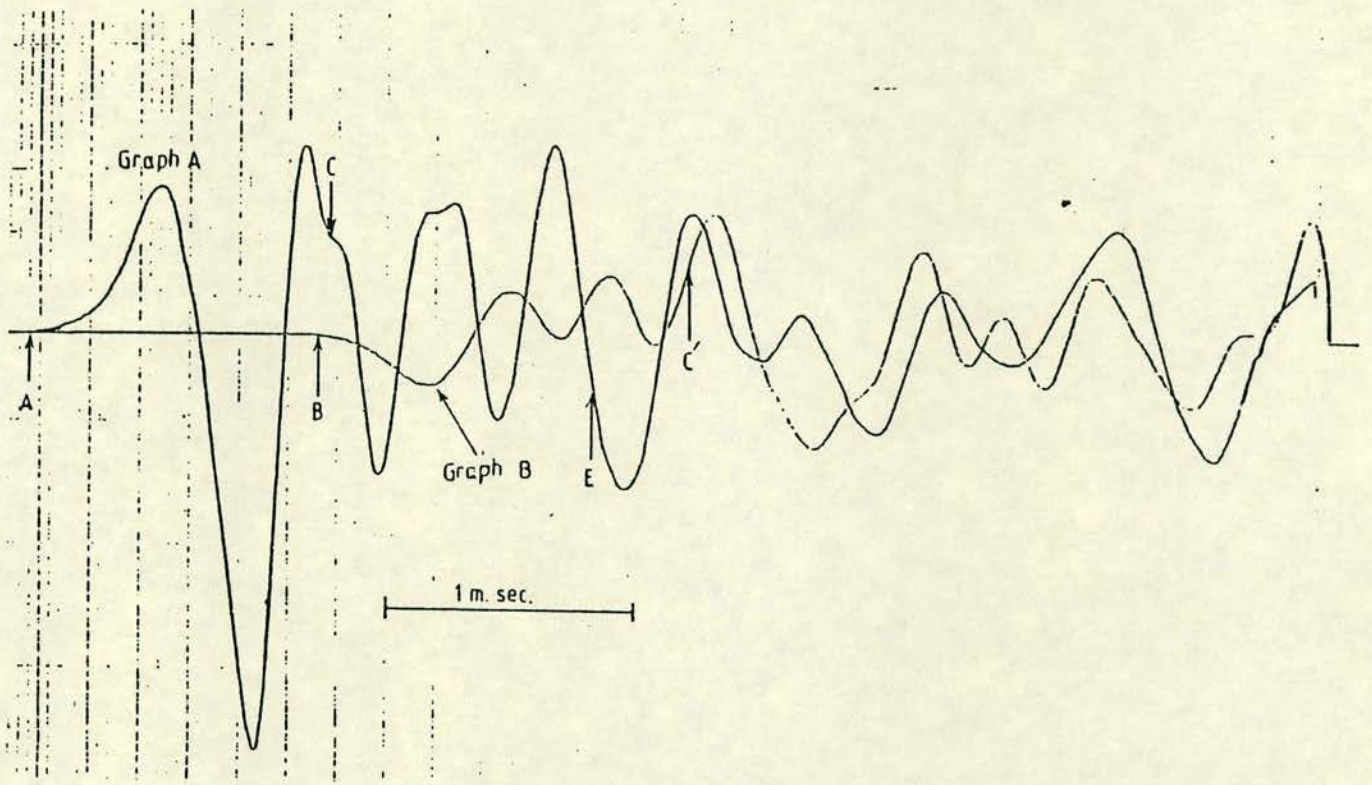

Fig. 5.10 Point B2-11

POINT	VEL_{AB} (m/s)	CRACK LOCATION							
		MAIN DIAGONAL CRACK			NEXT SEVERE CRACK			NOT OBSERVED DISCONTINUITY	
		ass'd.vel. (m/s)	obsr'd. ℓ_{AC}(m)	msr'd. ℓ_{AC}(m)	assm'd. vel.(m/s)	obsr'd. ℓ_{AC}(m)	msr'd. ℓ_{AC}(m)	assm'd. vel.(m/s)	ℓ_{AC}(m)
C1-1	2900	3000	3.17	3.15	3000	2.48	2.40	3100	1.50
C1-2	2900	2.97	2.95					3100	1.80
C1-3	2600	2.58	2.60					3100	2.30
C1-4	2700	3000	2.48	2.50				3100	1.60
C1-5	2400	3100	2.28	2.35	2700	2.70	2.70		
C1-6	2600	3100	2.02	1.95	2900	2.25	2.30		
C1-7	2600	2900	2.14	2.05	3100	1.91	1.90		
C1-8	2600	3000	1.92	1.90	3100	1.75	1.65	2800	2.50
C1-9	2700	3000	1.67	1.65	3100	1.60	1.50		
C1-10	2600	3100	1.50	1.60		3.42		2900	2.00
C1-11	2800	3100	1.08	1.10	2900	1.85	1.85	2800	2.30
C1-12	2700	3100	0.90	0.90	2800	1.76	1.70		
C1-2 Cav.	2800	3600	2.58	2.50					
Conc. Base	4000								

Table 5.3 Experimental Results of Wall C1

POINT	VEL_{AB} (m/s)	CRACK LOCATION							
		MAIN DIAGONAL CRACK			NEXT SEVERE CRACK			NOT OBSERVED DISCONTINUITY	
		ass'd.vel. (m/s)	obsr'd. ℓ_{AC}(m)	msr'd. ℓ_{AC}(m)	assm'd. vel.(m/s)	obsr'd. ℓ_{AC}(m)	msr'd. ℓ_{AC}(m)	assm'd. vel.(m/s)	ℓ_{Ac}(m)
C2-1	2700	2.52	2.50					3100	1.75
C2-2	2700	2900	2.40	2.40				3100	1.90
C2-3	2700	2900	2.05	2.20				3000	1.65
C2-4	2600	3100	1.92	1.90					
C2-5	2600	3100	1.68	1.70	2600	3.27	3.20		
C2-6	2600	3100	1.55	1.60	2900	3.03	2.90		
C2-7	2700	3000	1.34	1.35	2800	2.42	2.40		
C2-8	2500	3000	1.17	1.20	2800	2.23	2.10		
C2-9	2700	3100	1.02	0.95	2800	1.98	1.90		
C2-10	2600	3100	0.87	0.90	2700	1.82	1.90		
C2-11	2900	3100	0.70	0.70	2900	1.57	1.60		
C2-12	2800	3100	0.55	0.65		1.43		3000	1.80
C2-5 Cav.	2700	3600	1.02	1.00	3000	1.98	1.85		
C2-4 Cav.	2800	3500	1.34	1.35					
C2-3 Cav.	2900	3600	1.68	1.60					
Conc. Base	4800								

Table 5.4 Experimental Results of Wall C2

POINT	VEL_{AB} (m/s)	CRACK LOCATION							
		MAIN DIAGONAL CRACK			NEXT SEVERE CRACK			NOT OBSERVED DISCONTINUITY	
		ass'd.vel. (m/s)	obsr'd. ℓ_{AC}(m)	msr'd. ℓ_{AC}(m)	assm'd. vel.(m/s)	obsr'd. ℓ_{AC}(m)	msr'd. ℓ_{AC}(m)	assm'd. vel.(m/s)	ℓ_{AC}(m)
B2-1	2700	3000	2.15					3100	0.95
B2-2	2600	2900	2.02					3100	1.15
B2-3	2600	2900	1.55	1.70				3100	0.85
B2-4	2600	3100	1.39	1.30					
B2-5	2500	2900	1.22	1.20				3100	0.30
B2-6	2300	3100	1.07	1.05	2600	2.36	2.15	2800	**1.70
B2-7	2400	3100	0.95	0.90	2600	2.05	1.70		
B2-8	2400	3100	0.84	0.85	2700	1.75	1.55		
B2-9	2300	3100	0.69	0.70	2700	1.53	1.60		
B2-10	2300	3100	0.64	0.70	2500	1.44	1.50		
B2-11	2300	3100	0.45	0.50				2700	1.55
B2-12	2300	3100	0.26	*0.40					
B2-2 Cav.	2800	3200	1.55	1.60					
Conc. Base	3900								

* Difficult to interpret, multiple fractures, close to the toe
** Observed crack. (ℓ_{AC}) observed = 1.67 m

Table 5.5 Experimental Results of Wall B2

MATERIAL	AVERAGE TRANSMISSION VELOCITY M/S
Good Brickwork (Uncracked)	3100
Poor Brickwork	2500 - 2700
Uncracked Reinforced Cavity	3500
Cracked Reinforced Cavity*	2700 - 3000
Structural Concrete	4500
Granite Masonry Pier 1	3450
Granite Masonry Pier 2	3370
Red Sandstone Masonry Pier	1970
Yellow Sandstone Masonry Pier	2040
Whinstone Masonry Pier	2500
White Sandstone Pier	1700

Table 5.6 Transmission velocity values of different materials tested

* Depends on severity of cracks

As a result of this investigation it has been demonstrated that it is possible to distinguish more than one crack or discontinuity from a relatively complex trace, provided that they are well defined and not very closely spaced.

The results obtained for the reinforced collar joint indicated the presence of the observed cracks at the same level in the brickwork. This confirms the fact that shear cracks were developed through the entire thickness of the wall. This was not, however, true for the less severe cracks due to the presence of heavy reinforcement in the collar joint.

The transmission velocity for an uncracked reinforced collar joint was estimated to be 3500 m/s. This was obtained by comparing the transmission velocities of cracked brickwork and reinforced

collar joints and the transmission velocity of uncracked brickwork, as an uncracked reinforced collar joint was not available for direct measurement.

MATERIAL	VELOCITY (Km/s)	SOURCE
Good brickwork	Ave. 3100	Lab Investigation - Chapter 5
Reinforced Cavity	3500	" " " "
Structural Concrete	>4000	Neville (72)
Dry Sandy Top Soil	200 - 300	Clayton (73)
Dry Sandy Clay	400 - 600	" "
Saturated Sandy Clay	1300 - 2400	" "
Water	1430 - 1680	" "
Limestone and Dolemite	4000 - 6000	" "
Sandstone	1400 - 4300	Runcorn (74) and Lab Investigation - Chapter 5
Steel	Rod: 5100)	Catchpool and Sutterly
	bulk: 6100)	(75)
Granite Masonry Pier	3300 - 3500	Lab Investigation - Chapter 5
Sandstone Masonry Pier	1700 - 2100	" " " "
Whinstone Masonry Pier	2500	" " " "

Table 5.7 Additional table of transmission velocity of different materials

Wall B2 showed a lower cracked transmission velocity, about 2500 - 2600 m/s on average, compared to 2700 m/s in walls C1 and C2. This was due to the fact that wall B2 had a shorter length and hence it was relatively more damaged during shear testing.

The results obtained for the reinforced collar joints and concrete beams, showed a wide scattering of the transmitted compression wave, although concrete and mortar are considered to be

relatively homogeneous materials. This was mainly due to the presence of the reinforcements in the concrete beams and collar joints.

The transmission velocities obtained for the stone masonry piers can be used as estimates of good quality masonry. It must, however, be noted that different masonries of the same stone contruction may have different sonic or transmission velocities. The workmanship, mortar quality, stone/masonry ratio value (76) and moisture condition of the masonry do have a significant influence upon the transmission velocity measurements.

The other point that must be taken into account when testing masonry structures is that the transmission velocity through the masonry is not the average value of the transmission velocities through the stone/brick and the mortar. Usually there are cavities and unfilled mortar joints particularly in the vertical joints. This has some effects on the transmission velocity obtained. Indeed, when the masonry piers were tested at different points, different velocities, but in the same reasonable range were obtained. The major factor for this variation was the presence of unfilled vertical joints.

5.6 Limitations of Work

The use of this technique in evaluating the quality of masonry as a composite material and its use in fault detection in stone or brickwork structures, is undoubtedly faced with some limitations. In this work only transmission velocity, as an indication of the quality of masonry, and studying of a time domain signal are utilised. Use of the equipment reported in this work is limited only to a time domain analysis. To utilise other techniques, for example a frequency analysis one, requires use of more sophisticated and expensive equipment.

The following are some of the limitations experienced in carrying out the reported work:

(1) Only major discontinuities such as large cracks or air voids can be detected.

(2) In the event of the presence of multiple cracks, only the first two or three cracks are detectable. The reflection from further away cracks make the later parts of the signal very complicated.

(3) When there is one side of the masonry available for testing, only one signal, for each point, is obtained. A second signal from transducer B is not available for cross-checking the results obained from first signal.

(4) The shorter the transmission length, the larger the error in measuring the transmission velocity. After exciting a point close to transducer A on the masonry, it will take a time t till transducer A is triggered. At the same time the wave has travelled twice that distance along the length of the masonry since the longitudinal wave velocity is twice that of the surface wave (65,66).

The transmission velocity obtained corresponds to a shorter length of the masonry and hence an overestimation of the actual velocity is obtained.

To overcome these limitations other methods, for example frequency analysis technique, must be exploited. The use of the frequency domain method and the relevant equipment is discussed in the later chapters.

5.7 CONCLUSIONS

Despite the limitations facing this technique, the following conclusions can be made with relative confidence:

(1) This technique can be applied to investigate the presence of major discontinuities in brick masonry as reported in this work.

(2) The use of two transducers is preferred for cross-checking the presence of discontinuities.

(3) Measurement of transmission velocity can be used to give an indication of the relative strength and quality of the material.

CHAPTER SIX

DEVELOPMENT IN SIGNAL PROCESSING AND ANALYSIS

6.1 INTRODUCTION

In the past few years there has been ongoing research and developments in digital analysis methods. Now with the continuing advancements being made especially in this area of technology, the use of digital techniques in solving problems is becoming more and more widespread. The old conventional analog methods are found to be time consuming and comparatively expensive. With a series of developments in the component industry and particularly the developments in the semi-conductor industry, digital analysers have become more economically feasible. As a result of this, in the past few years, several systems having Fast Fourier Transform, FFT, as their operating base, have been introduced to the commercial market. Their operating principle is based on sampling the captured data rather than continuous data and they are finite instead of being infinite.

6.2 DIGITAL ELECTRONICS

As mentioned above, digital electronic analysers sample analog waveforms at discrete time intervals and have Fast Fourier Transform, FFT, as their operating principle. The function of this Fourier Transform integral pair is to provide a means of transforming a time function f(t) into its complex function F(w), and back again (77). In other words, the essence of Fourier Transform is the decomposition of a waveshape into the sum of sinosoids. This is if the time domain history of the signal, f(t), is known, using the Fourier Transform, the amplitudes of the component sines and cosines can be found and be plotted in the frequency domain. See Fig. 6.1.

The Fourier Transform integral pair can be written as (78):

$$F(f) = \int_{-\infty}^{\infty} f(t)e^{-J2\pi ft}dt \quad \text{i.e. resultant frequency function} \qquad (6.1)$$

$$f(t) = \int_{-\infty}^{\infty} F(f)e^{Jft}df \quad \text{i.e. time domain function} \qquad (6.2)$$

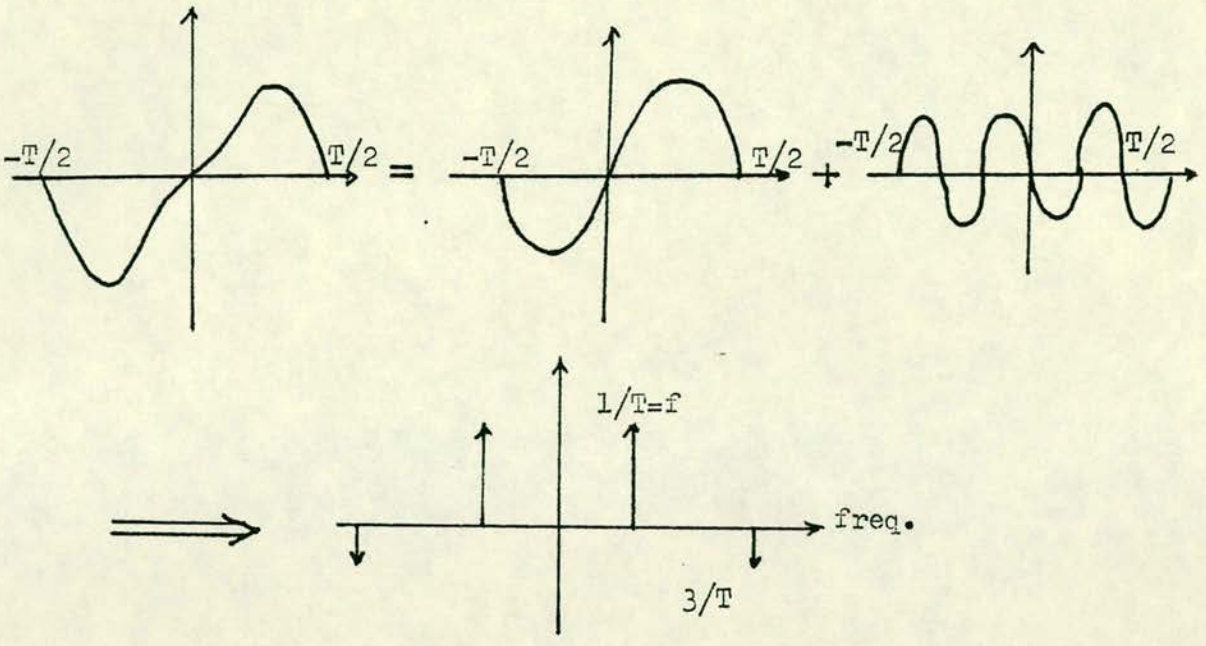

i.e. Complex waveform = sum of two sinosoids F.T. diag.

Fig. 6.1 Continuous F.T. (based on ref. 78)

In order to sample a finite length of a waveform, a truncation of its data is necessary. The Discrete Fourier Transform, DFT, was developed to handle this sample truncated data (77). The DFT equivalents, which are the summation forms of the two equations 6.1 and 6.2, can be written as:

$$F(k) = \frac{1}{N} \sum_{n=0}^{N-1} f(n) e^{-J2\pi nK/N} \qquad \text{i.e. frequency discrete function (6.3)}$$

$$f(n) = \sum_{K=0}^{N-1} F(k) e^{J2\pi nK/N} \qquad \text{i.e. time discrete function (6.4)}$$

However, in the digital analysers, these functions are calculated and plotted in real, imaginary or magnitude form. That is, the analyser considers the above functions in trigonometric forms rather than the exponential form described above. In this form, the function is a complex spectrum and is written as follows:

$$F(k)\ \text{real} = \frac{1}{N} \sum_{n=0}^{N-1} f(n)\ \text{Cos}\ (2\pi nk/N) \qquad (6.3.1)$$

$$F(k)\ \text{imaginary} = \frac{1}{N} \sum_{n=0}^{N-1} f(n)\ \text{Sin}\ (2\pi nk/N) \qquad (6.3.2)$$

And the Fourier amplitude, or magnitude is plotted as the square root of the sum of the squares of the two above transforms, i.e.

$$F(k)\ \text{mag.} = [(F(k)\ \text{real})^2 + (F(k)\ \text{imag}))^2]^{\frac{1}{2}}$$

It must be noted that the computation of the Discrete Fourier Transform involves multiplication and additions proportional to the square of the number of data points, i.e. N^2. For this reason, in the digital analysers the DFT calculations take longer by increasing the points.

The advantages of FFT analyers are numerous. Using these types of analysers, very good linearity of both frequency and amplitude, extreme stability, easy analysis, linear averaging, reference memories, spectrum comparison and so on can be obtained. In addition, they are easily connected to other types of digital equipment. This will clearly allow further treatment of data and hence obtaining more detailed and accurate results. It also enables one to analyse results with a speed of several spectra per second and the results are reliable and reproducible. However, there are a few limitations, for example time limit and aliasing. These can easily be avoided when the assumption on which the Discrete Fourier Transform work and the approximations involved, are known (79).

6.3 SIGNAL PROCESSING

Modern digital FFT analysers which work on the principle of fast and efficient calculation of Discrete Fourier Transform, perform in both time and frequency domain. This is a direct calculation in a digital processor. What the Discrete Transform basically does is process the time signal in blocks of data. Samples of the time signal are stored in a digital memory, and when this is filled up, the whole memory is transformed into the frequency domain as one block. Now to achieve discrete frequency components, this block is assumed to represent one period of a periodic signal (77).

It must be noted that both time compression and FFT analysers work only on a small part of the time signal and treat this as part of a periodic signal. The reason for this is that the original input signal has been "time limited" before the analysis. This time limitation has important consequences on the result of the analysis in both time compression and FFT analysers. These effects are sometimes more pronounced with an FFT analyser.

Another problem which may be encountered during signal processing is the occurrence of aliasing. Aliasing occurs if a waveform is undersampled, e.g. in the example illustrated below, undersampling has caused the "alias" or apparent frequency to be much lower than the actual waveform.

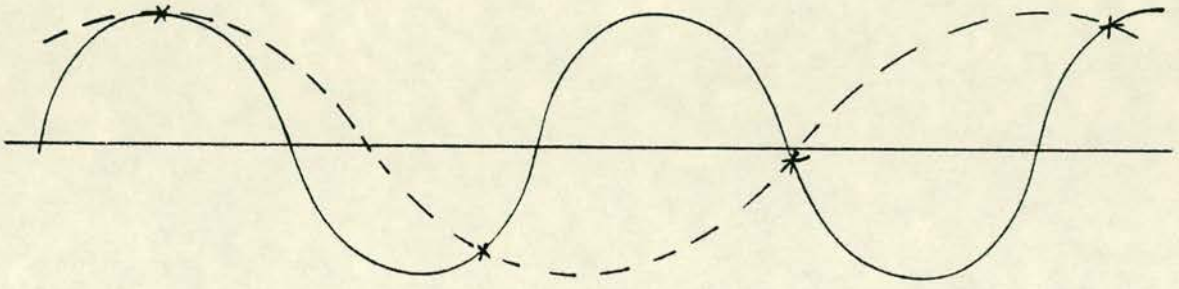

Fig. 6.2 Aliasing occurrence due to undersampling

To overcome the problem of aliasing, the sampling theory requires a sampling rate of slightly more than twice the signal frequency (80).

Now knowing the principle of signal processing and its possible difficulties, it must be said that the process of signal analysis is based on two principle methods. They are:

(a) processing time domain functions.
(b) processing frequency domain functions.

Each of these two principle methods employ their own functions and relevant applications. For the purpose of this work only a limited number of these functions are discussed and their relevant applications and advantages are mentioned.

6.3.1 Time Domain Functions

The two main time domain functions used in the proceeding work are auto correlation and cross correlation functions. Each one has its own advantages and relevant applications, i.e. detection of echoes (or reflections) in a signal using the auto correlation function and identification of transmission paths using the cross correlation function.

6.3.1.1 Auto correlation

The auto correlation function is a measure of how similar a time signal a(t) is with its time delayed replica a(t + τ) where τ is the amount of delay between the time signal a(t) and its displaced replica a(t + τ). Therefore this function is a very good detector of periodicity within a signal. The mathematical definition of the function is as follows:

$$R_{aa}(\tau) = \lim_{T\to\infty} \frac{1}{T} \int_{T} a(t)a(t + \tau)dt \qquad (6.5)$$

The discrete form of this function is:

$$R_{aa}(\tau) = \sum_{k=0}^{N-1} a(k)\ a(k + \tau) \qquad (6.5.1)$$

It is noted that at τ = 0, the auto correlation function is always at a maximum. Also in practice, the normalised auto correlation function is usually used (42), and it is defined as follows:

$$\rho_{aa}(\tau) = [R_{aa}(\tau)]/[R_{aa}(0)] \qquad (6.6)$$

where

$$R_{aa}(0) = \lim_{T\to\infty} \frac{1}{T} \int_{T} a^2(t)dt \qquad (6.6.1)$$

and ρ_{aa} is called the auto correlation coefficient function, and R_{aa} is called the total power in the signal b(t).

The relevant applications of the auto correlation function are:

(1) To detect echoes or reflections in the signal: That is if there is an echo or reflection, for example from a void or crack, at a time delay of τ_1 in the signal, the auto correlation function will have a peak at $\tau = \tau_1$. The auto correlation value at this point will then be $R_{aa}(\tau_1)$ and its coefficient $\rho_{aa}(\tau_1)$ (see equations 6.6, 6.6.1 and 6.5). The coefficient $\rho_{aa}(\tau)$ is clearly a measure of the relative strength of the echo. This is an obvious application in fault detection of materials such as masonry concerned in this work.

(2) To detect periodic signals hidden in random noise: The reason for this is that the auto correlation function of a periodic signal is also a periodic function with a periodic delay time of T, 2T, 3T and so on. Therefore this periodic signal will correlate at the above delay times, T, 2T, 3T,..... Now, the interfering background noise has an auto correlation function which tends to zero with increasing delay time, and therefore the periodic signal can be detected. Fig. 6.3 shows a typical auto correlation coefficient function ρ_{aa} for an echo detection. Fig. 6.4 shows the conventional time-delayed spectrum of the same signal.

However, for this application, use of cepstrum is preferred, because the cepstrum is less sensitive to the shape of the autospectrum. A description of cepstrum method is given in section 6.4.

6.3.1.2 Cross correlation

The concept of cross correlation is applied to two separate waveforms. Its principle application is in the detection of similarity between the two signals in the time domain. The mathematical definition of it is:

$$R_{ab}(\tau) = \lim_{T\to\infty} \frac{1}{T} \int_T a(t)b(t + \tau)dt \qquad (6.7)$$

where a(t) and b(t) are the two separate signals as a function of time t with a delay time of τ.

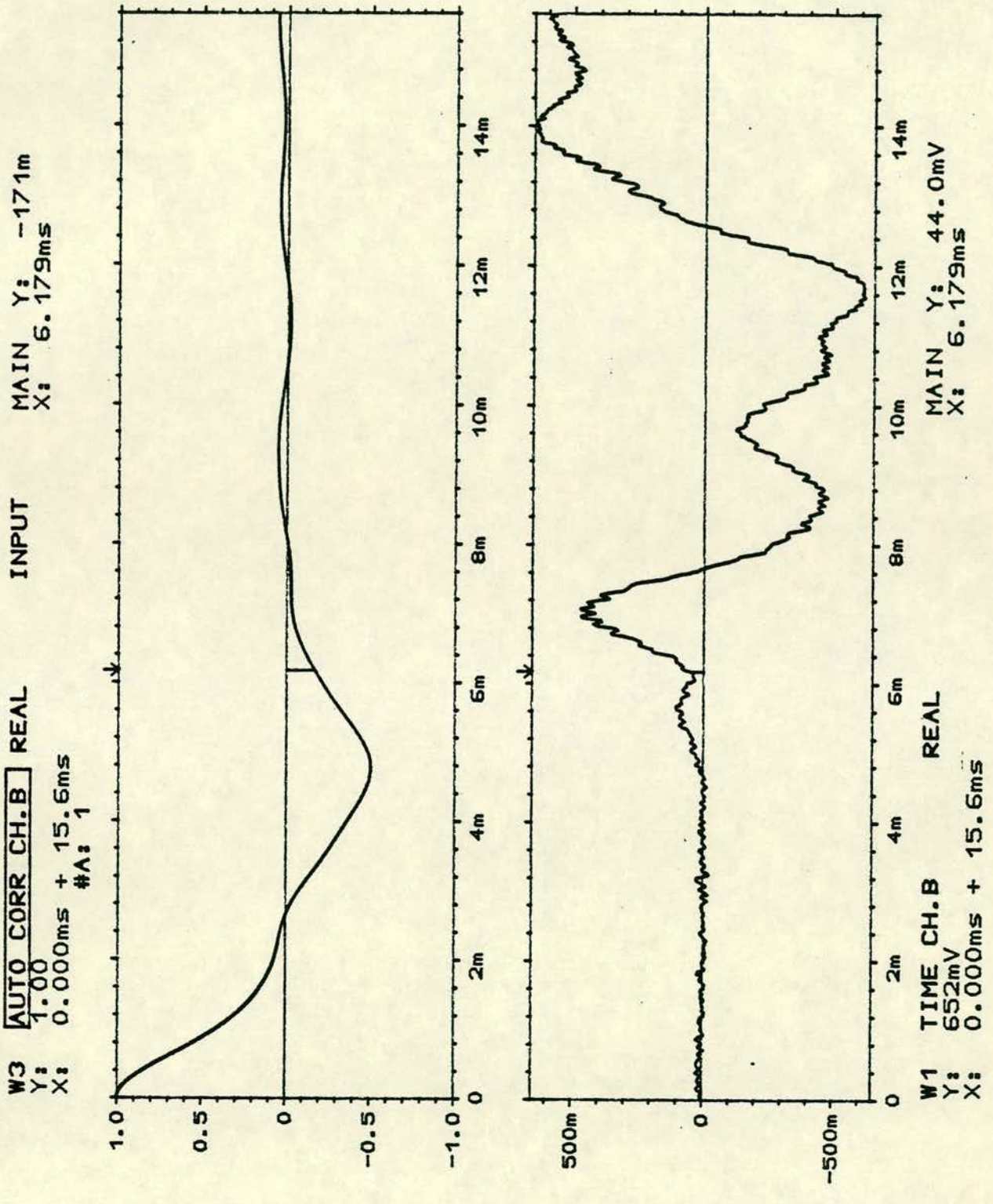

Fig. 6.3 A typical auto correlation spectrum for echo detection

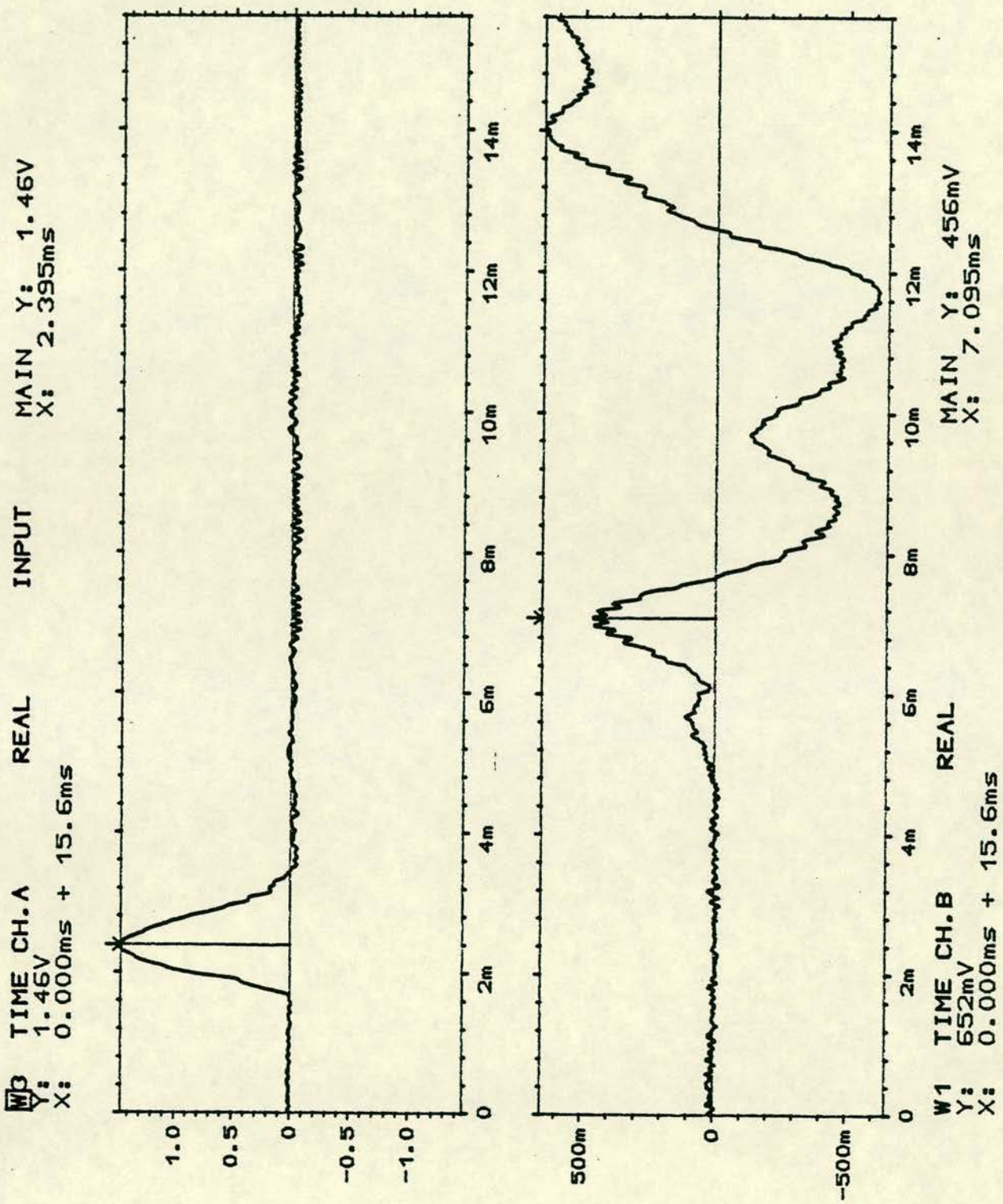

Fig. 6.4 A typical conventional time-delayed signal

$$R_{ab}(\tau) = \sum_{k=0}^{N-1} a(k)b(k + \tau) \qquad (6.7.1)$$

The practical interpretation of this function means that one waveform b is shifted in relation to the stationary waveform a, by equal time intervals of τ, and correlation takes place. In practice the cross correlation is also worked with its normalised form which is:

$$\rho_{ab} = [R_{ab}(\tau)]/[R_{aa}(0)\ R_{bb}(0)]^{\frac{1}{2}} \qquad (6.8)$$

where $$\rho_{bb}(0) = \lim_{T\to\infty} \frac{1}{T} \int_{T} b^2(t)dt \qquad (6.8.1)$$

and ρ_{ab} is called the cross correlation coefficient function, and $R_{bb}(0)$ is called the total power in the signal b(t).

The obvious relevant applications of cross correlation functions are the following:

(1) Determination of signal reflection delays: That is if a signal is transmitted between two points, A and B. The cross correlation function $R_{ab}(\tau)$ between the two signals a(t) and b(t), at the two points A and B, will peak at the time delay corresponding to the transmission time τ between the two points.

It was noted that, during the analysis of the experimental results of this work, some complications due to the dispersive nature of the signal propagation in the masonry, for determining the transmission time between A and B, was encountered. However, the main use of this method in this work was to determine the presence of discontinuities, and as long as these discontinuities were relatively close to the point A, the complications due to dispersion were not significant, since not much dispersion took place.

(2) Identification of transmission paths: If there are several transmission paths between the two points A and B, there will

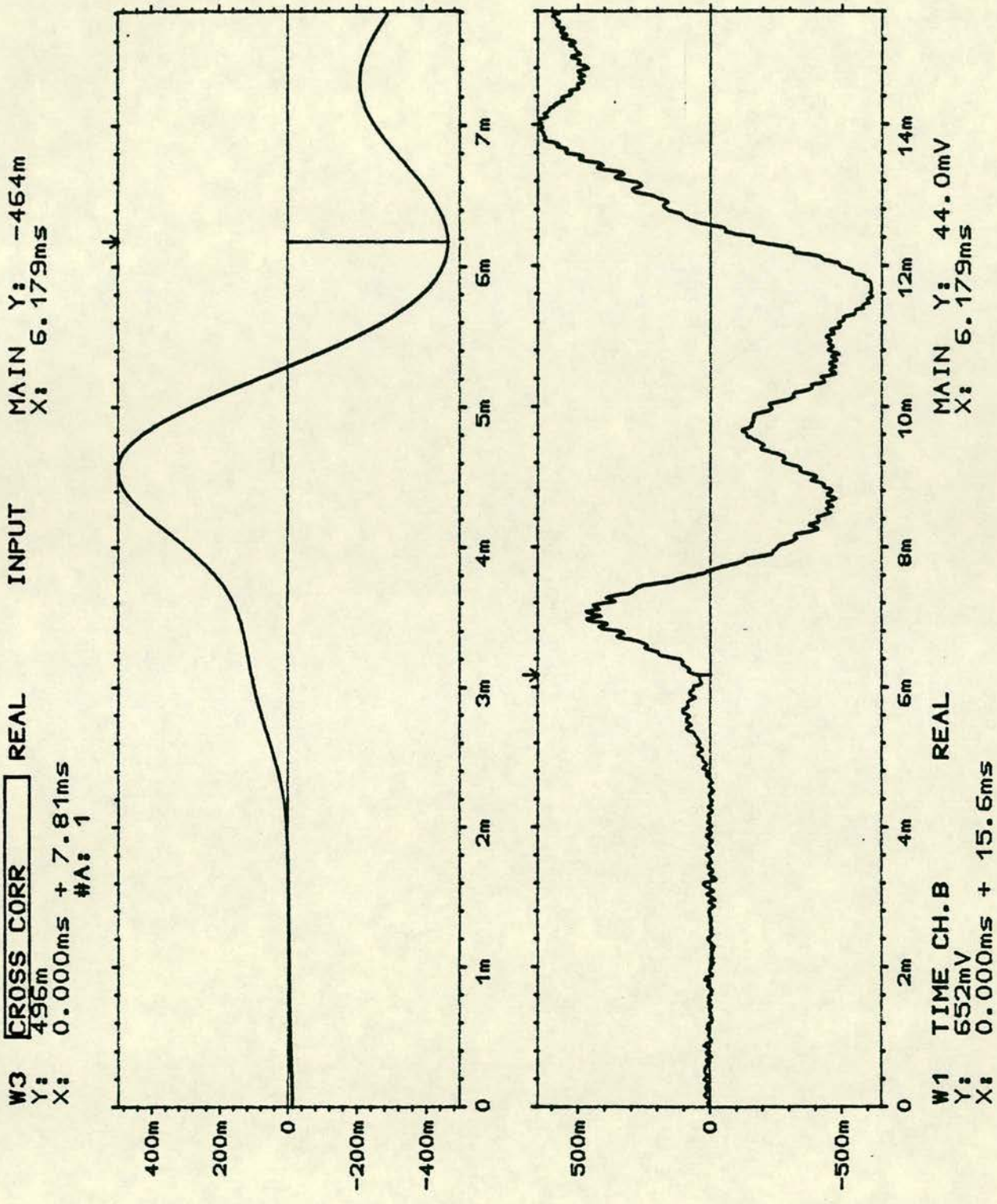

Fig. 6.5 A typical cross correlation spectrum for echo detection

be several maxima or minima peaks in the function and each peak corresponds to a transmission path. The magnitude of the peak is an indication of the relative strength of the transmission path. Here again it is recommended that the propagation should not be dispersive. Fig. 6.5 illustrates the first application above and shows a typical cross correlation coefficient function ρ_{ab} for time delay determination.

6.3.2 Frequency Domain Functions

6.3.2.1 Frequency response function definition and FFT analysers

One of the functions in the frequency domain most commonly used, in two channel system analysis, is the Frequency Response Function measurement of the system. What a dual channel FFT analyser does is to calculate the input and output functions of a system which describes its dynamic behaviour, assuming the system is linear.

Now if the input and output signals of a system are a(t) and b(t) respectively and their Fourier transform are A(f) and B(f), then in the frequency domain, the relation between input and output is given by:

$$B(f) = H(f).A(f) \qquad (6.9)$$

Therefore the frequency response function defined above in equation 6.9, as $H(f) = \frac{B(f)}{A(f)}$ describes the system in the frequency domain. The system can obviously be described in the time domain as well by h(t) = inverse Fourier transform of H(f). For the above function defined to be valid, several assumptions must be made so that the system can be described in terms of a frequency response function. They are:

(1) The system is stable, that is, it can respond with a limited amount of energy input when it is excited. Thus:

$\int_{-\infty}^{\infty} |h(t)|\, dt$ must be less than infinity.

2. The properties of the system are not changed with time, i.e. the system is time invarient. In a mathematical form:

$h(\tau + t) = h(\tau)$ and $H(f,t) = H(f)$ for $\infty < t < \infty$

3. The system is linear, that is, if the outputs of $a_1(t)$ and $a_2(t)$ are $b_1(t)$ and $b_2(t)$ respectively, then:

$a_1(t) + a_2(t) = b_1(t) + b_2(t)$

In other words, the function H(f) characterises the system independent of the signals involved.

Two common limitations sometimes encountered in practice are the violation of linearity assumption and time variations. In the first instance, the input signal may be so high in amplitude that the system will be excited beyond its range of linear behaviour. In the second instance, the system characteristics may change with temperature, pressure, humidity, etc. However, the two common problems mentioned hardly affect the system concerned in this work. This is due to the fact that masonry structures are so huge in size and resistant to short time effects of any temperature, pressure and linearity variation, that they are virtually considered non-effective for the purpose of this work.

It is worth mentioning here the advantages of using a dual channel FFT analyser. Firstly, it is possible to measure the frequency response function, even though there are some interfering signals, such as background noise, present in the input or output signal. Secondly, the estimated frequency response function will represent the best linear fit (in the least square form) to the system. The importance of this advantage becomes more clear when a non linear system is being analysed. In this case a best linear fit in the form of mathematical modelling is introduced. The estimated frequency response function will of course depend on the type of signals involved in the analysis.

To illustrate the use of the frequency response function-measurement, in practice, a more practical approach and its interpretation is followed here:

6.3.2.2 A practical approach to frequency response function and its interpretation

When a structure is subjected to vibration or excited by introducing a compression wave, i.e. applying a force to it, it will start vibrating with a certain frequency. This frequency depends on the structure's size, density, mechanical admittance and other resonance characteristics. Interpretation of the graph of mechanical admittance against frequency will lead to obtaining some useful physical characteristics of the structure and detection of some faults within its mass. To illustrate this, consider the diagram in Fig. 6.6.

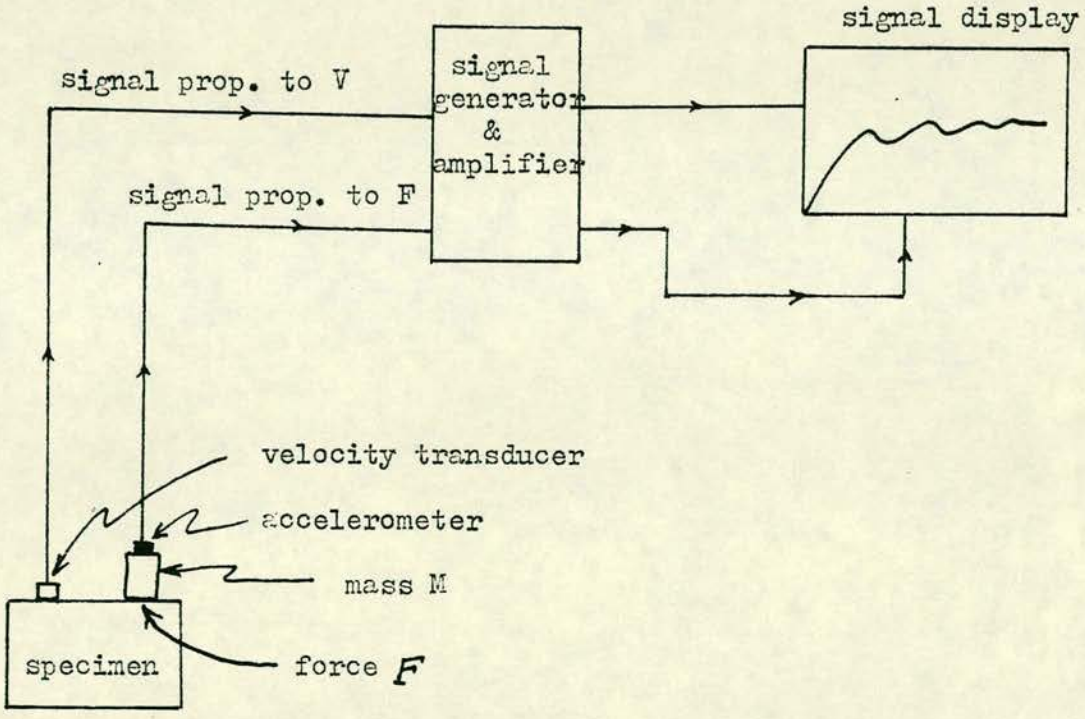

Fig. 6.6 Diagram of frequency testing equipment

Using the mass M, in the form of a built in load cell hammer, a force of F = Ma, where a is the acceleration of the hammer of mass M is applied. The acclerometer or the load cell built into the hammer is used to monitor the applied load. The velocity transducer

placed on the specimen, at the point being tested, is used to monitor the velocity of the structure at that point.

It is known that the movement of the structure at that point is a measure of the structure's excitation there. The compressional wave produced, travels longitudinally to the end of the structure and is reflected back to that point with a velocity of v which is dependent only on the density of the material of the structure. The velocity of the point tested is the resultant of the imposed and reflected waves (82).

The signal display X-Y recorder plots a signal proportional to mechanical admittance V_m/F_m against frequency f, where V_m is the maximum vertical velocity of the structure at the point of testing and F_m is the maximum vertical force applied at that point. Interpretation of the resulting graph gives a number of physical properties of the structure at the point of testing.

It must be noted that as the force is applied once to the testing point, the structure there is left to vibrate at a resonant frequency where $|(V_m/F_m)|$ is a maximum. However, due to energy absorbance by the surrounding material and damping effects of the structure itself, the amplitude of vibration is limited.

Consider that the structure at that point has a length L which is resting on or is in contact with an elastic very large infinite body. When a maximum force of F_m is applied and a maximum of velocity V_m is observed, it can be said that the resonant frequencies are spaced at equal frequency intervals of

$$\Delta f = \frac{V}{2L} \qquad (6.10)$$

where V = velocity of transmitted longitudinal plane wave
and L = length of the material along which the wave is propagated.

It is known and has been proved in practice that here, there exist two main possibilities (82):

(i) if the infinite elastic body is infinitely rigid, the lowest resonant frequency has a value of V/4L, Fig. 6.7(a).

(ii) if the elastic body is infinitely compressible, then the resonant frequency is very small, Fig. 6.7(b).

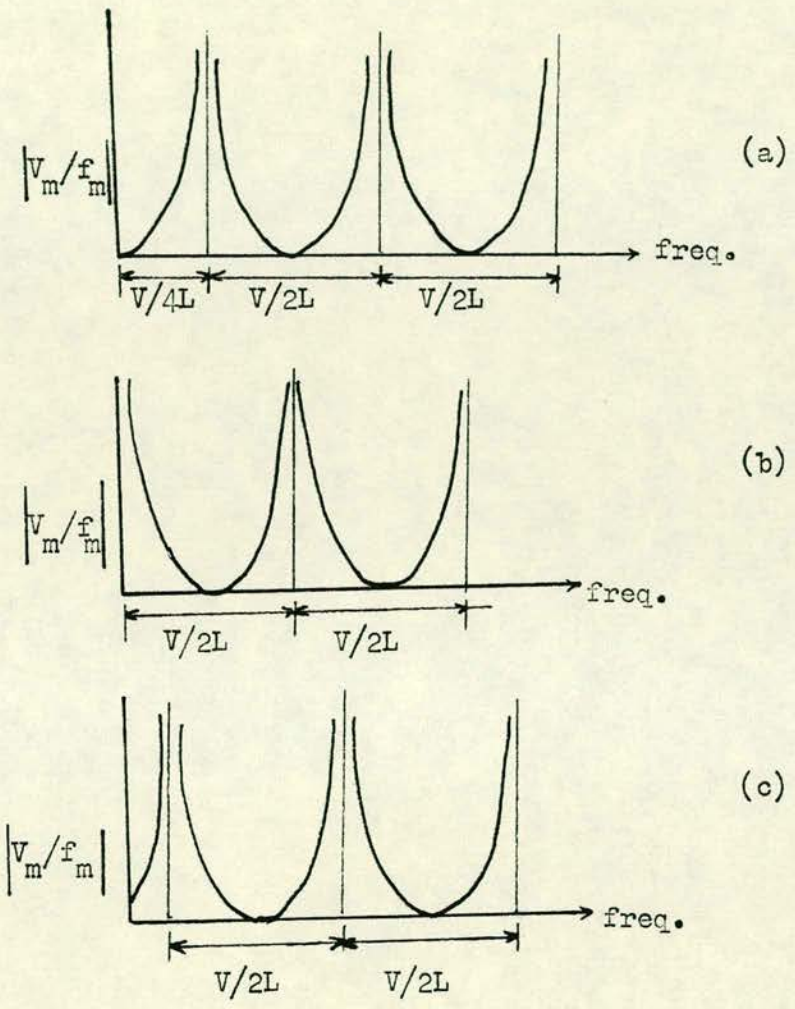

Fig. 6.7 Effect of compressibility of the infinite elastic body which is in contact with the structure under test. (a) infinitely rigid, (b) infinitely compressible, (c) intermediate rigidity or compressibility (based on ref. 82)

Also, as shown in Fig. 6.7(c), when the infinite contact body is an elastic one of normal compressibility the lowest resonant frequency has an intermediate value which is less than V/4L.

As a result of attenuation and damping effects of the structure

and the surrounding materials, i.e. in a real case rather than in an ideal undamped one, the response curve does not look like those in Fig. 6.7, but has a shape as shown in Fig. 6.8:

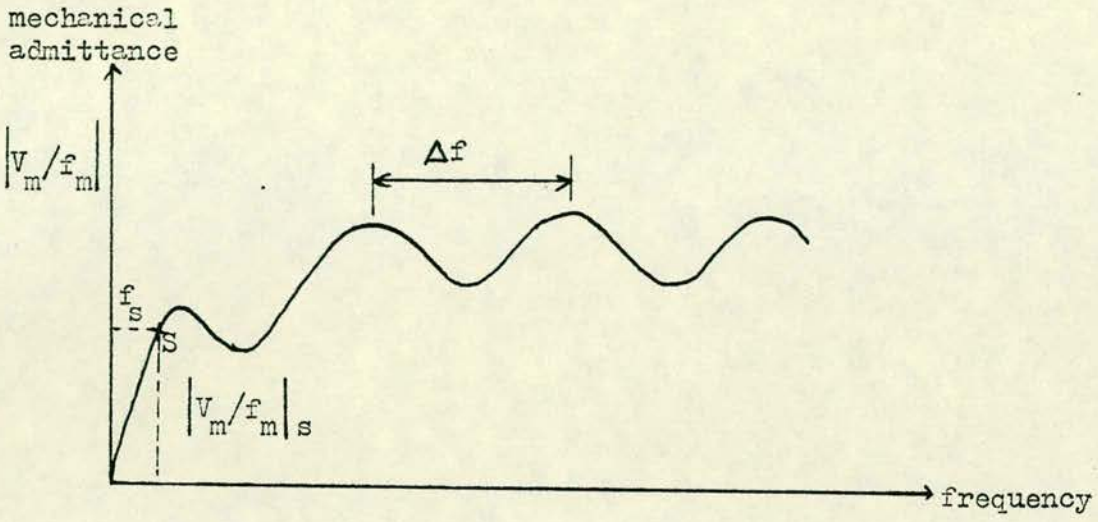

Fig. 6.8 Frequency response curve

Therefore the greater the attenuation, the smaller the difference between the maxima and minima of the curve in Fig. 6.8.

Apart from being able to estimate the degree of the compressibility of the base of the structure, there are several other physical properties to be obtained from the response curve. Here, two properties which may be of interest to NDT civil engineers are briefly outlined.

(1) When the structure is excited at low frequencies and other factors such as inertia effects are very small, the structure behaves like a spring, giving a straight line response at the start of the curve in Fig. 6.8. The inverse of the slope of that line is thought to be a measure of the apparent stiffness of the point being tested (82). It is given by:

$$E' = Kf_s / \left| V_m / F_m \right|_s \qquad (6.11)$$

where K is a constant

and f_s and $\left| V_m / F_m \right|_s$ are the coordinates of points s, on the response curve, beyond which the line is not straight any more.

(2) When there is an echo or reflection from a discontinuity, the reflected wave from that discontinuity is added to the reflected wave from the end of the structure. In other words, the body of the structure between the testing point and the discontinuity vibrates with a different resonant frequency. The two response curves are then superimposed and produce a resultant curve from which the resonant frequency of the structure between the testing point and the discontinuity can be obtained. If the velocity of the compression wave in that material is known, then using relationship (6.10), the length to the discontinuity in the structure can easily be obtained (see Fig. 6.9).

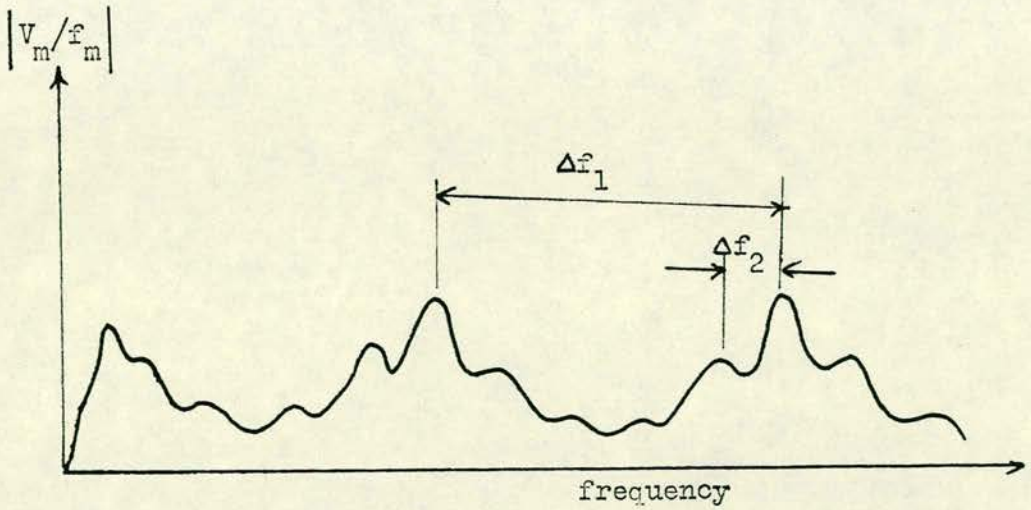

Fig. 6.9 The effect of the presence of a discontinuity on the frequency response curve

where the structure, at the point of testing, vibrates with a frequency of f_1 and the body of the structure between the testing point and the discontinuity vibrates with f_2.

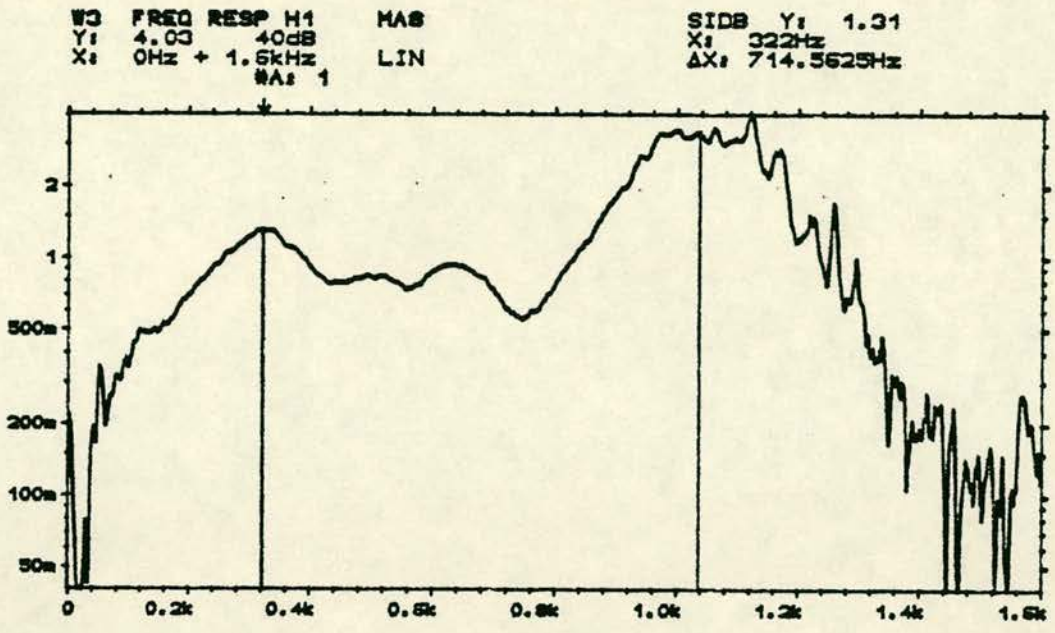

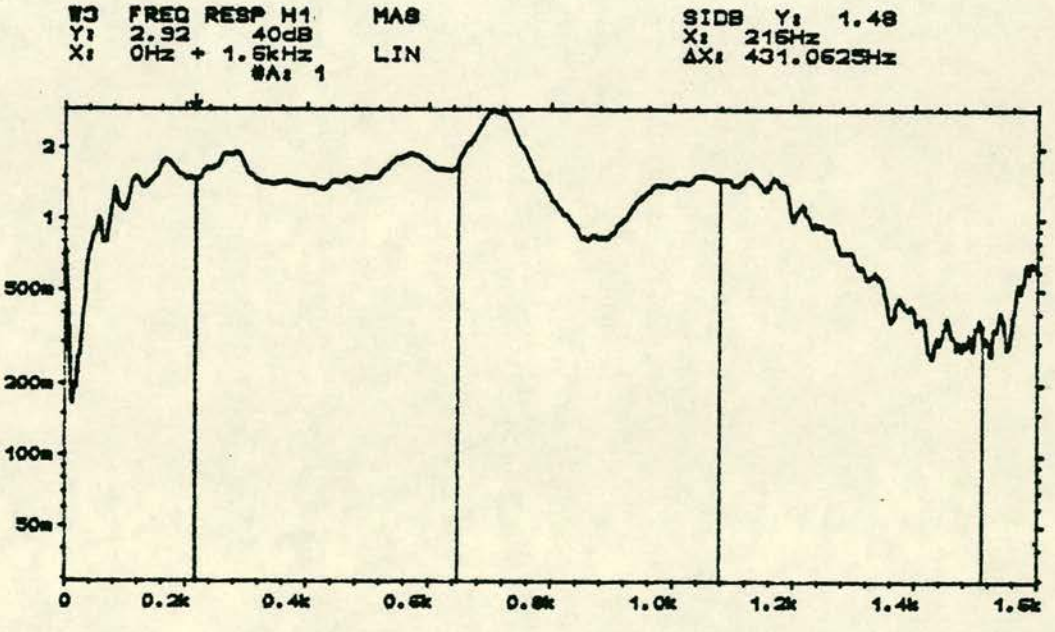

Fig. 6.10 Two typical frequency response curves

Fig. 6.10 shows a typical example taken.

6.4 CEPSTRUM ANALYSIS

The cepstrum is considered to be a spectrum of a logarithmic spectrum. Therefore it can be used for detection of periodic structure such as harmonics, or the effects of echoes in the spectrum. The reason for describing cepstrum as above is not known. A later definition of cepstrum as "the inverse Fourier transform of the logarithmic power spectrum" was introduced and apparently has some connections with the auto correlation (83).

The cepstrum was first introduced in the early 1960s, and it was defined as "the power spectrum of the logarithmic power spectrum". Its main application at that time was the analysis of seismic signals, because of its ability to give information about echoes useful in seismology (84).

Use of the cepstrum analysis technique with a modern FFT analyser has proved to be a highly valuable method of thickness measurement and echo detection in bridge testing.

6.4.1 Basic Theory

The basic definition of the cepstrum is:

$$C_p(\tau) = \text{inv.F}(\log F_{xx}(f)) \qquad (6.12)$$

where $F_{xx}(f) = \left|F(f_x(t)\right|^2$ (6.12.1)

$f_x(t)$ is time signal and F indicates the forward Fourier transform.

The above is called the power cepstrum and there exists a complex cepstrum defined as follows:

$$C_c = \text{inv.F}(\log F_x(f)) \qquad (6.13)$$

where $F_x(f) = F(f_x(t) = a_x(f) + ib_x(f)$ (6.13.1)

A practical problem which arises is whether the power cepstrum should be one-sided in frequency, i.e. whether negative frequency components should be set to zero or not. It concludes that for some diagnostic applications, it is more advantageous to use one-sided spectra. In the case of thickness measurements of bridge abutments, it was found useful to use two-sided spectra, otherwise some echoes would not have been detected.

It has been shown (83) that if a cepstrum has a frequency spectrum as shown in Fig. 6.11(a), its harmonic series is a series of positive harmonics as shown in Fig. 6.11(a). However, if the periodic components in the cepstrum are displaced a half spacing, the cepstrum will be a series of alternative harmonics, with the first one negative.

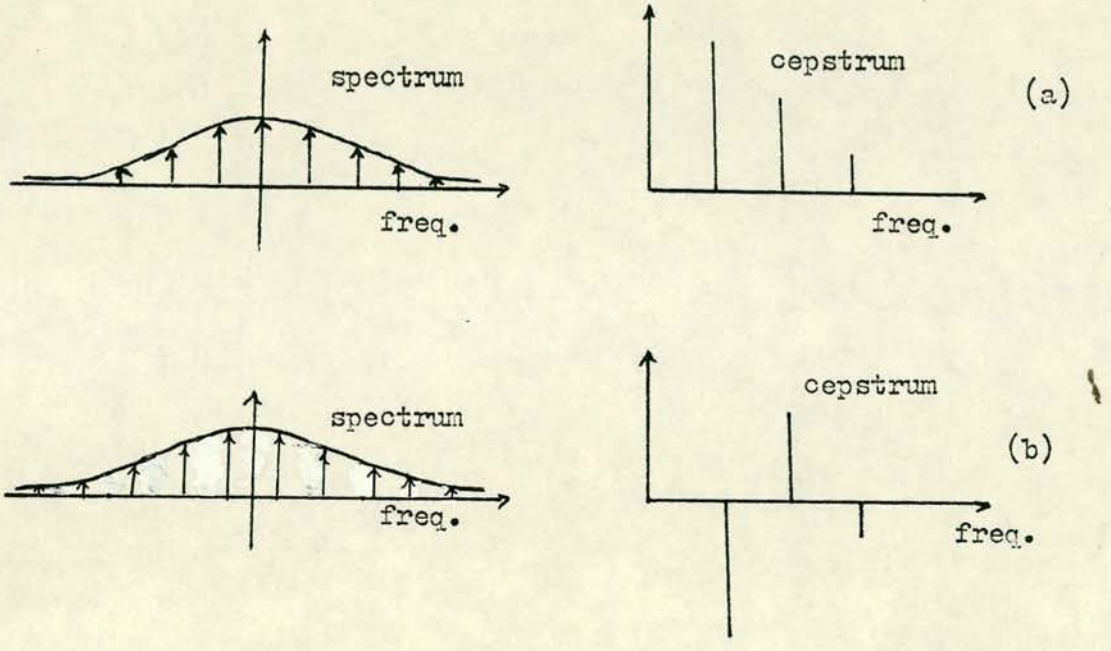

Fig. 6.11 Cepstrum of (a) a harmonic series, (b) an odd harmonic series

6.4.2 Applications of Cepstrum

One of the most commonly used application of cepstrum is echo detection which is very useful in fault detection in NDT of civil engineering materials and structures. The principle of this application is that echoes cause a periodic shape to the cepstrum

signal and it is easy to locate them. Also in the case of a non perfect and non ideal reflection, the cepstrum contains the impulse response of the reflection and it can therefore be used for measuring some properties of the refletive surface. This is another application of the cepstrum.

The essence of the main application mentioned above is that when a periodicity exists in the spectrum, it transforms by an inverse Fourier transform to a series of harmonics in the cepstrum, with a spacing equal to τ. τ is the delay time between these harmonics. Therefore, it is much easier to detect the presence of delay time echoes in the cepstrum than in the auto correlation function. There in the auto correlation function, even an ideal and perfect reflection gives a scaled down version of the signal at the echo delay time.

6.4.3 A Practical Approach to the use of Cepstrum in Civil Engineering

Using a dual channel modern FFT analyser where the cepstrum can be utilised, an echo within a spectrum can easily be located. The use of the digital liftering program increases the reliability of the concluded results. Digital liftering, equivalent of digital filtering, in cepstrum, enables the user to eliminate certain unwanted frequencies from a time domain signal. By calculating the Inverse Fourier Transform, the liftered frequency is then drawn on a frequency domain axis known as liftered spectrum. It includes all the frequencies except those which were selected out.

The cepstrum and the liftered spectra are then studied to locate the presence of a reflected echo or signal. To illustrate this the following example is considered:

A specimen of the size shown in Fig. 6.12 is to be tested. The length of the specimen is ℓ_{AB} and there is a void or crack at distance ℓ_{AC} along the length of the specimen:

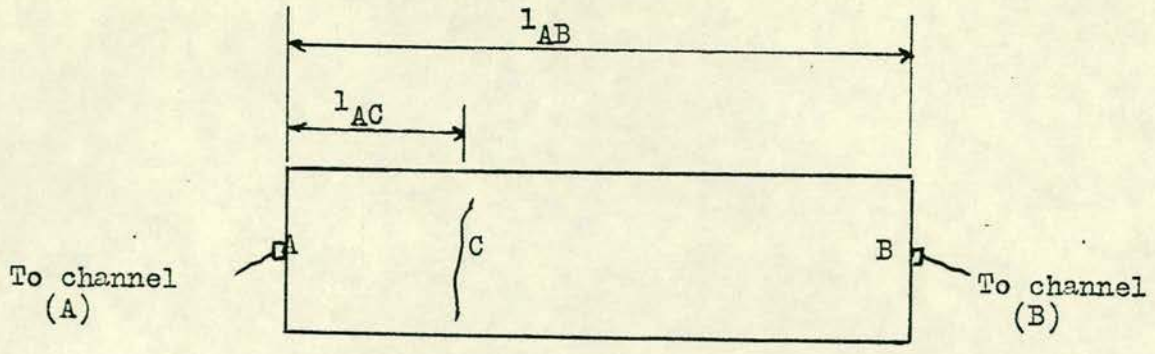

Fig. 6.12 Use of cepstrum in echo detection

When a compression wave is generated at point A, the whole structure between A and B vibrates with a resonant frequency of f_{AB}, and that part of the structure between A and C with a resonant frequency of f_{AC}. The resultant cepstrum and the liftered echo spectra are shown in Fig. 6.13.

There are two ways of liftering the unwanted echo. The first method is to use the short pass lifter of the analyser. In this way, initially the first harmonic frequency is taken into account and the rest are ignored (Fig. 6.13(a)). Then the next frequency is included (Fig. 6.13(b)). Each time the spectrum of the liftered frequencies is produced and is shown in the form of liftered spectrum $(f_{AC})_1$ (Fig. 6.13(a)), liftered spectrum $[(f_{AC})_1 + (f_{AB})_1]$, liftered spectrum $[(f_{AC})_1 + (f_{AB})_1 + (f_{AC})_2]$ and so on.

The second method known as long pass liftering instead of incorporating the first frequency and excluding the rest, excludes the first and includes the rest. In this way a more complicated signal is produced and the accumulated frequencies of the minute and small echoes are present. That is why a more complicated signal is obtained.

If the cepstrum at $(C_{AC})_1$ is the first resonant frequency harmonic of AC, then using the equation (6.10), Δf_1, will give the length AC. ℓ_{AC} is equal to the length corresponding to $O(C_{AC})_1$ on the time axis of the cepstrum. The second harmonic of AC at $(C_{AC})_2$ will result in a $\Delta f_2 = \frac{1}{2}(\Delta f_1)$.

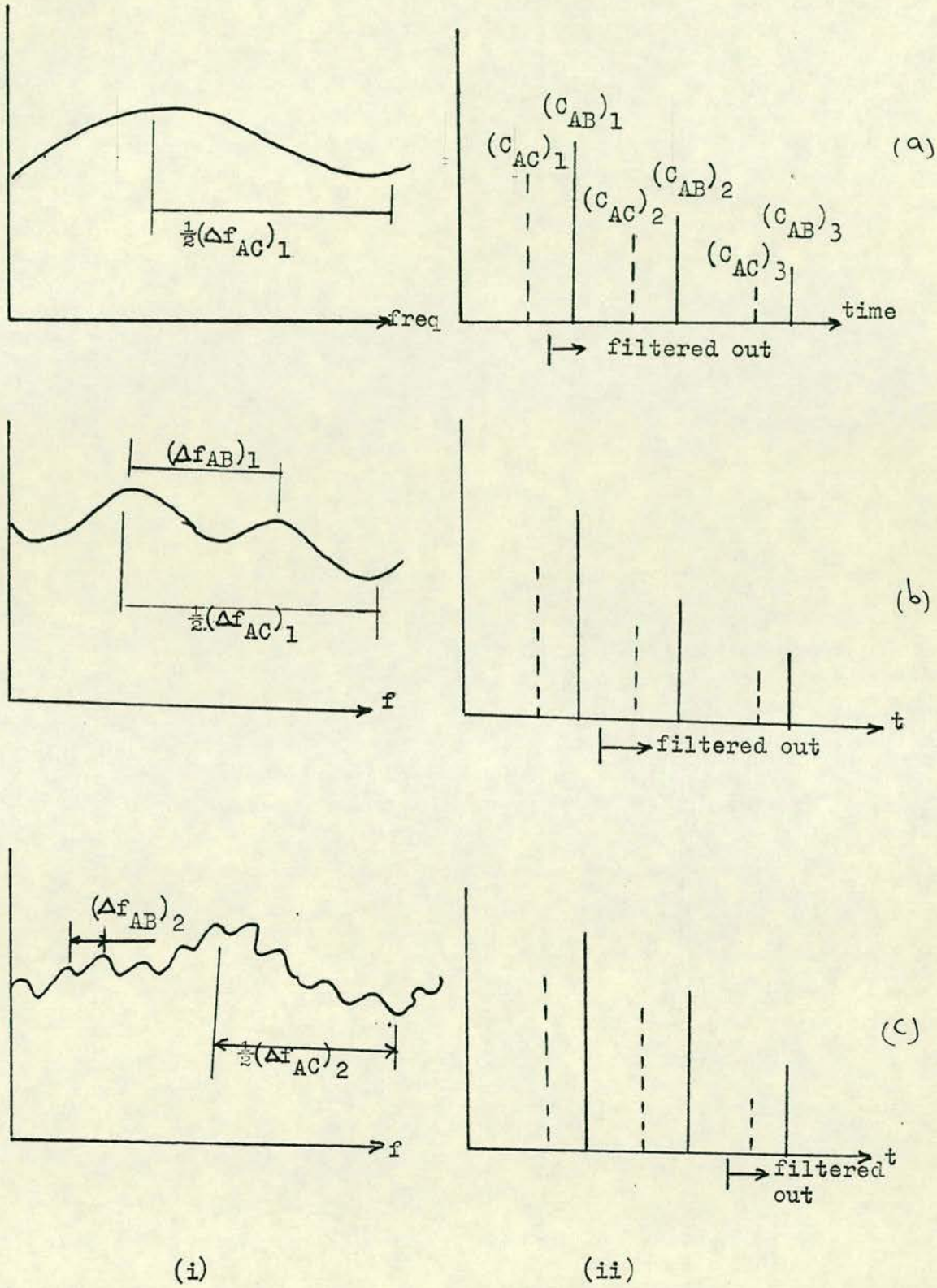

Fig. 6.13 The resultant signal output of the structure set into vibration in Fig. 6.12. (i) liftered spectrum and (ii) cepstrum

If the cepstrum in $(C_{AB})_1$ does result in a $\Delta f = \Delta f_{AB} \# \Delta f_{AC}$, then the length ℓ_{AB} can be calculated. The second harmonic of AB or AC will yield lengths twice the true values. In this case also, the nth harmonic gives:

$$O(C_{AB})_n = n\ (C_{AB})_1$$

and $$(\Delta f_{AB})_n = (\Delta f_{AB})/n$$

Therefore the use of this technique helps to identify two or more signals overlapped. The liftered spectrum helps to identify Δf and the cepstrum is useful in detecting the echoes. Use of the cepstrum alone in detecting several overlapped echoes is not possible and can lead to overestimating lengths.

6.4.4 Application to Civil Engineering

The use of the methods outlined earlier in this chapter were investigated and applied to a number of bridges. The results follow in the proceeding chapter. From the theory and experience it was demonstrated that auto correlation and cross correlation techniques are more useful in detecting cracks when there is access to two opposite sides of the structure being tested. The advantage of the cross correlation and auto correlation techniques compared to the cepstrum analysis method is that, as there is access to two sides of the structure, cross-checking can be performed and the reliability increased. However, when there is access to one surface of the structure, as in the case of thickness measurement of abutments, the cepstrum is considered to be of major importance. This again should be used together with the liftered spectrum method, because the presence of multiple reflections from cracks or other discontinuities complicate the analysis.

The transmission velocity through a civil engineering material, as an indication of the strength of that material, can be performed in the method described - Chapters Four and Five. However, the introduction of digital electronic instruments with high resolution functions, for example zoom facilities and pre triggering, have contributed to the accuracy and reliability of the test results.

6.5 Proposal for Further Research Development

To develop the research further and increase its accuracy, it is proposed that a numerical analysis on known quality and damaged models be carried out. A model of known materials with built in faults, but not as complicated of a bridge abutment can be made. The behaviour of the generated compressional wave at the boundaries can be studied in further detail. A detailed numerical analysis using, for example, the finite element methods, can yield to detection of inclination, nature and type of discontinuity.

6.6 SUMMARY OF INVESTIGATION

(1) With the development of the semi-conductor component industry, the use of digital analysers became economically feasible. The conventional analog methods were found to be time consuming and expensive. The conventional digital instruments and analysers had a 250 or 400 line resolution and an 8 bit span. The more modern analysers with an 800 line resolution and 12 bit span produce higher resolution signals and zooming features.

(2) In the time domain functions, the conventional time delayed functions and the algorithmic functions such as auto correlation and cross correlation functions were discussed. It was shown that the auto correlation and cross correlation functions can be used relatively easily for echo detection. Cross correlation is more advantageous in echo detection, when two opposite surfaces are available, as it compares the similarities between the two different functions with a certain delayed time. They are not, however, applicable for periodic signal detections.

(3) In the frequency domain functions, the frequency response function and its application in vibrational testing was discussed. It was shown that by studying the fundamental frequencies of the reflected waves, the length to the reflecting surface or the relative quality of the material can be obtained.

7.1 INTRODUCTION

In the previous chapters a study of ultrasonic non-destructive testing of masonry components was carried out. The conclusions and results obtained helped to apply sonic NDT to brick and stone masonry to evaluate their relative strength. The results in conjunction with a time domain analysis technique, were also used to measure and locate the presence of cracks in brick masonry walls. The aim of this section is to investigate the use and application of this NDT technique to full scale in situ masonry.

Four different bridges were tested and the results were compared with those obtained from other methods, e.g. coring, or with the information already known, when available. The bridges tested were:

(1) Middleton North Burn Bridge, situated on the A7 in Lothian Region between Edinburgh and Galashiels in Scotland.
(2) Bargower Bridge in Ayrshire, West Scotland.
(3) High Bridge, Struie, near Inverness, North Scotland.
(4) Victoria Bridge on River Tay, Tayside Region, Scotland.

7.2 MIDDLETON NORTH BURN BRIDGE (Plate 7.1)

Middleton North Burn Bridge is situated on the A7 in Lothian Region between Edinburgh and Galashiels, in East of Scotland. The bridge is a two span arch masonry structure with a masonry pier in the water. During piling for constructing a new bridge deck a large air gap in the bridge had been encountered. The sonic non-destructive testing technique was used to investigate the presence of the large air void and the extent of it. The test was repeated after repairing to ensure a satisfactory improvement in eliminating the air gap.

7.2.2 Experimental Equipment

The experimental equipment used to carry out the test consisted of:

(1) Two 54 kHz, 50 mm diameter flat surface piezoelectric transducers.
(2) Telequipment four channel storage oscilloscope.
(3) 75 ohm coaxial screened cables.

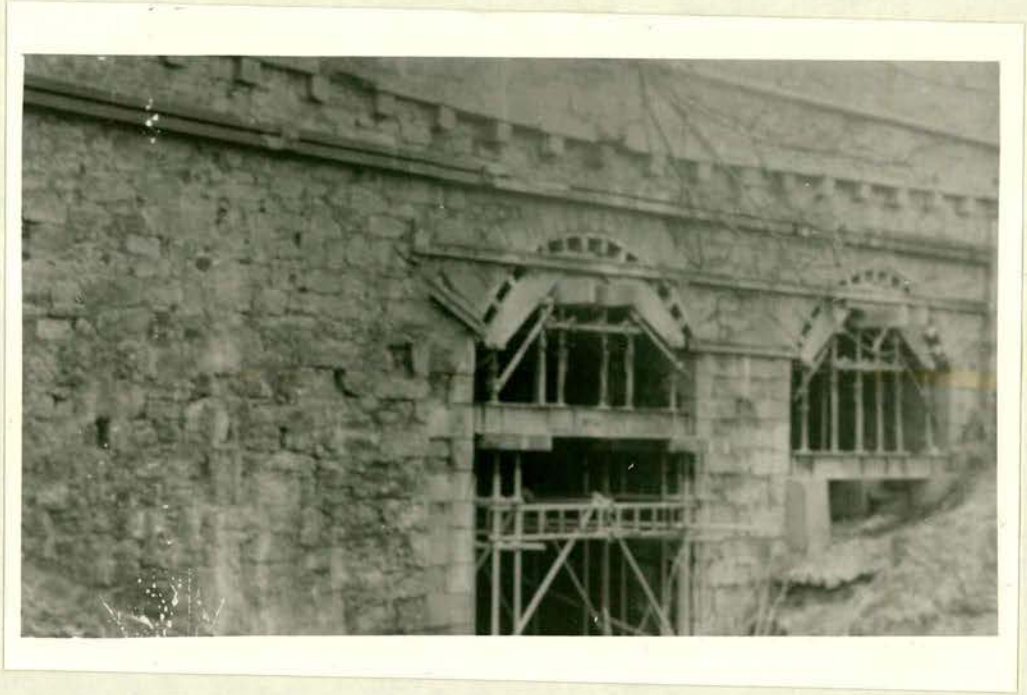

Plate 7.1 Middleton North Burn Bridge

(4) An ordinary all purpose steel tipped hammer.

7.2.2 Experimental Procedure

The two piezoelectric transducers were mounted onto the downstream and upstream faces of the bridge. One transducer was connected to one channel of the Telequipment storage oscilloscope and the other transducer was connected to the second channel of the oscilloscope, using the screened cables. A short sharp shock of energy in the form of a steel tipped hammer blow was then applied to the wall close to the first transducer, on the downstream face. The start of the resulting compression wave was picked up almost immediately by the first transducer A, which triggered the oscilloscope and after a time interval, by the second transducer B. By measuring the time interval between the two triggering points A and B, which were recorded on the oscilloscope screen, the time taken for the compression wave to travel through the bridge between the two transducers, was obtained. Then by using the relationship $V_{AB} = \frac{\ell_{AB}}{t_{AB}}$ the transmission velocity between A and B was obtained.

The procedure was then repeated but this time by exciting the wing wall on the upstream face as channel A. This approach would yield sensitivity in detecting voids or cracks very close to the wall surface.

The test was carried out for a matrix of points on the Southern abutment/wing wall and on two points on the Northern wing walls.

7.2.3 Results and Analysis

7.2.3.1 Locating large air voids in the bridge

In order to locate the presence of large air voids in the bridge, a transmission velocity test was required. The experimental procedure was described above. The test involved calculating the transmission velocity for each point tested on the wing walls. When there was no transmission observed for a point at both upstream and downstream faces, then an air void existed there. Calculating the transmission velocity was similar to the manner described in section 5.4.1. The results in Table 7.1 show that there was only one point,

that is point 3, where no transmission was obtained for both upstream and downstream wing walls, before grouting. This indicated the presence of a large air void in the bridge preventing the compression wave energy reaching the other side.

The results obtained for this point, after grouting, showed an improvement. A transmission velocity of 740 m/sec was obtained when triggering at the upstream and no transmission was produced when triggering at the other face. This indicated the presence of a gap at the downstream face very close to the wing wall there. The reason for this analysis is explained in section 7.2.3.2 below.

Location	Before Grouting trans. vel. (m/s)		After Grouting trans. vel. (m/s)	
	Upstream Trigger	Downstream Trigger	Upstream Trigger	Downstream Trigger
1	1556	1217	1333	1556
2	875	NT	718	848
3	NT	NT	737	NT
4	667	NT	933	NT
5	1333	1273	1400	1333
6	984	NT	862	NT
7	1000	NT	848	NT
8	824	NT	848	875
9	1037	NT	1217	1167
10	1556	NT	1931	2000
11	1556	1556	1474	1273
12	1474	1474	1217	1120
13	1076	1000	1037	800
14	1474	1400	1556	1750
15	1273	NT	1556	1400
16	2154	2154	-	-
17	3294	3111	-	-
18	2154	2545	-	-
19	2800	2000	-	-
20	3500	3500	-	-
21	2667	2545	-	-
22	900	NT	-	-

Table 7.1 Middleton North Burn Bridge - Transmission velocity values before and after grouting

7.2.3.2 Locating air gaps very close to wing walls

The results in Table 7.1 again show that, for several of the points tested on the south wing wall, no transmission was obtained when the upstream side was excited. This indicated voiding immediately behind the downstream wing wall. Fig. 7.1 illustrates this form of analysis.

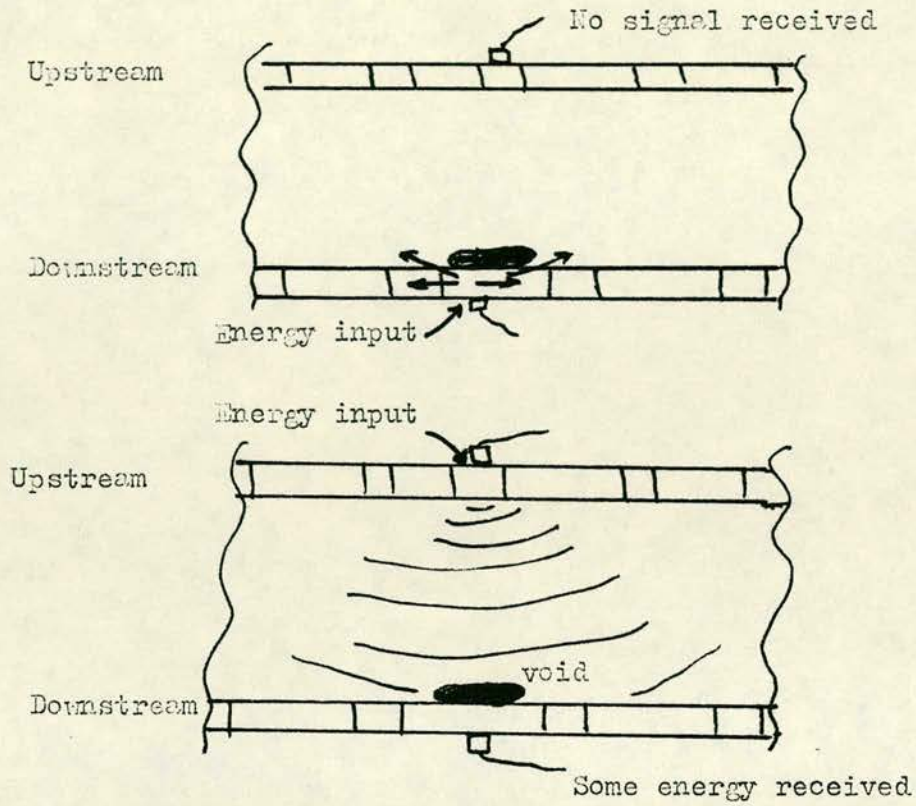

Fig. 7.1 Plan section of the bridge voiding very close to a surface under test

Fig. 7.1 shows that when a point on the wall is excited at one end, the input compression wave is propagated radially outwards from the exciting point. The propagation takes place as spherical wavefronts. When these wavefronts encounter a large void, they get reflected and diffracted around. They may eventually reach the other face and trigger the receiving transducer B. If the large void encountered is very close to the input energy source, the reflection and diffraction are so large that virtually no energy or very small amounts of it reach the other face. On the other hand, if the void is not very close to the input energy source, some energy gets transmitted around the void and reaches the other face. It must be noted that the void encountered in this case must not be so large that no energy can get round it to be transmitted to the other end.

Table 7.1 shows that there were a number of such points, e.g. points 7, 4, 22, etc, on the southern wing wall. When the wall was excited on the downstream face, no signal was transmitted to the upstream face. The wave was being reflected from the void very close to downstream face. On the other hand, when the upstream face was excited at the same point, a signal was received on the other side. The received signal, however, had a very low amplitude. This indicated that a much smaller amount of energy was transmitted in comparison with other signals when there was no void encountered.

The bridge was then grouted using 11 m^3 of a sand/cement grout. Several days later another sonic survey was carried out on the bridge. Table 7.1 shows that the transmission velocities obtained this time were higher with more transmission. A few unfilled points were, however, still present. Figs. 7.2 and 7.3 summarise the results of suspected void areas before and after grouting.

7.2.4 Discussion of Results

The results obtained show that a large void existed very close to the downstream face. Since several points were next to each other (2 and 4 plus 6 to 10, see Table 7.1), the cavity was in the fill immediately behind the masonry. The voids therefore cannot be due to unfilled vertical mortar joints. This indicated the separation of the wing wall and the rubble fill. The wall did not, however, show any bulging. Hence the void can be said to be a cavity. It might have been created by washing out of the fill by rain water penetrating into the bridge. The observations of the wing wall indicated the latter possibility.

The transmission velocities obtained varied widely. This indicated the possibility of the transmission path materials with differing densities. A transmission velocity of approximately 500 m/sec indicated a transmission path of uncompacted fill (see Table 5.7 in chapter 5). This low velocity might also be due to a long path around a void. It is not usually easy to distinguish between these two possibilities. One way of differentiating between these two possibilities is the comparison of the results obtained. If such a velocity for a point very close to another which has not

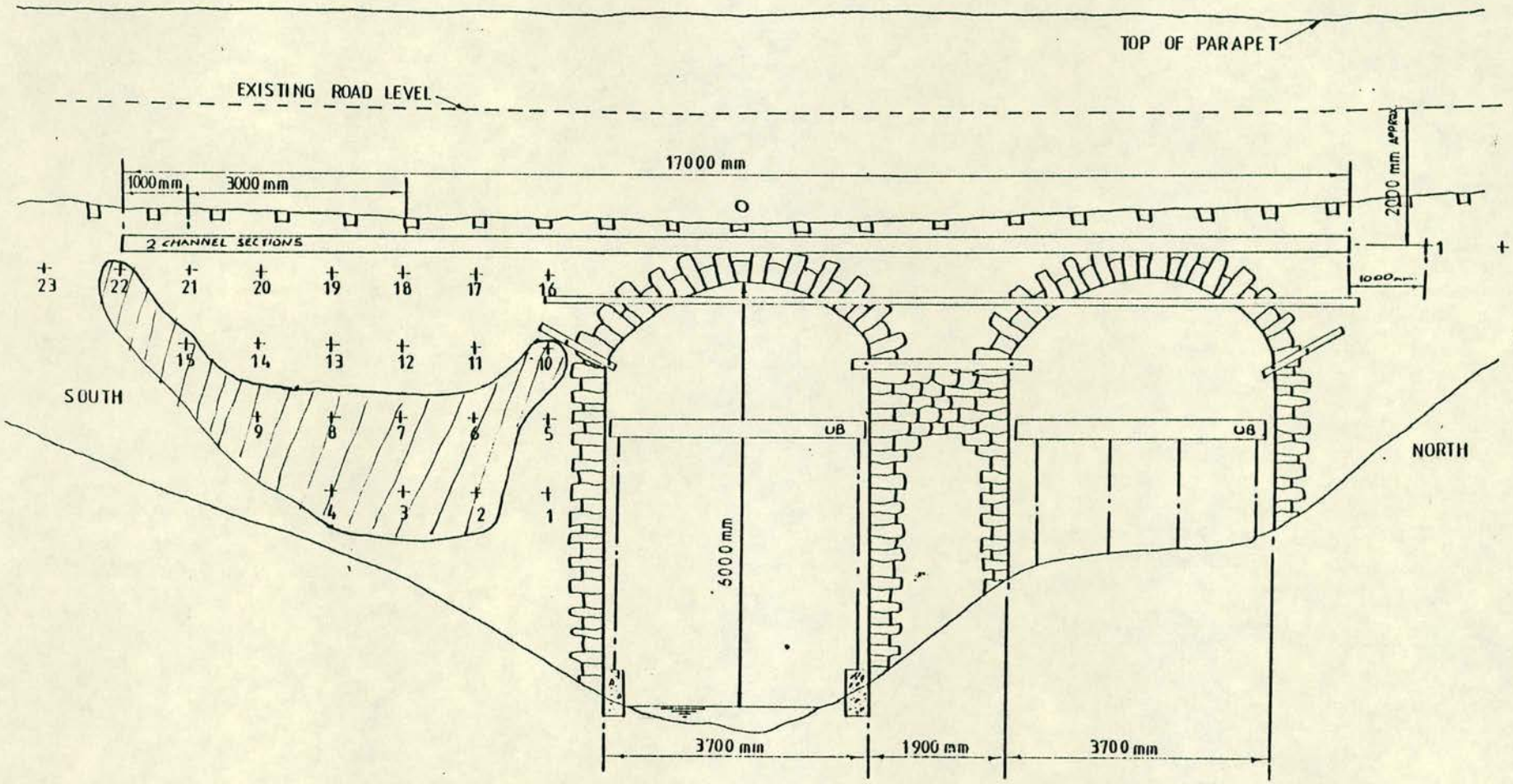

Fig. 7.2 Middleton North Burn Bridge, downstream elevation, suspected void area (shaded) before grouting

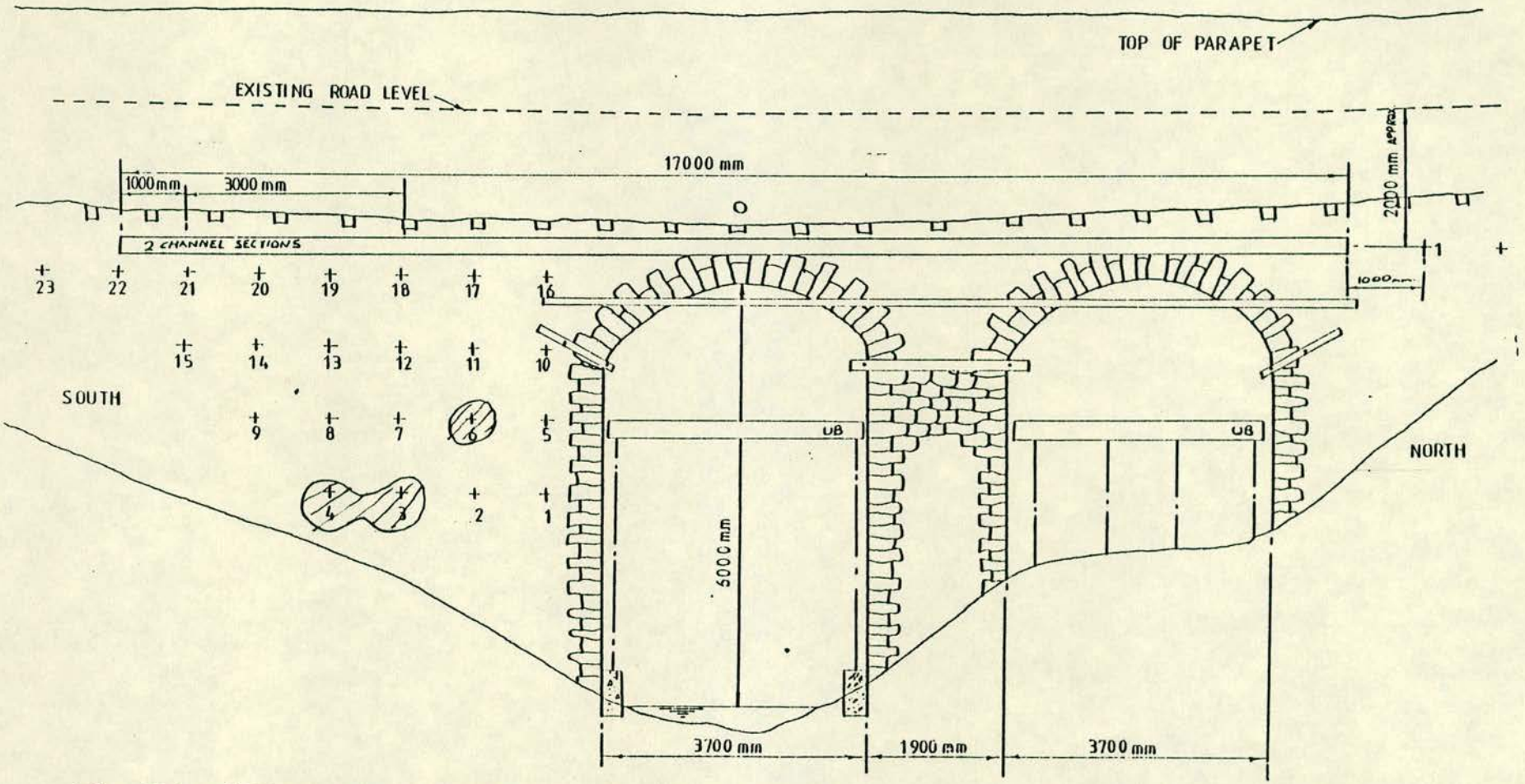

Fig. 7.3 Middleton North Burn Bridge, downstream elevation, suspected void area (shaded) after grouting

produced any transmission velocity, is obtained, then the low value reading can be said to be due to the long path of signal around the void.

The transmission velocities obtained for some points, e.g. 16 to 23, had values between 2000 m/sec to 3500 m/sec. This clearly indicated transmission through good quality masonry or even concrete. Indeed it was known that during previous strengthening operations on the bridge, a concrete slab had been placed in that area over the bridge deck.

7.2.5 Conclusions

The sonic NDT survey carried out on the Middleton North Burn Bridge showed that:

(a) A large cavity existed beween the south wing wall and the fill at the downstream face of the bridge.

(b) After grouting the cavity had mostly been filled with only a few patches unfilled.

(c) The transmission velocity values indicated the presence of varying materials used in the bridge. They included concrete, good quality masonry and uncompacted rubble fill.

(d) The transmission velocity survey can be used to detect the presence of voids even if they are very close to the surface.

7.3 BARGOWER BRIDGE

Bargower Bridge in Ayrshire, Scotland, previously known as Bridgehouse Bridge, is situated on old route A76 in Ayrshire. It is a single span masonry arch bridge. A sonic survey of the bridge was undertaken to locate the presence of good quality masonry and possible air voids in the bridge. A reflection test on the Northern abutment was also carried out to estimate the width of the masonry abutment at different levels. In other words, an integrity test, using sonic non-destructive testing techniques, was carried out on the bridge.

7.3.1 Experimental Procedure

7.3.1.1 Transmission velocity test

This test was carried out to locate the presence of possible

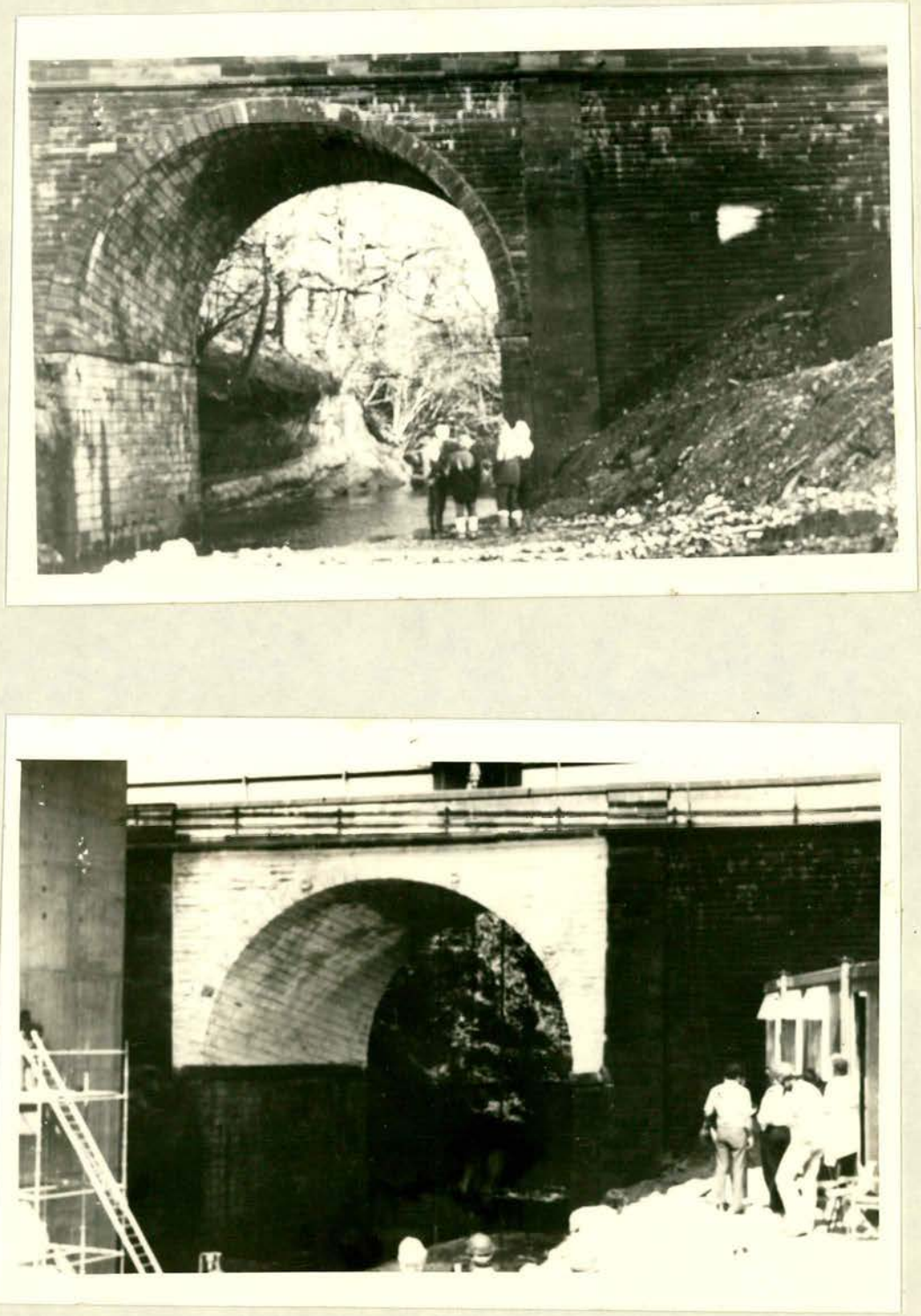

Plate 7.2 Bargower Bridge

air voids and areas of good or poor quality masonry in the bridge. The procedure was very similar to the method described in section 7.2.2. The difference being that instead of using the Telequipment DM2 storage oscilloscope, a digital two channel Nicolet 4094 oscilloscope was used. The Nicolet 4094 has a 12 bit A/D convertor, 16K memory, 16 bit processor and twin 5.25 inch 360K disk drive. Use of this equipment had the advantage of recording the results onto double sided 5.25 inch floppy discs, to be studied and analysed in the laboratory. This permitted a more sophisticated analysis. The other major advantage of using the Nicolet oscilloscope was that it had zoom facilities which gave more accurate and detailed results.

The principle of testing method was again similar to the method already described. It involved the measurement of time delay for a compression wave to travel between two known points. A high transmission velocity of the order of 2000 m/sec indicated the presence of good quality masonry. Also in the case of a very low or no transmission velocity measurement, a void or crack in the path of the wave was suspected.

7.3.1.2 Thickness measurement

In order to measure the thickness of the abutments, an accelerometer with built in charge amplifier was mounted onto the abutment wall surface. The point close to the accelerometer, on the wall, was then excited using an instrumented hammer with a two and a half tonne load cell. The consequent dynamic response of the wall at that point was then received and transmitted to an FM high frequency tape recorder by the accelerometer. The recorded signal was used for later analysis. Three or four readings were taken for each point.

This procedure was then repeated for each point on the Northern abutment which was divided into a 1 m x 1 m grid. It must be noted that due to bad surface conditions, for example, wet, weathered or unreachable, some points were not tested.

The analysis of the recorded signals in the laboratory involved playing the tape signals into a Bruel & Kjaer 2034 two channel signal analyser. This equipment converts signals from analog to digital form using a twelve bit A/D converter (Plate 7.3).

Two different analyses were then carried out on the signals in the laboratory. The analyses involved investigating the reflection time delay for the compression wave from a discontinuity such as the other face of the abutment wall. Cepstrum and liftered spectrum (see chapter 6) functions with a short pass filter were used as the first method to measure the reflection time. The second method of analysis involved using the same analog response record to be analysed in the time domain functions of auto correlation and cross correlation (see chapter 6).

The advantage of using cepstrum analysis is that when a periodicity exists in the spectrum it transforms by an inverse Fourier transform to a series of harmonics in the cepstrum. The harmonics then have spacings equal to the delay time. Therefore it is relatively easy to detect the presence of delay time echoes in the cepstrum (see section 6.4). Use of the liftered (or filtered) spectrum function with a short pass filter enables one to distinguish between the fundamental harmonic of a reflection delay time and the subsequent harmonics (see section 6.4.3). A fundamental harmonic of a periodicity in the cepstrum corresponds to a certain frequency interval in the liftered spectrum equal to half of the first one. Use of short pass filters allows one to remove the effects of other frequencies beyond the corresponding periodicity.

In order to enhance the quality of interpretation, the mathematical algorithms of cross correlation and auto correlation functions in the time domain were also used. The results then were compared (see the proceeding sections). The auto correlation function is basically a measure of how similar a function is in its time delayed replica. The cross correlation function, on the other hand, is the detection of similarity between two signals in the time

Plate 7.3 Bruel & Kjaer 2034 and FM high frequency tape recorder

domain. These two methods are used to detect reflections from a discontinuity, in this case the reflection from the other face of the abutment wall. The conventional approach of analysing the time domain signal can prove difficult for a complex structure as in this case where multiple reflections were suspected and only one surface was available.

7.3.2 Results and Analysis

7.3.2.1 Transmission velocity measurement

The transmission velocities were measured and calculated in the same manner as described in sections 7.2.2 and 7.2.3 for the Middleton North Burn Bridge. As the purpose of the test was to locate the presence of large voids and poor or high quality masonry, only a simplification of the results is shown. The quality of masonry was divided into categories A, B, C, D and E, with A corresponding to velocities of above 2000 m/sec and E corresponding to those below 500 m/sec. A and B were considered good quality masonry, where D and E indicated very poor masonry or transmission through the fill (see Table 5.7). The notation N in Table 7.2 where transmission velocity values are given, indicates no transmission took place. The notation H in the first column of this table corresponds to height in the vertical direction where, for example, H2-13 means second level in the vertical direction, at point 13 on the horizontal axis.

It is shown that the best transmission (i.e. highest velocity) took place through the abutments from one side of the bridge to the other and also through the voussoir of the structure. Additionally it will be noted that high velocities were obtained behind the springers of the bridge, thus indicating the possibility that the masonry was continuous behind the springers - continuing into the wing wall at a low level.

At other locations on the wing walls, it will be noted that there were large areas where no transmission was recorded. One side of the spandrel walls of the bridge also indicated no transmission - i.e. the south side of the structure. The interpretation of the lack of transmission through the south spandrel walls and the south

Point	Trans. Vel. Ups	Trans. Vel. Dns	Point	Trans. Vel. Ups	Trans. Vel. Dns	Point	Trans. Vel. Ups	Trans. Vel. Dns	Point	Trans. Vel. Ups	Trans. Vel. Dns
H1-6	N	B	H2-20	N	N	H4-16	N	B	H9-16	B	B
H1-7	N	B	H2-21	N	N	H4-17	C	N	H9-17	A	A
H1-8	N	B	H2-26	C	C	H4-18	N	N	H9-18	A	A
H1-9	N	C	H2-27	N	C	H4-19	B	B	H10-16	A	A
H1-10	N	C	H2-28	N	B	H4-28	A	A	H10-17	A	A
H1-13	N	B	H2-29	N	C	H4-29	B	B	H10-18	A	A
H1-14	N	N	H2-30	A	A	H4-30	N	N	H11-16	A	A
H1-15	N	D	H2-31	B	B	H4-31	A	A	H11-17	A	A
H1-16	N	C	H2-36	N	B	H5-9	N	C	H11-18	A	A
H1-17	C	N	H3-5	N	B	H5-10	C	N	H12-17	A	A
H1-18	B	B	H3-8	N	B	H5-12	N	N	H12-18	A	A
H1-19	N	N	H3-10	N	C	H5-15	N	C			
H1-20	N	N	H3-12	N	N	H5-16	N	C			
H1-21	N	N	H3-13	C	C	H5-17	C	N			
H1-22	N	N	H3-14	N	N	H5-18	B	B			
-	-	-	H3-15	E	E	H5-29	B	B			
H1-24	B	B	H3-16	N	D	H5-30	C	C			
H1-26	C	C	H3-17	C	N	H5-31	D	D			
H1-27	N	C	H3-18	N	N	H5-32	C	C			
H1-28	N	C	H3-19	B	N	H6-12	B	B			
H1-29	D	D	H3-20	B	N	H6-14	B	B			
H1-30	C	C	H3-28	B	B	H6-15	B	B			
H1-31	B	B	H3-29	C	C	H6-16	N	B			
H1-32	B	B	H3-30	N	D	H6-17	C	C			
H2-8	N	B	H3-31	D	D	H6-18	B	B			
H2-10	N	E	H3-33	B	B	H6-29	A	A			
H2-12	N	A	H3-35	D	D	H7-14	C	C			
H2-13	D	D	H3-36	B	B	H7-15	B	B			
H2-14	N	B	H4-9	N	N	H7-16	B	B			
H2-15	N	N	H4-11	N	N	H7-17	B	B			
H2-16	N	B	H4-12	N	N	H7-18	A	A			
H2-17	C	N	H4-13	N	N	H8-16	B	B			
H2-18	N	N	H4-14	N	N	H8-17	B	B			
H2-19	N	N	H4-15	N	N	H8-18	A	A			

Table 7.2 Bargower Bridge - Transmission velocity classification. A and B very good quality, D and E very poor.

wing wall could be that there was a significant void in the middle of the structure. A more probable explanation might be that there was some degree of voidage or leaf separation behind the wall at those particular locations. The subsequent investigation showed that a secondary abutment, resulting in double skin, existed at that area.

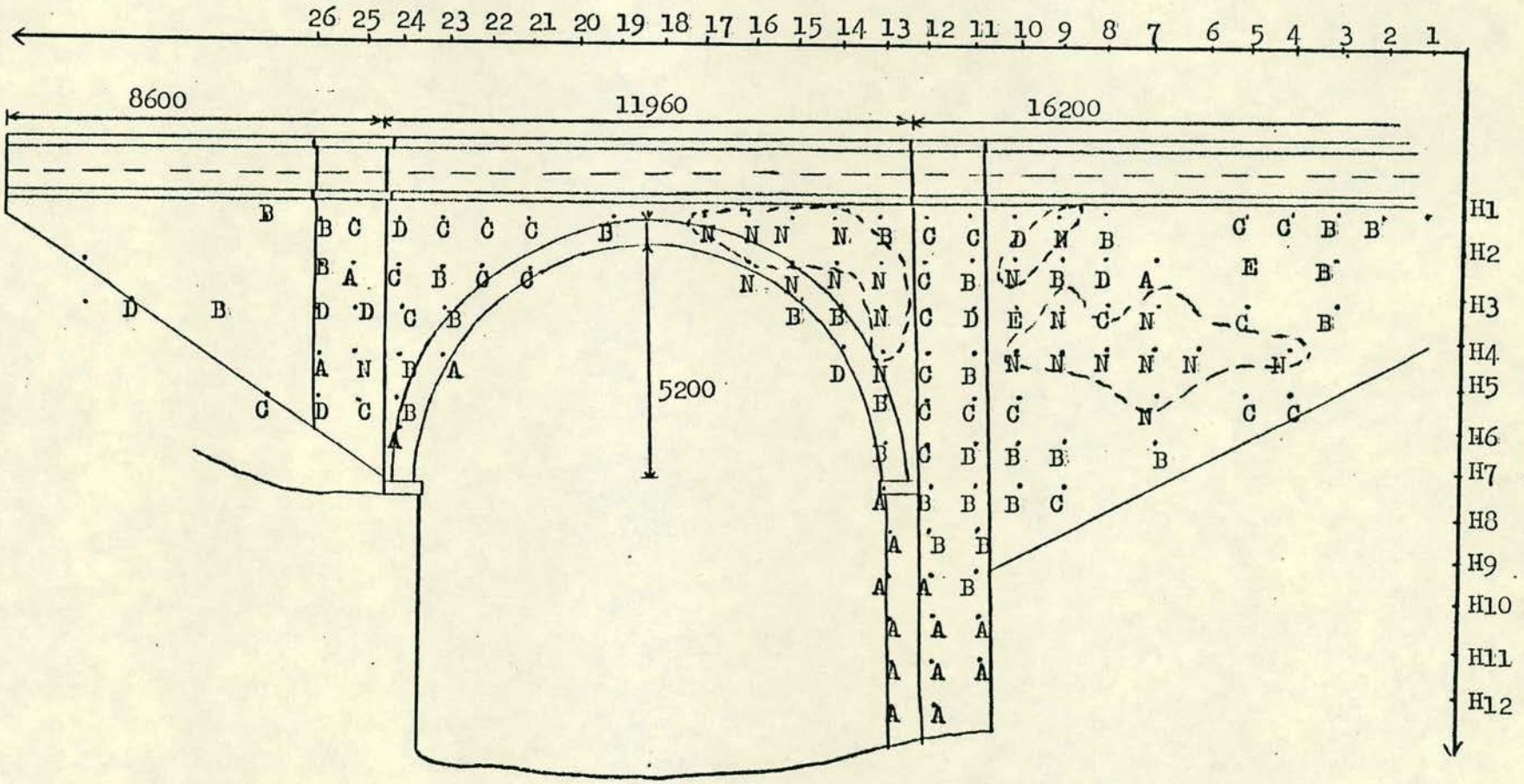

Fig. 7.4 Bargower Bridge, downstream face, location of large voids or discontinuities (shaded) and good quality masonry

It will be noted that in general the transmission velocities through the wing walls and the spandrel walls (away from the immediate vicinity of the voussoir and the possible stone immediately behind the springer) were in the category of C to E, i.e., relatively poor transmission. This indicated that transmission was taking place through the masonry, then through fill and then back to the masonry. This was as opposed to continuous transmission through masonry as might be the case behind the springer on the southern abutment. It is seen that relatively fast transmission speeds were noted above the springer point and into the wing walls immediately behind this part of the structure. Behind the northern springer of the bridge, there was also relatively high velocity, indicating again some continuous masonry existing.

7.3.2.2 Abutment thickness measurement

(a) Signal Analysis methods

As was mentioned earlier, three different methods of analysis were used for abutment thickness measurement. The results were then compared and then one set of results was used to determine the average width of the abutment at each level. Fig. 7.5 shows the location of test points on the north abutment.

One method of analysis involved the use of the auto correlation and the cross correlation functions in the time domain. Figs. 7.6, 7.7 and 7.8 show three typical results obtained in this manner.

From Fig. 7.8, it is seen that the first peak corresponding to a reflection from a discontinuity, occurs at 0.75 mil. sec. The second peak occurs at 2.5 mil. sec. The relative magnitude of these two peaks on the auto correlation function graph indicates reflections from major discontinuities such as a crack, void or a material very different from masonry. The other peaks on these graphs are very small in magnitude and therefore they can indicate reflections from a less severe or small crack or from a mortar joint. The reflection time delays of these later peaks are so large that they indicate discontinuities far from the expected range of the abutment thickness. Figs. 7.7 and 7.8 are other examples of this

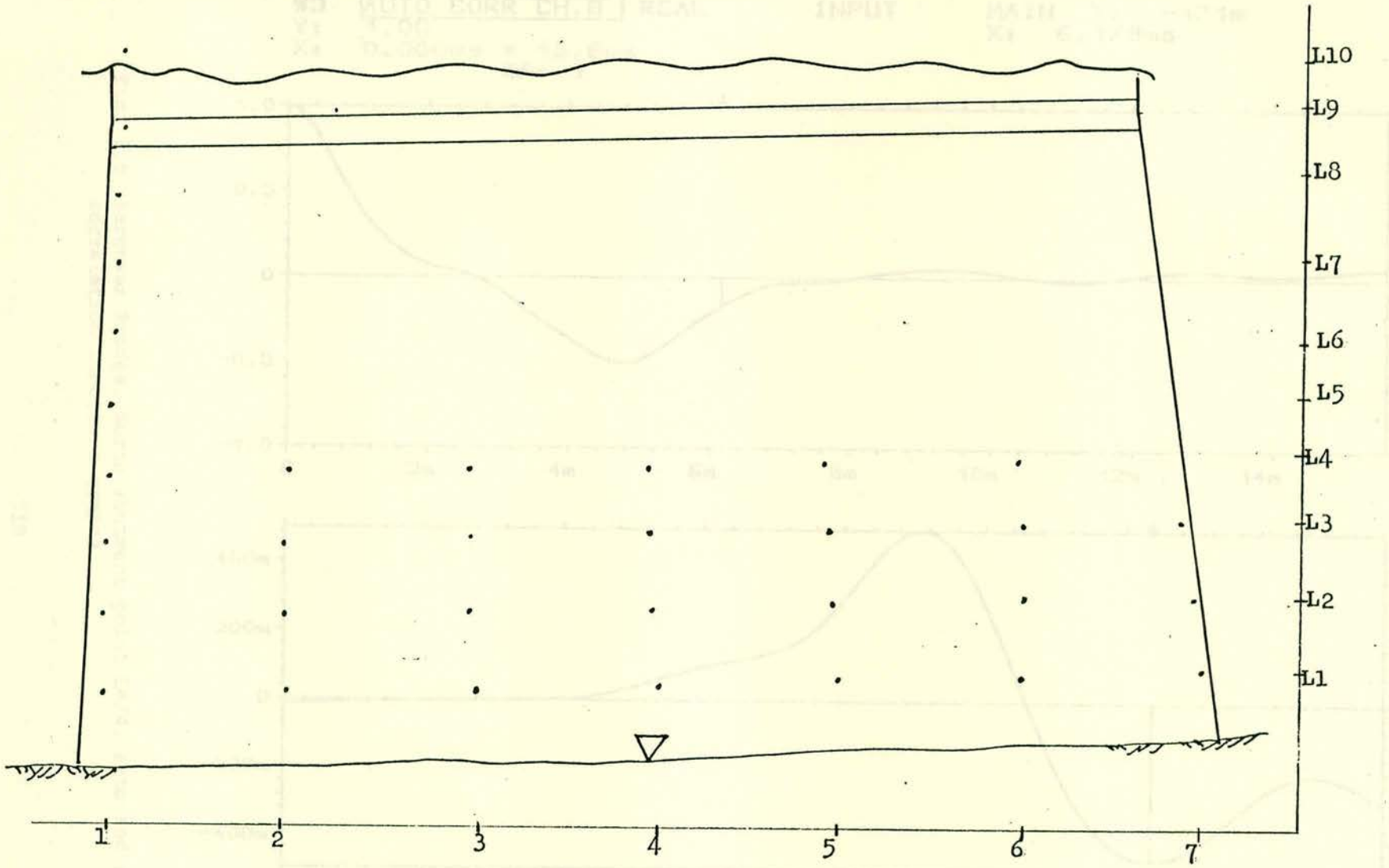

Fig. 7.5 Bargower Bridge, North abutment elevation, location of test point for thickness measurement

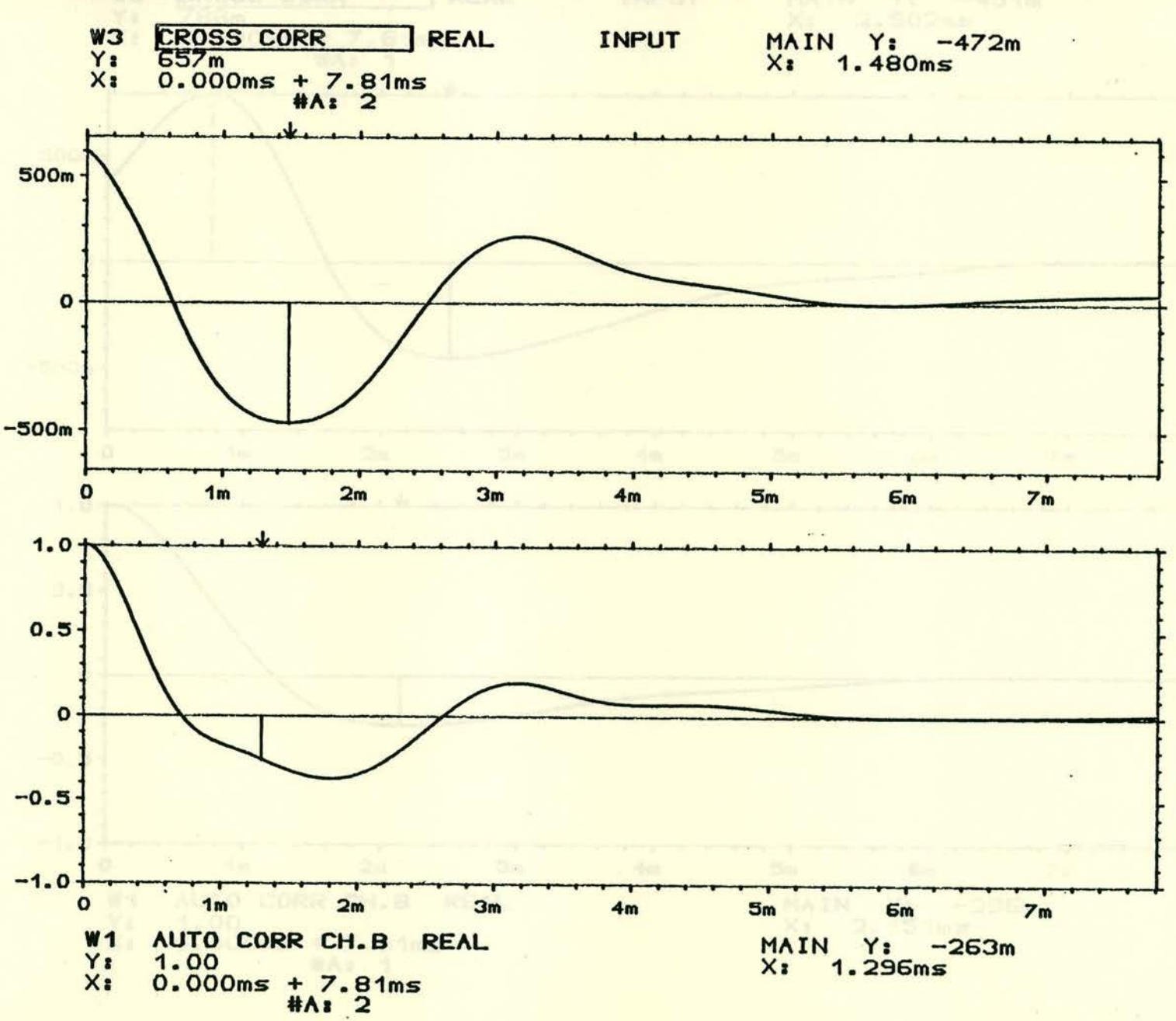

Fig. 7.7 Bargower Bridge, North abutment point L1/6, auto and cross correlation functions graphs

method of analysis. It is seen from these two figures that point L1/6 has two major discontinuities apparent at 1.3 and 3.1 mil. sec.

The corresponding points on the cross correlation graphs of point L4/4 show that two suspected discontinuities are observed. One discontinuity is at 1.01 mil. sec and the second one is at 2.3 mil. sec.

Assuming an average transmission velocity of 2000 m/sec, these discontinuities at L4-4 correspond to reflections at distances of 1.0 m and 2.3 m. Similarly the apparent reflections from the cross correlation graphs at L1-6 are at 1.5 m and 3.0 m distances. The presence of multiple reflections show that there is more than one discontinuity in the masonry. They may also be due to a second reflection from the same point, though in this case the magnitude of the reflection is usually very small.

Fig. 7.9 shows the result for the same point at L4-4 using the Liftered spectrum and cepstrum functions with short pass lifters (or filters). It is seen that the first major peak on the cepstrum graph corresponds to a frequency interval of 1031 Hz on the liftered spectrum. The second major peak at 1.95 mil. sec corresponds to a frequency interval of $\frac{1}{2}$(1031) Hz. This indicates that this peak is the second harmonic of the first reflection. The next major peak on cepstrum and liftered spectrum are shown in Fig. 7.10.

Here it is seen that the frequency interval is 315 Hz and it is unlikely to be the second, third, ... harmonic of the first reflection. The liftered spectrum graph in fact has become more complicated and the reflection from the first discontinuity has a marked effect on the smooth shape of the graph. The other reflections on these two graphs for L4-4 are too small in magnitude, or are beyond the expected range of the abutment thickness.

Use of the short pass filter has the advantage that it filters out the frequencies beyond the reflection under investigation. It includes the frequencies which are in the reflection time range under study, e.g. in the case of Fig. 7.10, it includes all the

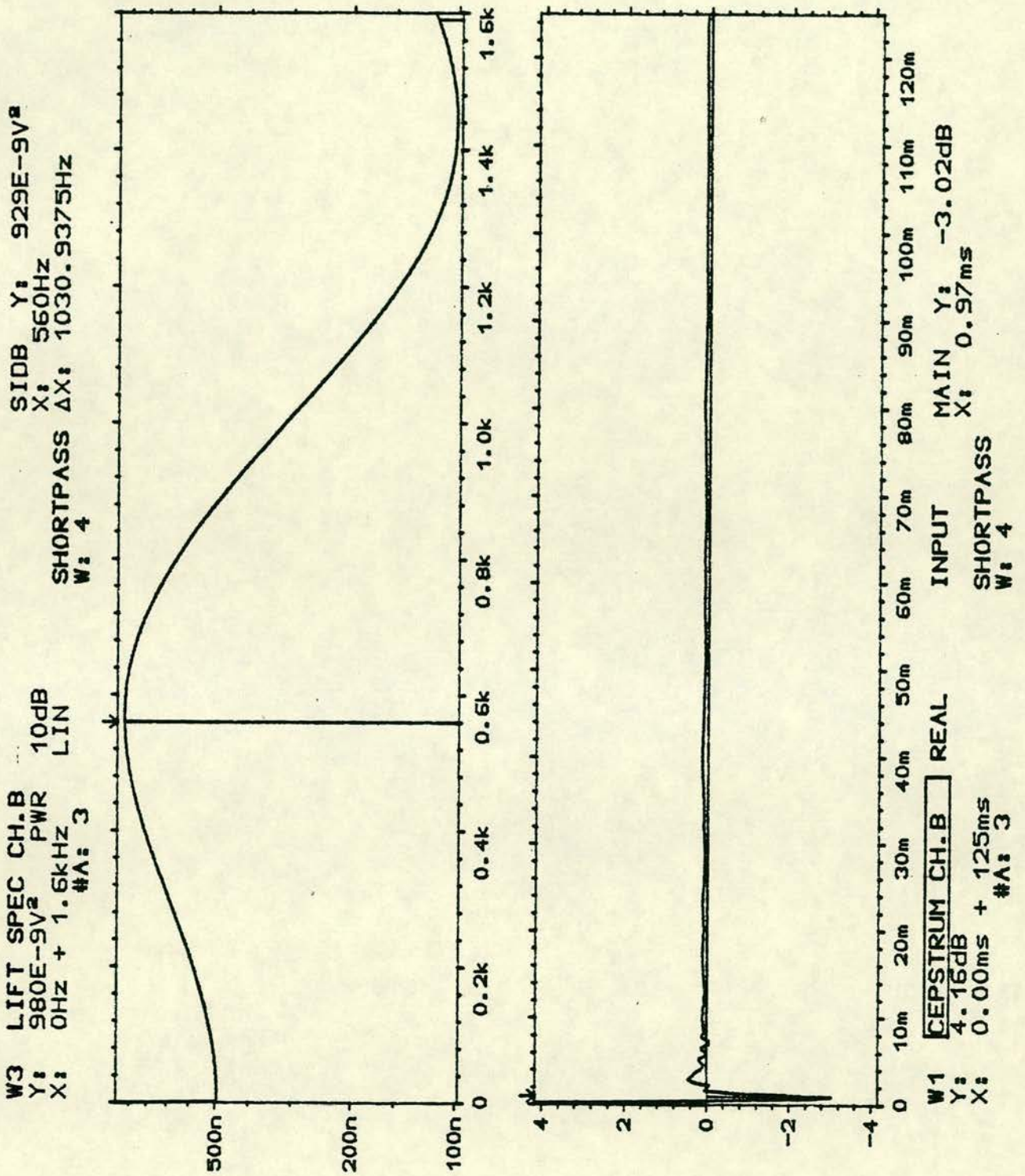

Fig. 7.9 Bargower Bridge, North abutment point L4/4, liftered spectrum and cepstrum, reflection at 0.97 mil. sec.

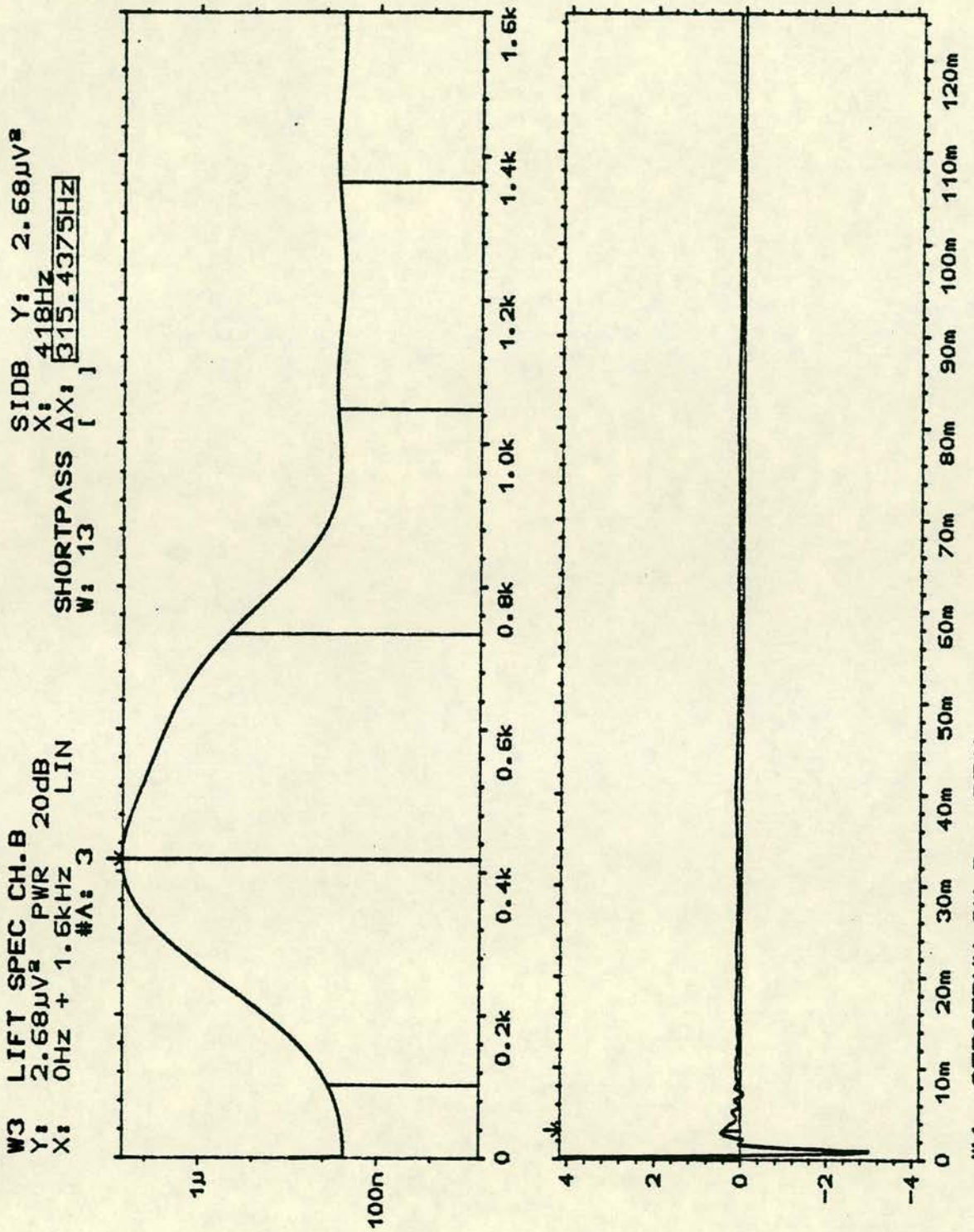

Fig. 7.10 Bargower Bridge, North abutment point 14/4, liftered spectrum and cepstrum , reflection at 3.17 mil. sec.

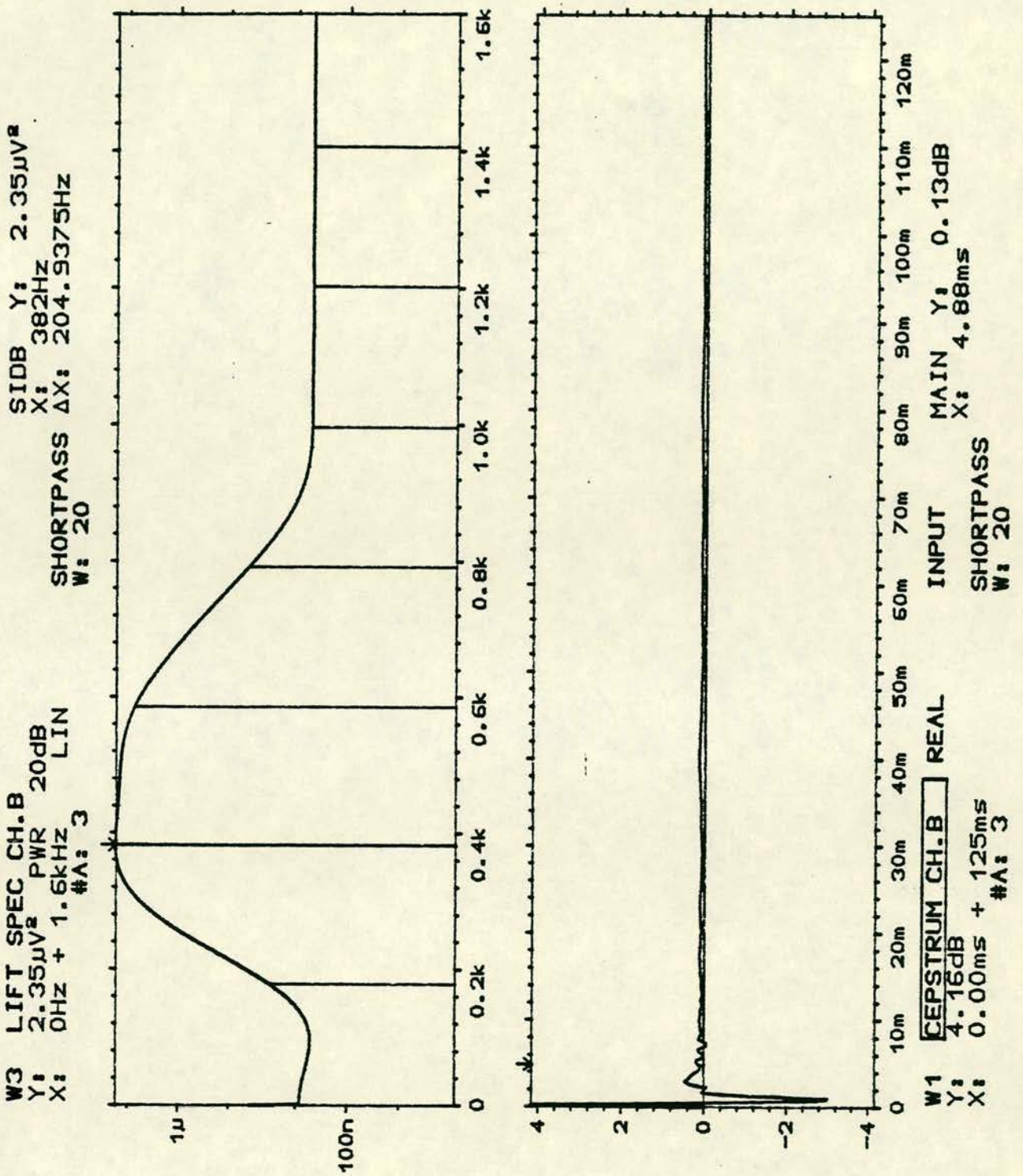

Fig. 7.11 Bargower Bridge, North abutment point L4/4, liftered spectrum and cepstrum reflection at 4.88 mil. sec.

frequencies in 3.17 mil. sec range. On the other hand, the long pass filter will start to exclude the frequencies when the reflection time begins to increase. Therefore the results obtained by using the long pass filter are very complicated, since all other frequencies from all the reflections in the signal are present at the start of filtering.

The results obtained by using these three methods of analysis are shown in Table 7.2 It is seen from this table that there was more than one discontinuity in the masonry. The results also show that cross correlation and auto correlation readings are quite similar and compare well with each other. The results from the liftered spectrum cepstrum analysis method are treated with more confidence. The reason for this "extra" confidence is that use of liftered spectrum and cepstrum together act as cross-checking each other. They are relatively easy to use and enable one to distinguish between reflections from the same point. Chapter 6 describes the advantages of cepstrum in differentiating between the reflections from the same point.

(b) Method of estimating the thickness

Table 7.4 shows that several points at each level on the abutment were tested. Each point showed several major reflections. To distinguish which of these reflections correspond to reflection from the other face of the abutment wall, transmission velocity v and thickness ℓ are varied. To illustrate this, take the example of test results on level 1. From the general information available, it was certain that the width or thickness of abutment at this level could not be less than 1 m and more than 5 m. Also from the table of transmission velocities in Tables 7.2 and 5.6, the expected transmission velocity through this sandstone masonry abutment was between 1500 m/sec and 2000 m/sec. First assuming a transmission velocity of 1500 m/sec resulted in the thickness shown (Table 7.4). Second, knowing the assumed range of thickness and the results obtained by a transmission velocity of 1500 m/sec, a new transmission velocity for each point was obtained. The calculated transmission velocities of 1st and 2nd reflections were seen to be too high to correspond to sandstone masonry. Now if the most likely

Location	Cepstrum-Liftered Spect. Refl. time 1st, 2nd, 3rd (ml. sec.)	Auto Correlation Refl. time 1st, 2nd, 3rd (mil. sec.)	X-Correlation Refl. time 1st, 2nd, 3rd (mil. sec.)
L1/1	1.22,2.19,4.39	1.48,3.10, -	1.45,3.13, -
L1/2	0.97,3.90, -	0.50,0.95,1.65	0.85,2.55, -
L1/3	1.46,2.19,4.39	No result	No result
L1/4	0.97,4.63	1.17,2.30, -	0.97,2.07,3.29
L1/5	1.46,2.19,3.41	No result	No result
L1/6	1.22,2.92,4.88	1.30,3.1, -	1.49,3.12, -
L1/7	0.73,1.70,4.63	0.60,1.16,1.66	0.91, -, -
L2/1	0.97,2.92, -	0.99,1.83,3.00	0.20,1.23,3.16
L2/2	0.73,1.95,2.92	0.99,1.90, -	0.91,2.06, -
L2/3 (very big crack)	1.22,1.95, -	1.69,3.86, -	0.15,1.63,3.62
L2/4	1.22,3.41,5.37	1.66,3.28,4.38	1.30,3.04,4.29
L2/5	0.97,1.70,3.17	0.84,1.63, -	0.84, -, -
L2/6	1.70,4.39, -	1.95,5.66, -	1.54,4.70, -
L2/7	0.73,3.17,3.90	0.82, -, -	0.79,1.56, -
L3/1	1.22,2.68,4.63	2.15, -, -	0.78,2.52, -
L3/2	1.22,2.19,3.90	1.16,2.75, -	1.20, -, -
L3/3	1.70,2.44,4.15	0.72,1.36,1.97	0.95,2.35,3.25
L3/4	1.22,1.95,3.41	0.64,1.08,1.42	1.33,3.02,4.34
L3/5	1.70,2.68,3.90	No result	No result
L3/6	2.44,3.17, -	1.72, -, -	1.83,3.95, -
L3/7	0.97,3.41, -	0.96,2.67, -	1.07,2.56,3.98
L4/2	0.97,1.95, -	1.14,2.36, -	0.95,2.27, -
L4/3	0.97,1.95,3.41	0.99,1.97,2.73	0.91,1.97,2.84
L4/4	0.97,3.17, -	0.99,2.73, -	1.01,2.30, -
L4/5	0.97,1.70, -	No result	No result
L4/6	1.46,2.68, -	1.62, -, -	0.91,2.43,4.24
L5/1	0.73,3.17, -	0.91, -, -	0.75,1.60,3.32

Table 7.3 Bargower Bridge - Comparison of reflection time results using different functions

Location	Reflection Time (mil. sec.)	Ass'd. V (Km/sec)	Cal'd. Refl. Length, ℓ (m)	Ass'd. ℓ (m)	Cal'd. t.V. (Km/sec)	Est'd ℓ (m)
L1-1	1.22,2.19,4.39	1.5	0.9,1.6,3.3	3.5	5.7,3.2,1.6	3.4
L1-2	0.97,3.90, -	"	0.7,2.9, -	"	7.2,1.8, -	3.1
L1-3	1.46,2.19,4.39	"	1.1,1.6,3.3	"	4.8,3.2,1.6	3.4
L1-4	0.97,4.63, -	"	0.7,3.5, -	"	7.2,1.5, -	3.5
L1-5	1.46,2.19,3.41	"	1.1,1.6,2.6	"	4.8,3.2,2.1	2.9
L1-6	1.22,2.92,4.88	"	0.9,2.2,3.7	"	5.7,2.4,1.4	3.6
L1-7	0.73,1.70,4.63	"	0.5,1.3,3.5	"	9.6,4.1,1.5	3.5
L2-1	0.97,2.92, -	1.5	0.7,2.2, -	2.8	5.7,1.9, -	2.5
L2-2	0.73,1.95,2.92	"	0.5,1.5,2.2	"	7.7,2.9,1.9	2.5
L2-3	1.22,1.95, -	"	0.9,1.5, -	"	4.6,2.9, -	-
L2-4	1.22,3.41,5.37	"	0.9,2.6,4.0	"	4.6,1.6,1.0	2.7
L2-5	0.97,1.70,3.17	"	0.7,1.3,2.4	"	5.7,3.3,1.8	2.6
L2-6	1.70,4.39, -	"	1.3,3.3, -	"	3.3,1.3, -	3.1
L2-7	0.73,3.17,3.90	"	0.5,2.4,2.9	"	7.7,1.8,1.4	2.9
L3-1	1.22,2.68,4.63	1.5	0.9,2.0,3.5	2.7	4.4,2.0,1.2	3.0
L3-2	1.22,2.19,3.90	"	0.9,1.6,2.9	"	4.4,2.5,1.4	2.8
L3-3	1.70,2.44,4.15	"	1.3,1.8,3.1	"	3.2,2.2,1.3	2.9
L3-4	1.22,1.95,3.41	"	0.9,1.5,2.6	"	4.4,2.8,1.6	2.6
L3-5	1.70,2.68,3.90	"	1.3,2.0,2.9	"	3.2,2.0,1.4	2.8
L3-6	2.44,3.17, -	"	1.8,2.4, -	"	2.2,1.7, -	2.5
L3-7	0.97,3.41, -	"	0.7,2.6, -	"	5.6,1.6, -	2.6
L4-2	0.97,1.95, -	1.5	0.7,1.5, -	2.3	4.7,2.4, -	-
L4-3	0.97,1.95,3.41	"	0.7,1.5,2.6	"	4.7,2.4,1.3	2.5
L4-4	0.97,3.17, -	"	0.7,2.4, -	"	4.7,1.5, -	2.4
L4-5	0.97,1.70, -	"	0.7,1.3, -	"	4.7,2.7, -	-
L4-6	1.46,2.68, -	"	1.1,2.0, -	"	3.2,1.7, -	2.1
L5-1	0.73,3.17, -	1.6	0.6,2.5, -	2.5	6.8,1.6, -	2.5

Table 7.4 Bargower Bridge, North abutment's width estimation - Method of varying ℓ and v.

calculated transmission velocity was close to 1500 m/sec, then a thickness was estimated. If the calculated transmission velocity was very different from 1500 m/sec, originally assumed, then the original assumed transmission velocity was altered and the procedure was repeated, For example, point L1-1 had a calculated transmission velocity of 1600 m/sec which was close to 1500 m/sec first assumed. The calculated length was 3.3 m and the assumed one, which resulted in a reasonable transmission velocity, was 3.5 m. Therefore the estimated length was thought to be 3.4 m. For all levels, the thickness was estimated in this manner and the result for each level was averaged.

From Table 7.4 it is also seen that the thickness at each level was not constant. This could be due to the uneven shape of the hidden face of the abutment, reflection from a dense fill, or from a crack close to a hidden face.

Location	Ass'd.Vel. (m/sec)	Av'd.Cal'd. Length (m)	Ass'd. Length (m)	Av'd.Cal'd. Velocity (m/sec)	Av'd.Length Estimation (m)
L1	1500.	3.3	3.5	1600	3.3
L2	1500	2.6	2.8	1600	2.7
L3	1500	2.9	2.7	1500	2.7
L4	1500	2.0	2.3	1500	2.3
L5	1600	2.5	2.5	1600	2.5

Table 7.5 Bargower Bridge, North abutment width estimation - summary

Table 7.5 shows the estimated thickness of the abutment. It is seen that the average thickness of the abutment decreased with height as expected. It is also seen that the assumed transmission velocities are very similar to calculated ones.

It is noted that the accuracy of the approximation of the results is within an acceptable range. The transmission velocities are corrected to the nearest 100 m/sec and the transmission time values are taken to one decimal place. In the later case, the difference in calculated transmission velocity Δv, is given by:

$$\Delta v = 2\left(\frac{\ell o}{t_2} - \frac{\ell o}{t_1}\right)$$

where ℓo = assumed thickness

and t_1 and t_2 = transmission times.

Assuming a transmission path of 4.0 m, and a transmission time of $t_1 = 2.05 \times 10^{-3}$ sec and its approximation to one decimal place $t_2 = 2.0 \times 10^{-3}$ sec, gives:

$\Delta v = 98$ m/sec $\cong$ 100 m/sec.

This is again within the acceptable range of accuracy. This is clear from the fact that a variation of 200 m/sec within a transmission velocity of 2000 m/sec results in a 10% approximation. This percentage of approximation for the purpose of this test was considered to be acceptable.

7.3.3 Conclusions

The sonic NDT survey on Bargower Bridge in Ayrshire, Scotland, was carried out in two stages. The first stage was to monitor the transmission velocity through the wing walls, buttress, arch and spandrel walls to locate the areas of good quality masonry. It was also used to detect the presence of suspected voids in the bridge. The second stage was to estimate the thickness of the Northern abutment of the bridge. The results obtained and analysed showed that:

(1) A large area of void or cavity existed inside the bridge on the south west wing wall. The fact that no transmission was obtained at that area might well be due to a high degree of attentuation of the wave energy in the possible loose fill.

(2) A relatively large void area corresponding to a double skin due to presence of a secondary abutment also existed in the south west spandrel wall section of the bridge. In addition in the southern central arch under the bridge a large crack was observed. The presence of this crack plus the suspected voidage inside the bridge resulted in no transmission velocity being obtained at that section.

(3) The good quality masonry areas were shown to be in the buttress and arch sections of the bridge as expected.

(4) A few good transmission velocity readings on the wing walls and in the south west wing walls close to the buttress were also obtained. This is due to the presence of stone blocks or very densely compacted fill at those locations. In fact the subsequent investigations showed that a large area of stone blocks did exist near the south west buttress at the southern part of the south west wing wall.

(5) Several points especially on the wing walls indicated that some degree of voidage existed very close to the wing walls at the upstream side.

(6) The auto correlation and cross correlation reflection results of thickness measurement compared well with each other.

(7) Cepstrum and liftered (or filtered) spectrum method of analysing thickness measurements was found to be more reliable. This technique of analysing and measuring thickness showed that it is simpler to distinguish between the first and second reflections from the same reflecting surface.

(8) The results showed that there was more than one discontinuity in the abutment.

(9) The abutment hidden surface was suspected to have irregular shapes, since for each level, the thickness varied from point to point.

(10) It was also suspected that the abutment thickness decreased with increasing height as was expected.

(11) The accuracy of approximation, particularly for abutment thickness measurement, was found to be of the order of 10 per cent. This was thought to be an acceptable range for the purposes of this test.

7.4 HIGH BRIDGE - STRUIE

High Bridge in Struie in North Scotland is a single span masonry arch bridge. As in the case of Bargower Bridge, a sonic NDT survey was carried out on this bridge to locate the presence of good quality masonry and possible air voids in the bridge. In addition a reflection test was performed on the abutments to estimate their average widths at different levels. The test, however, was more extensive and thorough and it is similar to a full scale integrity test that may be carried out on a structure (Plate 7.5).

7.4.1 Method of Investigation

The method of investigation was identical to that of Bargower Bridge. A transmission velocity test was used to estimate the quality of the masonry and to locate the presence of suspected voids or major cracks in the bridge. In addition a transmission velocity measurement test was carried out on two cross-sections of the bridge from road level to wing walls. These results were used for cross-checking the presence of air voids or high attenuation of wave energy through the wing walls.

The abutment thickness measurement method was also similar to that of Bargower Bridge. Here again by exciting a point close to the accelerometer with an instrumented hammer, the dynamic response of the wall was monitored. Several readings for each point, several points at each level, were taken and then averaged.

The main experimental equipment again consisted of a digital two channel Nicolet 4094 oscilloscope, an accelerometer with built in charge amplifier, an instrumented hammer with a two and half tonne load cell and an FM high frequency tape recorder. The transmission velocity readings were recorded onto double sided 360K 5.25 inch floppy discs on the digital oscilloscope. The reflection test readings on the abutments were transmitted by the accelerometer to the FM high frequency tape recorder. The tape signals were then played into a Bruel & Kjaer 2034 two channel signal analyser, which converts analog signals into digital ones using a twelve bit A/D converter.

Plate 7.4 High Bridge-Struie

The reflection test results were analysed by using cepstrum and liftered spectrum functions. It was shown in the previous sections that the use of these functions results in reliable analysis measurements. The cepstrum function enables one to locate a harmonic of a periodicity in the cepstrum and the liftered (or filtered) spectrum function is used to differentiate between a fundamental harmonic or the subsequent ones (see sections 6.3.2 and 6.3.3). The conventional approach of time domain signal analysis could again prove difficult as there were multiple reflections and there was only one surface available.

7.4.2 Results and Analysis

7.4.2.1 Transmission velocity measurement

Table 7.6 shows the transmission velocity readings from either upstream to downstream or alternatively downstream to upstream. Fig. 7.12 gives a visual indication of these transmission results. It will be noted from this figure that there were significant areas of the bridge that no transmission was recorded. This can be due to one of the two following resons:

(i) Large voids or discontinuities existed in the structure.

(ii) A high degree of attenuation of the transmitted wave energy, due to the very loose nature of the infill, took place.

It will be noted from Table 7.6 that at certain points transmission could be obtained by exciting one face but not by the other. Therefore, as explained earlier for Middleton North Burn Bridge, a void existed very close to such points.

An examination of Fig. 7.12 and Table 7.6 shows that the quality of masonry in the vicinity of the barrel was much higher than that in other areas of the bridge. It is also shown that the east abutment had significantly poorer quality material and/or infill than the west abutment.

In order to investigate whether the no transmission areas in Fig. 7.12 were due to high attenuation or presence of voids, a complementary analysis technique was used. The test involved performing transmission velocity measurements on two cross-sections

of the bridge, one at point H1/7 and the other at point H1/4. These measurements were taken from the bridge or road deck/surface through to the spandrel/wing walls. Therefore the procedure involved exciting the surface of the road with transmission through the fill to the wing wall or spandrel wall. The test results are shown in Tables 7.7 and 7.8 and in Figs. 7.13 and 7.14.

Point	Trans. Vel. (Km/sec) Ups	Dns	Point	Trans. Vel. (Km/sec) Ups	Dns	Point	Trans. Vel. (Km/sec) Ups	Dns	Point	Trans. Vel. (Km/sec) Ups	Dns
H1-1	00	00	H2-17	1.4	1.1	H4-22	00	00	H7-24	00	00
H1-2	00	00	H2-18	00	1.1	H4-23	00	0.7	H7-25	00	00
H1-3	00	00	H2-19	0.3	00	H4-24	0.5	1.2	H7-26	00	00
H1-4	00	00	H2-20	00	0.6	H4-25	00	00	H8-5	00	0.4
H1-5	1.2	00	H2-21	00	00	H4-26	00	00	H8-6	0.7	0.5
H1-6	00	00	H2-22	00	00	H5-3	00	00	H8-20	00	00
H1-7	00	00	H2-23	00	00	H5-4	0.3	00	H8-21	00	00
H1-8	00	0.3	H2-24	00	0.6	H5-5	00	00	H8-22	00	00
H1-9	0.4	0.4	H2-25	0.9	0.8	H5-6	00	00	H8-23	00	00
H1-10	0.9	0.8	H2-26	00	00	H5-19	2.4	2.6	H8-24	00	00
H1-11	1.3	2.1	H3-1	0.9	00	H5-20	00	0.7	H8-25	00	00
H1-12	2.1	2.0	H3-2	00	00	H5-21	00	00	H8-26	00	00
H1-13	2.1	2.0	H3-3	00	00	H5-22	00	0.3	H9-6	1.1	00
H1-14	1.5	2.1	H3-4	00	0.4	H5-23	00	00	H9-20	00	00
H1-15	1.1	1.9	H3-5	00	00	H5-24	00	00	H9-21	00	00
H1-16	1.1	0.9	H3-6	0.9	0.5	H5-25	00	00	H9-22	00	00
H1-17	0.9	1.1	H3-7	00	1.9	H5-26	00	00	H9-23	00	00
H1-18	0.6	0.5	H3-18	2.2	2.2	H6-3	00	00	H10-6	1.3	1.3
H1-19	0.7	0.7	H3-19	0.6	0.9	H6-4	1.8	00	H10-20	00	00
H1-20	0.8	0.6	H3-20	00	00	H6-5	1.5	00	H10-21	0.9	0.9
H1-21	00	00	H3-21	00	00	H6-6	1.5	1.7	H10-22	1.0	0.9
H1-22	0.7	0.7	H3-22	0.6	0.5	H6-20	00	0.9	H11-20	00	1.2
H1-23	00	00	H3-23	0.4	0.4	H6-21	0.6	00	H11-21	1.6	00
H1-24	00	0.7	H3-24	00	00	H6-22	00	00	H12-20	1.7	1.0
H1-25	o.6	00	H3-25	00	00	H6-23	00	0.3			
H1-26	00	00	H3-26	00	00	H6-24	00	00			
H2-1	00	00	H4-2	00	00	H6-25	00	0.6			
H2-2	1.7	2.1	H4-3	00	00	H6-26	00	0.6			
H2-3	00	00	H4-4	0.6	00	H7-4	0.4	00			
H2-4	1.9	2.5	H4-5	0.8	00	H7-5	1.7	00			
H2-5	1.2	00	H4-6	1.0	00	H7-6	1.0	00			
H2-6	1.7	00	H4-7	2.2	1.5	H7-20	00	00			
H2-7	0.8	0.6	H4-19	1.6	1.6	H7-21	00	00			
H2-8	0.7	0.7	H4-20	0.7	0.5	H7-22	00	00			
H2-9	2.0	2.0	H4-21	0.9	0.4	H7-23	00	00			

Table 7.6 High Bridge, Struie - Transmission velocity values

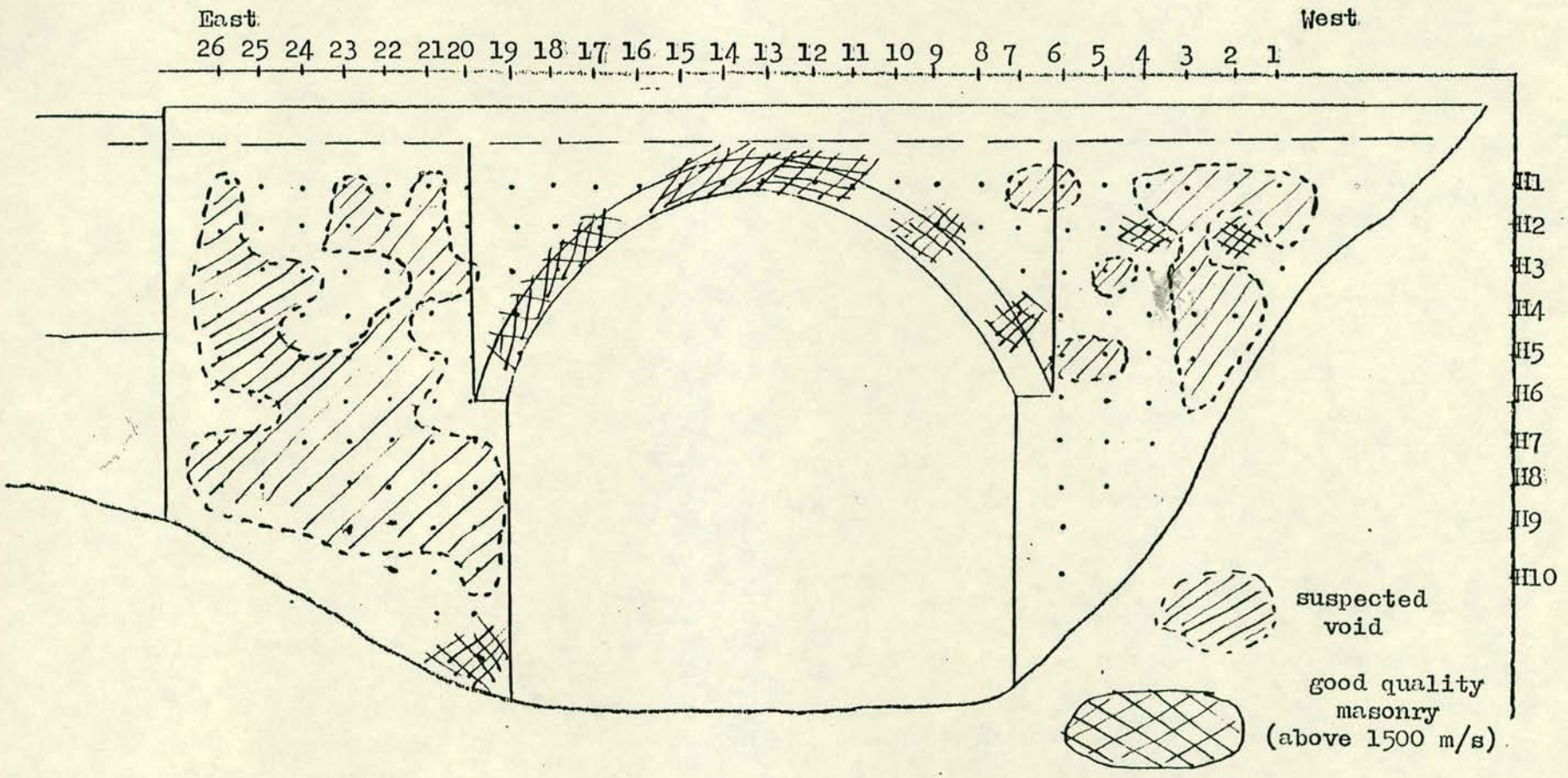

Fig. 7.12 High Bridge - Struie, downstream face, location of suspected voids and good quality masonry

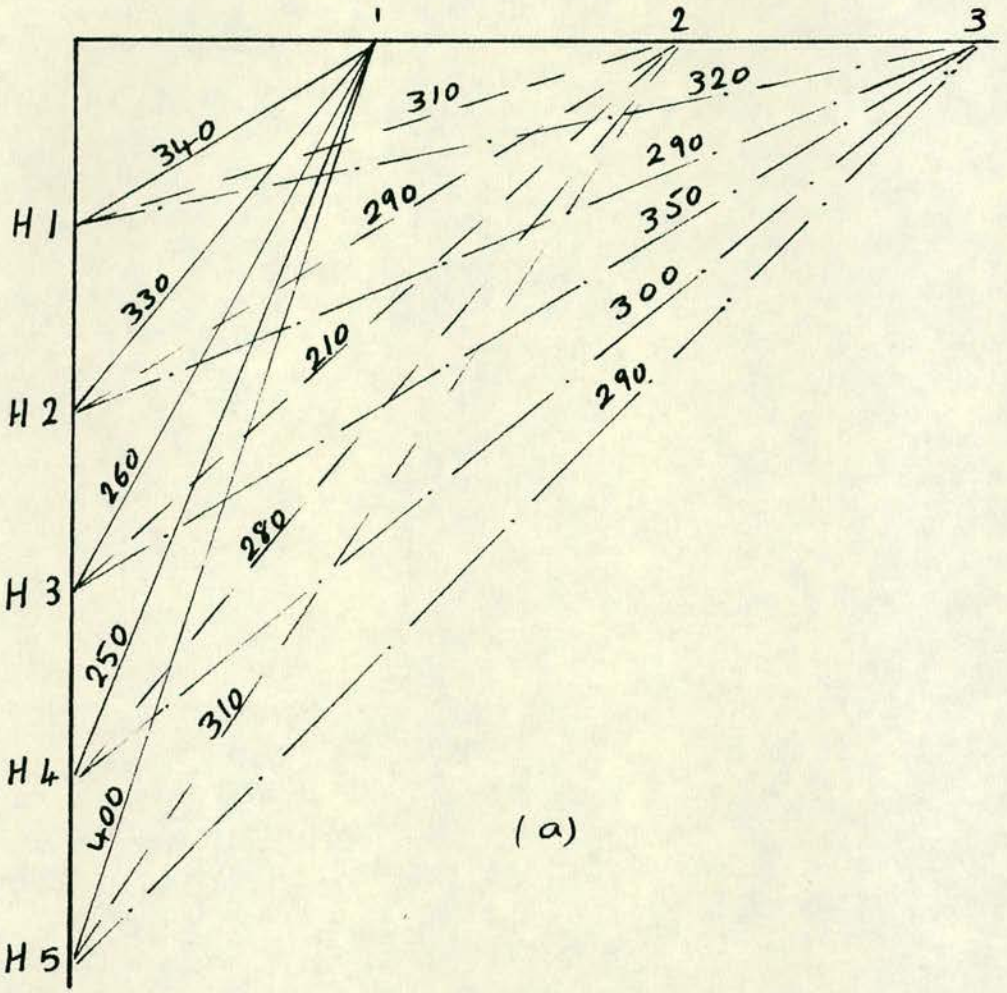

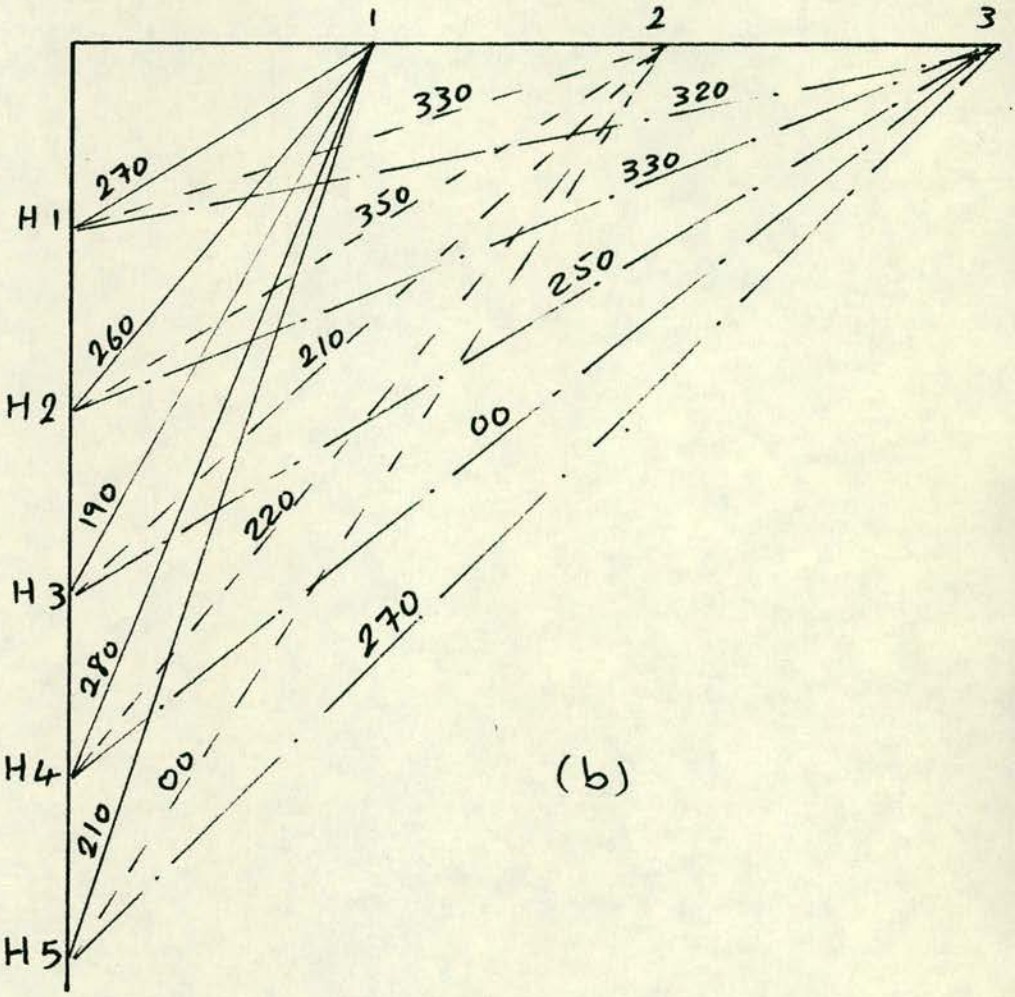

Fig. 7.13 High Bridge - Struie, transmission velocity values on cross-section H1/7 to H5/7, (a) upstream, (b) downstream

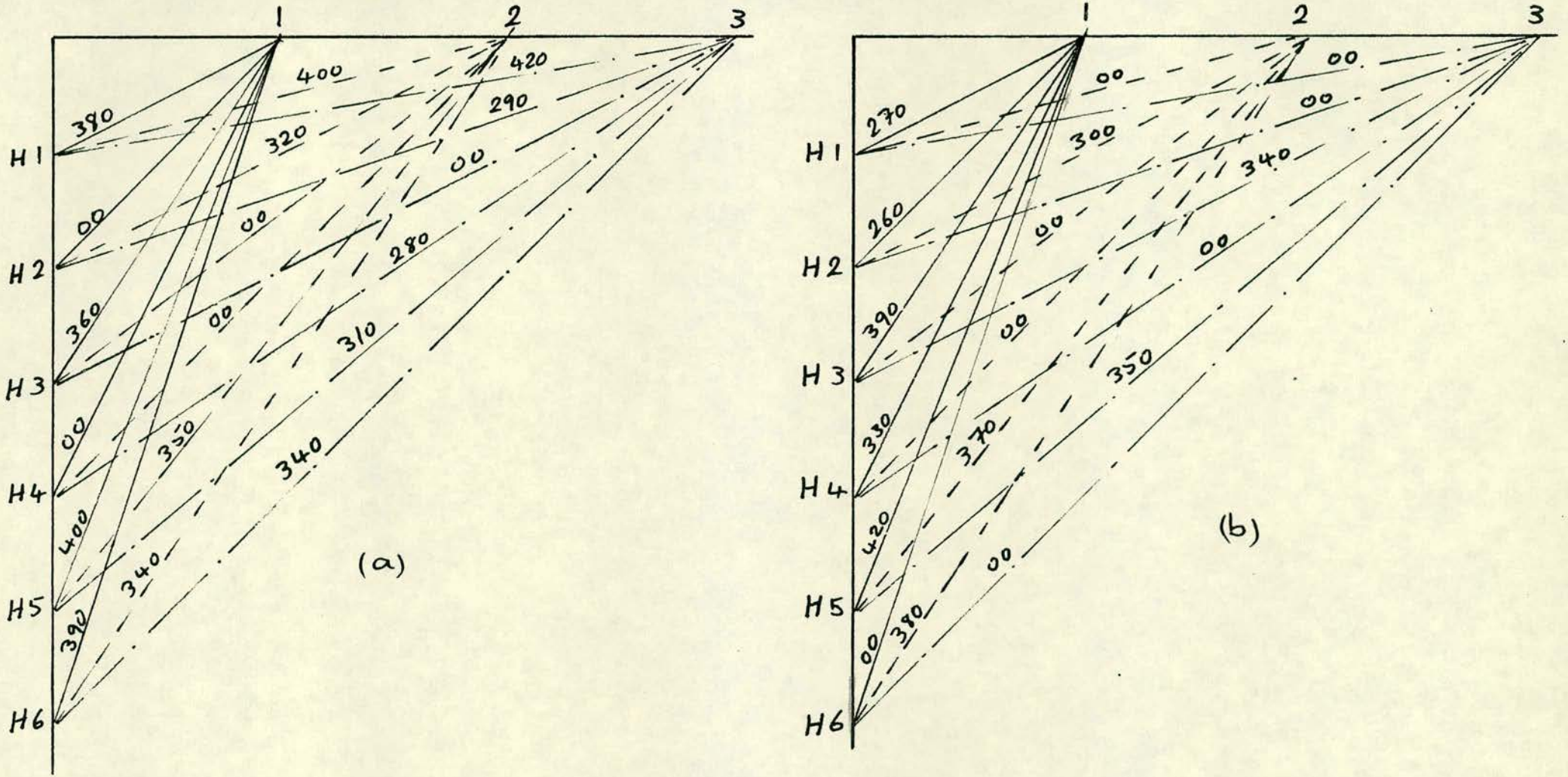

Fig. 7.14 High Bridge - Struie, transmission velocity on cross-section at H1/4 to H6/4, (a) upstream, (b) downstream

When a point on the road surface was excited, a compression wave was generated. The wave travelled in plane spherical shapes longitudinally. After a time interval the wave reached the area where the receiving accelerometer was mounted onto the wall and triggered it. The transmission velocity was then calculated by dividing the shortest distance between the exciting point and the accelerometer by the time interval recorded.

From visual inspection of Figs. 7.13 and 7.14, it is seen that the transmission velocities from the road deck through to the upstream face of the bridge were generally higher than those through to the downstream face. This could be due to a poorer coupling between the soil fill and wing wall masonry in the vicinity of the downstream face than the upstream face. It is also seen that the transmission velocity through the fill material was of the order of 400 m/sec. An important conclusion drawn from this investigation at cross-section (shown in Fig. 7.13) is that there was significant voidage in the downstream area of the bridge behind the wing walls. This was not only because the upstream transmission velocities were higher but also because no transmission was recorded at the upstream side when the downstream side was excited (see Fig. 7.12 and Table 7.6). Also it was not considered that the voidage continued laterally across the structure, but it was seen to occur in the vicinity of the wall.

Examination of Table 7.8 and Fig. 7.14 shows that on both sides of the bridge, close to masonry wing walls, a significant degree of voidage existed. The voidage at the downstream side was considered to be significantly larger and more widespread, whereas the voidage at the upstream side was mainly concentrated around points H3/4 and H4/4. The reason for not being able to obtain transmission velocities across the bridge at that vicinity was therefore clearly due to the presence of these voids and their widespread extent. Hence no energy was able to be transmitted. The transmission velocity through soil fill was again of the order of 400 m/sec.

Point	Wall from road level (m)		Road from wall across (m)		Velocity (m/sec)	
	Upst.	Dnst.	Upst.	Dnst.	Upst.	Dnst.
H1-7	0.0	0.0	1.5	1.5	340	270
H1-7	0.0	0.0	3.0	3.0	310	330
H1-7	0.0	0.0	4.5	4.5	320	320
H2-7	1.0	1.0	1.5	1.5	330	260
H2-7	1.0	1.0	3.0	3.0	290	350
H2-7	1.0	1.0	4.5	4.5	290	330
H3-7	2.0	2.0	1.5	1.5	260	190
H3-7	2.0	2.0	3.0	3.0	210	210
H3-7	2.0	2.0	4.5	4.5	350	220
H4-7	3.0	3.0	1.5	1.5	250	280
H4-7	3.0	3.0	3.0	3.0	280	220
H4-7	3.0	3.0	4.5	4.5	300	250
H5-7	4.0	4.0	1.5	1.5	400	210
H5-7	4.0	4.0	3.0	3.0	310	-
H5-7	4.0	4.0	4.5	4.5	290	270
H6-7	-	5.0	-	1.5	-	660
H6-7	-	5.0	-	3.0	-	950
H6-7	-	5.0	-	4.5	-	-

Table 7.7 High Bridge - Struie - Transmission velocity on cross-section exciting point on road deck/surface at point H1/7 to H6/7.

Point	Wall from road level (m)		Road from wall across (m)		Velocity (m/sec)	
	Ups.	Dnst.	Upst.	Dnst.	Upst.	Dnst.
H1-4	1.0	1.0	1.5	1.5	380	270
H1-4	1.0	1.0	3.0	3.0	400	-
H1-4	1.0	1.0	4.5	4.5	420	-
H2-4	2.0	2.0	1.5	1.5	-	260
H2-4	2.0	2.0	3.0	3.0	320	300
H2-4	2.0	2.0	4.5	4.5	290	-
H3-4	3.0	3.0	1.5	1.5	360	390
H3-4	3.0	3.0	3.0	3.0	-	-
H3-4	3.0	3.0	4.5	4.5	-	340
H4-4	4.0	4.0	1.5	1.5	-	330
H4-4	4.0	4.0	3.0	3.0	-	-
H4-4	4.0	4.0	4.5	4.5	280	-
H5-4	5.0	5.0	1.5	1.5	400	420
H5-4	5.0	5.0	3.0	3.0	350	370
H5-4	5.0	5.0	4.5	4.5	310	350
H6-4	6.0	6.0	1.5	1.5	390	-
H6-4	6.0	6.0	3.0	3.0	340	380
H6-4	6.0	6.0	4.5	4.5	340	-

Table 7.8 High Bridge - Struie - Transmission velocity on cross-section exciting point on road deck/surface at point H1/4 to H6/4.

7.4.2.2 Abutment thickness measurement

The method used to determine the average abutment thicknesses at different levels was similar to that used for Bargower Bridge. Here only one method of analysis, that is use of cepstrum and liftered spectrum functions, was used. Figs. 7.15 and 7.16 show the position of the points tested on the abutments. Figs. 7.17 and 7.18 show some typical results obtained using the above functions with short pass filter.

The method of interpretation is described in 7.3.2.2 for the Bargower Bridge.

Table 7.9 summarises the results for the East abutment and Table 7.10 for the West abutment. The method of estimating the width for each point was again by varying transmission velocity v and thickness ℓ. Studying these two tables shows that there was more than one discontinuity in the abutment. They could be due to stone mortar vertical joint or from a discontinuity beyond the abutment face. The thickness obtained for each point was averaged for each level and the results are summarised in Table 7.11. From Table 7.11 it is seen that the abutments did not have a constant width but they decreased with height as expected. The thickness at level 9 on the east abutment showed that there was a sudden decrease in thickness compared to previous level 8. This was due to the fact that level 9 was above the springer level and it was an arch surface which had a lesser thickness in comparison to the abutments.

The transmission velocity of the abutment masonry was estimated to be of the order of 1600 to 2000 m/sec. This is again typical for sandstone masonry as in the case of this bridge. The accuracy of the approximation of the results was estimated to be again of the order of 10%.

7.4.3 Conclusions

The test carried out on High Bridge, Struie, showed that:

(1) Large areas of the wing walls did not permit transmission from one side of the structure to the other.

Location Point	Trans. Time (mil.sec)	Ass'd Vel. (Km/sec)	Cal'd Length (m)	Ass'd Length (m)	Cal'd Vel. (Km/sec)	Est'd Length (m)
L1-1	3.2,5.1	1.6	2.6,4.1	4.1	1.6	4.1
L2-1	1.7,3.2	1.6	1.4,2.6	3.7	4.4,2.3	3.0)Av.
2	2.3,4.2	"	1.8,3.4	"	3.2,1.8	3.3)3.6
3	2.4,6.3	"	1.9,5.0	"	3.1,1.2	4.5)
L3-1	2.4,5.6	1.6	1.9,4.5	3.4	2.8,1.2	4.1)
2	4.2	"	3.4	"	1.6	3.4)
3	4.4	"	3.5	"	1.5	3.5)
4	3.7	"	3.0	"	1.8	3.2)Av.
5	2.3,4.2	"	1.8,3.4	"	3.0,1.6	3.4)3.4
6	2.2,4.6	"	1.8,3.7	"	3.1,1.5	3.5)
7	3.9	"	3.1	"	1.7	3.1)
8	3.4	"	2.7	"	2.0	3.0)
L4-1	2.4,3.9	1.7	2.0,3.3	3.2	2.7,1.6	3.3)
2	-	-	-	-	-	-)
3	3.17	"	3.1	"	1.7	3.1)
4	1.7,4.4	"	1.4,3.7	"	3.8,1.5	3.4)Av.
5	4.4	"	3.7	"	1.5	3.4)3.2
6	2.0,3.4	"	1.7,2.9	"	3.2,1.9	3.0)
7	3.9	"	3.3	"	1.6	3.3)
8	3.4	"	2.9	"	1.9	3.0)
L5-1	2.4,3.4	1.7	2.0,2.9	2.9	2.4,1.7	2.9)
2	2.4,3.9	"	2.0,3.3	"	2.4,1.5	3.1)
3	3.7	"	3.1	"	1.6	3.0)
4	2.4,3.2	"	2.0,2.7	"	2.4,1.8	2.8)Av.
5	1.7,3.4	"	1.4,2.9	"	3.4,1.7	2.9)2.8
6	2.7	"	2.3	"	2.1	2.5)
7	2.0,2.9	"	1.7,2.5	"	2.9,2.0	2.6)
8	1.7,3.2	"	1.4,2.7	"	3.4,1.8	2.8)

L6-1	1.7,2.2	1.7	1.4,1.9	2.6	3.1,2.4	2.0)
2	2.2,2.9	"	1.9,2.5	"	2.4,1.8	2.6)
3	3.2	"	2.7	"	1.6	2.7)
4	1.7,2.7	"	1.4,2.3	"	3.1,1.9	2.5)Av.
5	1.7,2.9	"	1.4,2.5	"	3.1,1.8	2.5)2.4
6	2.2	"	1.9	"	2.4	2.0)
7	1.7,2.7	"	1.4,2.3	"	3.1,1.9	2.5)
8	2.7	"	2.3	"	1.9	2.5)
L7-1	1.7	1.8	1.5	2.2	2.6	-)
2	1.2,2.4	"	1.1,2.2	"	3.7,1.8	2.2)
3	2.4	"	2.2	"	1.8	2.2)
4	1.7,2.4	"	1.5,2.2	"	2.6,1.8	2.2)Av.
5	1.5,2.4	"	1.3,2.2	"	2.9,1.8	2.2)2.2
6	1.7	"	1.5	"	2.6	-)
7	1.2,2.2	"	1.0,2.0	"	3.7,2.0	2.0)
8	1.2,1.7	"	1.0,1.5	"	3.7,2.6	-)
L8-1	2.2	1.8	2.0	2.0	1.8	2.0)
2	1.2,2.7	"	1.0,2.4	"	3.3,1.5	2.2)
3	1.2,2.7	"	1.0,2.4	"	3.3,1.5	2.2)
4	1.2	"	1.0	"	3.3	-)Av.
5	2.2	"	2.0	"	1.8	2.0)2.1
6	1.7	"	1.5	"	2.4	-)
7	2.4	"	2.2	"	1.7	2.0)
8	2.4	"	2.2	"	1.7	2.0)
L9-1	2.0	2.0	2.0	1.0	1.0	-)
2	1.0	"	1.0	"	2.0	1.0)
3	1.2,2.2	"	1.2,2.2	"	1.7,0.9	1.0)Av.
4	1.0	"	1.0	"	2.0	1.0)1.0
5	1.0	"	1.0	"	2.0	1.0)
6	1.0	"	1.0	"	2.0	1.0)
7	1.0	"	1.0	"	2.0	1.0)

Table 7.9 High Bridge - Struie - East abutment width estimation - method of varying v and ℓ

Location Point	Trans. Time (mil.sec)	Ass'd Vel. (Km/sec)	Cal'd Length (m)	Ass'd Length (m)	Cal'd Vel. (Km/sec)	Est'd Length (m)
L1-1	2.4,5.6	1.7	2.0,4.8	4.2	3.5,1.5	4.4)
2	2.9,4.2	"	2.5,3.6	"	2.9,2.0	3.8)
3	3.2	"	2.7	"	2.6	-)
4	3.0	"	2.5	"	2.8	-)Av.
5	-	-	-	-	-	-)4.2
6	4.2	"	3.6	"	2.0	3.4)
7	2.4,5.6	"	2.0,4.8	"	3.5,1.5	5.0)
8	2.0,5.1	"	1.7,4.3	"	4.2,1.6	4.4)
L2-1	1.7,4.2	1.7	1.4,3.6	3.7	4.4,1.8	3.6)
2	2.44,4.6	"	2.1,3.9	"	3.0,1.6	3.8)
3	2.7,4.2	"	2.3,3.6	"	2.7,1.8	3.6)
4	1.2	"	1.0	"	6.2	-)Av.
5	1.5	"	1.3	"	4.9	-)3.6
6	2.9,4.2	"	2.5,3.6	"	2.6,1.8	3.6)
7	2.7	"	2.3	"	2.7	-)
8	2.7	"	2.3	"	2.7	-)
L3-1	2.9,4.9	1.8	2.6,4.4	2.9	2.0,1.2	2.8)
2	1.9,3.4	"	1.7,3.1	"	3.1,1.7	3.1)
3	1.5,2.7	"	1.3,2.4	"	3.9,2.1	2.6)
4	1.2,2.2	"	1.1,2.0	"	4.8,2.6	-)Av.
5	1.5,2.4	"	1.3,2.2	"	3.9,2.4	-)2.9
6	2.4	"	2.2	"	2.4	-)
7	2.4	"	2.2	"	2.4	-)
8	1.5,3.2	"	1.3,2.9	"	3.9,1.8	2.9)
L4-1	1.7,3.7	1.8	1.5,3.3	2.6	3.1,1.4	2.9)
2	1.5,3.2	"	1.3,2.9	"	3.5,1.6	2.7)
3	1.5,2.2	"	1.3,2.0	"	3.5,2.4	2.0)
4	2.2	"	2.0	"	2.4	2.0)Av.
5	2.4,3.2	"	2.2,2.9	"	2.2,1.6	2.7)2.5
6	1.5,2.7	"	1.3,2.4	"	3.5,1.9	2.5)
7	1.9,3.6	"	1.7,3.2	"	2.7,1.4	3.0)
8	2.4	"	2.2	"	2.2	2.4)

L5-1	1.5,3.2	1.8	1.3,2.9	2.2	2.9,1.4	2.6)
2	1.5,2.4	"	1.3,2.2	"	2.9,1.8	2.2)
3	2.4	"	2.2	"	1.8	2.2)
4	2.2	"	2.0	"	2.0	2.1)Av.
5	1.5	"	1.3	"	2.9	-)2.2
6	2.0	"	1.8	"	2.2	2.0)
7	1.7,2.7	"	1.5,2.4	"	2.6,1.6	2.3)
8	1.5,2.7	"	1.3,2.4	"	2.9,1.6	2.3)
L6-1	2.2,3.4	1.8	2.0,3.1	1.8	1.6,1.1	1.9)
2	1.7,2.9	"	1.5,2.6	"	2.1,1.2	1.9)
3	2.0	"	1.8	"	1.8	1.8)
4	1.5	"	1.4	"	2.4	1.4)Av.
5	2.0	"	1.8	"	1.8	1.8)1.8
6	1.5	"	1.4	"	2.4	1.6)
7	1.7,2.7	"	1.5,2.4	"	2.1,1.3	2.0)
8	1.5,2.7	"	1.4,2.4	"	2.4,1.3	2.0)
L7-1	2.4	1.9	2.3	1.6	1.3	2.0)
2	1.5	"	1.4	"	2.1	1.4)
3	1.2,2.4	"	1.1,2.3	"	2.7,1.3	2.0)Av.
4	1.7	"	1.6	"	1.9	1.6)1.7
5	1.5	"	1.4	"	2.1	1.3)
6	1.7	"	1.6	"	1.9	1.6)
7	2.0	"	1.9	"	2.6	1.8)

Table 7.10 High Bridge - Struie - West abutment width estimation - method of varying v and ℓ

(2) The barrel/arch area of the bridge was shown to have a reasonably high transmission velocity, thus indicating a good quality masonry there. The transmission velocities were of the order of 1500 to 2500 m/sec.

(3) Complementary investigation techniques involving transmission velocity measurement from the road deck through to wing walls, at two cross-sections, showed that the deck soil fill/wing wall coupling quality was significantly poorer in the downstream side in comparison to the upstream side.

(4) It was also shown from the downstream side of the structure that voidage existed at where the cross-sections were taken. The voidage was thought to occur immediately behind the wing wall at a depth of the order of 3 to 5 metres approximately. The voidage was not seen to be occurring across the bridge but only in the vicinity of the wing wall.

(5) The sonic transmission velocity test showed the area of the structure which could be considered for repair such as grouting.

(6) The abutment thickness measurement showed that the average width at each level varied. The lowest level had a width of around 4.0 m and it decreased to around 2.0 m below springer level. The average transmission velocity estimated for the abutment masonry was shown to vary between 1600 and 2000 m/sec.

(7) The above sonic NDT survey illustrates a complete non-destructive testing technique which can be carried out on a masonry structure with reasonable confidence and reliability. The results can be used for possible repair and improvement recommendations.

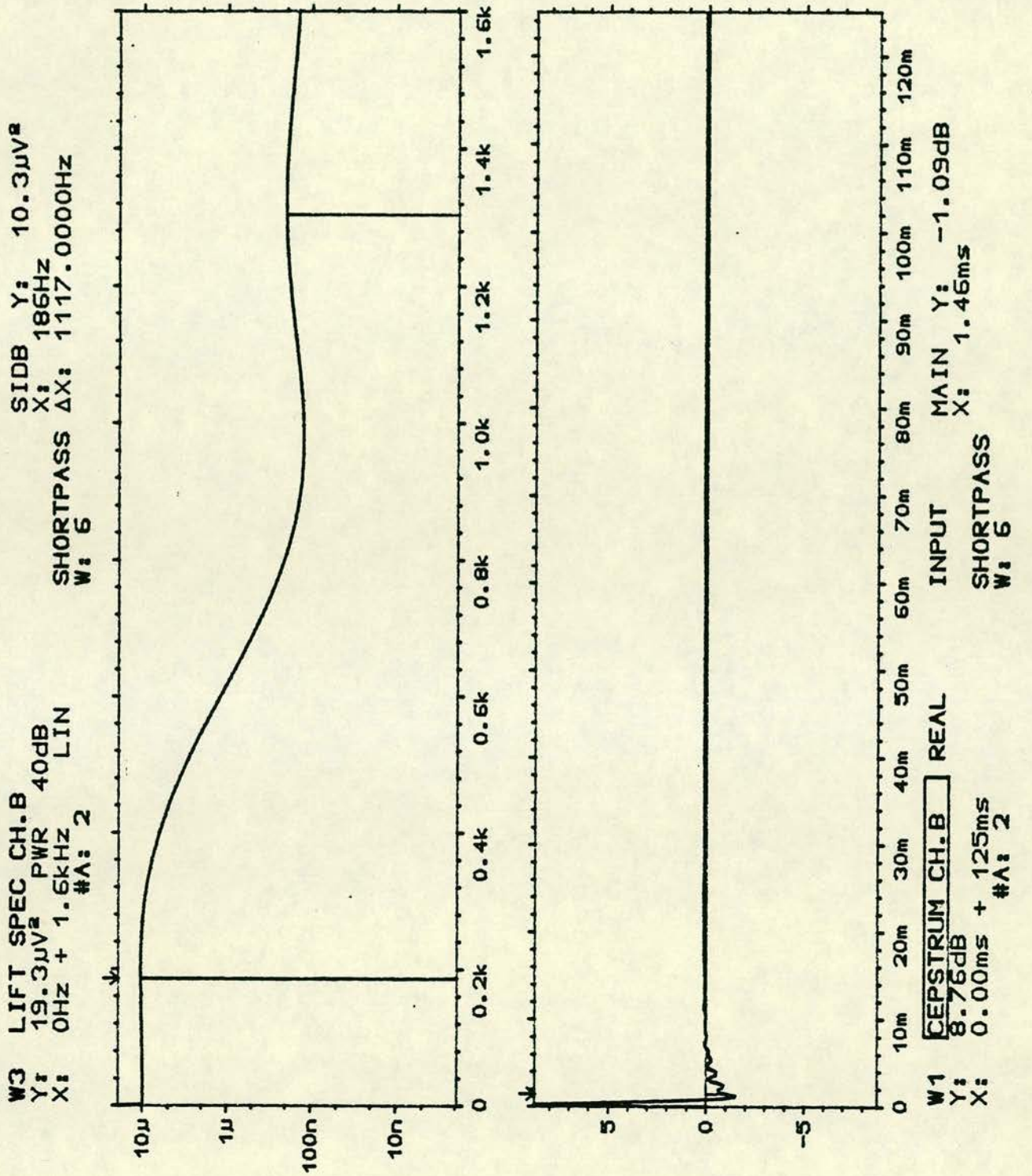

Fig. 7.15(a) High Bridge - Struie - west abutment point L3/5, reflection at 1.46 ms

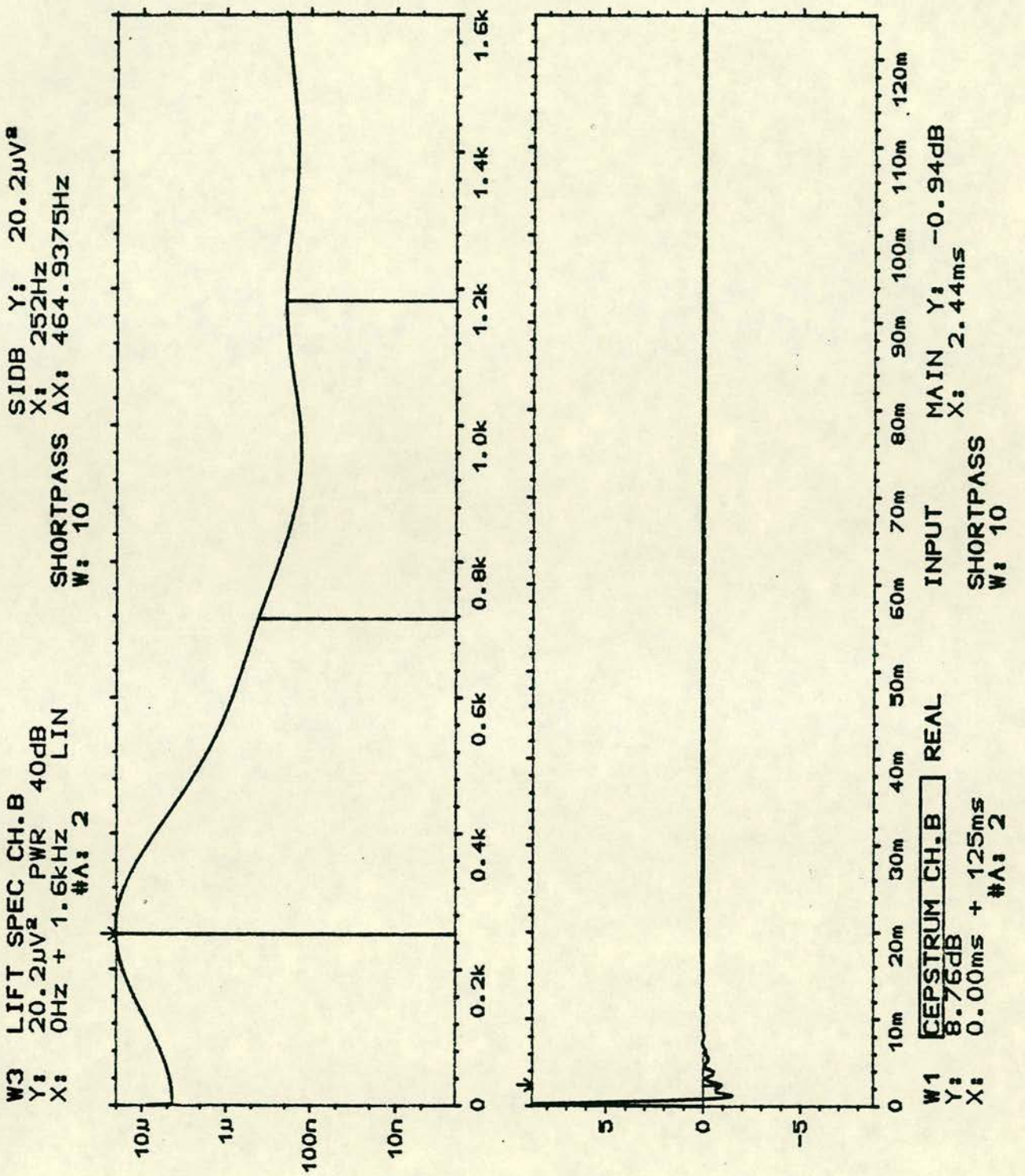

Fig. 7.15(b) High Bridge - Struie - west abutment point L3/5,. reflection at 2.44 ms

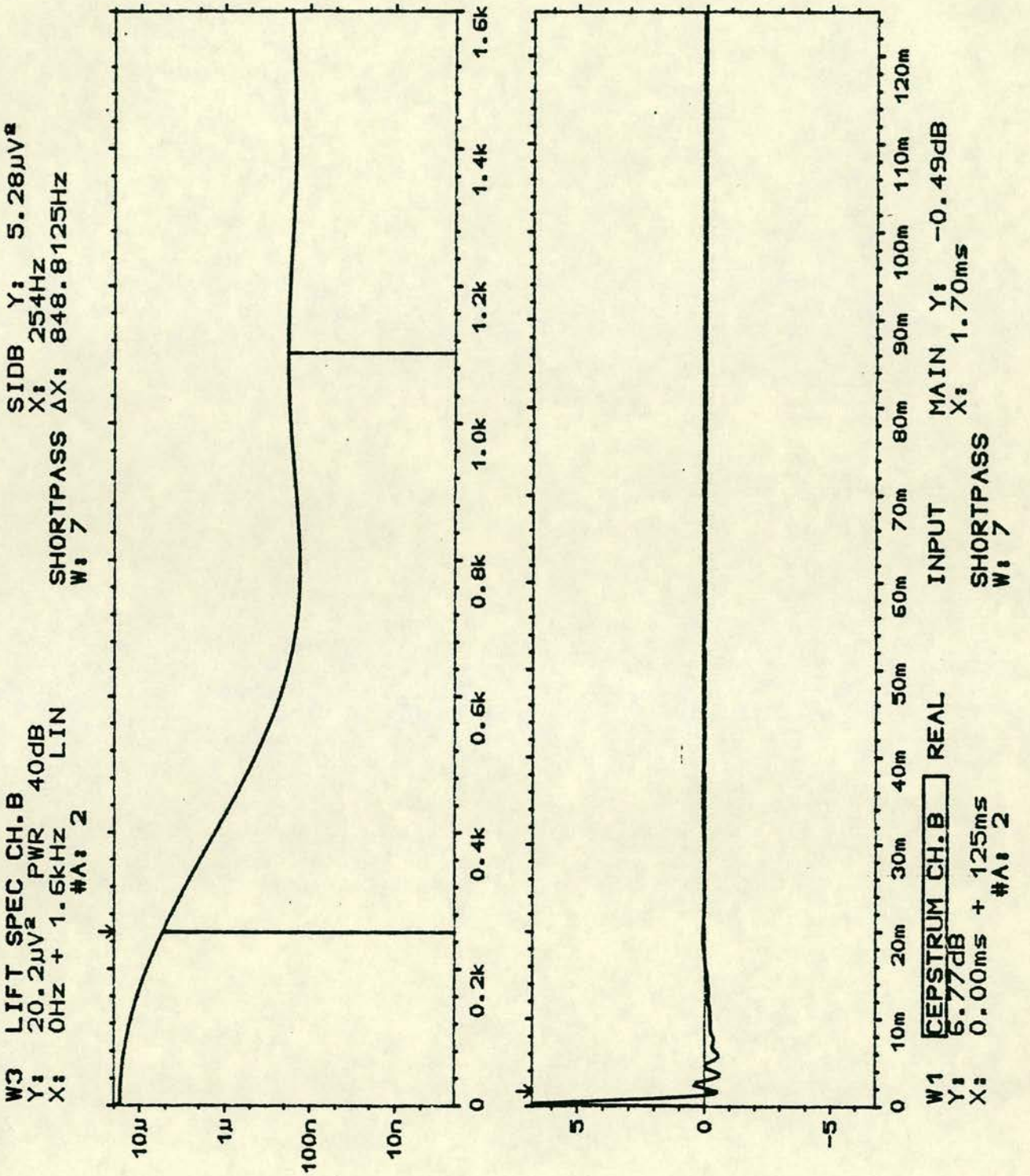

Fig. 7.16(a) High Bridge - Struie - west abutment point L5/7, reflection at 1.70 ms

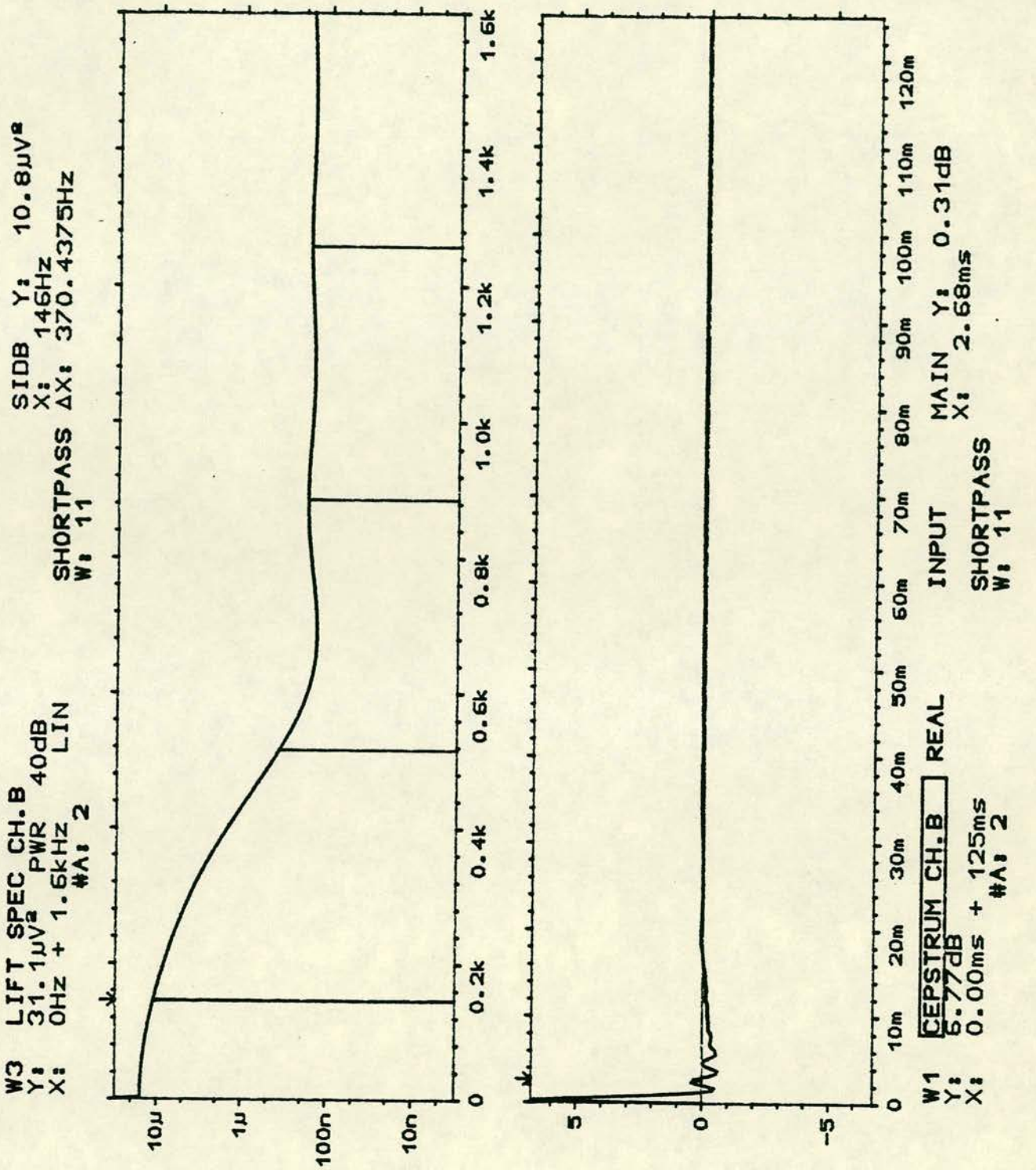

Fig. 7.16(b) High Bridge - Struie - west abutment point L5/7, reflection at 2.68 ms

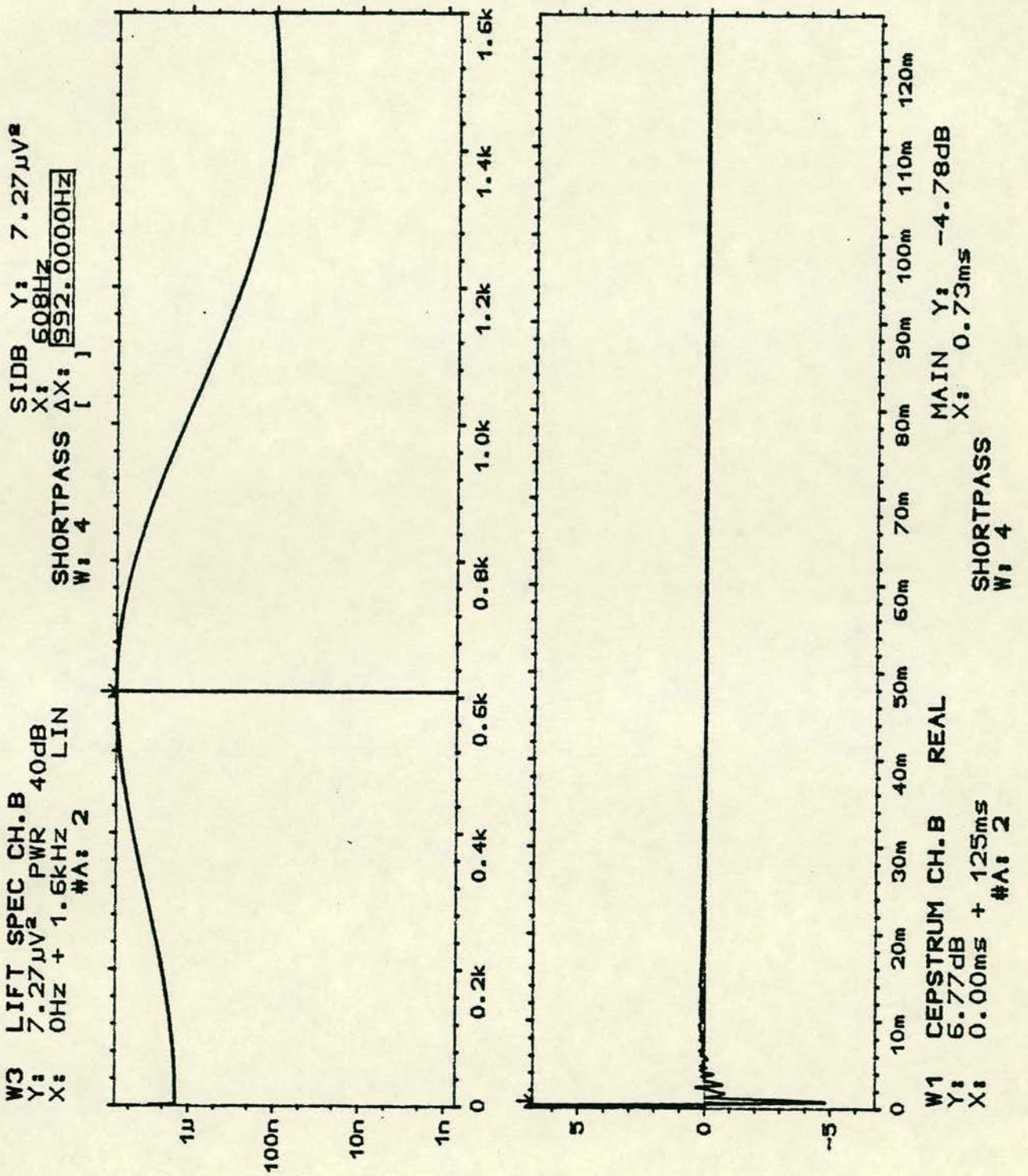

Fig. 7.17(a) High Bridge - Struie - east abutment point L2/3, reflection at 0.73 ms

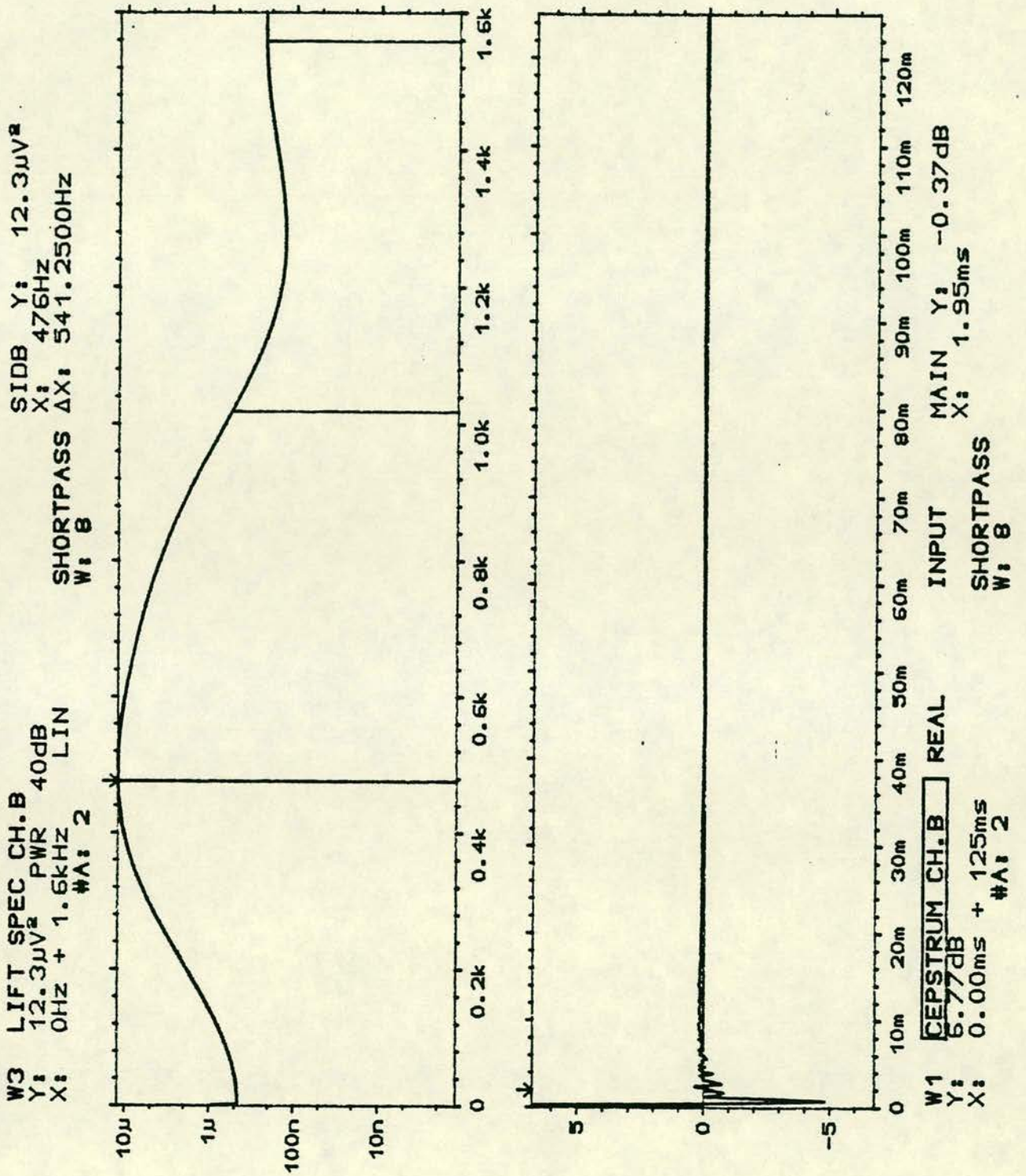

Fig. 7.17(b) High Bridge - Struie - east abutment point L2/3, reflection at 1.95 ms

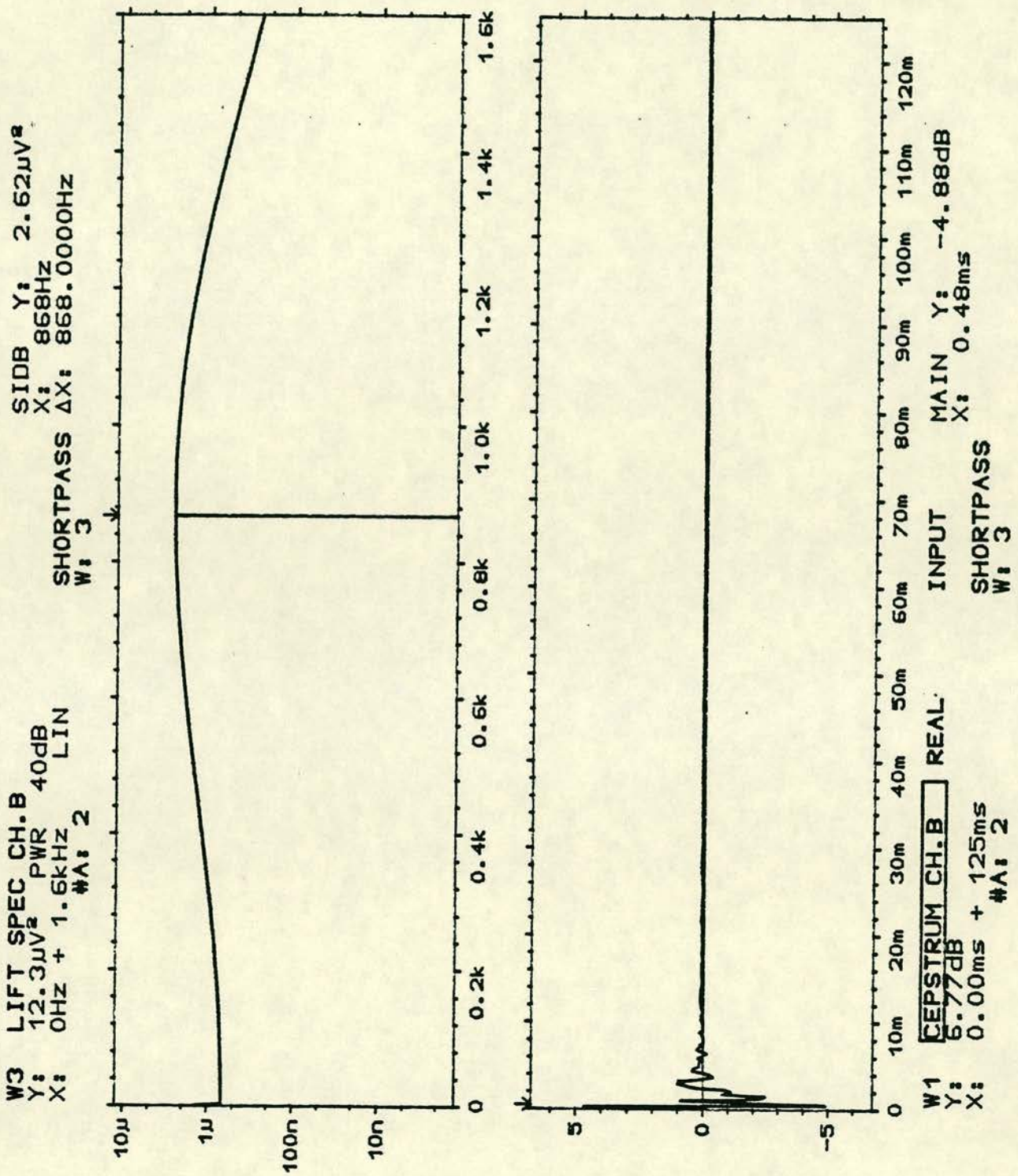

Fig. 7.18(a) High Bridge - Struie - east abutment point L4/3, reflection at 0.48 ms

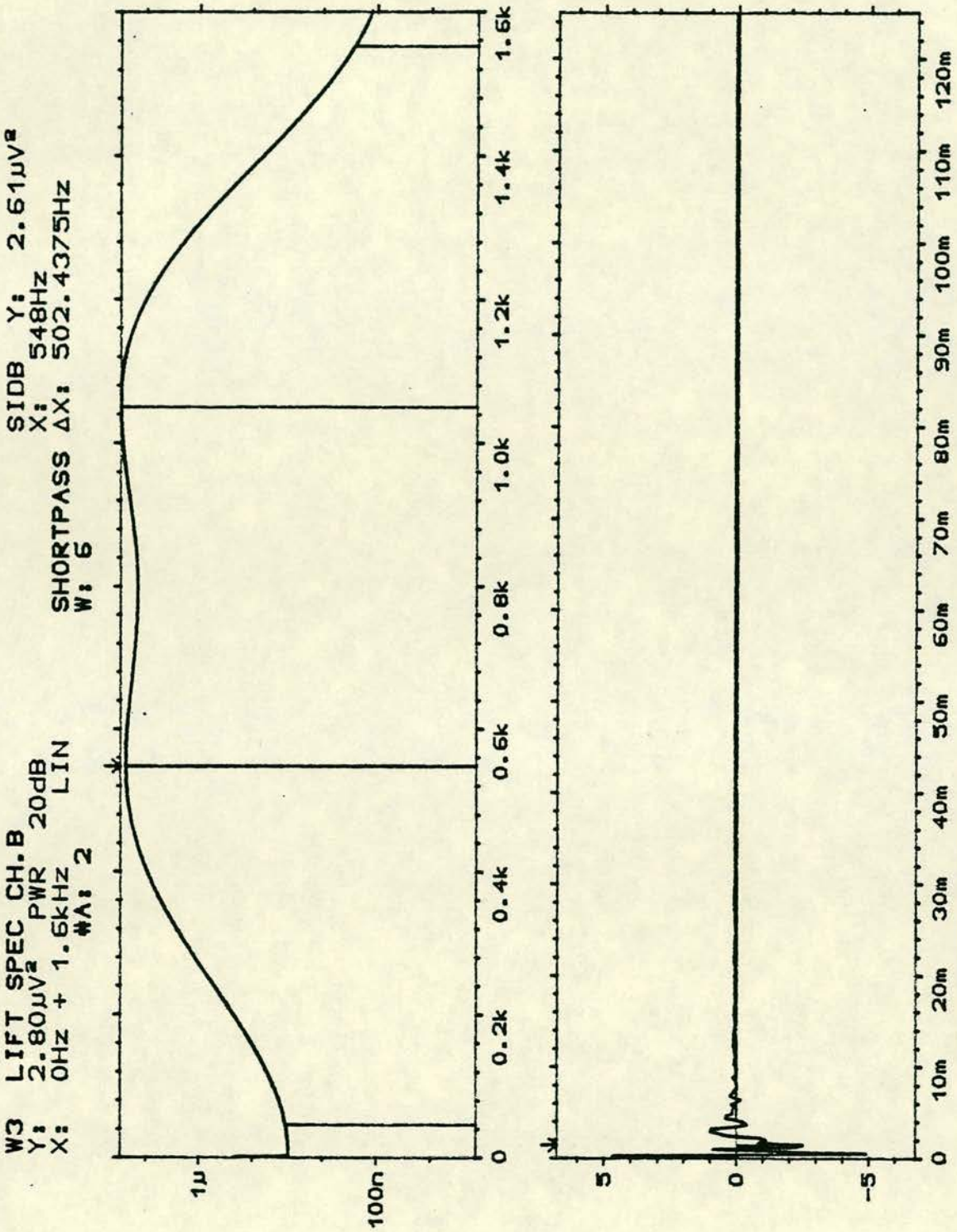

Fig. 7.18(b) High Bridge - Struie - east abutment point L4/3, reflection at 1.46 ms

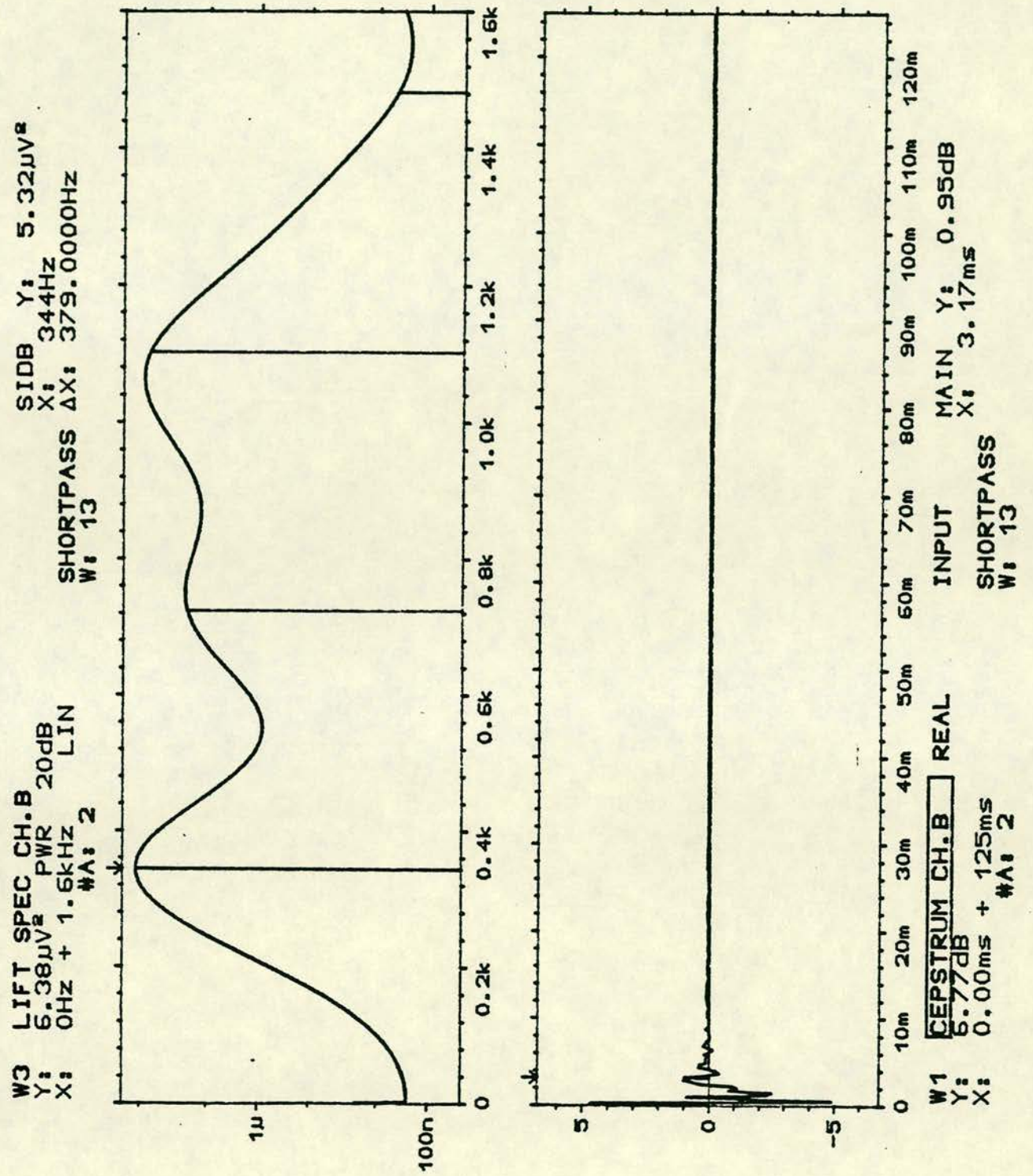

Fig. 7.18(c) High Bridge - Struie - east abutment point L4/3, reflection at 3.17 ms

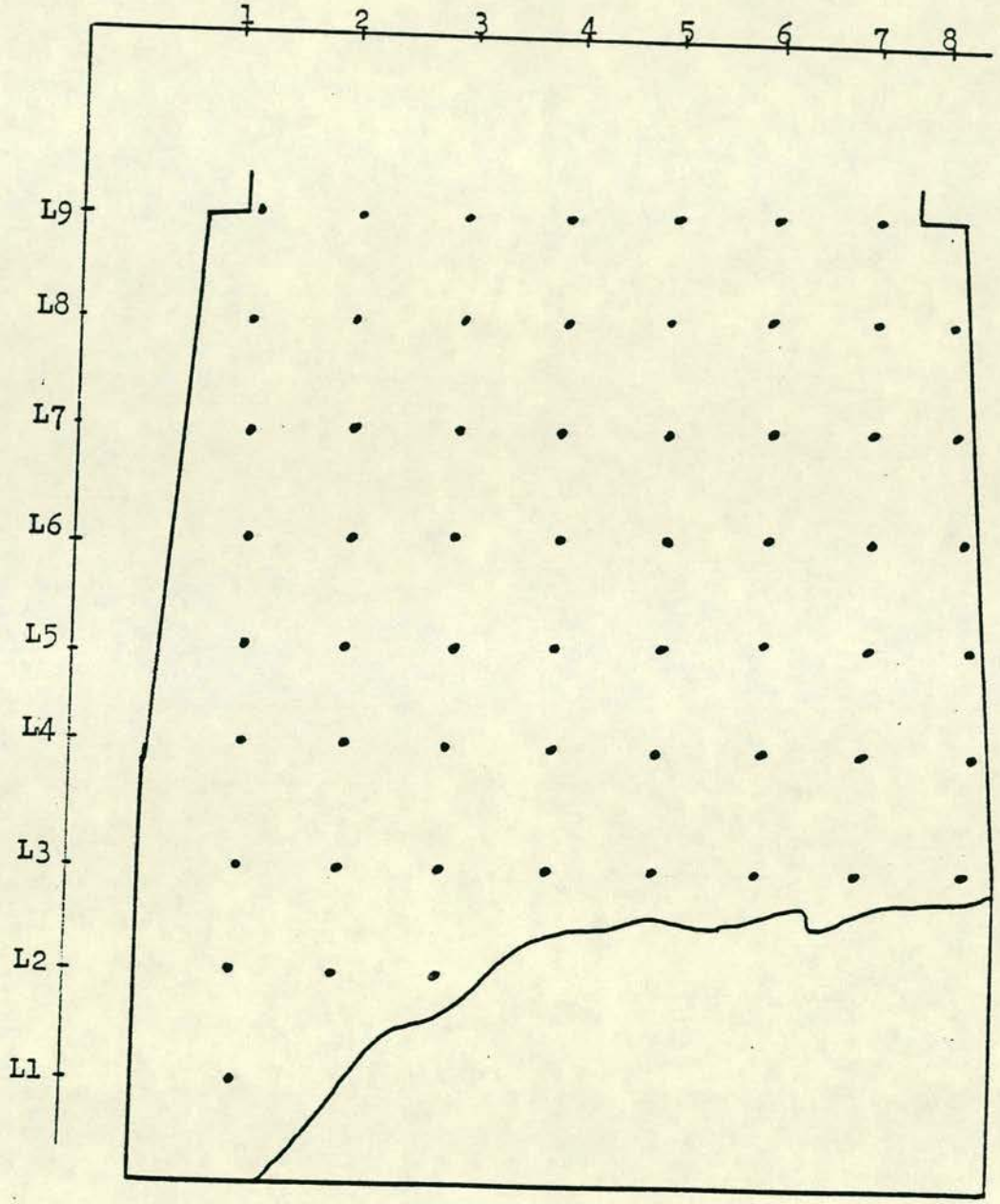

Fig. 7.19 High Bridge - Struie - east abutment, location of reflection test points

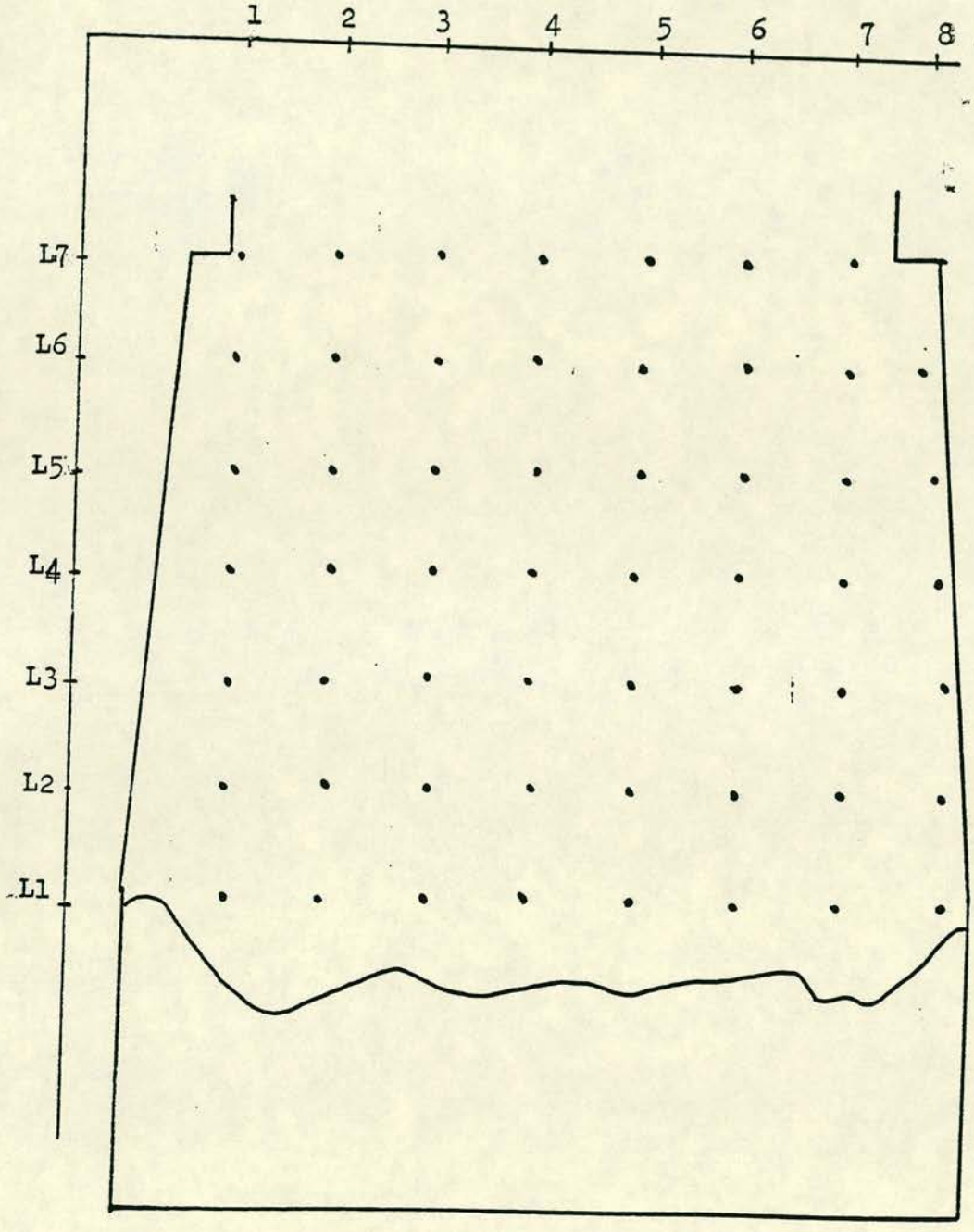

Fig. 7.20 High Bridge - Struie - west abutment, location of reflection test points

Location	Ass'd Vel.	Averaged Cal'd Length	Ass'd Length	Averaged Cal'd Vel.	Length Estimated
L1-East	1600	4.1	4.1	1600	4.1
L2-East	1600	3.7	3.7	1800	3.6
L3-East	1600	3.5	3.4	1600	3.4
L4-East	1700	3.3	3.2	1700	3.2
L5-East	1700	2.8	2.9	1800	2.8
L6-East	1700	2.3	2.6	2000	2.4
L7-East	1800	1.9	2.2	2100	2.2
L8-East	1800	2.0	2.0	2000	2.1
L9-East	2000	1.2	1.0	1800	1.0
L1-West	1700	3.8	4.2	1700	4.2
L2-West	1700	2.7	3.7	2100	3.6
L3-West	1800	2.7	2.9	2100	2.9
L4-West	1800	2.6	2.6	1900	2.5
L5-West	1800	2.2	2.2	1800	2.2
L6-West	1800	2.0	1.8	1700	1.8
L7-West	1900	1.6	1.6	1700	1.7

Table 7.11 High Bridge - Struie - Abutment thickness measurement, average results for each level

7.5 VICTORIA BRIDGE - CAPUTH

Victoria Bridge on the River Tay in Tayside Region is located on the B9099, on the edge of the village of Caputh. The bridge is a three span lattice girder structure with two piers in the river. The piers are resting on "quarried" foundations which extend to some depth below the river bed. The "quarried" foundations are thought to be concrete (Plate 7.5).

The purpose of the test was to establish as much information as possible regarding the quality of the piers below the masonry columns. Therefore it was proposed to carry out transmission velocity testing laterally from one side of the piers to the other to determine quality of material above water level. In addition, further tests were suggested to be undertaken vertically downwards from the top of the piers above the water level.

The experimental equipment was similar to that used for the two previous bridges of Bargower and Struie.

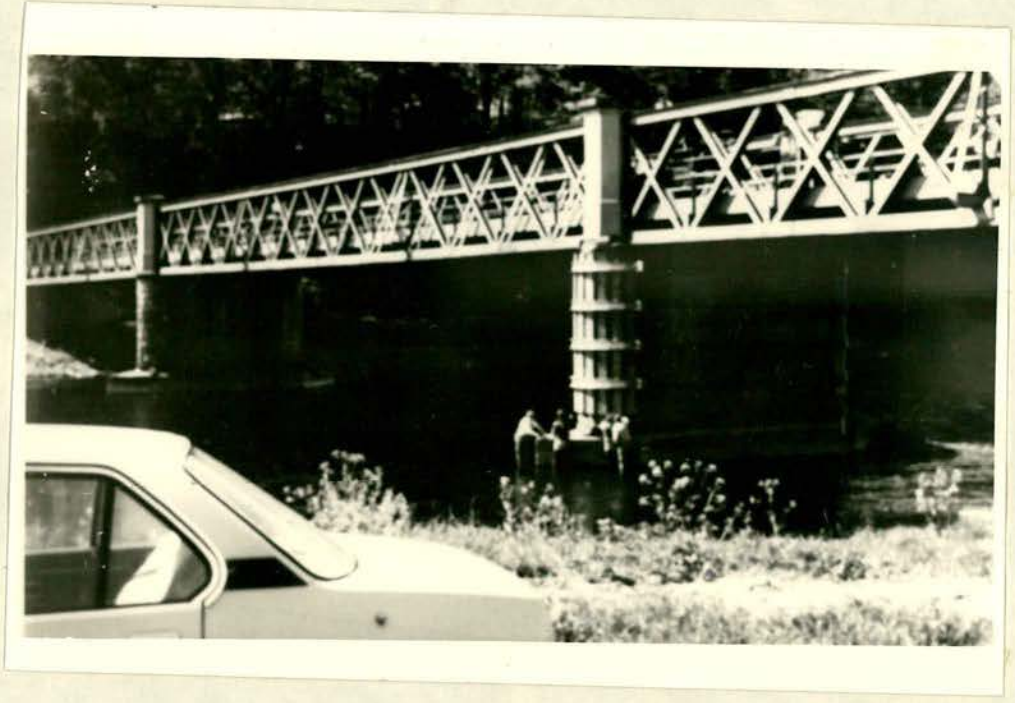

Plate 7.5 Victoria Bridge, Caputh

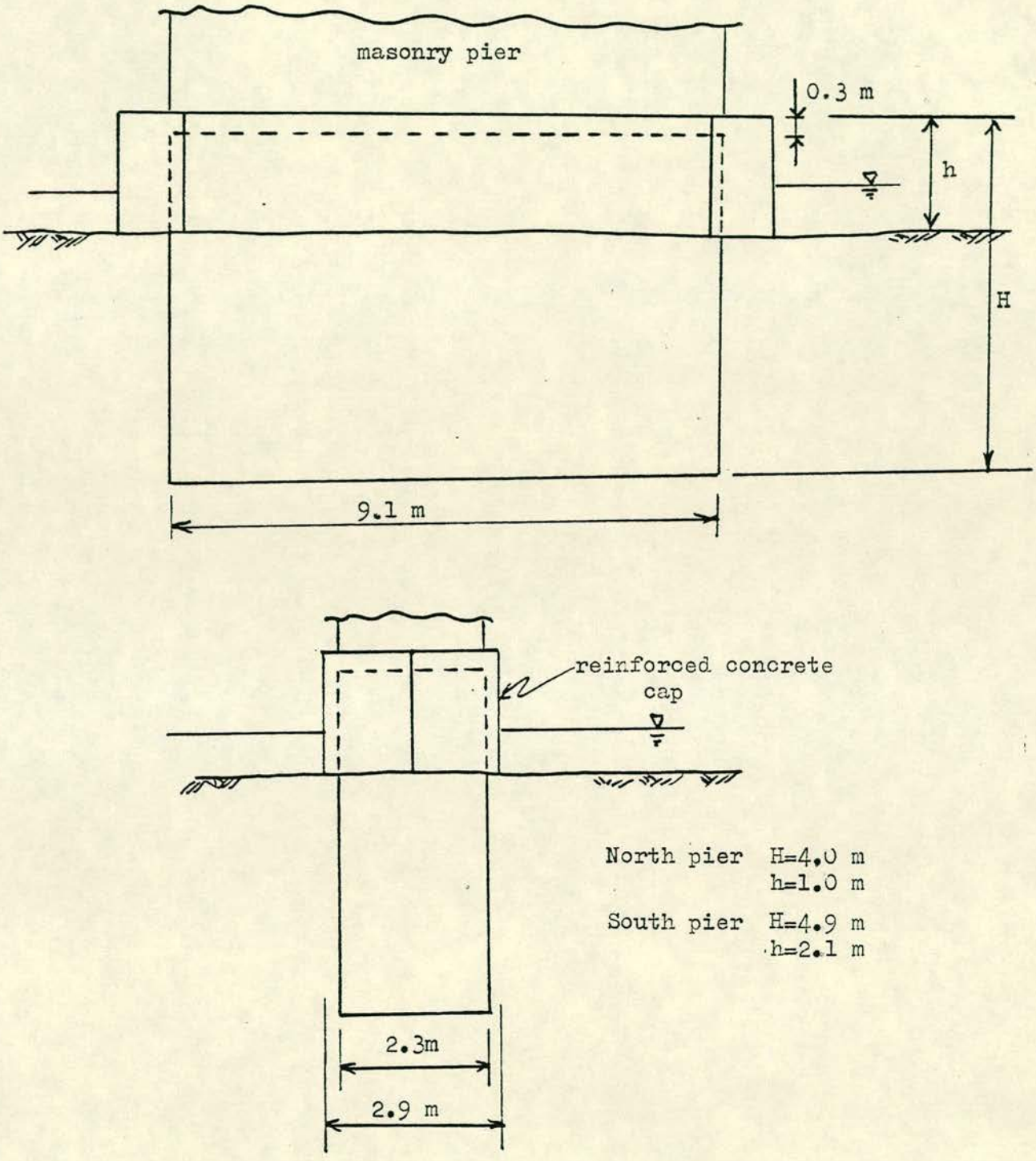

Fig. 7.21 Victoria Bridge - Caputh - elevation, piers dimensions and details

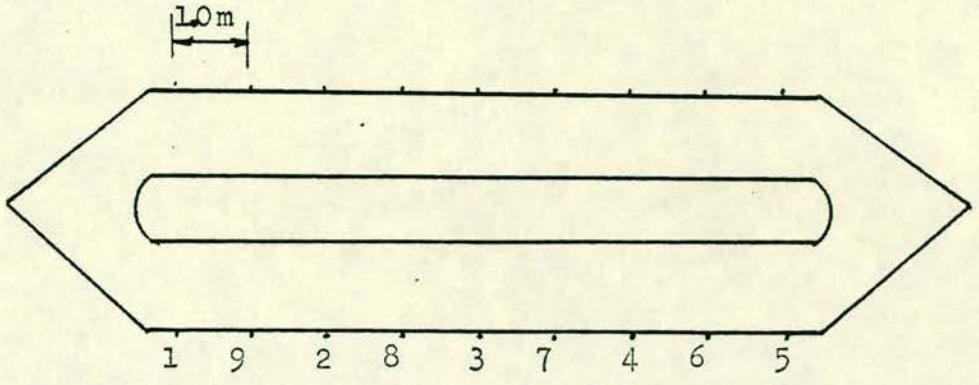

Plan

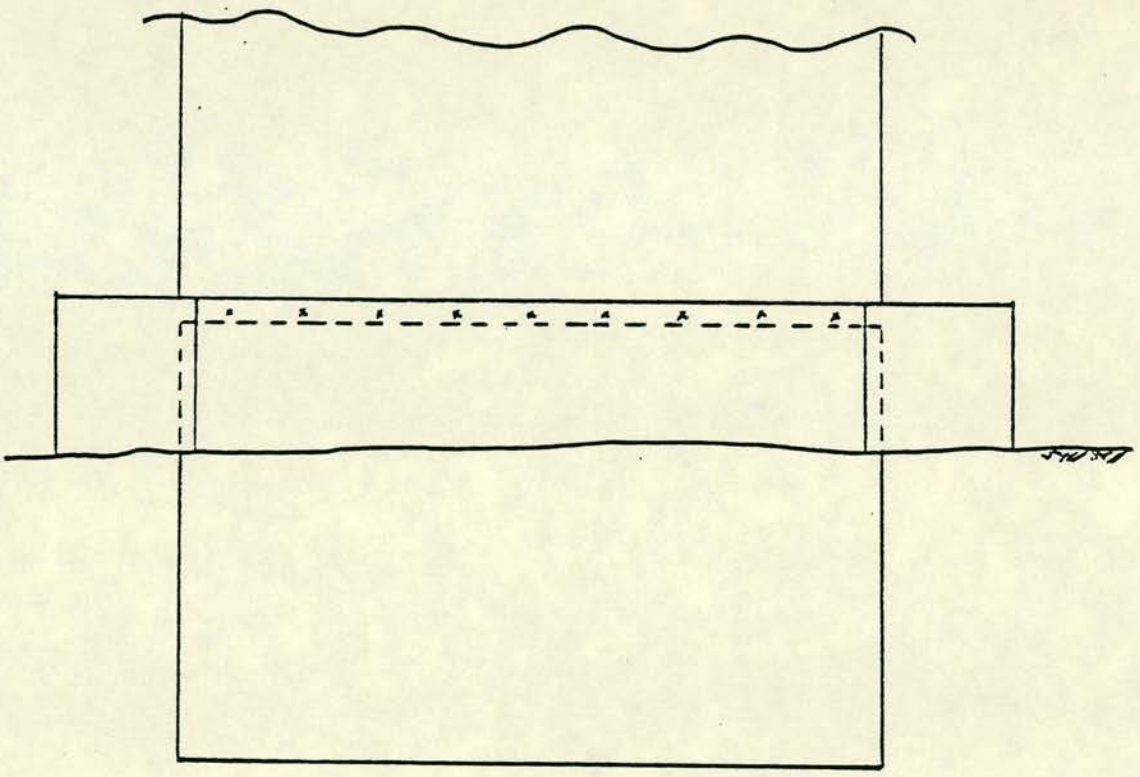

Elevation

Fig. 7.22 Victoria Bridge - Caputh - North pier, location of test points for horizontal transmission velocity measurement

7.5.1 Experimental Method and Procedure

7.5.1.1 Horizontal transmission velocity testing of piers

The transmission velocity measurement here again involved measuring the time taken for the transmitted compression wave to travel from one side of the structure to the other side. This technique was used to evaluate the quality of the piers protruding above the water level. The transmission time was measured by striking the pier opposite the point where the accelerometer was attached, using the instrumented hammer. The signal was being recorded on the FM high frequency tape recorder.

The interpretation of the results was based on the following:

(i) if no transmission was observed, then voidage, leaf separation or discontinuity from a crack was present.

(ii) where transmission did take place, the faster the velocity the higher the quality of the material was.

As a basis for preliminary inspection of the transmission velocities obtained, the reader may refer to Tables 5.6 and 5.7 in chapter 5. These tables give indications of the different velocities through a range of different materials. It is seen that the transmission velocity through good quality concrete is of the order of 4000 metres per second and through good quality sandstone masonry about 2000 metres per second.

7.5.1.2 Vertical testing of piers

The two piers were tested from the horizontal surface exposed above water level in a vertical direction towards the river bed. The procedure involved mounting the accelerometer with built in charge amplifier onto the horizontal surface of the pier above water level. Then using the instrumented hammer with a built in two and a half tonne load cell, the pier was excited at a point close to the accelerometer. The consequent dynamic response of the pier at that point was recorded onto the FM high frequency tape recorder. Then by using the Bruel & Kjaer 2034 two channel signal analyser, the results were analysed later on in the laboratory.

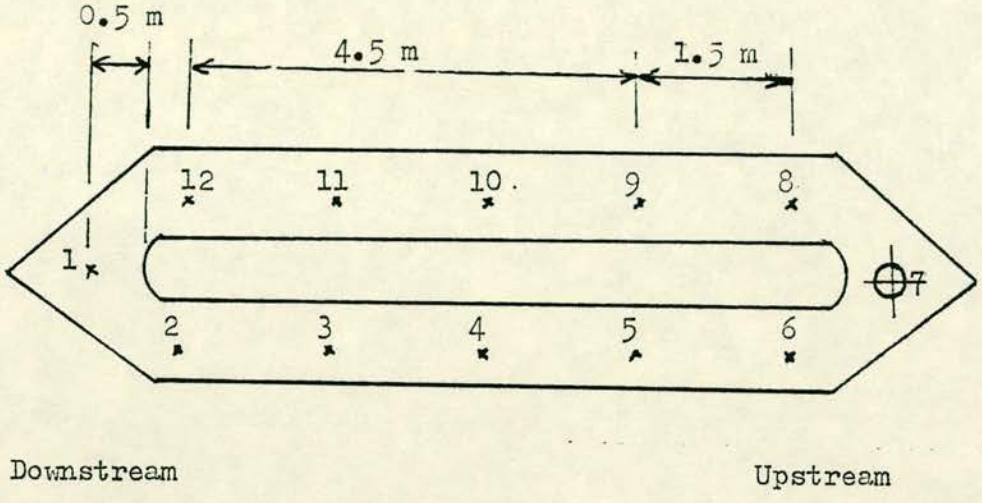

Fig. 7.23 Victoria Bridge - Caputh - plan North pier, location of test points for vertical measurement

The analysis undertaken involved investigating the longitudinal vibrational response of the piers, using the frequency response function facility of the analyser (see 6.2.2.1 and 6.2.2.2). It is noted that this analysis would have been undertaken until recently by mounting an electro dynamic shaker on the horizontal surface and sweeping through a range of discrete frequencies using an exciter (82).

The principle of the analysis is described in section 6.3.2.2. Therefore it can be said that the intact depth of the pier is given by:

$$D = V/2\Delta f$$

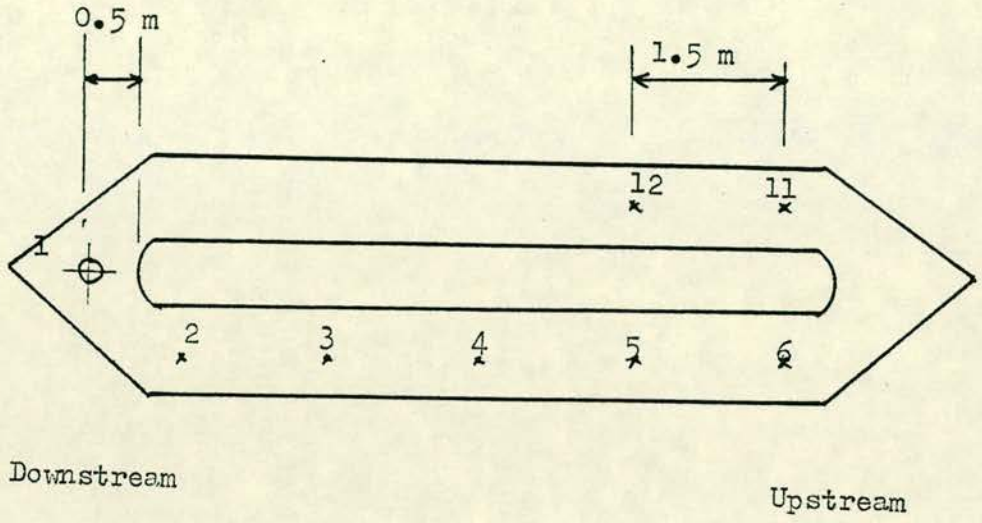

Fig. 7.24 Victoria Bridge - Caputh - plan South pier, location of test points for vertical measurement

where D = intact depth of the pier

V = the velocity through the material

Δf = the resonant frequencies interval as indicated on the FFT frequency domain plot.

D was known from general information from the design drawings and Δf was read from the analyser. Therefore V, the velocity, was calculated as an indication of the quality of the overall depth of the material.

In addition a second conclusion was also drawn from the analysis. That was the fixity of free ended nature of the piers was

calculated. To achieve this, as explained in chapter 6, the fundamental frequency f_o was read from the frequency domain plot. Then:

If $f_o = \Delta f$, the pier was free ended

If $f_o < \Delta f/2$, the pier was fixed ended

7.5.2 Results and Analysis

7.5.2.1 Transmission velocity test horizontally across piers

The transmission velocity results obtained from the horizontal testing of the top of the piers are summarised in Table 7.12. It will be noted that two transmission velocities are given in the table. The transmission velocities reported in column 4 represent the overall average velocity through the material. The corrected transmission velocities in column 6 represent the velocity corrected for the assumed thickness of the outer skin of concrete. It will also be noted from the table that transmission velocity readings were taken at 9 locations. The measurements were taken from both sides of the pier. It was seen that the velocity from one side to the other was not necessarily the same when the excitation took place on the opposite side. This was due to some degree of non-homogeneity in the structure.

Comparing the results in Table 7.12 with Tables 5.6 and 5.7, it was seen that the structure above water level was most probably masonry of variable quality or compacted rubble fill. These values did not indicate concrete since concrete transmission velocity is thought to vary between 3500 metres per second to 4500 metres per second. The above comparison with other materials in the tables, therefore, indicated that the material was either masonry or possibly extensively grouted or compacted soil fill.

7.5.2.2 Vertical tests on the piers

The vibration analysis results on the two piers are given in Table 7.13. It can be seen that, given the pier depth, different velocities were calculated. The calculated velocities varied between the low value of 2040 m/sec and the very high value of 5410 m/sec. Figs. 7.25 to 7.32 give typical results of frequency response function analysis.

Location	Pier Width (m)	Trans.Time (mil.sec)	Trans.Vel. (m/sec)	Corrected Time (mil.sec)	Corrected Vel. (m/sec)
1 South	2.90	1.65	1757	1.50	1533
1 North	2.90	1.12	2589	0.97	2371
2 South	2.90	1.34	2164	1.19	1933
2 North	2.90	1.40	2071	1.25	1840
3 South	2.90	1.34	2164	1.19	1933
3 North	2.90	1.32	2197	1.17	1966
4 South	2.90	1.32	2197	1.17	1966
4 North	2.90	1.14	2544	0.99	2323
5 South	2.90	1.54	1883	1.39	1655
5 North	2.90	1.25	2320	1.10	2091
6 South	2.90	1.40	2071	1.25	1840
6 North	2.90	1.36	2132	1.21	1901
7 South	2.90	1.50	1933	1.35	1704
7 North	2.90	1.20	2417	1.05	2190
8 South	2.90	1.30	2231	1.15	2000
8 North	2.90	1.31	2214	1.16	1983
9 South	2.90	1.40	2071	1.25	1840
9 North	2.90	1.39	2086	1.24	1855

Table 7.12 Victoria Bridge - Caputh - North pier, transmission velocity values across the pier above water level

corrected transmission velocity values:

Maximum value = 2371 m/sec
Minimum value = 1533 m/sec
Average value = 1940 m/sec

It is seen that the calculated velocity values were in the range of 2500 to 3500 metres per second. The few points which gave very high or very low calculated velocities were thought to represent reflections from horizontal cracks, reflections from the river bed or from a material below the pier end.

From these velocities, it was estimated that the material used was a high quality masonry or compacted soil fill. Indeed, the subsequent investigations showed that the piers were made of very compacted rubble fill.

Pier Location	Fundamental Freq. (Hz)	Freq. Interval (Hz)	Depth (m)	Calculated Velocity (m/sec)	Comments
North 1	72	368	4.0	2944	Fixity
2	230	406	"	3248	Fixity
3	260	580	"	4640	Fixity
4	282	338	"	2704	Free
5	152	293	"	2344	Fixity
6	300	340	"	2720	Free
7	338	335	"	2680	Free
8	174	265	"	2120	Fixity
9	264	255	"	2040	Free
10	474	560	"	4480	Free
11	294	303	"	2424	Free
12	240	404	"	3232	Fixity
South 1	290	342	4.9	3352	Free
2	274	296	"	2900	Free
3	254	296	"	2900	Free
4	294	380	"	3724	Partial Fixity
5	288	305	"	2989	Free
6	332	363	"	3557	Free
11	366	552	"	5410	Partial Fixity
12	290	502	"	4920	Fixity

Table 7.13 Victoria Bridge - Caputh - vibrational analysis results for the two piers

It will also be noted that in the frequency domain analysis that reference is made to fixity, free or partial fixity. Fixity indicates a rigid contact of the base against a solid object such as rock or very dense gravel. On the other hand, free ended indicates contact on a loose material or apparently suspended above any rigid contact. Partial fixity is a situation between these two extremes. For example, points 1 and 2 on North pier were thought to be in very good contact with the stratum at foundation formation level.

In general it is seen that certain parts of the piers appeared uniform with regard to calculated velocity measurements. Typical points were 1, 2, 5, 6 and 7 of North pier and 1, 2 and 3 of South pier. At other locations anomalies might exist.

7.5.3 Conclusions

(1) From the transmission analysis on the piers above water level, the velocities indicated the presence of a fair to good quality of masonry or grouted compacted fill rather than concrete or voided loose fill.

(2) Below water level, the piers were seen to be of consistent quality at certain locations but variable at other locations.

(3) The constant velocities indicated presence of very good high strength masonry or very compacted rubble fill. The inconsistent velocities indicated reflections from necking, horizontal cracks, river bed or a material below the foundation formation level. The reflection might be due to other anomalies such as plum, i.e. change of density at a certain level.

(4) At certain locations reported in Table 7.13, fixity with the stratum at foundation formation level was identified. At other locations a lack of fixity was observed. This was thought to be due to the presence of some kind of discontinuity.

(5) The foundations were thought to be constructed of either
   (a) historical quality concrete containing large plums, overbreaks or neckings.
   (b) heavily voided granular fill which had been subsequently extensively grouted to produce what was in effect a low quality masonry.
   (c) very good quality masonry made of stone blocks of higher strength than sandstone.

7.6 DISCUSSION

The sonic NDT survey carried out on the four bridges mentioned, serves to illustrate the use of this method for testing masonry structures. In comparison to other methods, it is a fast, extensive and relatively inexpensive one. Although the results may not be comparable with those of some other methods such as load testing, for strength evaluation, they can be used to obtain an indication of

the strength of the structure. The tests show that it can be used with reliability and confidence for detections of faults such as presence of large voids in the bridge or leaf separation in the walls and the adjacent materials. It is well established that the transmission sonic velocity results are a good indication of the quality of masonry tested.

A general review of the results obtained for the four bridges also shows that with the development of the instruments, some advanced and sophisticated methods of interpretation can be utilised. The use of auto correlation and cross correlation in the time domain has improved the reliability and accuracy of fault and discontinuity detection. In addition, the introduction of analog to digital convertors and analysers improved the accuracy of the results considerably. These newly developed instruments enable the use of some advanced mathemetical functions such as cepstrum, liftered spectrum and frequency response functions in fault detection, thickness measuremnt and sonic velocity measurement.

It is seen that in the event of a complex structure and also where there is one surface available for testing the structures, the conventional method of analysis in the time domain is not possible or very complicated. However, the transmission sonic velocity measurement in time domain is still the major method of determining the quality of the structure. The use of digital signal analysers, such as digital oscilloscopes with non-destructive zoom facilities or the Bruel & Kjaer two channel digital signal analysers, has helped significantly in increasing the accuracy of the results obtained. For location of faults and thickness measurement, however, it is shown that frequency analysis techniques and the use of frequency based function such as liftered spectrum or frequency response are the most accurate and reliable.

It is suggested that use of other conventional methods, to a lesser extent, such as coring, will improve greatly the reliability and accuracy of the results. For example, if one or two points on a bridge abutment are cored and the results compared with those of sonic NDT technique for thickness measurement, there cannot be any doubt about the reliability of the final results.

In brief, it can be said that this method of testing masonry structures has been shown to be very effective and useful for quality assessment of the structure and for fault detection. With the improvement and introduction of digital signal analysers, advanced mathematical functions can be utilised to improve the accuracy. The following are some general conclusions drawn from testing the four described masonry bridges:

(i) Sonic transmission velocities are an indication of the quality of the material and hence an indication of the quality of the structure. It must, however, be noted that other factors such as large multiple cracks or poor foundations must be taken into account and not to be underestimated, when assessing the quality of the structure. When there are two surfaces available, this method can also be used to locate the presence of large voids in the structure.

(ii) A transmission velocity test may not in some cases produce any results due to a rapid and heavy degree of attenuation. In this case, as in the case of High Bridge - Struie, a cross-sectional velocity test must also be carried out. This is used for cross-checking the presence of suspected voids and to find out whether the no transmission reading is due to high attenuation or due to the presence of large voidage.

(iii) This method has shown that the presence of major discontinuities can be determined and thicknesses measured. The method in comparison to other ones such as coring is inexpensive, time saving and more extensive. This is in addition to being non-destructive.

(iv) The use of this method for quality assessment, thickness measurement and detection of large voids is shown to be generally reliable. It is suggested that when this test is used together with other methods such as coring, but in a much lesser extent, the accuracy and reliability of the results improve greatly and can increase the confidence of the NDT engineer.

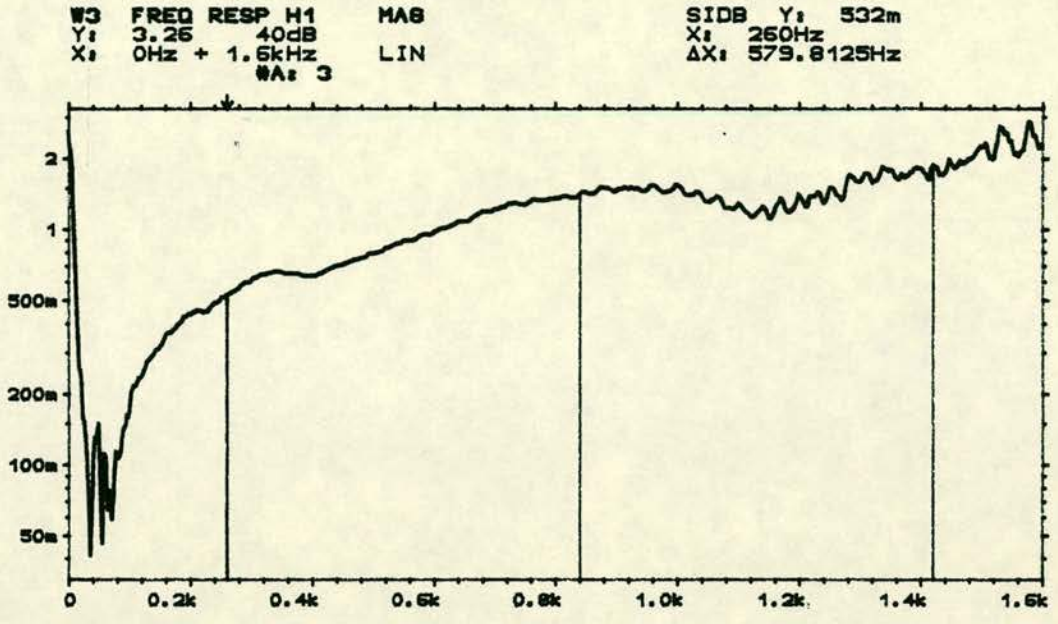

Fig. 7.25 Victoria Bridge, North pier, vibration test, point 3

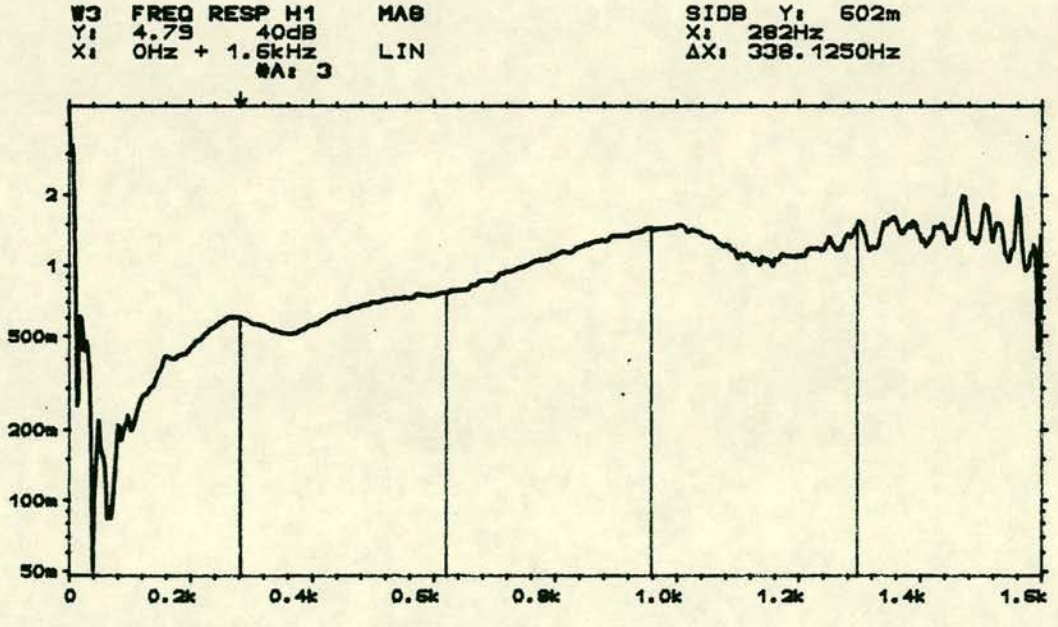

Fig. 7.26 Victoria Bridge, North pier, vibration test, point 4

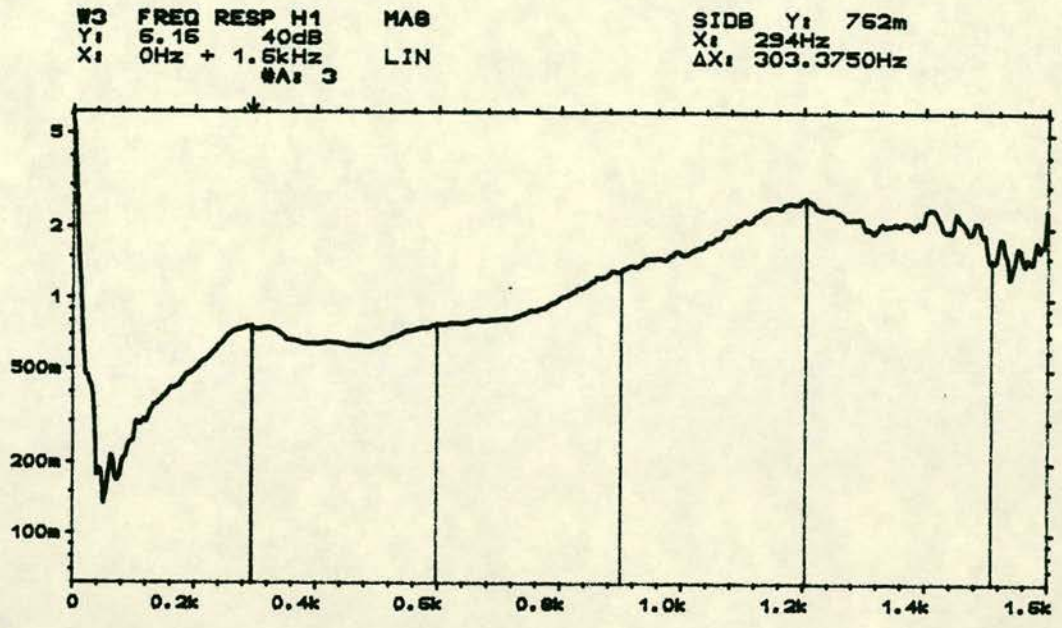

Fig. 7.27 Victoria Bridge, North pier, vibration test, point 11

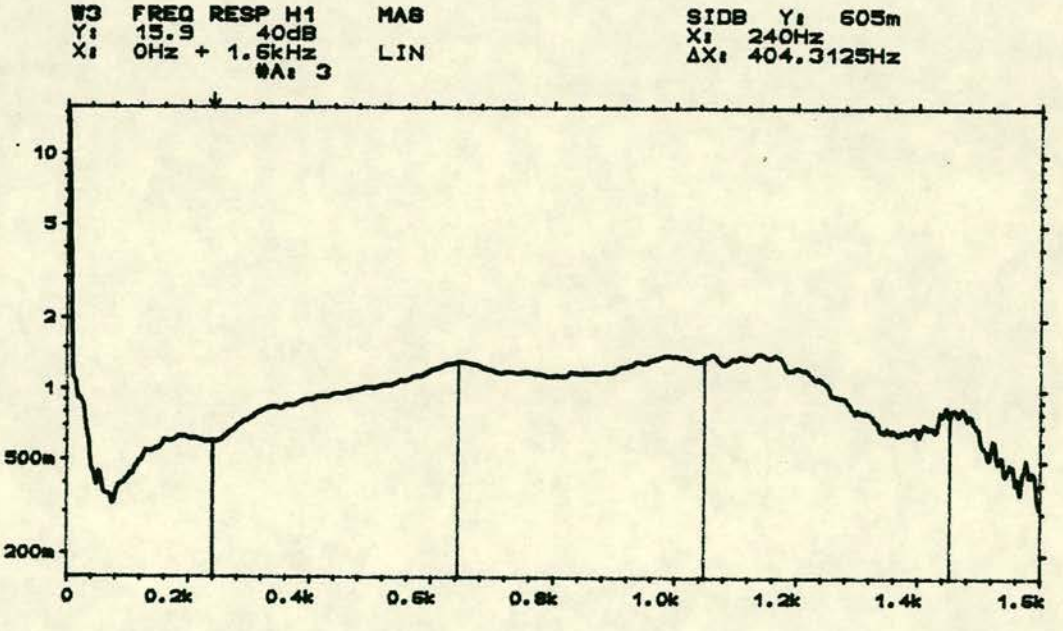

Fig. 7.28 Victoria Bridge, North pier, vibration test, point 12

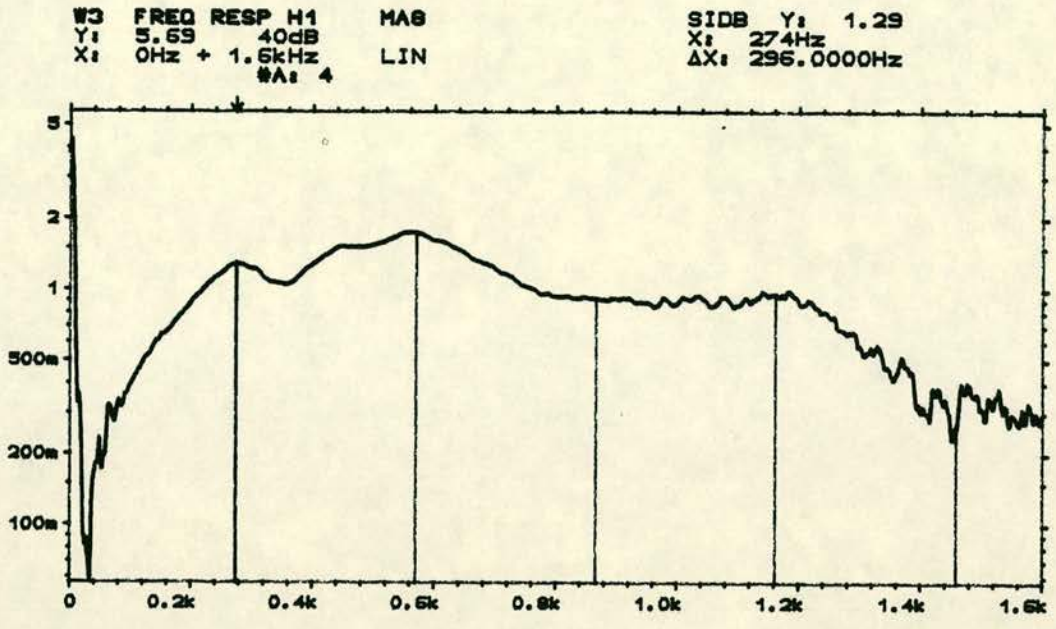

Fig. 7.29 Victoria Bridge, South pier, vibration test, point 2

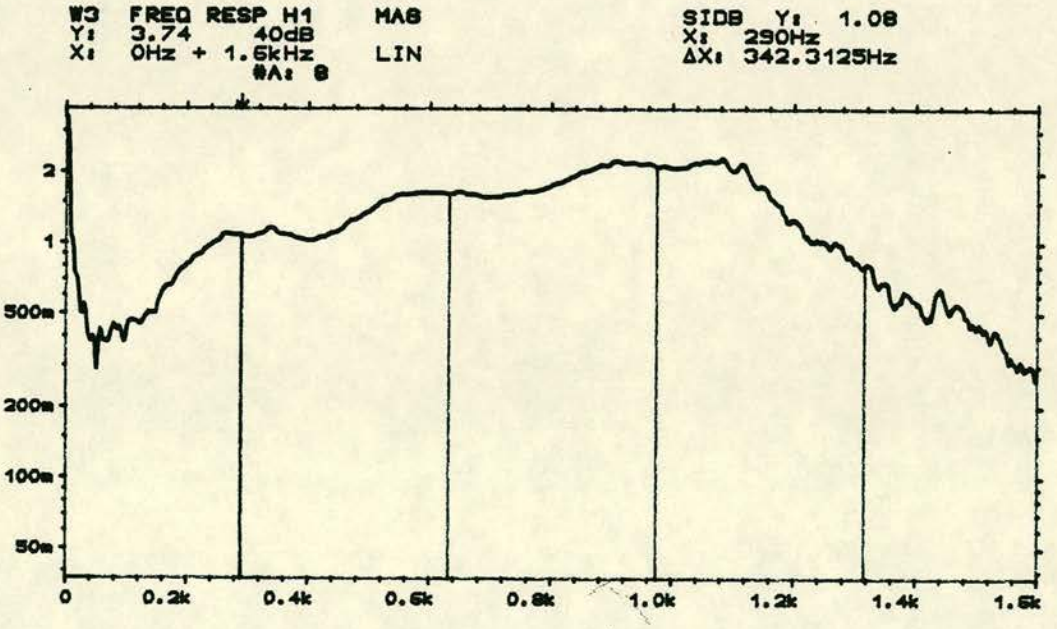

Fig. 7.30 Victoria Bridge, South pier, vibration test, point 1

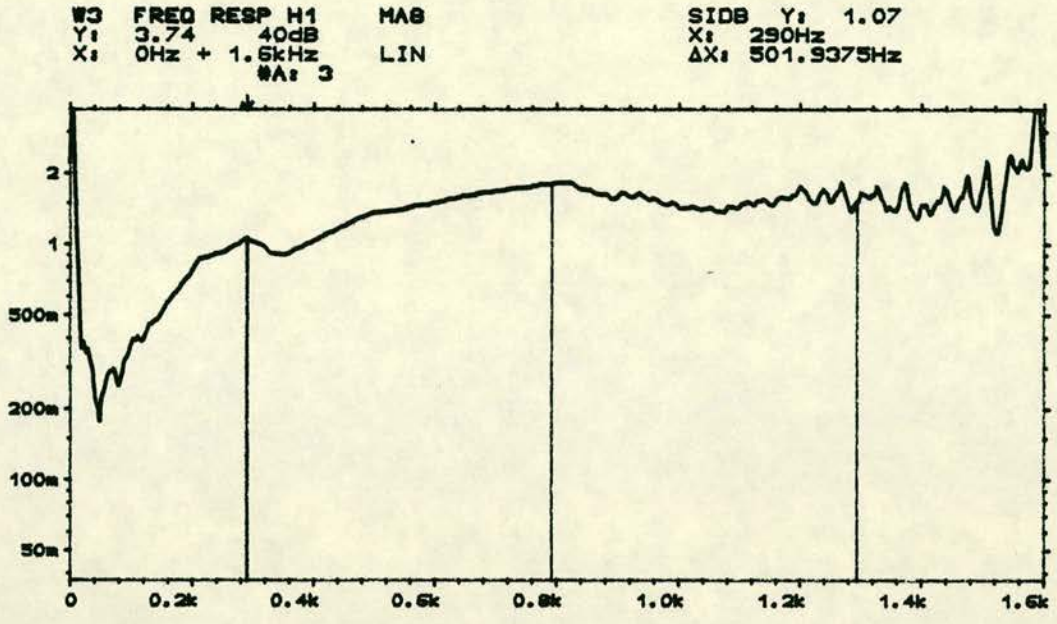

Fig. 7.31 Victoria Bridge, South pier, vibration test, point 12

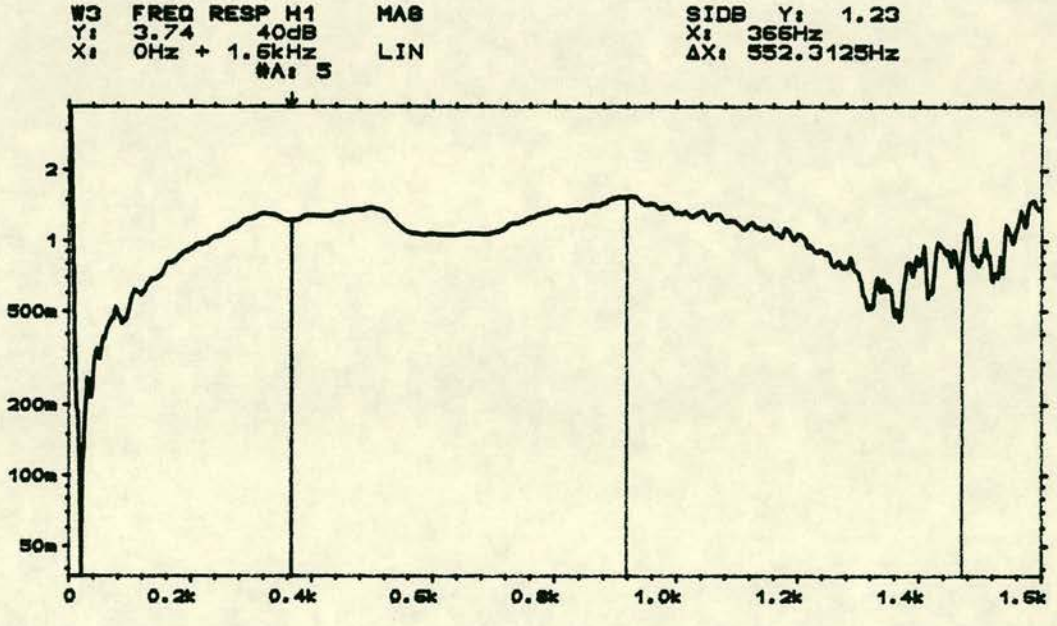

Fig. 7.32 Victoria Bridge, South pier, vibration test, point 11

CHAPTER EIGHT

DISCUSSION OF DEVELOPMENTS

8.1 INTRODUCTION

Until approximately two decades ago, testing of structures was confined to load testing a small proportion of them or core taking. The cost of load or core taking testing is very high in addition to the inconvenience caused. It is clear that it is not economical and sometimes not practical to use load or core taking tests for routine control testing of structures.

However, over the past 15 years it is becoming increasingly acceptable that integrity testing can be used to routinely control civil engineering structures such as piles. Over the past several years there has been ongoing research and development of sonic NDT methods of testing concrete and masonry structures in this Institute. The cost advantage of this method of integrity testing makes it possible to widen the zone of testing and extend it in such a way to cover a larger area of the structure over a short time, instead of being confined to a small proportion of the structure.

The research reported in this work clearly shows the extent of developments in testing masonry structures, along with the application of sophisticated digital signal processors and analysers.

8.2 CONVENTIONAL TIME DOMAIN ANALYSIS

The main experimental work undertaken for transmission or pulse velocity measurement, as an indication of the integrity and strength of brick/stone masonry, was on three shear failed reinforced brick masonry and several stone masonry piers. The testing equipment consisted of a two channel transient recorder and flat bed recorder, together with a conventional hammer. The results of the transmission velocity test gave an indication of the relative strength of the brick/stone masonry. However, due to the lack of high resolution equipment the results were not considered to be highly accurate. The operator had to generate a compression wave as close to the transmitting transducer as possible and there was an inevitable overestimation within the results obtained in this way (see section 5.6, part 4). When using this method of analysis the complication of the signal due to multiple reflections, scattering

and absorption, would not also yield very accurate and detailed results. It was with the introduction of digital analysers to the commercial and research market that more detailed signal processing and analysis was undertaken.

8.3 USE OF DIGITAL EQUIPMENT IN TIME DOMAIN ANALYSIS

With the introduction of digital signal processors and analysers, such as the digital two channel Nicolet 4094 oscilloscope which has a twin 5.25 inch floppy disk drive together with non-destructive zoom facility, a more detailed analysis of wave propagation and signal analysis was undertaken. This data capture system included a PCB instrumented hammer with a built in 2.5 tonne load cell. This permitted the problem of transmission velocity overestimation to be overcome (see section 5.6).

Use of PUNDIT (34) for measuring the transmission velocity of small dimension masonry components and the above digital equipment for larger scale masonry members proved to be of considerable value. Following this work, full scale testing of first Middleton North Burn Bridge and then Bargower Bridge was undertaken.

The results on Middleton North Burn Bridge, using the conventional time domain analysis technique, permitted the location of a large void inside the bridge to be identified. The results on the Bargower Bridge proved more promising. The use of the PCB built in load cell hammer and digital oscilloscope resulted in a thorough integrity test of this bridge. The advantages of the new equipment to the conventional one used for the Middleton North Burn Bridge, was then demonstrated.

8.4 INTRODUCTION OF FFT ANALYSERS AND USE OF FREQUENCY DOMAIN ANALYSIS TECHNIQUE

With the introduction of highly sophisticated FFT dual channel analysers, another stage in signal processing and analysis was reached. The use of this type of equipment enabled the researcher to make use of Fast Fourier Transform and Discrete Fourier Transform functions to study in more depth the signals obtained in testing masonry structures such as a bridge.

Auto correlation and cross correlation functions were used to locate the presence of voids and cracks with a much improved confidence. Frequency domain functions and particularly cepstrum (see sections 6.3.2 and 6.4) proved invaluable compared with older techniques in determining the hidden depth of a structure such as determining the thickness of a bridge abutment. The results obtained from the tests carried out on High Bridge, Struie and Caputh Bridge (see Chapter 7) are illustrations of the reliability of this method of integrity and fault detection technique.

Therefore in brief, it can be said that from an early stage of assessment of transmission velocity measurement and "visual" inspection of the time domain signals, a higher degree of resolution was achieved. Instead of the then existing unsophisticated method of fault detection, Fourier transform and the relevant frequency functions were utilised.

It must be noted that although this technique of testing masonry structures has developed substantially, further developments and research are required. It is recommended that this technique still has to be used in conjunction with some older conventional methods of testing such as coring. One of the main areas of research and development could be considered to be the distinction between a major discontinuity in a structure which could prove vital for structural stability and performance, and other types of discontinuity such as the presence of some void or crack, though large but not vital. This area of research can also be developed to the stage that a more quantitative analysis of faults in structures could be made, e.g. the extent, inclination, depth and type of a discontinuity, to be determined. Another area of research which may prove of substantial use is determining a more precise and accurate relationship between overall strength of the structure and sonic testing parameters such as transmission velocity, absorption, frequency and so on. The advantage of this development is that it will extend beyond the area of integrity testing and would cover structural analysis as well.

CHAPTER NINE

CONCLUSIONS

The aim of this work was to investigate the use of sonic non-destructive testing techniques for masonry structures. Sonic techniques were used to measure the transmission velocity in masonry as an indication of quality and strength, to detect large voids or cracks and to measure the thickness of the masonry such as the thickness of a bridge abutment. To this end various tests were carried out and the conclusions drawn are summarised as follows:

9.1 TESTING MASONRY COMPONENTS

In this work, relationships between pulse velocity and age, and pulse velocity and path length for mortar were found. A relationship between pulse velocity and strength for mortar and masonry stone cubes was also established. It was found that:

(i) The stronger the mix, the higher the pulse velocity.

(ii) Pulse velocity is also proportional to the strength of masonry stone.

(iii) Pulse velocity decreases with a decrease in path length shorter than a certain length.

(iv) The strength of mortar increases rapidly during the first few days of construction and then the rate of increasing strength reduces and after 28 days, as in the case of concrete, reaches a near constant strength.

(v) Yellow sandstone is usually higher in strength than white sandstone and granite is much higher than many other stone blocks used in masonry.

(vi) Pulse or transmission velocity can be used to obtain an indication of the quality and strength of the material used in masonry and hence the masonry itself.

9.2 TESTING MASONRY AS COMPOSITE

The tests on three shear failed reinforced brick masonry walls and several stone masonry piers resulted in:

(i) The technique can be applied to investigate the presence of major discontinuities in brick masonry as reported in chapter 5, using a time domain analysis technique.

(ii) The use of two transducers for the above purpose is preferred for cross-checking the presence of discontinuities, from the signals obtained.

(iii) Measurement of transmission velocity can be used to give an indication of the relative strength and quality of masonry.

9.3 TESTING FULL SCALE STRUCTURES

The sonic survey carried out on on four masonry bridges illustrated the use of sonic non-destructive testing of full scale masonry (and also concrete) structures. The investigations undertaken on the four bridges described in chapter 7 showed that:

(i) The transmission velocity survey of a structure gives an indication of the overall quality of the structure. In assessing the quality of the structures other factors such as poor foundations, presence of large multiple cracks and so on must not be overlooked.

(ii) The transmission velocity survey can also be used for cross-checking the presence of large voids or poor quality material in the structure.

(iii) The presence of major discontinuities can be determined quickly and cheaply with relative reliability.

(iv) In the case of one surface being available, for example when investigating thickness of a bridge abutment, cepstrum analysis can prove to be more reliable and accurate.

(v) When there is access to two surfaces of a structure, the transmission velocity technique can be used to detect the presence of large voids very close to a surface.

In short, it was concluded that the use of sonic non-destructive testing technique in quality assessment, thickness measurement and detection of large faults, proved to be generally reliable. When this method of testing is used together with other methods such as coring, the accuracy and reliability of the results will be increased.

Further developments in this field such as estimation of the structure's stiffness, determining the overall strength of the structure and its structural performance, which is today in progress, will no doubt reduce the need for the old conventional expensive and time consuming methods. Further developments to determine the strength and structural performance of masonry buildings must include the study of such factors as effects of joints, number of courses, size of the blocks and so on.

REFERENCES

REFERENCES

1. Mitchell D., Harris P.J. and Lai F.W.K. "Evaluation and Repair of Slabs Containing Improperly Placed Reinforcement". Structural Faults 85, Proceedings of Second International Conference on Structural Faults and Repair, April-May 1985, London.

2. Cairns J. and Hutt C. "Replacement of Corroded Reinforcement, Locked Out Stresses". Structural Faults 83, Proceedings of International Conference on Structural Faults, March 1983, Edinburgh.

3. Romaya R. "Structural Appraisal of a Multi-Storey Building Frame Containing H.A.C. Concrete Contents". Structural Faults 85, Proceedings of Second International Conference on Structural Faults and Repair, April-May 1985, London.

4. B.S. CP110 - 1972. "The Structural Use of Concrete". British Standards Institution, London.

5. Swamy R.N. and Jones R. "Polymer Grid Reinforcement for Corrosion Control and Concrete Repair". Structural Faults 85, Proceedings of Second International Conference on Structural Faults and Repair, April-May 1985, London.

6. Hendry A.W. "Inspection of Brick and Stone Masonry Structures". Structural Faults 83, Proceedings of First International Conference on Structural Faults, March 1983, Edinburgh.

7. Maurenbrecher A.H.P. "Use of the Prism Tests to Determine the Compressive Strength of Masonry". Proceedings of North American Masonry Conference, Colorado, August 1978.

8. Suter G.T. and Keller H. "Reinforced Brickwork Lintel Shear Study Utilising Small Scale Bricks". Proceedings of North American Masonry Conference, Colorado, August 1978.

9. Hegemier G.A., Krishnam G.K., Nunn R.N. and Moorthy T.V. "Prism Tests for the Compressive Strength of Concrete Masonry". Proceedings of North American Masonry Conference, Colorado, August 1978.

10. B.S. 5628 Part 1, 1978. "Code of Practice for Structural Use of Masonry". British Standards Institution, London.

11. Maurenbrecher A.H.P. "Use of the Prism Tests to Determine the Compressive Strength of Masonry". Proceedings of North American Masonry Conference, Colorado, August 1978, p. 91-2.

12. Sinha B.P. and Hendry A.W. "The Effect of Brickwork Bond on the Load Bearing Capacity of Model Brick Walls". Proceedings of British Ceramic Association, No 11, Load Bearing Brickwork 2, 1968, pp. 55-67.

13. Baur J, Noland J.L. and Chinn J. "Compression Tests of Clay-Unit Stack Bond Prisms". Proceedings of North American Masonry Conference, Colorado, August 1978.

14. Jessop E.L., Sherives N.G. and England G.L. "Elastic and Creep Properties of Masonry". Proceedings of North American Masonry Conference, Colorado, August 1978.

15. Noland J.L., Hanada K.T. and Feng C.C. "The Effect of Slenderness and End Conditions on the Strength of Clay Unit Prisms". Proceedings of North American Masonry Conference, Colorado, August 1978.

16. Hatzinikolas M, Longworth J. and Warwaruk J. "The Effect of Joint Reinforcement on Vertical Load Carrying Capacity of Hollow Concrete Block Masonry". Proceedings of North American Masonry Conference, Colorado, August 1978.

17. B.S. 1881, Part 4. "Methods of Testing Concrete for Strength". British Standards Institution, London.

18. Concrete Society. "Concrete Core Testing for Strength". Concrete Society Technical Report No 11, London, 1976.

19. Bungey J H. "An Appraisal of Pull-Out Methods of Testing Concrete". NDT 83, Proceedings of International Conference on Non-Destructive Testing, November 1983, London.

20. Keiller A.P. "An Investigation of Test Methods for the Assessment of Strength of in Situ Concrete". NDT 83, Proceedings of International Conference on Non-Destructive Testing, November 1983, London.

21. Chabowski A.J. and Bruden Smith A.W. "A Simple Pull-Out Test to Assess the Strength of in Situ Concrete". B.R.E. Current Paper, CP 25/77, June 1977, p. 5.

22. Chabowski A.J. and Bruden Smith A.W. "Assessing the Strength of in Situ Portland Cement Concrete by Internal Fracture Tests". Magazine of Concrete Research, Vol 32, No 112, September 1980, pp. 164-172.

23. Long A.E. "A Review of Methods of Assessing the in Situ Strength of Concrete". NDT 83, Proceedings of International Conference on Non-Destructive Testing, November 1983, London.

24. Swamy R.N. and Ali A.M.A.H. "Assessment of in Situ Concrete Strength by Various Non-Destructive Tests". NDT 83, Proceedings of International Conference on Non-Destructive Testing, November 1983, London.

25. Murray A.McC. and Long A.E. "Applications of Pull Off Test for the Reduction of Structural Faults". Structural Faults 85, Proceedings of Second International Conference on Structural Faults and Repair, April-May 1985, London.

26. Murray A.McC. and Long A.E. "A New Method of Assessing the Strength of 'Suspect' Concrete". Structural Faults 83, Proceedings of International Conference on Structural Faults, March 1983, Edinburgh.

27. Densicon Inc. "Windsor Probe Test System". Technical Data Manual, Elmswood, Connecticut, USA.

28. Bungey J.H. "The Testing of Concrete in Structures". Surrey University Press, London, 1982, pp. 62-63.

29. Blyth F.G.H. and de Freitas M.H. "A Geology for Engineers". Sixth Edition, Edward Arnold, London 1974, Re-printed 1977, p. 76.

30. Bungey J.H. "The Testing of Concrete in Structures". Surrey University Press, London 1972, p. 68.

31. Johansen R. "In Situ Strength Evaluation of Concrete - the Break-Off Method". Concrete International, 1, No 9, September 1979, pp. 45-51.

32. SNELL L.N. "Non-Destructive Testing Techniques to Evaluate Existing Masonry Construction". Proceedings of North American Masonry Conference, August 1978, Colorado.

33. Savage R.J. "Critical Review and Appraisal of NDT Methods". Structural Faults 83, Proceedings of International Conference on Structural Faults, March 1983, Edinburgh.

34. CNS Instruments Ltd. PUNDIT Manual, CNS Instruments Ltd, 61-63 Holmes Road, London.

35. Birse R.M. and Currie D. "Ultrasonic Examination of Concrete Structures". Structural Faults 83, Proceedings of the International Conference on Structural Faults, March 1983, Edinburgh.

36. B.S. 4408, Part 5, 1974. "Non-Destructive Methods of Test for Concrete - Measurement of the Velocity of Ultrasonic Pulses in Concrete". British Standards Institution, London.

37. Bungey J.H. "The Testing of Concrete in Structures". Surrey University Press, 1982, London, pp. 55 and 57.

38. B.S. 4408, Part 5, 1974, Cl. 1.3. "Non-Destructive Methods of Test for Concrete - Measurement of the Velocity of Ultrasonic Pulses in Concrete". British Standards Instititon, London.

39. Hutten P.H. and Ord R.D. "Acoustic Emission", Research Techniques in Non-Destructive Testing, Vol 1, Academic Press, London and New York, 1970.

40. Arrington M. "Monitoring Structural Integrity by Acoustic Emission Methods". Structural Faults 83, Proceedings of International Conference on Structural Faults, March 1983, Edinburgh.

41. Hanacek and Winkler H. "Inspection of a Heat Exchanger of the Saphir Reactor Using the Acoustic Emission Technique". Structural Faults 83, Proceedings of International Conference on Structural Faults, March 1983, Edinburgh.

42. Hendry A.W. and Royles R. "Acoustic Emission Observations on a Stone Masonry Bridge Loaded to Failure". Structural Faults 85, Proceedings of Second International Conference on Structural Faults and Repair, April-May 1985, London.

43. Gericke O.R. "Ultrasonic Spectroscopy". Research Techniques in Non-Destructive Testing, Vol 1, Academic Press, London and New York, 1970.

44. McGonnagle W.J. "Non-Destructive Testing". Second Edition, Gordon and Breach Science Publishers, New York, London, Paris.

45. Halmshaw R. "Direct View Radiological Systems". Research Techniques in Non-Destructive Testing, Vol 1, Academic Press, London and New York, 1970.

46. Berger H. "Neutron Radiography". Research Techniques in Non-Destructive Testing, Vol 1, Academic Press, London and New York, 1970.

47. B.S. 4408, Part 3, 1970. "Non-Destructive Methods of Testing Concrete - Gamma Radiography, British Standards Institution, London.

48. Morelli R. "Resistivity Testing of Concrete". PhD Thesis, University of Edinburgh, 1985, Edinburgh.

49. Waidelich D.L. "Pulsed Eddy Currents". Research Techniques in Non-Destructive Testing, Vol 1, Academic Press, 1970, London and New York.

50. Lawson W,D, and Sabey J.W. "Infra-red Techniques". Research Techniques in Non-Destructive Testing, Vol 1, Academic Press, 1970, New York and London.

51. Render A.S. "Use of Photo-elastic and Moire' Fringe Techniques". Experimental Methods in Concrete Structures for Practitioners, American Concrete Institute, Detroit, 1979.

52. Rad P.F. "A Simple Technique for Determining the Strength of Brick". Proceedings of the North American Masonry Conference, Colorado, August 1978.

53. Sahlin S. "Structural Masonry". Englewood Cliffs Prentice-Hall, 1971, p. 25.

54. Hendry A.W., Sinha B.P. and Davies S.R. "Load Bearing Brickwork Design". John Wiley and Sons Inc., Chichester, 1981, pp. 56-61.

55. B.S. 1200, 1976. "Specifications for Building Sands from Natural Sources". British Standards Institution, London.

56. Hendry A.W., Sinha B.P. and Davies S.R. "Load Bearing Brickwork Design". John Wiley and Sons Inc., Chichester, 1981, p. 32.

57. B.S. 5628, Part 1, 1978, Table 1. "Code of Practice for Structural Use of Masonry". British Standards Institution, London.

58. CP 121, Part 1, 1973. "Code of Practice for Walling, Brick and Block Masonry". British Standards Institution, London.

59. B.S. 5390, 1976. "Code of Practice for Stone Masonry". Formerly CP 121.201 and CP 121.202, British Standards Institution, London.

60. Currie D.W. "Survey of Scottish Sands and the Investigation of their Characteristics in Relation to the Compressive Strength of Mortar". M.Phil Thesis, University of Edinburgh, 1981, Edinburgh.

61. Neville A.M. "Properties of Concrete". "Pitman Publishing, 1977, pp. 318-321.

62. Kaplan M.F. "Flexural and Compressive Strength of Concrete as Affected by the Properties of Coarse Aggregate". Journal of American Concrete Institute, 55, pp. 1193-208, May 1959.

63. Bungey J.H. "The Validity of Ultrasonic Pulse Velocity Testing of in Place Concrete for Strength". NDT International, December 1980, pp. 296-297.

64. C.P. 110, 1972. "The Structural Use of Concrete". British Standards Institution, London.

65. Fegen I. "Testing Concrete Foundation Piles by Sonic Echo". PhD Thesis, University of Edinburgh, 1981, Edinburgh.

66. Filipczynski L., Pawlowski Z. and Wehr J. "Ultrasonic Methods of Testing Materials". London, Butterworth, 1966.

67. Szilard J. "Ultrasonic Testing - Non-Destructive Testing Techniques". Chichester, Wiley, 1982.

68. Krautkramer J. and Krautkramer H. "Ultrasonic Testing of Materials". Translation of the Second Revised German Edition, Springer-Verlag, Heidelberg New York, 1969, pp. 4-20.

69. Scrivener J.C. "Shear Tests of Reinforced Brick Walls". Masonry International, No 2, 1984, pp. 24-31.

70. Sharpe R.S. (ed.). "Research Techniques in Non-Destructive Testing". Academic Press, London and New York, 1970, Vol 1, p. 31.

71. Sharpe R.S. (ed.). "Research Techniques in Non-Destructive Testing". Academic Press, London, New York and San Francisco, Vol 3, 1977, p. 101.

72. Neville A.M. "Properties of Concrete". Second Edition, 1975, Pitman Publishing Ltd, London, p. 506.

73. Clayton C.R.I., Simons N.E. and Mathews M.C. "Site Investigation". London, 1982.

74. Runcorn S.K. "Methods and Techniques in Geophysics". 1960, Vol 1, pp. 62-103.

75. Catchpool E. and Sutterly J. Text Book of Sound, 1949, 7th Edition.

76. Sahlin S. "Structural Masonry". Edglewood Cliffs Prentice-Hall, 1971.

77. Thrane N. "The Discrete Fourier Transform and FFT Analysers". Digital Signal Analysis, Selected Reprints from Technical Review, Bruel and Kjaer, 1985.

78. Nicolet Oscilloscope. "Fourier Transform Concepts and the FFT". Nicolet Oscilloscope 4094, Waveform Analysis, p. 13, Nicolet Instrument Corporation.

79. Upton R. "The Objective Comparison of Analog and Digital Methods of Real Time Frequency Analysis". Bruel and Kjaer Technical Review, No 1, 1977.

80. Nicolet Oscilloscope. "Aliasing and the Nyquist Frequency". Nicolet Oscilloscope 4094, Waveform Analysis, p. 10, Nicolet Oscilloscope Corporation.

81. Herlufsen H. "Auto Correlation and Cross Correlation". Signal Analysis, Selected Reprints from Technical Review, Bruel and Kjaer, 1985.

82. Davis A.G. and Dunn C.S. "From Theory to Field Experience with the Non-Destructive Vibration Testing of Piles". Proceedings, Part 2, Research and Theory, December 1974, Vol 57, The Institute of Civil Engineers, London.

83. Raundall R.B. and Hee J. "Cepstrum Analysis". Digital Signal Analysis, Selected Reprints from Technical Review, Bruel and Kjaer, 1985.

84. Bogert B.P., Healy M.J.R. and Tukey J.W. "The Quefrency Analysis of Time Series for Echoes: Cepstrum". Proceedings of Symposium on Time Series Analysis, M. Rosenblatt (ed.), Wiley, New York, 1963.

APPENDIX ONE

MORTAR MIX SPECIFICATIONS

A1.1 SIEVE ANALYSIS B.S. 1200, 1976

Table of Results

Sieve Size (mm)	Retained (g)			Passed (%)		
	Coarse	Medium	Fine	Coarse	Medium	Fine
5.00	0.0	0.0	0.0	100.00	100.00	100.00
2.36	0.5	1.5	4.0	99.8	99.37	98.77
1.18	6.0	4.0	9.0	97.4	97.69	96.01
0.600	100.0	14.5	20.0	56.8	91.59	89.88
0.300	89.0	82.0	83.0	20.7	57.06	64.42
0.150	38.0	110.5	167.0	5.3	10.53	13.19
0.075	10.0	20.0	37.0	1.2	0.85	1.84
passed 0.075	3.0	2.0	6.0	-	-	-

Table A1.1 Sand used for mortar cubes

Sieve Size (mm)	Retained (g)	Passed (%)
5.0	0.0	100.00
2.36	2.0	99.00
1.18	5.5	96.24
0.600	10.0	91.23
0.300	43.0	69.67
0.150	99.0	20.05
0.075	34.0	3.01
passed 0.075	6.0	-

Table A1.2 Sand used for mortar beams

A1.2 MIX PROPORTIONS

Using 100 mm cubes

Three cubes for each mix

beams, (a) and (b), sizes = 4" x 20"

No	Mix	Grading	Water (Cm^3)	Cement m^3x10^{-3}	Cement (g)	Lime m^3x10^{-3}	Lime (g)	Sand m^3x10^{-3}	Sand (g)
1	1:1/4:3	Coarse*	1184	1.129	1316	0.282	157	3.388	4774
2	"	Medium	1330	"	"	"	"	"	5021
3	"	Fine	1250	"	"	"	"	"	4774
4	1:½:4.5	Coarse*	1120	0.800	933	0.400	223	3.600	5288
5	"	Coarse	1306	"	"	"	"	"	5288
6	"	Medium	1410	"	"	"	"	"	5335
7	"	Fine	1420	"	"	"	"	"	5072
8	1:1:6	Coarse*	1120	0.600	700	0.600	334	3.600	5288
9	"	Coarse	1330	"	"	"	"	"	5288
10	"	Medium	1390	"	"	"	"	"	5335
11	"	Fine	1420	"	"	"	"	"	5072
12	1:2:9	Coarse*	1119	0.400	466	0.800	445	3.600	5288
13	"	Coarse	1166	"	"	"	"	"	5288
14	"	Medium	1420	"	"	"	"	"	5335
15	"	Fine	1299	"	"	"	"	"	5072
Beam (a)	1:1/4:3	-	1946	1.765	2058	0.441	246	5.295	7778
Beam (b)	"	-	1957	"	"	"	"	"	7778

Table A1.3 Mix design proportions for mortar cube and beam construction

N.B. * used for investigating age-strength relationship

APPENDIX TWO

TESTING OF MORTAR BEAMS AND CUBES

Tables of Results

Age (Day)	Average Transmission Velocity (m/sec) 1:1/4:3	1:1/2:4.5	1:1:6	1:2:9
1	2247	1790	1489	1181
2	2523	2128	1890	1517
3	2804	2331	2065	1707
4	2962	2492	2208	1852
5	3033	2566	2278	1914
6	3083	2620	2329	1924
7	3155	2693	2379	1987
8	3215	2737	2445	2027
9	3264	2770	2471	2052
10	-	-	-	-
11	-	-	-	-
12	3337	2857	2536	2102
13	3337	2862	2540	2108
14	3352	2885	2564	2125
15	-	-	-	-
16	3382	2907	2591	2138
17	-	-	-	-
18	-	-	-	-
19	-	-	-	-
20	3405	2935	2620	2168
21	-	-	-	-
22	3421	2950	2618	2175
23	-	-	-	-
24	-	-	-	-
25	-	-	-	-
26	3432	2961	2637	2199
27	-	-	-	-
28	3432	2973	2650	2195

Table A2.1 Mortar cube strength against age for the FINE grade sand (see Table A1.3)

Age (Day)	Average Transmission Velocity (m/sec) 1:1/4:3	1:1/2:4.5	1:1:6	1:2:9
1	1899	1724	1449	1070
2	2571	2138	1901	1514
3	2838	2368	2141	1745
4	2956	2479	2249	1842
5	3046	2568	2293	1923
6	3128	2646	2394	1996
7	3209	2717	2461	2028
8	3261	2755	2500	2056
9	-	-	-	-
10	-	-	-	-
11	3352	2843	2577	2110
12	3352	2852	2586	2138
13	3386	2890	2622	2163
14	-	-	-	-
15	3417	2904	2641	2174
16	-	-	-	-
17	-	-	-	-
18	-	-	-	-
19	3452	2950	2681	2198
20	-	-	-	-
21	3472	2956	2693	2212
22	-	-	-	-
23	-	-	-	-
24	-	-	-	-
25	3470	2970	2710	2244
26	-	-	-	-
27	-	-	-	-
28	3484	2979	2725	2268

Table A2.2 Mortar cube strength against age for the MEDIUM grade sand (see Table A1.3)

Age (Day)	Average Transmission Velocity (m/sec) 1:1/4:3	1:1/2:4.5	1:1:6	1:2:9
1	2356	2285	1718	1315
2	2656	2625	2117	1624
3	2899	2760	2274	1856
4	2954	2893	2433	1918
5	3077	2973	2496	1969
6	3135	3030	2591	2045
7	3284	3080	2617	2078
8	3236	3106	2634	2088
9	3252	3080	2641	2070
10	3220	3067	2667	2098
11	3262	3112	2703	2140
12	3257	3148	2708	2160
13	3300	3155	2717	2160
14	3300	3171	2730	2168
15	3317	3205	2757	2193
16	3355	3219	2760	2190
17	3390	-	-	-
18	-	-	-	-
19	-	3240	2791	2204
20	3407	3240	2783	2203
21	3413	3260	2812	2216
22	3419	-	-	-
23	-	3275	2814	2232
24	3431	-	-	-
25	-	-	-	-
26	-	-	-	-
27	-	3289	2854	2244
28	3454	3289	2846	2257

Table A2.3 Mortar cube strength against age for the COARSE grade sand (see Table A1.3)

Age (day)	Beam (a) Trans. Vel. (m/sec)	Beam (a) Curing Temp. (deg. C)	Beam (b) Trans. Vel. (m/sec)	Beam (b) Curing Temp. (deg. C)
2	2865	27	2224	-
3	3046	28	2918	-
4	3163	27	3131	-
5	3242	26	3273	-
6	3303	27	3344	18
7	3351	27.5	3421	17
8	3391	28.5	3475	16
9	3475	29	3491	16
10	3449	27.5	3535	15.5
11	3484	27.5	3543	14.5
12	3501	-	-	14
13	3516	-	-	15
14	-	24.5	3583	15.5
15	-	26	3580	15.5
16	3560	26.5	3600	15
17	3552	-	-	15
18	3562	-	3613	-
20	3572	-	-	13
22	-	25	3623	14.5
24	3613	-	3631	-
26	3613	-	-	-
28	3620	24	3644	12

Table A2.4 Mortar beam strength against age at different curing temperatures (see Table A1.3)

APPENDIX THREE

PUBLISHED PAPERS FROM THIS THESIS

PUBLISHED PAPERS FROM THE THESIS ARE:

"Sonic Investigation of Shear Failed Reinforced Brick Masonry"
Masonry International, No. 3, November 1983

"Fault Detection in Stone Masonry Bridges by Non-Destructive Testing"
Structural Faults 85, Proc. of Second Int. Con. on Structural Faults and Repair, April-May 1985, London.

Sonic Investigation of Shear Failed Reinforced Brick Masonry

F. Komeyli-Birjandi, B.Eng.
Research Student, Department of Civil Engineering and Building Science, University of Edinburgh

M.C. Forde, B.Eng., M.Sc., Ph.D. C.Eng., M.I.C.E., M.I.H.T.,
Senior Lecturer, Department of Civil Engineering and Building Science, University of Edinburgh

H.W. Whittington, B.Sc., Ph.D., C.Eng., M.I.E.E.
Senior Lecturer, Department of Electrical Engineering, University of Edinburgh

A sonic investigation of three shear failed reinforced brick masonry walls was carried out. The objectives were to identify the position of shear cracks and to obtain an estimate of transmission velocity through cracked and uncracked brickwork and a reinforced collar joint filled with mortar. The sonic velocities obtained gave an indication of the relative strengths of the different materials.

INTRODUCTION

In the past few decades, there has been ongoing research into the ultrasonic testing of materials and its application in industry, The emphasis, however has been on testing of homogeneous materials, for example metals at high frequency (≥50 kHz). Work on civil engineering materials has been confined to concrete and also undertaken using high frequency ultrasonic devices, for example "PUNDIT" [1]. Research into the non-destructive investigation of composite systems has been confined to concrete piles in soil where the concrete member has been the subject of integrity testing[2].

The work reported in this paper represents the initial stages of an attempt to develop a technique for the inspection and diagnosis of composite materials, for example brick masonry. Low frequency 1 to 2 kHz sonic investigation methods have been developed to locate cracks in, and to establish transmission velocities through, three shear failed reinforced brick masonry walls.

MASONRY WALLS TESTED

Three shear failed reinforced brick masonry walls B2, C1 and C2 were tested[3]. Each wall was of stretcher bond construction with steel embedded in the collar joint and 240 mm thick. The leaves were constructed from 102 mm wide pressed bricks and reinforcing steel was embedded in the collar joint which was 36 mm wide. Thirty-six courses of brickwork to a height of 2.7 m were capped with a 236 mm deep concrete beam. The wall base was a 300 mm deep reinforced concrete beam. Wall B2 was of 2.5 m nominal length and walls C1 and C2 of 3.5 m nominal length.

The vertical reinforcement used in each wall consisted of two 16 mm dia bars at each end and 12 mm dia bars uniformly distributed along the centre line of the wall. Six 8 mm dia bars were also used horizontally and additional short starter bars, suitably anchored in the concrete base, were incorporated along the base.

Table 1[3] gives details of the dimensions and reinforcement for each wall.

EXPERIMENTAL TECHNIQUE

The basic principle of the experimental technique entailed the propagation of a compression wave along the length of the wall, using a conventional hammer covered with several layers of soft paper, to avoid damaging the brick surface. Two piezo-electric transducers were attached to the two opposite ends of the wall, using water pump grease as an acoustic coupling medium. They were placed opposite each other at the same height above the base of the wall, 5 to 7 courses of brickwork below the concrete cap. They were connected to a two channel transient recorder and flat-bed recorder by screened cables. One transducer (A) was connected to channel (A) of the flat-bed recorder, and the other transducer (B) to the other channel (B) Fig 2. Transducer (A) triggered first.

The time scale and sensitivity of the transient recorder were adjusted such that a relatively light hammer blow, very close to transducer A, would generate a compression wave which would travel along the length of the wall. A suitable recording was then obtained on the transient recorder for display on the plotter.

This procedure was repeated, moving the transducers downwards every two or three courses of brickwork. Additionally, several points on the reinforced collar joint were chosen for testing. The procedure was repeated on the concrete beams at the base of the walls.

The above technique was used on a 1.55 m uncracked length of similar brickwork in order to obtain an estimate of transmission velocity through uncracked brickwork.

The locations of the main diagonal crack and other severe visible cracks were measured with a steel tape, relative to the ends of the walls.

In setting up the transient recorder and flat-bed plotter, a suitable time scale, for accurate interpretation of results, had to be found. This was achieved by carrying out some preliminary trials to obtain sharp and well defined signals.

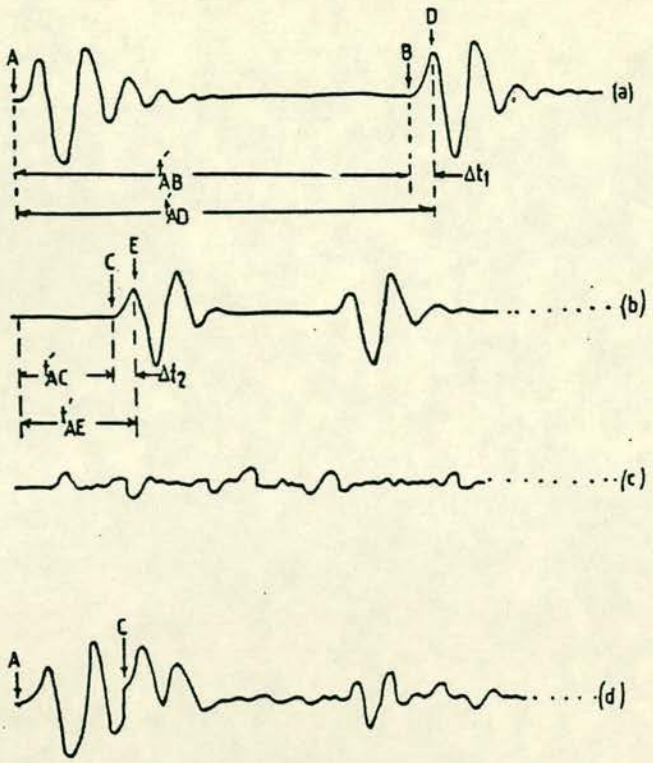

Figure 1 Waveforms for cracked brickwork.

a. Transmitted signal, b. reflected signal from a crack face, c. reflected signal from brick-mortar joints, d. resultant signal i.e. the trace obtained.

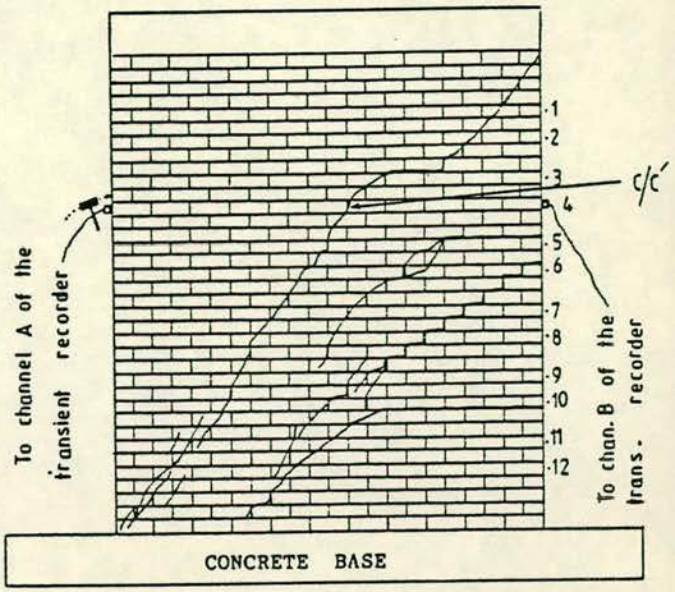

Figure 2. Wall B2 - Observed crack pattern.

INTERPRETATION OF RESULTS

Under idealised conditions, when a compression wave propagates through the wall, it will have a shape similar to Fig 1(a) which can be derived by Fourier's analysis[4].

This type of signal, with an exponential rise and decay, is common in ultrasonic testing[4]. Indeed all the traces obtained do have this exponential rise and decay in common.

However, brickwork is a heterogeneous material and additionally the walls tested were cracked. Therefore the traces obtained were more complicated than the idealised case. The complication arises from interference of reflected waves from brick-mortar joints, any crack of discontinuity and the surface waves generates at the transducer. This is illustrated diagramatically in Fig 1.

The relative proportion of the initial signal transmitted against proportion reflected from a discontinuity, is dependent upon the magnitude, shape and orientation of the discontinuity[5]. For example a vertically continuous void results in no transmission to the end of the wall, as the characteristic impedence of air is much higher than that of brickwork and hence almost total reflection occurs[5].

As shown in Fig 1, t^1_{AC} and t^1_{AB} correspond to delay times required by the transmitted compression wave to reach the reflectors, a crack and the end B of the wall respectively, and return to the transducer. The peak of the reflected wave from the end B of the wall occurs after a time interval of t'_{AD} and that of the reflected wave from the crack after t'_{AE}, where it can be seen from Fig 1:

$$t'_{AD} = t'_{AB} + \Delta_{\epsilon_1}$$

$$t'_{AE} = t'_{AC} + \Delta_{t_2}$$

Δ_{t_1} and Δ_{t_2} are determined by the shape of the transmitted compression wave and the response of the transducer[6].

Also by using two transducers, Fig 2, placed opposite each other, at the same level at the two ends of the wall, the time of arrival of a sonic pulse at each transducer could be identified and the transmission velocity measured.

Referring to Fig 3, when a point close to transducer A, was excited by a hammer blow a longitudinal compression wave travelled along the length AB. This triggered first transducer A and after a time interval t_{AB}, triggered transducer B. The distance between the two triggering points A and B, on the chart, corresponded to t_{AB} ie the time taken for the compression wave to travel from A to B. Therefore transmission velocity V_{AB}, along the length AB was given by:

$$V_{AB} = \ell_{AB}/t_{AB}$$

where ℓ_{AB} = length of the wall between transducers A and B.

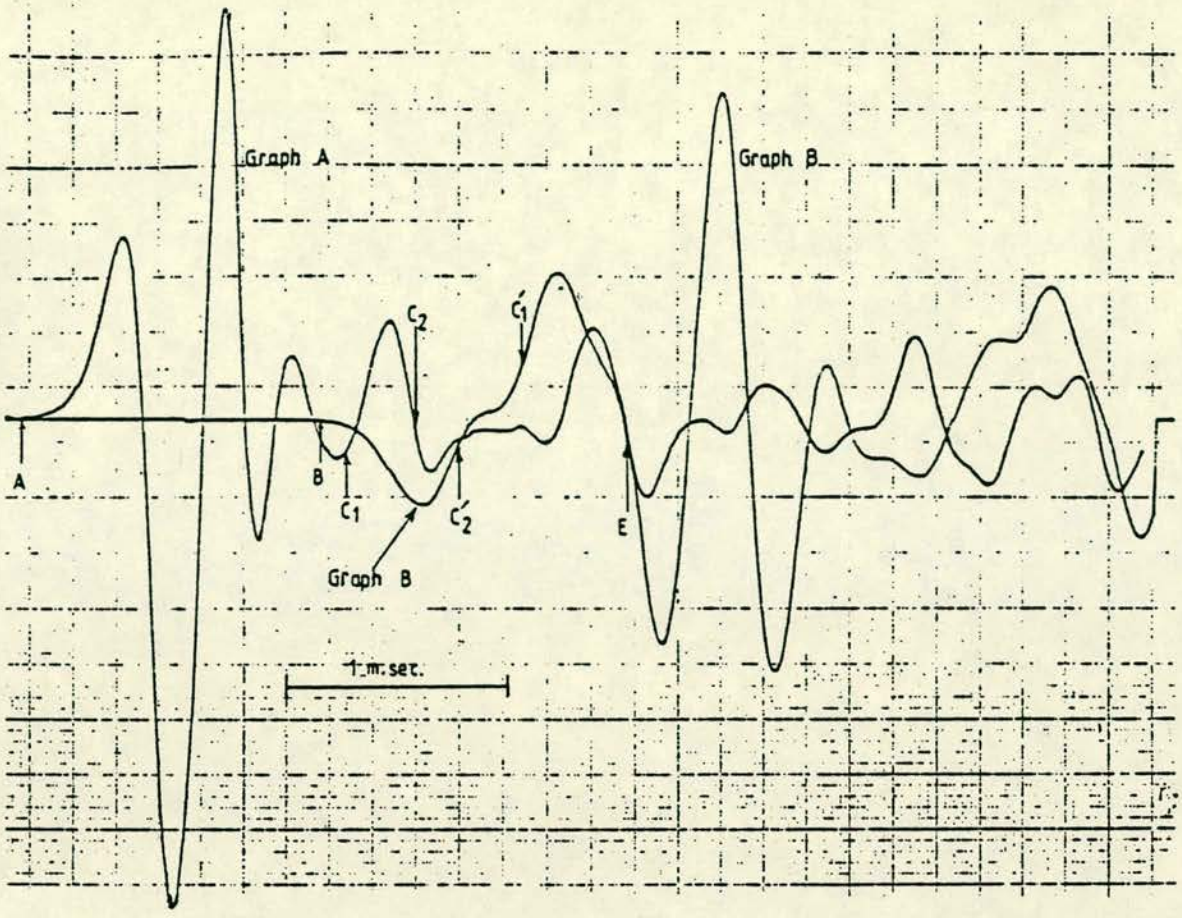

Figure 3 Point C1-3

SONIC ASSESSMENT OF WALLS

In order to identify the effect of a crack or a major discontinuity along the length of the wall, on the recorded trace, the following procedure was carried out:

(1) $(V_{AB})_{uncracked}$, which had already been measured on a similar uncracked brickwork section was noted.

(2) $(V_{AB})_{cracked}$ was calculated by knowing length ℓ_{AB} and measuring t_{AB} on the trace. The distance between the start of graph A and the start of graph B, on the trace, corresponds to t_{AB}.

(3) The start of the first major distortion on the trace was marked on graph A as C. By assuming a suitable velocity V_{AC} such that $(V_{AB})_{cracked} \leq V_{AC} \leq (V_{AB})_{uncracked}$, and measuring t_{AC} on the trace, the length of the crack from face A, ℓ_{AC} was calculated.

(4) Similarly, the corresponding distortion on graph B was located and marked as C^1. This helped in cross checking the existence of the discontinuity at c/c^1, Fig 2.

It was found that the most of the significant distortions in the traces obtained corresponded to a reflection from a crack face or from the opposite face of the wall. However, on several occasions, the discontinuities indicated by the sonic technique in this way were not visible on the walls, and the authors suggest that these correspond to hidden discontinuties - for example a major void gap or an internal crack.

ILLUSTRATIVE EXAMPLE

To illustrate this procedure take the example of Fig 3, which corresponds to point 3 on wall C1, as a typical example:

(1) $(V_{AB})_{uncracked} = 3100$ m/s

(2) From the trace : $t_{AB} = 1.368$ ms

length of the wall C1 : $\ell_{AB} = 3.50$ m

$$\therefore (V_{AB})_{cracked} = \frac{3.5 \times 10^3}{1.368} \approx 2600 \text{ m/s}$$

(3) Point C1 on graph A of Fig. 3, indicates the start of a reflecting wave as there is a sudden increase in the amplitude of the graph starting at C1.

It is assumed that this is the first major discontinuity on graph A of the trace, as there is no other major distortion of the graph before C1. Hence a maximum velocity of 3100 m/s is used to calculate ℓ_{AC1} = ie $V_{AC1} = 3100$ m/s

From the graph: $t_{AC1} = 0.737$ ms

$\therefore \ell_{AC1} = V_{AC1} \cdot t_{AC1} = 2.28$ m which corresponds to point C1-5, Table 2 and Fig. 6.

Note that t_{AC} = (the time taken for the transmitted signal to travel from A to C) = $\frac{1}{2}t_{AC}$ Fig 1.

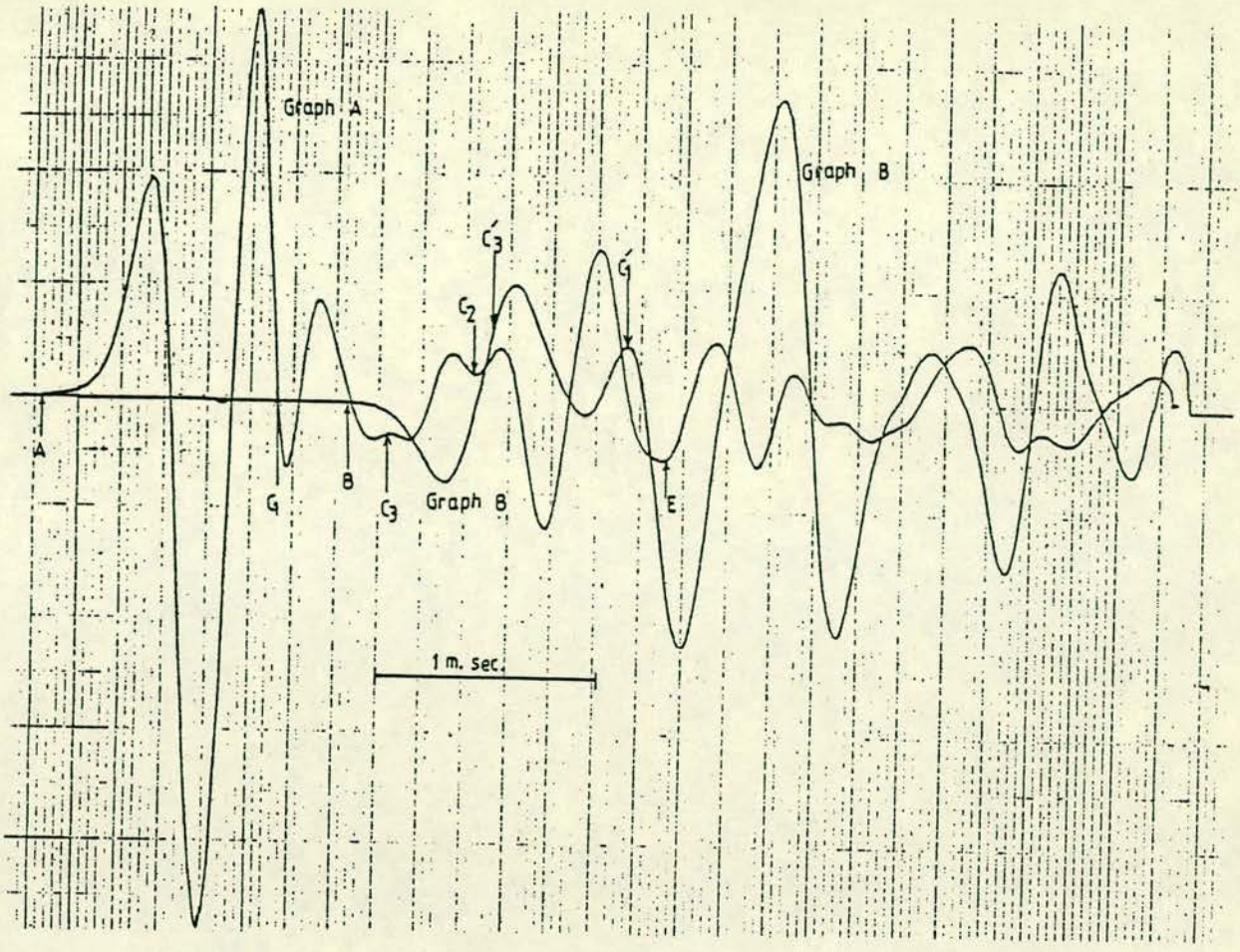

Figure 4. Point C2-6.

The next major distortion on graph A, starts at C2. Measuring the distance ℓ_{AC2} in the manner described above gives: ℓ_{AC} = 2.60 m which corresponds to the diagonal crack observed at 2.58 m from A.

The trace distortions immediately following C2, on graph A, are ignored as they are very close to the end B. Interpretation of these distortions is very complicated as they may be due to interference of multiple reflections from brick-mortar joints with each other and with the reflections from C1 and C2. An attempt to interpret these complex composite signals, can lead to the apparent detection of non-existent discontinuities, unless there is a large distortion corresponding to a significant discontinuity.

(4) The existence of C1 and C2 must be checked on graph B of the trace, to ensure that these are not due to the sum of minor reflections from brick-mortar joints. Indeed a major distortion does exist at $C^1 2$ (corresponding to C2) on graph B of the trace in Fig. 3. Using the method described above yields $\ell_{BC^1 2}$ = 1.0 m

The start of the next major distortion on graph B of Fig. 3 is considered to be at $C^1 1$, therefore the presence of a discontinuity at $C^1 1$ (corresponding to C1) is certain. Referring to Table 2 and Fig. 6, there is no observable discontinuity at C1. Therefore the trace distortion at C1 is considered to indicate a hidden discontinuity for example an internal crack, at a distance 2.30 m from face A of the wall C1.

The trace distortion at C2 and $C^1 2$ corresponds to the diagonal crack observed at 2.6 m from face A.

Figs. 4 and 5 corresponding to C2-6, Table 3 and Fig. 4, and B2-11, Table 4 and Fig. 5., respectively, were interpreted in the same manner as described above.

GENERAL DISCUSSION OF RESULTS

In general, when interpreting the results, it was found that when there was a discontinuity very close to face A (and hence when the reflecting signal fell within the first two or three peaks of graph A of a trace) it was difficult to distinguish it on graph A alone. To a lesser extent this was also true when interpreting the results from graph B alone, (when the reflecting signal fell within the first two peaks). Using two transducers in the manner described above, helped to overcome this by permitting cross-checking of the presence of a discontinuity on two graphs A and B of a trace. Several of the measured distances of cracks, from face A in these tests, were first calculated from graph B and then marked on graph A.

In general, graph A for all the traces proved more difficult to interpret, compared to graph B. This was considered to be due to surface wave effects at A.

In Tables 2,3 and 4, there were apparent discontinuities which were not observed on the walls. These were calculated from graph distortion and were considered to be hidden cracks or large void gaps in brick mortar joints.

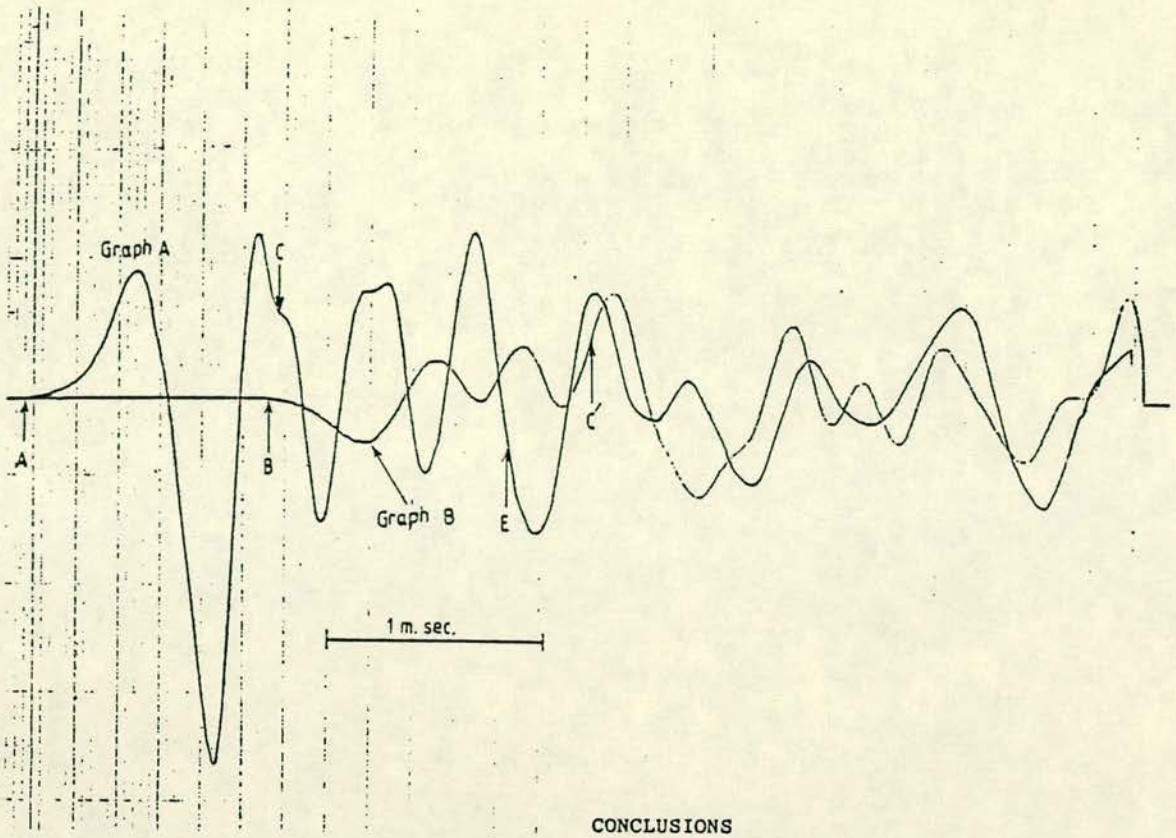

Figure 5. Point B2-11

As a result of this investigation it has been demonstrated that it is possible to distinguish more than one crack or discontinuity from a relatively complex trace, provided that they are well defined and not very closely spaced.

The results obtained for the reinforced collar joint indicated the presence of the observed cracks at the same level in the brickwork. This confirms the fact that shear cracks were developed through the entire thickness of the wall. This was not, however, true for the less severe cracks due to the presence of heavy reinforcement in the collar joint.

The transmission velocity for an uncracked reinforced collar joint was estimated to be 3500 m/s. This was obtained by comparing the transmission velocities of cracked brickwork and reinforced collar joint and the transmission velocity of uncracked brickwork, as an uncracked reinforced collar joint was not available for direct measurement.

Wall B2 showed a lower cracked transmission velocity, about 2500 - 2600 m/s on average, compared to 2700 m/s in walls C1 and C2. This was due to the fact that wall B2 had a shorter length and hence it was relatively more damaged during shear testing.

The results obtained for the reinforced collar joints and concrete beams, showed a wide scattering of the transmitted compression wave, although concrete and mortar are considered to be relatively homogeneous materials. This was clearly due to the presence of the reinforcements in the concrete beams and collar joints.

CONCLUSIONS

1. This technique can be applied to investigate the presence of major discontinuities in brick masonry as reported in this work.
2. The use of two transducers is preferred for cross-checking the presence of discontinuities.
3. Measurement of transmission velocity can be used to give an indication of the relative strength and quality of the material.

ACKNOWLEDGEMENTS

The authors wish to thank Professor A W Hendry of the Department of Civil Engineering and Building Science and Professor J Mavor of the Department of Electrical Engineering at the University of Edinburgh, for placing the facilities of their respective departments at their disposal.

REFERENCES

[1] CNS Electronics Ltd., Pundit Mark IV Manual, CNS Electronics Ltd., London, 1979.

[2] Fegen, I., Testing Concrete Foundation Piles by Sonic Echo, Ph.D. Thesis, University of Edinburgh, 1981.

[3] Scrivener, J.C., Shear Tests of Reinforced Brick Walls, Masonry International, No.2, 1984, pp 24-31.

[4] Sharpe, R.S. (ed), Research Techniques in Non-Destructive Testing, Academic Press, London and New York, 1970, Vol. 1, p 31.

[5] Filipczynskil, Pawlowski, Z.and Weir, J., Ultrasonic Methods of Testing Materials, Butterwortj, London, 1966.

[6] Sharpe, R.S. (ed), Research Techniques in Non-Destructive Testing, Academic Press, London, New York, San Francisco, 1977, Vol.3, p 101.

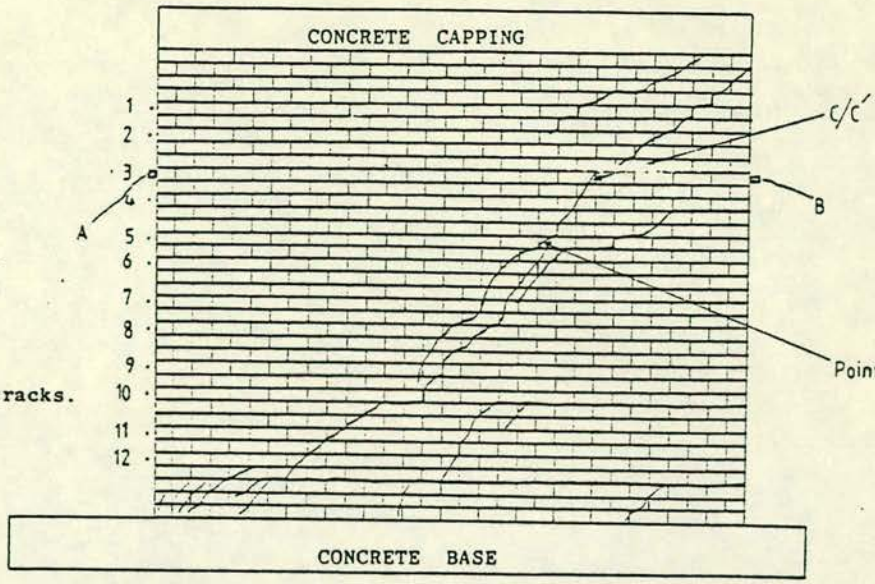

Figure 6. Wall C1, observed cracks.

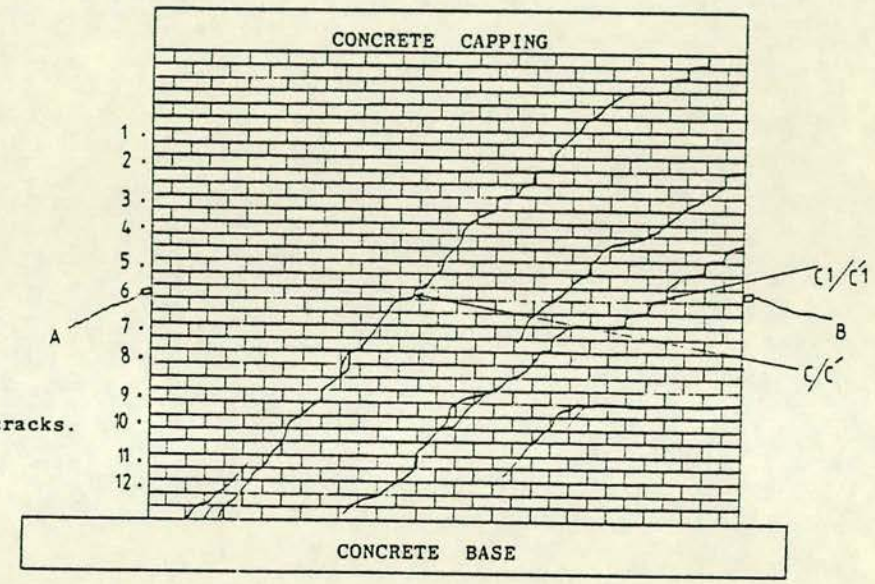

Figure 7. Wall C2, observed cracks.

WALL DESIGNATION	WALL LENGTH (mm.)	VERTICAL REINFORCEMENT IN CENTRAL PORTION No. of 12mm-dia bars	PERCENTAGE* %
B2	2465	26	0.63
C1	3483	7	0.19
C2	3483	18	0.34

All walls:	Brickwork height	2.7m
	Total wall height	3.24m
	Thickness	240mm
	Horizontal reinforcement	Six 8mm-dia bars
	Vertical reinforcement	Two 16mm-dia bars at each end

* Percentage of reinforcement is calculated on gross cross-sectional area of the wall

TABLE 1 - WALL AND REINFORCEMENT DETAILS[3]

POINT	VEL_{AB} (m/s)	CRACK LOCATION							
		MAIN DIAGONAL CRACK			NEXT SEVERE CRACK			NOT OBSERVED DISCONTINUITY	
		assm'd.vel. (m/s)	obsr'd. ℓ_{AC}(m)	msr'd. ℓ_{AC}(m)	assm'd. vel.(m/s)	obsr'd. ℓ_{AC}(m)	msr'd. ℓ_{AC}(m)	assm'd. vel.(m/s)	ℓ_{AC}(m)
C1-1	2900	3000	3.17	3.15	3000	2.48	2.40	3100	1.50
C1-2	2900	2900	2.97	2.95				3100	1.80
C1-3	2600	2900	2.68	2.60				3100	2.30
C1-4	2700	3000	2.48	2.50				3100	1.60
C1-5	2400	3100	2.28	2.35	2700	2.70	2.70		
C1-6	2600	3100	2.02	1.95	2900	2.25	2.30		
C1-7	2600	2900	2.14	2.05	3100	1.91	1.90		
C1-8	2600	3000	1.92	1.90	3100	1.75	1.65	2800	2.50
C1-9	2700	3000	1.67	1.65	3100	1.60	1.50		
C1-10	2600	3100	1.50	1.60		3.42		2900	2.00
C1-11	2800	3100	1.08	1.10	2900	1.85	1.85	2800	2.30
C1-12	2700	3100	0.90	0.90	2800	1.76	1.70		
*C1-2 CJ	2800	3600	2.58	2.50					
Conc. Base	4000								

*The point on the collar joint

TABLE 2 - EXPERIMENTAL RESULTS OF WALL C1

POINT	VEL_{AB} (m/s)	CRACK LOCATION							
		MAIN DIAGONAL CRACK			NEXT SEVERE CRACK			NOT OBSERVED DISCONTINUITY	
		assm'd.vel. (m/s)	obsr'd. ℓ_{AC}(m)	msr'd. ℓ_{AC}(m)	assm'd. vel.(m/s)	obsr'd. ℓ_{AC}(m)	msr'd. ℓ_{AC}(m)	assm'd. vel.(m/s)	ℓ_{AC}(m)
C2-1	2700	3000	2.52	2.50				3100	1.75
C2-2	2700	2000	2.40	2,40				3100	1.90
C2-3	2700	2900	2.05	2.20				3000	1.65
C2-4	2600	3100	1.92	1.90					
C2-5	2600	3100	1.68	1.70	2600	3.27	3.20		
C2-6	2600	3100	1.55	1.60	2900	3.03	2.90		
C2-7	2700	3000	1.34	1.35	2800	2.42	2.40		
C2-8	2500	3000	1.17	1.20	2800	2.23	2.10		
C2-9	2700	3100	1.02	0.95	2800	1.98	1.90		
C2-10	2600	3100	0.87	0.90	2700	1.82	1.90		
C2-11	2900	3100	0.70	0.70	2900	1.57	1.60		
C2-12	2800	3100	0.55	0.65		1.43		3000	1.80
C2-5 CJ	2700	3600	1.02	1.00	3000	1.98	1.85		
C2-4 CJ	2800	3500	1.34	1.35					
C2-3 CJ	2900	3600	1.68	1.60					
Conc.Base	4800								

TABLE 3 - EXPERIMENTAL RESULTS OF WALL C2

POINT	VEL. AB (m/s)	CRACK LOCATION							
		MAIN DIAGONAL CRACK			NEXT SEVERE CRACK			NOT OBSERVED DISCONTINUITY	
		meas'd. vel. (m/s)	obser'd ℓ_{AC} (m)	mar'd. ℓ_{AC} (m)	meas'd. vel. (m/s)	obser'd. ℓ_{AC} (m)	mar'd. ℓ_{AC} (m)	meas'd. vel. (m/s)	ℓ_{AC} (m)
B2-1	2700	3000	2.15	2.20				3100	0.95
B2-2	2600	2900	2.02	2.00				3100	1.15
B2-3	2600	2900	1.65	1.70				3100	0.85
B2-4	2600	3100	1.30	1.30					
B2-5	2500	2900	1.22	1.20				3100	0.30
B2-6	2300	3100	1.07	1.05	2600	2.30	2.15	2800	1.70**
B2-7	2400	3100	0.95	0.90	2600	2.05	1.70		
B2-8	2400	3100	0.84	0.85	2700	1.75	1.65		
B2-9	2300	3100	0.69	0.70	2700	1.53	1.60		
B2-10	2300	3100	0.64	0.70	2500	1.44	1.50		
B2-11	2300	3100	0.45	0.50				2700	1.55
B2-12	2300	3100	0.26	0.40					
B2-2 CJ	2800	3200	1.65	1.60					
Conc.Base	3900								

* Difficult to interpret, multiple fractures, close to the toe.

** Observed crack. (ℓ_{AC}) observed = 1.67m.

TABLE 4 - EXPERIMENTAL RESULTS OF WALL B2.

MATERIAL	AVERAGE TRANSMISSION VELOCITY M/S
Good Brickwork (Uncracked)	3100
Poor Brickwork (Cracked)*	2500 - 2700
Uncracked Reinforced Cavity	3500
Cracked Reinforced Cavity*	2700 - 3000
Structural Concrete	4500

* Depends on the severity of cracks

TABLE 5 - COMPARISON OF RESULTS

FAULT DETECTION IN STONE MASONRY BRIDGES BY NON-DESTRUCTIVE TESTING

M. C. Forde, BEng, MSc, PhD, CEng, MICE, MIHT
F. Komeyli-Birjandi, BEng
University of Edinburgh
A. J. Batchelor, Civil Tech NDT Ltd, Galashiels

The role of masonry bridges in the transportation network is discussed, together with the influence of increased traffic loadings upon impact loading and low frequency excitation

The types of defect in masonry bridges are discussed.

Conventional methods of masonry bridge inspection are discussed, together with their advantages and disadvantages.

Ultrasonic and sonic methods of investigation are discussed. A case study of the application of a sonic investigation technique is described. The results of a survey before and after remedial measures are described.

INTRODUCTION

The U.K. Transport infrastructure contains a large number of stone masonry bridges of size varying from single span low height to multi span high viaducts. The infrastructure belongs largely to three different categories of transport system:

(I) Road Bridges

(II) Rail Bridges

(III) Waterway Bridges

Most of the stone masonry bridges are of the order of 100 years old and have had varying amounts of maintenance over the years. In the case of the road bridges they might well have been designed with horse drawn traffic as the intended loading.

The major problems which have occurred have been due to the steadily increasing loads due to motorised traffic. Although individual axle loads may have been limited to a certain value the ever increasing load of the trucks has resulted in total loads on arch spans increasing. This has resulted in the intensity of low frequency vibration also increasing. A further factor has been the reduction in maintenance budgets which has resulted in lower standards of waterproofing of masonry bridge decks.

Water penetration of masonry bridge decks results in erosion of the soil fines from the fill behind the spandrel walls and behind the wing walls of the abutments. Water penetration combined with freeze thaw cycles results in the propagation of cracks in the barrel and the spandrel walls.

Compaction of the eroded soil fill can also cause problems due to the movement of the spandrel walls.

The rail bridges have suffered from similar cycles of problems as the road bridges. In order to maintain competitiveness with road and air, passenger traffic speeds on the inter city lines have increased quite dramatically in the last 10 years. Likewise in order to remain competitive with road freight, rail freight traffic has had to increase speed and distribution. The net result has been an acceleration in the rate of deterioration of masonry rail bridges.

The Engineer responsible for masonry bridges is therefore faced with an increase in maintenance costs which have to be met from possibly a reducing budget. There is therefore an urgent need for diagnostic tools in order to permit carefully targeted distribution of scarce resources with respect to maintenance. The options facing the masonry bridge owner may be extremely limited in the sense that it may not be possible to demolish bridges as they are increasingly becoming listed structures with preservation orders placed upon them.

TYPES OF DEFECTS OCCURRING IN MASONRY BRIDGES

Some of the defects which may occur in masonry bridges include the following:

(a) Voids created due to erosion of fines from ingress of water/lack of waterproofing of the deck.

(b) Cracks in the arch/barrel - due to movement of the soil fill, frost action, increased traffic loads and lack of maintenance.

(c) Bulging of the spandrel walls due to movement of the fill, frost action, increasing stresses of the traffic.

(d) Bulging of the wing walls - due to failure within the fill, erosion of fines, continuing vibration from traffic.

Ongoing research within the U.K. by Dundee University, Edinburgh University, S.D.D., and T.R.R.L., is indicating that failure of the masonry arch purely due to overloading is relatively rare. However, repeated loading may lead to earth

pressures through the soil/rubble fill transmitted laterally to the spandrel walls and wing walls which is in excess of the walls lateral load carrying capacity. Thus primary failure of the arch itself may not take place but the structure may "fail" for secondary reasons directly associated with the load carrying capacity.

It is probable that the single most important source of potential damage to masonry bridges in the U.K. is that due to water ingress through the deck and the approach road to the abutments. The water ingress results in:

(1) Erosion of fines thus causing voids.

(2) In cold climates severe frosts cause cyclical expansion and contraction with freeze thaw.

The potential magnitude of the maintenance and operation of masonry bridges will be appreciated when it is considered that many of the U.K. road and rail trunk routes make extensive use of these masonry structures. For example the Borders Regional Council in Scotland is responsible for approximately 1200 to 1300 bridges of which approximately 800 are masonry bridges; Strathclyde Regional Council is responsible for 4,000 bridges of which 2,000 are masonry. Other regions have similar percentages of stone masonry bridges. Whilst a number of these masonry bridges are on very minor routes a large number of them are also on major trunk routes. It is thus totally out of the question, from a financial standpoint, to contemplate major replacement of these structures. Additionally the structures are elegant items of cultural and engineering heritage which should be preserved. The largest single owner of masonry bridges in the U.K. is British Rail. The cost of repair to a simple single arch masonry bridge would vary depending upon the amount of attention required. A major reinstatement of a single arch 30 metre span masonry bridge could be of the order of 200,000 pounds. Thus, within the overall U.K. context the potential maintenance cost of stone masonry bridges is extremely high.

The inspection of steel and concrete structures may prove relatively straighforward. However the inspection of masonry bridges can often prove more difficult due to the composite nature of the masonry and the soil fill. Accurate drawings of the structure as constructed rarely exist.

Against the above background it is the authors view that there is an urgent need for low cost effective diagnostic tools for assessing the quality and integrity of stone masonry structures which neither structurally damage nor scar the bridge. The techniques to be reported within this paper are equally applicable to brick masonry and stone masonry.

TRADITIONAL METHODS OF ASSESSMENT OF MASONRY BRIDGES

The standard engineering approach to the evaluation of masonry bridges is largely based on visual inspection accompanied by coring techniques - typically 100mm diameter. The coring techniques are clearly expensive and can scar the structure.

The obvious limitations of traditional evaluation procedures include:

(I) Visual inspection, typically by a tradesman trained inspector, does not reveal internal deterioration and degradation of the structure.

(II) Coring techniques are expensive and are statistically valid only in relation to the point at which the core has been taken.

(III) Large important areas of the structure may be totally ignored.

(IV) It is often impossible to gain an insight into the quality of the soil fill as the coring technique using a water flush will wash out the soil fines from the core taken - it is therefore only relevant to the masonry part of the structure.

(V) If extensive coring is used the drilling process using a water flush may in fact do more damage to the structure than no inspection.

NON-DESTRUCTIVE INVESTIGATION TECHNIQUES

Ultra Sonic Techniques

The availability of low cost ultra sonic testing devices, such as PUNDIT, has increased the availability and access to non destructive investigation techniques. The first class ultra sonic device, PUNDIT, is a low energy input high frequency, 50,000 hertz, device. If one assumes a transmission velocity through masonry of 2000 metres per second this yields a wave length of 0.04 metres. With such a short wavelength and such a high frequency the device will prove inappropriate for masonry structures for the following reasons:

(I) Energy input is inadequate for penetration to any significant depth.

(II) The high resolution from the high frequency and short wave length is inappropriate for the heterogeneous material which comprises stone masonry with lime mortar.

(III) The net outcome of an investigation is that superficial surface discontinuities or change in the nature of the material will be identified.

(IV) Significant major defects cannot be identified due to the low energy input.

Ultra sonic techniques have proved powerful and increasingly used tools for the investigation of steel and concrete structures.

SONIC TECHNIQUES

As a result of the ready availability of ultra sonic instrumentation systems (sometimes described as "black boxes"), this technique has been readily used within civil engineering. The application of ultra sonics described above has been shown to be inappropriate to other than small sample testing where there is a ready and appropriate place for their application. Ultrasonics refers to frequencies of excitation outside the audible range. Thus sonic testing refers to frequencies below 20kHz.

It has been shown by the authors that the advantages of sonic investigation techniques include:

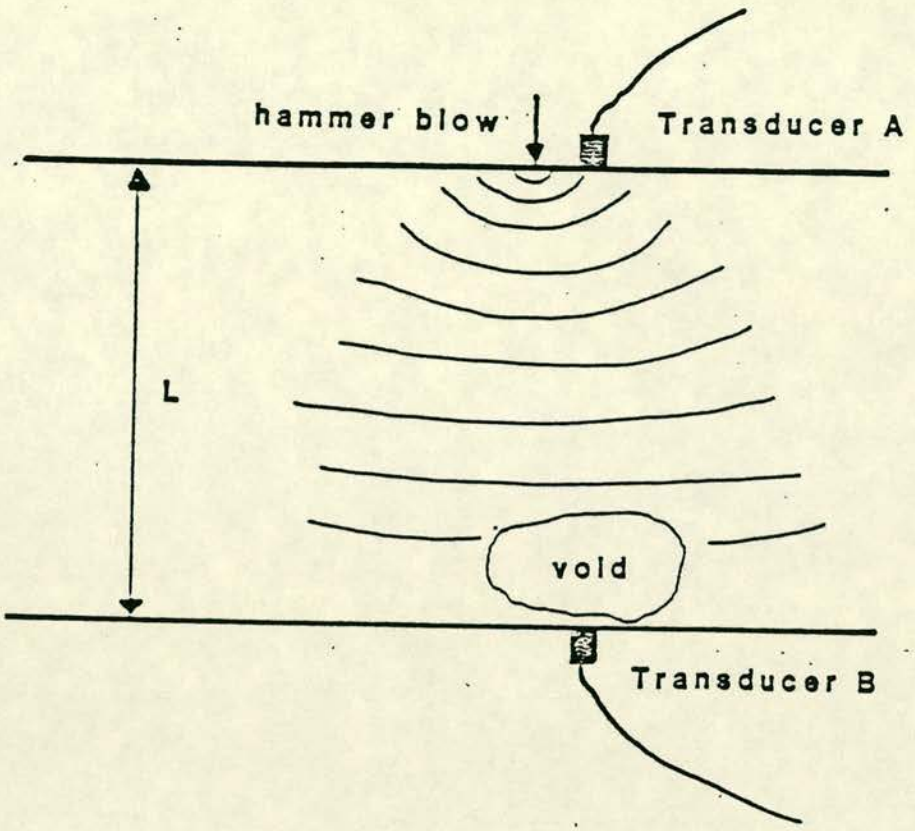

FIG. 1

a) longer wavelengths
b) greater depth of penetration
c) less attenuation of the signal

Asscciated with the advantages of the sonic technique are a number of potential disadvantages. The primary disadvantage of the sonic investigation technique lies in the poor resolution of the technique at shallow depth. One would therefore not use sonics for the investigation of defects or cracks in aircraft wing structures.

The method of investigation used in the investigation reported herein is based upon that used by the authors previously (ref 1). The technique involves the excitation of the structure using a steel tipped hammer. (It should be noted that further research is being undertaken using hammers of different hardness of tip.) An analysis of the frequency of the signal propogated was undertaken using an 8 bit transient recorder downloading to a Hewlett-Packard HP 85 Microcomputer. The signal downloaded onto the HP 85 Microcomputer was analysed using the mathematical algorithm of the fast fourier transform. The analysis was undertaken using a standard Hewlett-Packard waveform analysis package. From the investigation, it was established that typically the predominant frequency generated by the 450 gram hammer was approximately 2kHz.

With respect to the investigation to be undertaken, the engineering implication of using a sonic signal as opposed to an ultrasonic signal can be appreciated when one considers that with a transmission velocity through old stone masonry of approximately 2,000 m/s and a frequency of 2 kHz, the wavelength of the compression wave generated is approximately 1 metre. Having regard to the advantages and disadvantages discussed above, it will be apparent that the technique will be sensitive only to significant defects within the heart of the structure. Practising Engineers of course are primarily interested in these major defects in masonry structures rather than a detailed map of every individual joint.

The principle of the method used was to mount piezo-electric accelerometers to either side of the structure to be investigated - see Figure 1. For the purposes of this investigation, each accelerometer was then attached to a separate channel of a dual-beam storage oscilloscope. The wall adjacent to accelerometer "A" was excited. The resultant compression wave was then recorded as trace 1 on the oscilloscope. Accelerometer 2 resulted in trace 2 on the oscilloscope. This trace resulted from the compression wave which passed through the structure and was received at accelerometer "B". Essentially, one was using the delay technique to measure the time interval between the receipt of the hammer blow on transducer A and the receipt of the propogated signal through the structure to transducer B - Fig 2.

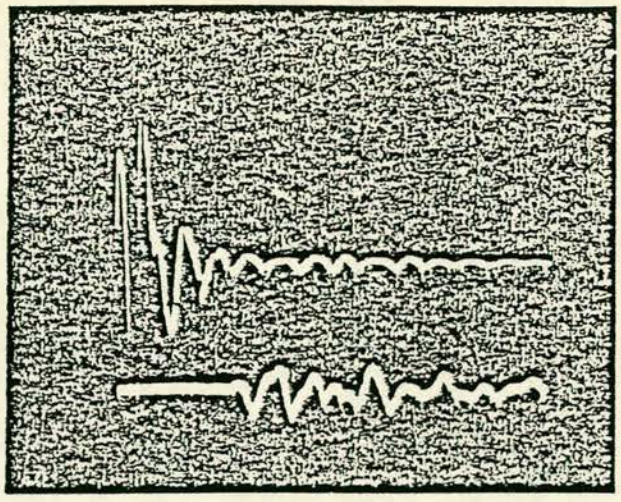

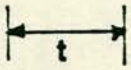

TYPICAL TRACE

SHOWING TRANSMISSION

FIG. 2

The compression wave velocity, v, may be calculated from:

v = transmission velocity = t/L

where t = time interval from oscilloscope trace
L = distance between transducers

FULL SCALE INVESTIGATION OF MASONRY BRIDGE PRIOR TO AND POST GROUTING

The ongoing research at Edinburgh University has involved the development and application of non-destructive techniques to repair, maintenance and operation in the soil structure environment. As part of this ongoing research at both the laboratory and full scale, an investigation was undertaken of a 120 year old stone masonry bridge - Fig. 3.

The objective of the investigation was to determine voiding, if any, in the southern abuttment/wing wall and compare this with the northern wing wall.

The experimental procedure was as described in the previous section and as reported in more detail elsewhere (Ref 1).

The experimental procedure comprised marking a grid of survey points on the wing wall/abuttments of this 120 year old masonry bridge. The delay time investigation was then undertaken at the marked locations on the structure. From an analysis of the polaroid photograph records taken, it was established that there was no transmission from the

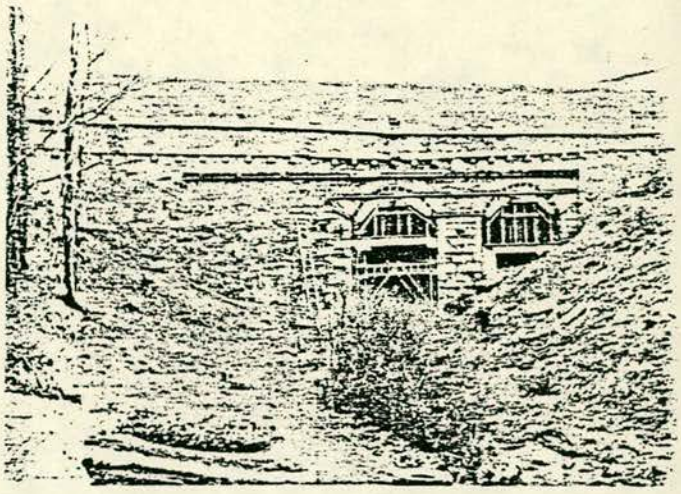

FIG. 3

downstream abuttment in the area hatched on Fig. 4. However, upon undertaking the delay method from the other side of the structure, it was found possible to obtain transmission from the upstream face propogating to the downstream face. The interpretation of this apparent initial anomaly was that voiding of significant magnitude was present behind the downstream wing wall but not the upstream wing wall.

The physical explanation of this can be appreciated from Fig. 1. A point compression wave injected by the steel headed hammer on the downstream face will not propogate through the voided area. However, a point compression wave injected into the upstream face will propogate through the fill and become plain fronted. Thus, when the plain fronted wave comes to the void a proportion of the signal will travel either side of the void and excite the downstream wing wall - albeit with reduced energy.

Following the findings of this investigation, the Engineer responsible for the works specified sand cement grouting of the wing wall. Eleven cubic metres of sand cement grout were introduced to the structure. Subsequent to the grouting operation, the authors undertook a follow-up investigation using the tecniques reported earlier. The follow-up survey revealed a significantly improved quality of the structure - see Fig. 5. From this it can be seen that most of the voiding reported previously was now filled.

CONCLUSIONS

(1) A low frequency, 2kHz, time delay sonic system has been used for the investigation of a 120 year old masonry bridge.

(2) The sonic investigation technique identified a large voided area behind one wing wall of the structure.

(3) Following grouting with 11 cubic metres of sand cement grout, the structure was retested.

(4) Subsequent to grouting, the retest indicated a substantial improvement with only very limited areas of voiding behind the wing wall.

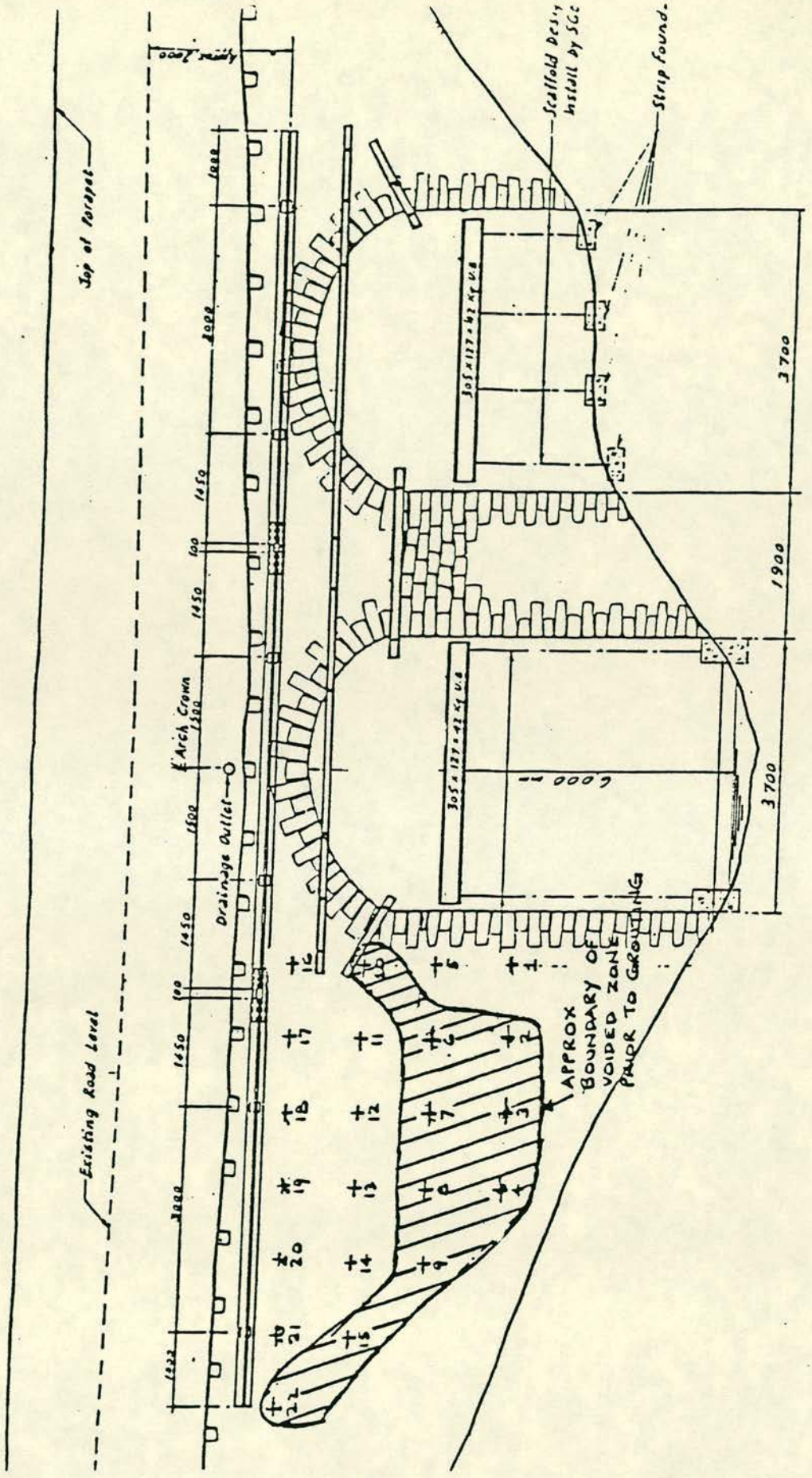
Top of Parapet
Existing Road Level
Drainage Outlet
Arch Crown
Scaffold Deck
Strip found.
3700
1900
3700
APPROX BOUNDARY OF VOIDED ZONE PRIOR TO GROUTING

FIG. 4

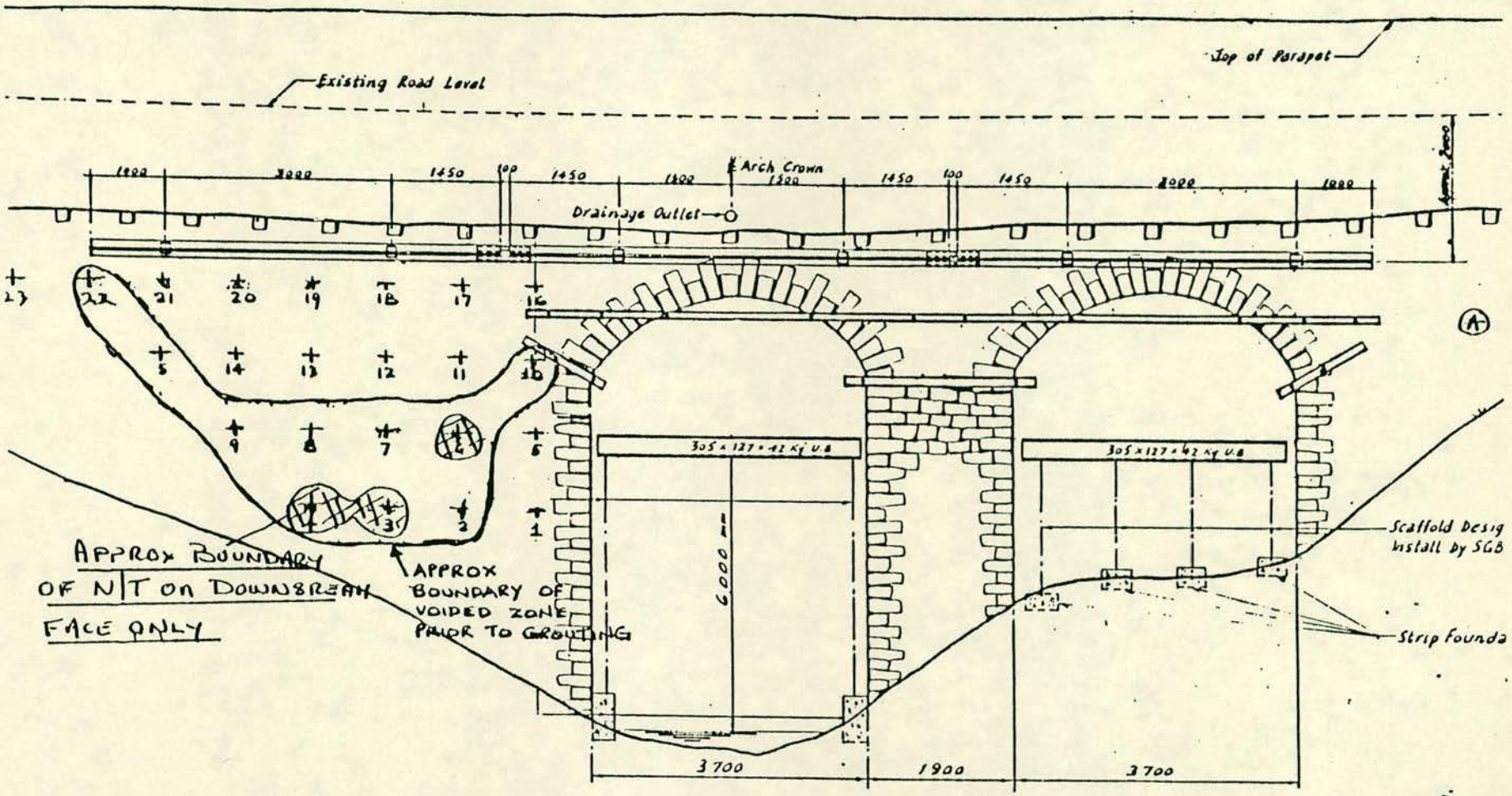
Top of Parapet
Existing Road Level
Drainage Outlet
E Arch Crown
305 x 127 x 42 Kg U.B
305 x 127 x 42 Kg U.B
6000
APPROX BOUNDARY OF N|T ON DOWNSTREAM FACE ONLY
APPROX BOUNDARY OF VOIDED ZONE PRIOR TO GROUTING
Scaffold Desig
Install by SGB
Strip Founda
3700
1900
3700

FIG. 5

ACKNOWLEDGEMENTS

The authors acknowledge the provision of facilities and ongoing encouragement of Professor A.W. Hendry, Department of Civil Engineering and Building Science, University of Edinburgh. Valuable discussions with Messrs. K. Teh and R. Mendleson of Blyth & Blyth, Edinburgh are also acknowledged.

REFERENCE

(1) Kameyli-Birjandi, F.,Forde, M.C., and Whittington, H., "Sonic Investigation of Shear Failed Reinforced Brick Masonry Walls", Masonry International, November 1984.